

**GAS CHROMATOGRAPHY AND MASS SPECTROMETRY OF
SOME STERICALLY CROWDED TRIALKYLSILYL DERIVATIVES OF
MONOSACCHARIDES AND RELATED COMPOUNDS**

by

Peter K. T. Ng

A Thesis

**Submitted to the Faculty of Graduate Studies
in Partial Fulfillment of the Requirements for the
Degree of Master of Science**

Department of Chemistry

The University of Manitoba

Winnipeg, Manitoba

October, 1979

GAS CHROMATOGRAPHY AND MASS SPECTROMETRY OF
SOME STERICALLY CROWDED TRIALKYLSILYL DERIVATIVES OF
MONOSACCHARIDES AND RELATED COMPOUNDS

BY

PETER KA TAI NG

A dissertation submitted to the Faculty of Graduate Studies of
the University of Manitoba in partial fulfillment of the requirements
of the degree of

MASTER OF SCIENCE

©v1979

Permission has been granted to the LIBRARY OF THE UNIVERSITY OF MANITOBA to lend or sell copies of this dissertation, to the NATIONAL LIBRARY OF CANADA to microfilm this dissertation and to lend or sell copies of the film, and UNIVERSITY MICROFILMS to publish an abstract of this dissertation.

The author reserves other publication rights, and neither the dissertation nor extensive extracts from it may be printed or otherwise reproduced without the author's written permission.

to my parents

ACKNOWLEDGEMENTS

I am grateful to Dr. J. B. Westmore for his supervision, encouragement, and advice he provided throughout the course of this research.

I would like to thank Michael Quilliam for his continual enthusiasm and helpful advice on the technical aspects of gas chromatography. His encouragement is very much appreciated.

I would also like to thank K.L.Sadana and D.Buksak for helpful discussions and their assistance with various aspects of the study.

Abstract

A preliminary study on the gas chromatography and mass spectrometry (Gas Phase Analytical Chemistry) of a series of silyl ether derivatives of monosaccharides and related molecules is described. The silyl groups of interest all contain a bulky alkyl substituent, i.e. t-butyl or i-propyl and collectively are described as sterically crowded trialkylsilyl (SCTASi) groups. They are : tert-butyldimethylsilyl (TBDMSi); cyclo-tetramethylene-iso-propyl-silyl (TMIPSi); and cyclo-tetramethylene-tert-butylsilyl (TMTBSi). Monosaccharides (D-2-deoxyribose, D-ribose, D-xylose, D-glucose, D-galactose, D-mannose and D-fructose) as well as some related molecules (D-1,4 ribonolactone and β -D-benzylribofuranoside) were reacted with the silyl reagents in various proportions and the products were analyzed by gas chromatography and the peaks studied by electron impact mass spectrometry. By these methods partial and mixed silyl derivatives could be obtained, which yielded information on structure and rearrangement and fragmentation directing behavior of SCTASi-groups in mass spectra.

TABLE OF CONTENTS

	Page
ACKNOWLEDGEMENTS	ii
ABSTRACT	iii
TABLE OF CONTENTS	iv
LIST OF TABLES	vii
LIST OF SCHEMES	viii
LIST OF FIGURES	ix
ABBREVIATIONS	xiv
NOMENCLATURE	xvi
I. INTRODUCTION	1
Carbohydrates	1
Isomerism and stereochemistry of monosaccharides	2
Analytical chemistry of carbohydrates	6
Gas phase analytical chemistry	9
Chemical derivatization	10
Silylation	10
Gas phase analytical chemistry of carbohydrates	15
Gas phase analysis in carbohydrate structure determination	15
II. EXPERIMENTAL	20
Reagents	20
Synthesis of β -D-benzylribofuranoside	21
Preparation of analytical derivatives	22
Persilylation	22
Partial silylation	23

	Page
Mixed derivatization	23
Gas chromatography	24
Quantitative GC	25
Mass spectrometry	28
III. GAS CHROMATOGRAPHY	29
Introduction	29
Retention indices	30
GC system	31
Solvent systems	32
Silylated monosaccharides	36
Silylated 1,4-ribonolactones	48
Silylated β -D-benzylribofuranosides	55
Quantitative GC	65
Mutarotation of sugars	69
IV. MASS SPECTROMETRY	74
Introduction	74
Electron impact mass spectrometry	75
Electron impact behavior of trialkylsilyl ethers of carbohydrates	77
a) Mass spectra of TBDMSi-D-hexopyranose systems	83
1) Pentakis-O-TBDMSi-D-glucoses	83
2) Pentakis-O-TBDMSi-D-mannoses	91
3) Pentakis-O-TBDMSi-D-fructoses	91

	Page
b) Mass spectra of SCTASI-O-D-2-deoxyriboses	96
1) Per SCTASI-D-2-deoxyriboses	96
2) Partial SCTASI-D-2-deoxyriboses	104
c) Mass spectra of SCTASI- β -D-ribofuranosides	109
1) Per SCTASI- β -D-benzylribofuranosides	109
2) Partial SCTASI-O- β -D-benzylribofuranosides	117
3) Mixed Ac/TEDMSI derivatives of β -D-benzyl-ribofuranosides	129
4) Mass spectra of SCTASI-D-riboses	137
5) Mass spectra of SCTASI-D-xyloses	137
d) Mass spectra of SCTASI-1,4-ribonolactones	
1) Per SCTASI-1,4-ribonolactones	117
2) Partial SCTASI-1,4-ribonolactones	152
V. CONCLUSION	164
VI. BIBLIOGRAPHY	166

LIST OF TABLES

	Page
1) Classification of carbohydrates.	1
2) Classification of sugars.	2
3) Number of stereo-isomers for monosaccharides.	4
4) Analytical capabilities of a variety of instrumental techniques.	7
5) Derivatives from different protecting groups.	18
6) GC retention data of per-O-TMSi-sugars.	38
7) GC retention data of partial-O-TBDBSi-sugars.	43
8) GC retention data of per-O-TBDMSi-sugars.	46
9) Comparison of different studies of silylated sugars.	47
10) GC retention data of silylated 1,4-ribonolactones.	50
11) GC retention data of β -D-benzylribofuranoside derivatives.	56
12) Comparison of mutarotation studies in pyridine.	71

LIST OF SCHEMES

	Page
1) Cyclization of D-ribose in H ₂ O.	4
2) Formation of external acetals.	5
3) General outline for carbohydrate structure determination.	16
4) Formation of 1,4-lactones from aldoses.	48
5) TMSilylation of lactones.	48
6) Possible fissions of a trimethylsilyl ether.	79
7) Geneses of m/z 693, m/z 561, m/z 429, m/z 519 and m/z 445.	86
8) Formation of m/z 487, m/z 519 and m/z 445 from m/z 693.	87
9) Formation of m/z 231, m/z 245, and m/z 375 from M ⁺ ion.	88
10) Formation of m/z 288 from M ⁺ ion.	89
11) Formation of m/z 301 from pentakis-O-TBDMSi-glucofuranose.	70
12) Formation of (M-145) ⁺ ion from M ⁺ of pentakis-O-TBDMSi-D-fructose.	91
13) Mass spectral fragmentation of SCTASI-D-2-deoxyriboses.	102
14) Mass spectral fragmentation patterns of SCTASI- β -D-benzyl-ribofuranosides.	114
15) Mass spectral fragmentation patterns of SCTASI-D-ribofuranoses.	142

LIST OF FIGURES

	Page
1) Diagram of an aldo-pentose showing three chiral centres.	3
2) Diagram showing the number of chiral centres on an aldo-pentose if D- and L- configurations are distinguished.	3
3) Common SCTASI groups	14
4a) Gas chromatogram of the upper layer of a silylated sugar reaction mixture when DMF was used as a solvent.	37
4b) Mass spectrum of di- <i>tert</i> -butyltetramethylidisiloxane.	35
5) Gas chromatogram of silylated D-ribose.	39
6) Gas chromatogram of TBDMSi-D-2-deoxyribose.	40
7) Gas chromatogram of silylated D-ribose.	41
8) Gas chromatogram of TBDMSi-D-galactose.	42
9) Possible structures of bis-O-TBDMSi-D-2-deoxyribose.	44
10) Gas chromatogram of silylated 1,4-ribonolactones.	51
11) Gas chromatogram of partially silylated 1,4-ribonolactones.	52
12) Gas chromatogram of O-TMTBSi-1,4-ribonolactones.	53
13) Gas chromatogram of mixed TMSi/TBDMSi derivatives of 1,4-ribonolactones.	54
14) Gas chromatogram of O-silylated β -D-benzylribofuranosides.	58
15) Gas chromatogram of mono-O-TMTBSi- β -D-benzylribofuranosides.	59
16) Gas chromatogram of O-TMTBSi- β -D-ribofuranosides.	60
17) Gas chromatogram of TMPSi ₃ β -D-benzylribofuranoside.	61
18) Gas chromatogram of mixed TMSi/TBDMSi derivatives of β -D-benzylribofuranoside.	62

	Page
19) Gas chromatogram of TFA/TBDMSi mixed derivatives of β -D-benzylribofuranosides.	63
20) Gas chromatogram of mixed derivatives of β -D-benzyl-ribofuranosides.	64
21) FID response curves for silylated β -D-benzylribofuranosides and 1,4-ribonolactones.	67
22) FID response curves of silylated hexose, pentose and D-2-deoxyribose.	68
23) Equilibrium processes in mutarotation of sugars.	70
24) Formation of different ions from the molecular ion.	76
25) Mass spectrum of decafluorophenylphosphine.	78
26) Loss of trimethylsilanol from M-15 ⁺ .	81
27) Mass spectrum of pentakis-O-TBDMSi-D-glucose.	84
28) Mass spectrum of pentakis-O-TBDMSi-D-glucose.	85
29) Mass spectrum of pentakis-O-TBDMSi-D-mannose.	92
30) Mass spectrum of pentakis-O-TBDMSi-D-mannose.	93
31) Mass spectrum of pentakis-O-TBDMSi-D-fructose.	94
32) Mass spectrum of pentakis-O-TBDMSi-D-fructose.	95
33) Comparison between SCTASI-deoxyribonucleosides and SCTASI-D-2-deoxyriboses.	96
34) Major fragments of SCTASI-2-deoxyribose.	97
35) Mass spectrum of tris-O-TBDMSi-D-2-deoxyribose.	98
36) Mass spectrum of tris-O-TBDMSi-D-2-deoxyribose.	99

	Page
37) Mass spectrum of tris-O-TMTBSi-D-2-deoxyribose.	100
38) Mass spectrum of tris-O-TMTBSi-D-2-deoxyribose.	101
39) Mass spectrum of bis-O-TBDMSi-D-2-deoxyribose.	105
40) Mass spectrum of bis-O-TBDMSi-D-2-deoxyribose.	106
41) Mass spectrum of mono-O-TMSi-bis-O-TBDMSi-D-2-deoxyribose.	107
42) Mass spectrum of mono-O-TBDMSi-bis-O-TMSi-D-2-deoxyribose.	108
43) a) Comparison of SCTASi-ribonucleoside, SCTASI- β -D-benzylribofuranoside and SCTASI-D-ribofuranoside.	109
b) Major fragments of SCTASI- β -D-benzylribofuranosides.	109
44) Mass spectrum of tris-O-TMSi- β -D-benzylribofuranoside.	110
45) Mass spectrum of tris-O-TBDMSi- β -D-benzylribofuranoside.	111
46) Mass spectrum of tris-O-TMIPSi- β -D-benzylribofuranoside.	112
47) Mass spectrum of tris-O-TMTBSi- β -D-benzylribofuranoside.	113
48) Mass spectrum of mono-O-TBDMSi- β -D-benzylribofuranoside.	118
49) Mass spectrum of mono-O-TBDMSi- β -D-benzylribofuranoside.	119
50) Mass spectrum of mono-O-TBDMSi- β -D-benzylribofuranoside.	120
51) Mass spectrum of mono-O-TMTBSi- β -D-benzylribofuranoside.	121
52) Mass spectrum of mono-O-TMTBSi- β -D-benzylribofuranoside.	122
53) Mass spectrum of mono-O-TMTBSi- β -D-benzylribofuranoside.	123
54) Mass spectrum of bis-O-TBDMSi- β -D-benzylribofuranoside.	124
55) Mass spectrum of bis-O-TBDMSi- β -D-benzylribofuranoside.	125
56) Mass spectrum of bis-O-TBDMSi- β -D-benzylribofuranoside.	126
57) Mass spectrum of bis-O-TMTBSi- β -D-benzylribofuranoside.	127
58) Mass spectrum of bis-O-TMTBSi- β -D-benzylribofuranoside.	128

	Page
59) Mass spectrum of mono-0-TBDMSi-bis-0-Ac- β -D-benzylribofuranoside.	130
60) Mass spectrum of mono-0-TBDMSi-bis-0-Ac- β -D-benzylribofuranoside.	131
61) Mass spectrum of mono-0-TBDMSi-bis-0-Ac- β -D-benzylribofuranoside.	132
62) Mass spectrum of mono-0-Ac-bis-0-TBDMSi- β -D-benzylribofuranoside.	133
63) Mass spectrum of mono-0-Ac-bis-0-TBDMSi- β -D-benzylribofuranoside.	134
64) Mass spectrum of mono-0-Ac-bis-0-TBDMSi- β -D-benzylribofuranoside.	135
65) Mass spectrum of tris-0-Ac- β -D-benzylribofuranoside.	136
66) Mass spectrum of tetrakis-0-TBDMSi-D-ribose.	138
67) Mass spectrum of tetrakis-0-TBDMSi-D-ribose.	139
68) Mass spectrum of tetrakis-0-TBDMSi-D-ribose.	140
69) Mass spectrum of tetrakis-0-TBDMSi-D-ribose.	141
70) Mass spectrum of tetrakis-0-TMTBSi-D-ribose.	144
71) Mass spectrum of tetrakis-0-TBDMSi-D-xylose.	145
72) Mass spectrum of tetrakis-0-TBDMSi-D-xylose.	146
73) Mass spectrum of tris-0-TMSi-1,4-ribonolactone.	148
74) Mass spectrum of tris-0-TBDMSi-1,4-ribonolactone.	149
75) Mass spectrum of tris-0-TMIPSi-1,4-ribonolactone,	150
76) Mass spectrum of tris-0-TMTBSi-1,4-ribonolactone.	151

	Page
77) Mass spectrum of mono-0-TBDMSi-1,4-ribonolactone.	153
78) Mass spectrum of mono-0-TBDMSi-1,4-ribonolactone.	154
79) Mass spectrum of mono-0-TBDMSi-1,4-ribonolactone.	155
80) Mass spectrum of mono-0-TMTBSi-1,4-ribonolactone.	156
81) Mass spectrum of mono-0-TMTBSi-1,4-ribonolactone.	157
82) Mass spectrum of bis-0-TBDMSi-1,4-ribonolactone.	158
83) Mass spectrum of bis-0-TBDMSi-1,4-ribonolactone.	159
84) Mass spectrum of bis-0-TBDMSi-1,4-ribonolactone.	160
85) Mass spectrum of bis-0-TMTBSi-1,4-ribonolactone.	161
86) Mass spectrum of bis-0-TMTBSi-1,4-ribonolactone.	162
87) Mass spectrum of bis-0-TMTBSi-1,4-ribonolactone.	163

ABBREVIATIONS

Ac	acetyl
AcAnh	acetic anhydride
AcIm	acetyl imidazole
AcOH	acetic acid
B	base unit of nucleoside
CI	chemical ionization
DMF	N,N-dimethylformamide
EI	electron impact
Et	ethyl
FI	field ionization
FD	field desorption
GC	gas chromatography
HPLC	high performance liquid chromatograph
Im	imidazole
Im·HCl	imidazole hydrogen chloride
i-Pr	iso-propyl
M ⁺	molecular ion
PYR	pyridine
S	sugar unit of nucleoside
SCTASI	sterically crowded trialkylsilyl
TBDMSi	<u>tert</u> -butyl dimethylsilyl

<u>t</u> -Bu	<u>tert</u> -butyl
TFA	trifluoroacetyl
TFAA	trifluoroacetyl anhydride
TFAlm	trifluoroacetyl imidazole
THF	tetrahydrofuran
TMIPSi	<u>cyclo</u> -tetramethylene- <u>iso</u> -propylsilyl
TMSi	trimethylsilyl
TMTBSi	<u>cyclo</u> -tetramethylene- <u>tert</u> -butylsilyl

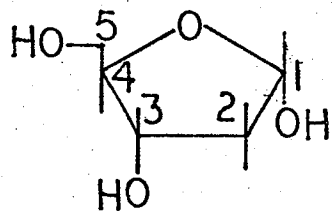
SYMBOLS

- ∞ separation factor
- ↖ single electron movement
- ↗ double electron movement
- > iso-propyl
- + tert-butyl
- ↔ cyclo-tetramethylene

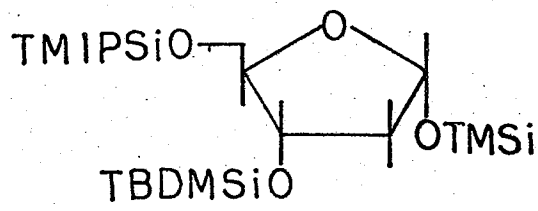
Nomenclature

I	= D-2-deoxyribose	a = TMSi
II	= D-ribose	b = TBDMSi
III	= D-xylose	c = TMPSi
IV	= D-glucose	d = TMTBSi
V	= D-galactose	e = TMHSi
VI	= D-mannose	p = TFA
VII	= D-fructose	q = Ac
VIII	= β -D-benzyl ribofuranoside	
IX	= 1,4-ribonolactone	

Each derivative is represented by a Roman numeral with subscripts in small letters. The first subscript denotes a substituent group at the lowest available carbon number on the molecule. The second subscript is for a substituent group at the second lowest available carbon number bearing the hydroxyl, etc.



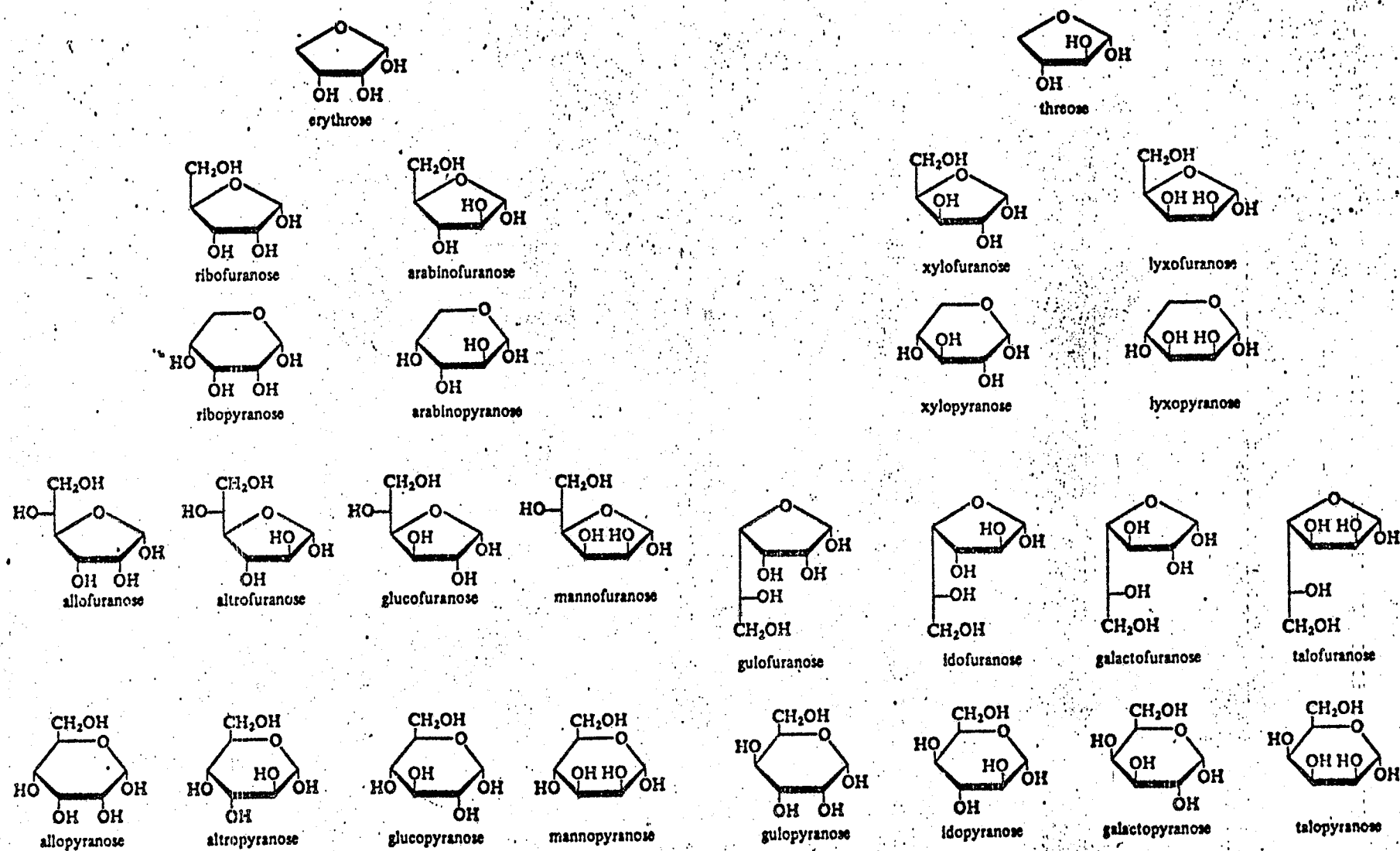
D-2-deoxyribose
with numberings on
each carbon atom



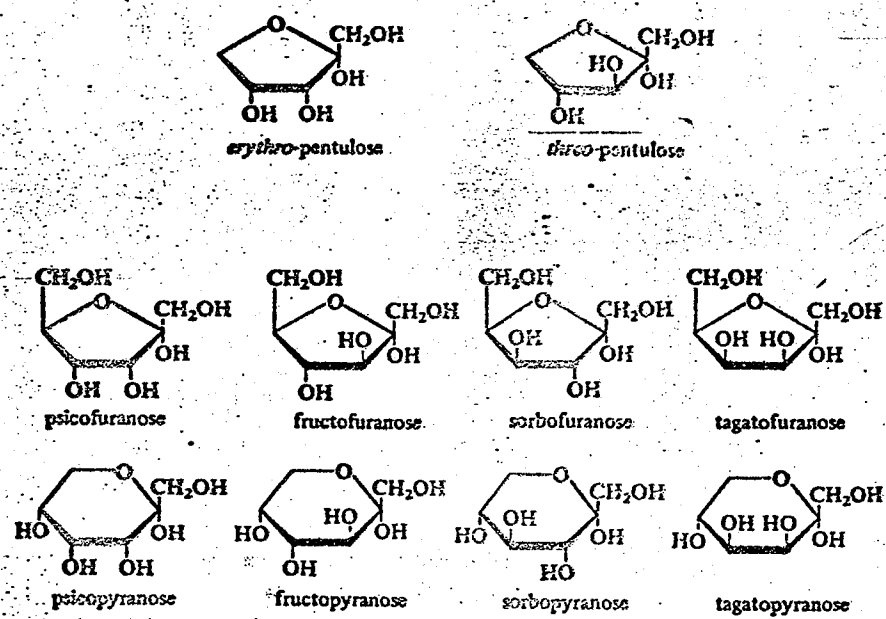
1-O-TMSi-3-O-TBDMSi-5-O-TMPSi-D-2-deoxy-
ribose or I_{abc}

I_{abc} = D-2-deoxyribose with TMSiO on carbon number 1; TBDMSiO on carbon number 3; and TMPSiO on carbon number 5.

When the subscripts are bracketed, no specification is made to assign substituent groups to individual carbon atoms.



: Cyclic forms of α -D-aldoses.



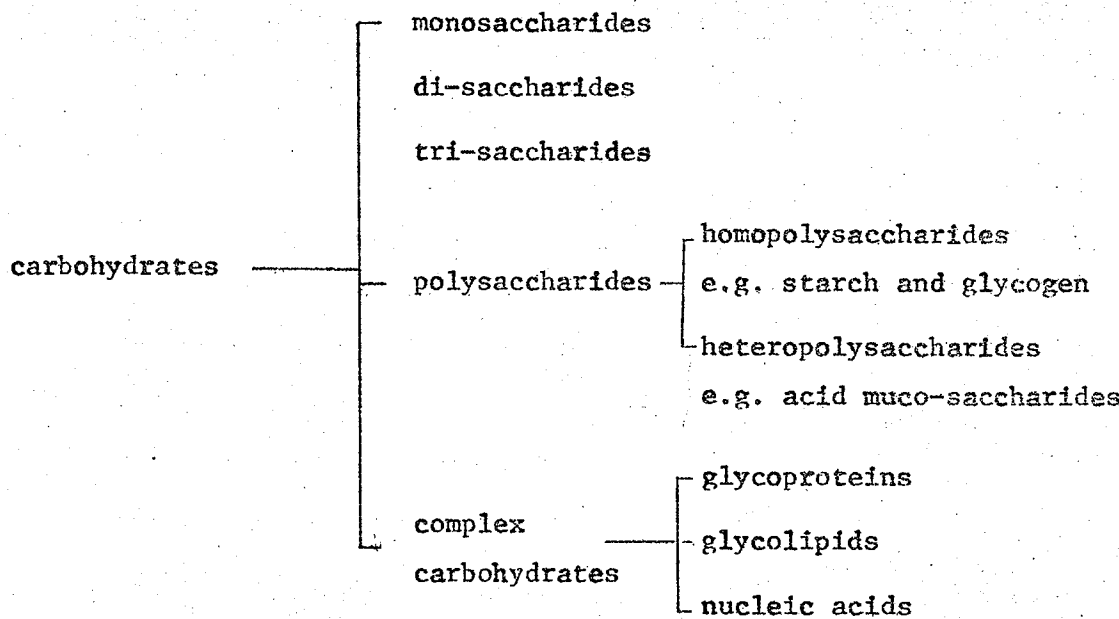
INTRODUCTION

Carbohydrates

Carbohydrates are among the most abundant chemical compounds in biological systems. They can be broadly defined as substances which upon hydrolysis, give polyhydroxy-aldehydes or polyhydroxy-ketones (1)

A brief classification of carbohydrates (2) is given as follows:

Table 1 : Classification of carbohydrates.



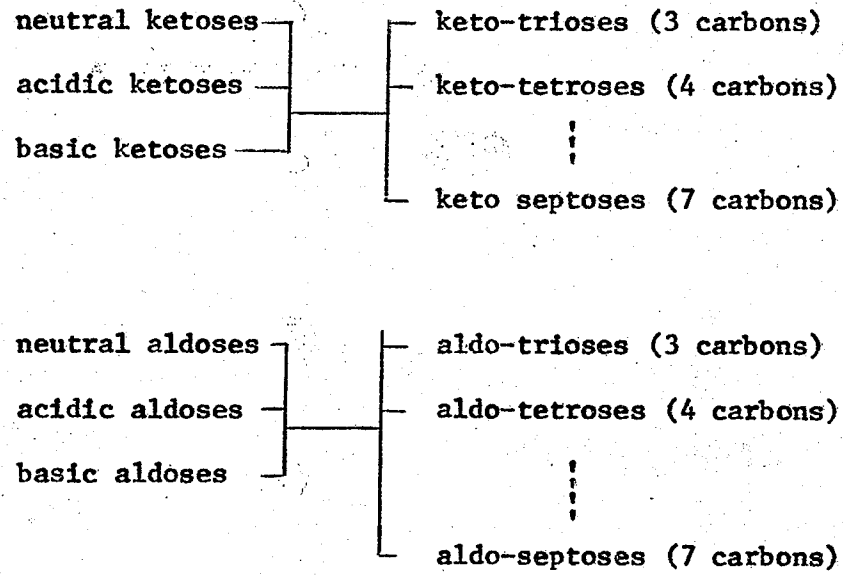
Together with lipids and proteins, carbohydrates are considered as the main building units of living organisms. In plants, they are the structural units, in the form of cellulose, hemi-cellulose and lignins, as well as the storage substances, in the form of starch, pectins and sugars. In higher animals, they are found as hyaluronic acid, glycogen, blood group substances, glucose, mucopolysaccharides, adenosine triphosphate (ATP), nucleic acids and hydroxy acids.

The simplest form of carbohydrate is the monosaccharide or "sugar" sub-unit. Monosaccharides can again be differentiated as aldoses and ketoses, depending on the nature of carbonyl group on the molecules. In terms of chemical functional groups, monosaccharides are classified into:

- 1) neutral sugars;
- 2) basic sugars (with NH_2 or $\text{CH}_2-\text{N}(\text{H})-$ groups); and
- 3) acidic sugars (with carboxyl groups).

Each sugar is also named according to the number of carbon atoms it carries. For example, a three "carbon" sugar is a triose. A schematic classification of simple sugars can be represented as follows:-

Table 2: Classification of simple sugars



Isomerism and stereochemistry of monosaccharides

Isomerism and stereochemistry of sugars have been studied since the 19th century. Because of the polyhydroxy nature of monosaccharide molecules, and hence chiral carbon atoms, many stereo-isomers are possible. Take

for example, an aldo-pentose which contains 5 carbon atoms in the molecule.

The highest number of chiral carbon atoms = 3. Thus, there can be 2^3 or 8 stereoisomers.

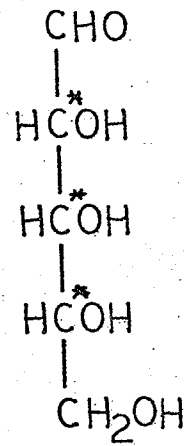
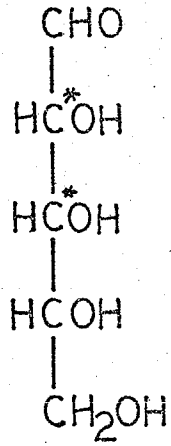


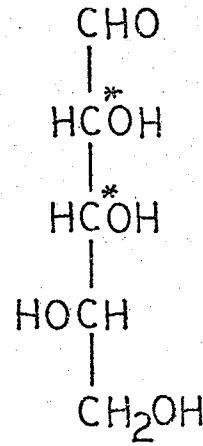
Figure: 1 Diagram of an aldo-pentose showing 3 chiral centres.

$$\text{Number of possible stereo-isomers} = 2^3 = 8.$$

If we fix one configuration of the penultimate carbon atom, and name it as a D-sugar, its mirror image can then be assigned as the L-sugar; and the number of remaining chiral carbons on each molecule is 2. Thus, the number of stereo-isomers for either D- or L- series reduces to 2^2 , e.g.



D-ribose



L-ribose

Figure: 2 Diagram showing the number of chiral carbons on an aldo-pentose if D- and L- configurations are distinguished.

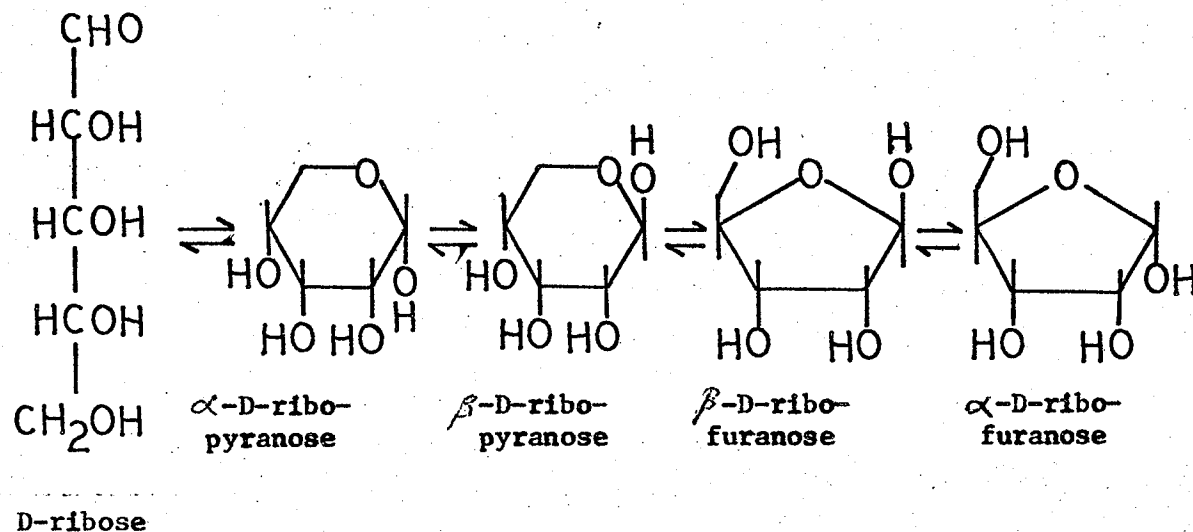
To provide a summary, the following table gives the highest number of stereoisomers from each kind of sugar.

Table: 3 Number of stereoisomers for monosaccharides.

Number of carbon atoms	Stereoisomers of monosaccharides	Stereo-isomers for D- or L-series
3	$2^1 = 2$	$2^0 = 1$
4	$2^2 = 4$	$2^1 = 2$
5	$2^3 = 8$	$2^2 = 4$
6	$2^4 = 16$	$2^3 = 8$
7	$2^5 = 32$	$2^4 = 16$

For thermodynamic reasons, many sugars readily form cyclic isomers.

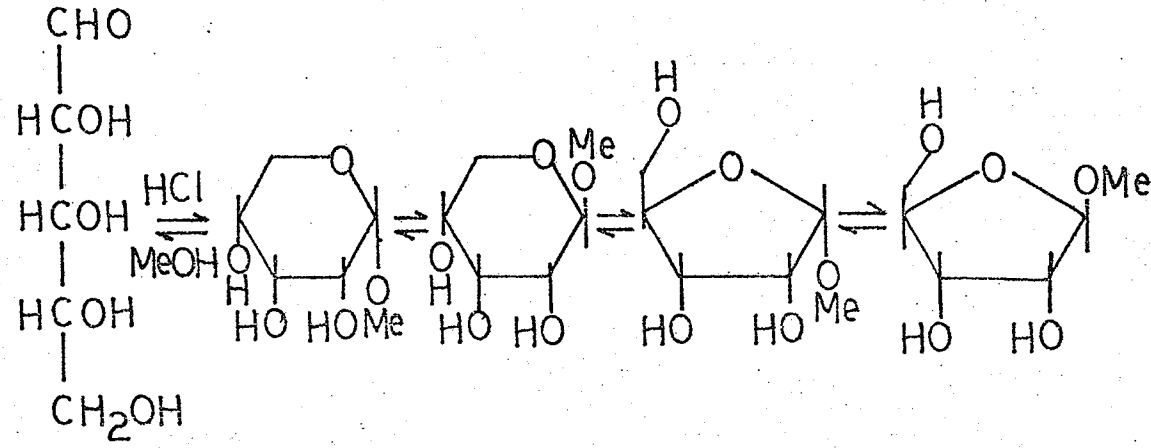
They may form 5 or 6 membered-rings, by cyclization involving a hydroxyl group and the carbonyl group on the molecule, e.g.



Scheme:1 Cyclization of D-ribose in solvents, e.g. H_2O

The formation of the cyclic acetal or ketal, leads to new chiral centres (anomeric carbons). As a result, and including the possibility of 5 or 6 membered-rings, 4 more stereo-isomers are formed, each of which is in equilibrium with each other and the acyclic isomer. The equilibrium depends also on a lot of external factors such as temperature, solvent system, pH, ionic strength, and oxidizing strength of the system. Thus, one would view a mono-saccharide in solution as a dynamic and flexible molecule capable of transforming from one configuration to another with relative ease at ambient temperature.

External acetals are also possible, with the formation of a number of reaction products.



Scheme: 2 Formation of external acetals, e.g. D-ribose with methanol/HCl.

Analytical chemistry of carbohydrates

Carbohydrates, no matter how complex in structure, eventually yield monosaccharides as hydrolysis products. The analytical chemistry of carbohydrates is essentially : 1) the identification of "sub-units" (monosaccharides); 2) the special sequence determination of the building-block sequence; 3) the branching characteristics of the molecule; 4) the special structural aspects of each monosaccharide (configuration) as well as 5) the biologically active sites. "Monosaccharide" analyses alone are constantly performed because of the ubiquitous nature of the sugars.

Monosaccharides, to a chemist, represent highly polar molecules, multi-functional, thermo-labile as well as very non-volatile. They are subject to biological degradation during analysis. In addition to handling problems, the structural and configurational differences between molecules are extremely slight. A hypothetically ideal method for sugar analysis should have the following characteristics:-

- 1) sufficiently high resolution to separate sugar molecules (including acyclic as well as cyclic anomers of 5 or 6 membered-ring sugar isomers) from each other,
- 2) the power to quantify each individual component of the sugar mixture,
- 3) absolute determination of the unique configuration and structural information of each component, and
- 4) a short analysis time, as well as ease of operation.

Table 4 gives a review and comparison on the capability of a variety of instrumental techniques.

Table 4 Analytical capabilities of a variety of instrumental techniques.

Table 4 (cont'd)

Techniques	Time	Separation	Resolution	Sensitivity	Specificity (selectivity)	Identification	quantitation
UV absorption spectrophotometry	s	/	/	g	f/g	g	g/exc.
Fluorometry & phosphorometry	s	/	/	g	f/g	g	g/exc.
IR & Raman spectroscopy	s	/	/	g	f/g	f/g	f
M.S.	s	/	/	exc.	g	exc.	g
NMR	s	/	/	f/g	g/exc.	g/exc.	f/g
X-ray diffraction	l	/	/	g	f	g/exc.	p
Immunochemical methods	l	/	/	g/exc.	exc.	g/exc.	g/exc.
GC	s	yes	exc.	g/exc.	g/exc.	g/exc.	g/exc.

Abbreviations: l = long; s = short; p = poor; f = fair; exc. = excellent; and / = not applicable.

UV = ultra violet, IR = infra-red , M.S. = mass spectrometry, NMR =nuclear magnetic resonance, GC = gas chromatography, TLC = thin layer chromatography , PC = paper chromatography and HPLC = high performance liquid chromatography.

With the above analytical capabilities of each method in mind, one is able to select the combination of 2 or 3 techniques which gives good separation, resolution, specificity, sensitivity, quantification and identification within a reasonable analysis time period. The combination of gas chromatography and mass spectrometry in particular offers a highly complementary system which nearly fulfills the criteria mentioned above for good analysis of sugar mixture.

Gas phase analytical chemistry

"Gas Phase Analytical Chemistry", a term coined by E.C. Horning (3), is a powerful analytical technique for separation, quantitation and identification of components in a sample mixture. Most important analytical processes of the above-mentioned technique occur in the gaseous phase, hence the name. In brief, the "gas-phase analysis" consists of 1) sample preparation (concentration, enriching, extracting etc); 2) derivatization (blocking of thermally labile polar groups on each component); 3) separation in gas phase (gas chromatography); 4) quantitation by gas chromatographic detectors and 5) identification (gas chromatographic retention times, mass spectral fragmentation patterns etc.). The main features, namely, GC/MS involve the properties of samples in gas phase. Over recent years, we have witnessed a relatively productive period for gas phase analyses due to advances in derivatization and GC/MS instrumentation (high temperature GC columns, temperature programming, highly selective absorbents, high pressure techniques, automation and high speed data processing). With the present day technology in micro-processing and control devices, gas phase analysis occupies an important position in modern analytical chemistry.

Chemical derivatization

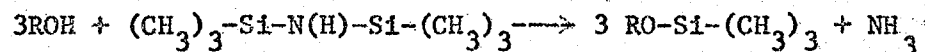
Sample derivatization is frequently an essential process in gas chromatography because separation depends on partition of gaseous sample molecules between the carrier phase (gas) and the liquid solvent on the column. Large or highly polar molecules are often non-volatile. Many of these compounds exert a measurable volatility only at temperatures at which they decompose. If sample decomposition occurs inside a GC system non-elution of sample and even destruction of the column may happen.

Enhancement of volatility and prevention of asymmetric chromatographic peaks can be achieved by a derivatization process that blocks the inter-molecular bonding of molecules through polar groups. A comprehensive review on chemical derivatization was recently given by J. Drozd. (4)

Silylation

a) Trimethylsilylation:

Trimethylsilylation (5,6) is a popular derivatization method for polar group protection. The reaction, originally investigated by C.C. Sweeley proceeds as:-



Over the years, other trimethylsilylation reagents, solvent systems, and different derivatization conditions have been devised to achieve different goals in protecting different labile groups. The huge volume of literature on trimethylsilylation bears witness to the tremendous success of trimethylsilylation on a great variety of compounds for GC purposes.

However, the quantitative and fast trimethylsilylation reaction has some disadvantages. The TMSi-samples are subject to hydrolysis, which causes handling and manipulative problems (e.g. in TLC sample isolation). For GC elutions, TMSi-derivatives may have small volatility differences and co-chromatograph as a single peak. For stereo-isomeric TMSi-derivatives, a high resolution (as much as 50,000-100,000 theoretical plates) may be required for good separation. Mass spectral fragmentation patterns for isomers are often very similar and may give very little stereochemical and structural information.

Wide varieties of silylating reagents have been developed to complement the trimethylsilylation reagents. Broadly speaking, the silylating agents can be divided into 3 types:-

- 1) alkyl dimethylsilyl types ($\text{RM}_2\text{Si}-$) where R = hydrogen (7,8), ethyl (9), propyl (9), allyl (15,16), chloromethyl (17-20), bromomethyl (18,21,22), iodomethyl (18,23), trifluoropropyl (24), heptafluoropentyl (24), pentafluorophenyl (24);
- 2) trialkylsilyl type ($\text{R}_3\text{Si}-$) where R = ethyl, n-propyl, n-butyl and n-hexyl;
- 3) sterically crowded trialkylsilyl (SCTASI-) (26-28): namely, tert-butyldimethyl silyl (TBDMSi) (10-15)(29-33), cyclo-tetramethylene-iso-propylsilyl (TMIPSi), cyclo-tetramethylene-tert-butyldimethylsilyl (TMTBSi) and diphenyl-tert-butylsilyl (34).

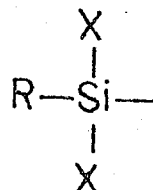
The halogen-containing alkylsilyl groups are known to enhance the detection limit of derivatized samples if electron-capture GC detectors are used. $\text{H}(\text{CH}_3)_2\text{Si}$ derivatives have shorter retention times than those of the TMSi-ethers; whereas if longer retention times are necessary, other trialkylsilylating reagents can be employed in place of TMSiCl. Trialkylsilyl groups are also more selective towards blocking of polar groups of different steric environments. Phenyl group containing silyl ethers are valuable in UV spectrophotometric analysis of polyglycol derivatives as well as nucleotide syntheses (34).

In a search for stable silyl ethers of prostaglandins in synthesis, E.J. Corey *et al* (29) reacted the silylating reagent *tert*-butyldimethylsilyl chloride, and imidazole in N,N-dimethyl formamide with the hydroxyl groups of prostaglandins. The derivatization was found to proceed under very mild conditions. Selectivity towards -OH groups was enhanced as compared with TMSi-groups. Stable TBDMSi-prostaglandins which were resistant to hydrogenolysis, mild oxidation, reduction, acid and base hydrolysis, were formed. Also, they were crystalline compounds with sharp melting points. The silyl groups can also be cleaved selectively in tetrahydrofuran with tetra-n-butyl ammonium fluoride or in acidic media.

Furthermore, Ogilvie (30), using selective derivatization, was able to block certain groups on ribose and 2-deoxyribose moieties of nucleosides for nucleotide synthesis.

b) Silylation with SCTASi reagents:

As more highly selective blocking agents were required, silyl groups with different sterically crowded environments around the silicon atom were prepared. They generally fall into the following structural category:



where R = iso-propyl, tert-butyl

X = methyl, iso-propyl

(2X) = cyclo-tetramethylene

The replacement of methyl group by a bulkier alkyl group (e.g. t-butyl or i-propyl) on a silicon atom drastically reduces the hydrolysis tendency of the silicon-oxygen ether bond, and yet retains enough volatility of the derivative for GC analysis.

Quilliam et al (36), employing SCTASi-derivatization on nucleosides and steroids have found the protected molecules exhibit good "gas phase analysis" characteristics:-

- 1) The derivatization is fast, simple, with quantitative yield, and reaction goes to completion under mild conditions.
- 2) SCTASi-products are usually stable, and are amenable to direct chromatographic analysis.
- 3) Gas chromatographic and mass spectral properties of derivatized stereoisomers were improved compared to TMSi-derivatives in the case of steroids and nucleosides.

The following figure shows the most commonly used SCTASi groups:-

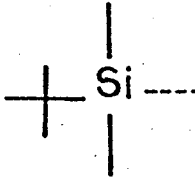
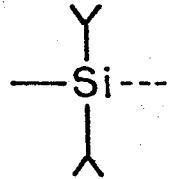
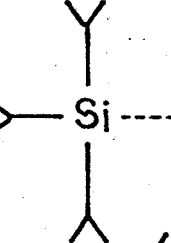
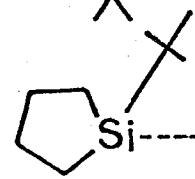
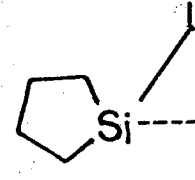
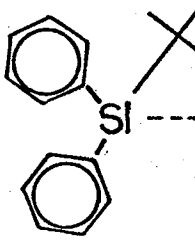
Structure	Protecting group	Abbreviation
	<u>tert</u> -butyldimethylsilyl	TBDMSi-
	methyl- <u>di</u> - <u>iso</u> -propylsilyl	MDIPSi-
	tri- <u>iso</u> -propylsilyl	TIPSi-
	cyclo-tetramethylene- <u>tert</u> -butylsilyl	TMIPSi-
	cyclo-tetramethylene- <u>iso</u> -propylsilyl	TMTBSi-
	di-phenyl- <u>tert</u> -butylsilyl	DPTBSi-

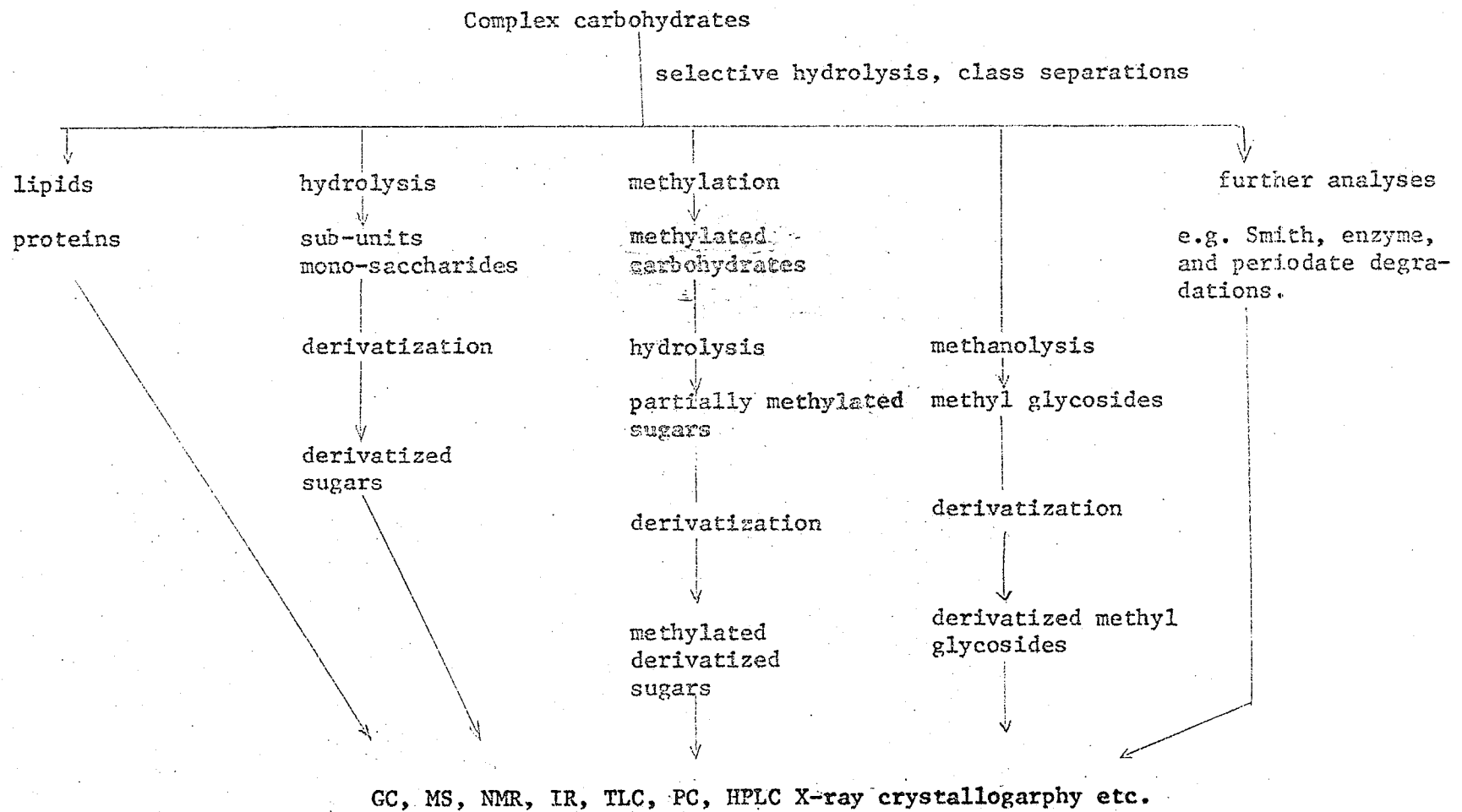
Figure: 3

Gas phase analytical chemistry of carbohydrates

Gas chromatography of carbohydrates was first performed in the form of methylated monosaccharides by A.G. McInnes and colleagues in 1958 (37). Since then, new chemical derivatization methods have been tried on carbohydrate samples in GC separations. The real breakthrough came about in 1963 when C.C. Sweeley and co-workers (38) gas-chromatographed trimethyl-silyl derivatives of sugars. The silylated sugars which were formed in quantitative yields possessed good chromatographic behavior and had good separation properties on different GC columns. Subsequently, trimethylsilylation became the most popular "protecting" procedure for saccharides, basic and acidic sugars, as well as for some complex molecules.

Gas phase analysis in carbohydrate structure determination

Structure analysis of carbohydrates includes identification of monomers as well as sequencing and "branching" of sub-units. A complete study of a complex carbohydrate structure is very involved and complicated; and it demands the most from analytical chemists. It may require many extra techniques such as NMR, IR, X-ray crystallography, etc. However, GC/MS has become the most popular technique for carbohydrate chemists in terms of versatility and reproducibility. One of the many general schemes for carbohydrate structure analysis is given as follows:-



Scheme: 3 General outline for carbohydrate structure determination

From all the possible information gathered from various steps, the structure and sequence of the monomers of the original molecule can be determined. (Scheme 3)

Whereas complex carbohydrates usually go through the outlined scheme, simple molecules in a sugar mixture can be directly derivatized and chromatographed. The usual volatile derivatives of monosaccharides are: 1) trimethylsilyl derivatives; 2) acetates; 3) methyl ethers; 4) butaneboronates; 5) trifluoroacetates; 6) benzoates; 7) benzyl ethers; 8) toluene-p-sulfonates and 9) propylidene acetals. Table 5 shows the "protected" derivatives as well as the common derivatizing reagents for sugars.

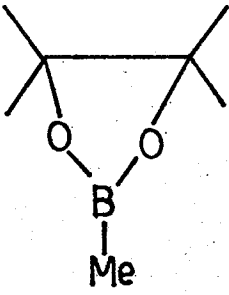
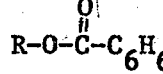
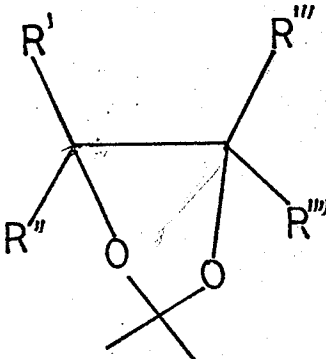
Some derivatives of neutral ketoses and aldoses present 2 major complications upon GC analysis. Firstly, the well-known multiple-peak formation in the chromatogram for derivatives from one sugar. Secondly, each peak, even when well-resolved, is very much similar to the other diastereomers structurally that absolute identification (e.g. mass spectrometry) is difficult. Silylation and methylation are known to cause such problems. (39)

One way to remove the troublesome anomeric carbon centre is to convert the carbonyl group into an oxime (38), a nitrile (39), a lactone (41) or an alditol by reduction.

Table 5 Derivatives from different protecting groups.

Reagents	Derivatives	Protected groups
trimethylsilyl-imidazole (TMSi-Im)	R-OSi(Me) ₃ trimethylsilyl ether R-C(=O)-O-Si(Me) ₃ trimethylsilyl ester R-N(H)-Si(Me) ₃ N-trimethylsilyl amine R'-N(R'')-Si(Me) ₃ N-trimethylsilyl amine R-N(Si(Me) ₃) ₂ N,N-di-trimethylsilyl amine	-OH -C(=O)OH -NH ₂ N-R'' -NH ₂
acetic anhydride	R-O-C(=O)-CH ₃ acetate R-NH-C(=O)-CH ₃ acetamide R'-NR''-C(=O)-CH ₃ acetamide	-OH -NH ₂ -NR''-H
N-(trifluoroacetyl)-imidazole	R-O-C(=O)-CF ₃ trifluoroacetate RNH-C(=O)-CF ₃ trifluoroacetamide	-OH -NH ₂

Table 5 (cont'd)

Reagents	Derivatives	Protected groups
methaneboronic acid		1,2 cis diol and 1,3 cis diol
methyl iodide/DMF	cyclic alkyl boronate	-OH
benzoyl chloride	R-O-Me methyl ether  benzoate	-OH
α -methyl hydroxyl-oxime	R-C(H)-N-OMe	-CHO
acetone/ H^+	$R'-C(R'')-N-OMe$ O-methyl oxime 	-CO
	isopropylidene acetal	 diol

EXPERIMENTALReagents

Reagent grade N,N-dimethyl formamide (DMF) was refluxed over calcium hydride, followed by distillation. The "centre cut" of the distillate was stored over Linde molecular sieves in a glass container. "Silylation grade" DMF was also obtained from Pierce Chemical Company, (Rockford, Ill.). Reagent grade pyridine (PYR) was distilled from p-toluenesulfonyl chloride, redistilled from calcium hydride, followed by storage over Linde molecular sieves. Tetrahydrofuran (THF) was first eluted through an activated alumina column and then refluxed with powdered lithium aluminum hydride, LiAlH₄. This distillate was stored and protected from light. Both PYR and THF were also purchased in the form of "silylation grade" from Pierce Chemical Co.

D-2-deoxyribose, D-ribose, D-xylose, D-galactose, D-glucose, D-mannose, D-fructose, and D-1,4-ribonolactone were purchased from SIGMA Chemical Company (St. Louis, Missouri). They were all "SIGMA Grade". All sugars were used without further purification, and were stored at 4°C inside a vacuum dessicator with phosphorus pentoxide as drying agent. Benzyl alcohol (Certified Grade) was obtained from Fisher Scientific Company (Fair Lawn, New Jersey). It was re-distilled at 205°C before use in the synthesis of β -D-benzyl-ribofuranoside. Imidazole was purchased from Eastman Kodak Company (Rochester, New York). N-alkanes ($n\text{-C}_{20}-n\text{-C}_{40}$) were purchased from Applied Science Labs (State College, Pennsylvania). Decafluorotriphenylphosphine was obtained from PCR Inc. (Gainesville, Florida). Pyrene, triphenylene and triphenylbenzene were kindly provided by M.A. Quilliam.

The reagents, N-trimethylsilyl imidazole (TMSiIm), Tri-sil Z (1.2M TMSiIm in PYR), bis-trimethylsilyltrifluoroactamide (with 1% trimethylsilylchloride) (BSTFA), acetylimidazole (AcIm), trifluoroacetylimidazole (TFAIm), and trifluoroacetic anhydride (TFAA) were purchased from Pierce Chemical Company (Rockford, Ill.). Reagent grade acetic anhydride (AcAnh) was distilled from phthalic anhydride, and stored in the dark before use.

tert-Butyldimethylchlorosilane (TBDMSiCl) m.p. 121-125°C was prepared according to the method of Sommer and Taylor (42); it was also purchased from Willow Brooks Labs (Waukesha, Wisconsin). cyclo-Tetramethylene-iso-propylchlorosilane (TMIPSiCl) b.p. 165-175°C., and cyclo-tetramethylene-tert-butyl-chlorosilane (TMTBSiCl), b.p. 182-184°C, were prepared by reacting iso-propyllithium and tert-butyllithium (Alpha Products, Ventron Corp., Danvers, Mass.), respectively, under N₂ with freshly distilled cyclo-tetramethylenedichlorosilane (PCR inc., Gainesville, Florida), b.p. 138-139°C, dissolved in pentane containing 10% THF, followed by fractional distillation. The TMIPSiCl and TMTBSiCl so prepared, were gift from M.A. Ouilliam.

Synthesis of β -D-benzyl-ribofuranoside

β -D-benzylribofuranoside was prepared according to the method of R. Barker (43). The preparation was performed as follows:-

5 gm of D-ribose was dissolved in 150 ml. of benzyl alcohol containing 1% of HCl. The solution was left overnight (16 hrs.) and protected from light. The reaction mixture was neutralized with sodium bicarbonate;

sodium chloride so precipitated was filtered. The residual benzyl alcohol was distilled off under vacuum. To the resulting product, ethyl acetate was added. The solution was filtered and β -D-benzyl ribofuranoside was concentrated in a rotary evaporator. After two recrystallizations from ethyl acetate, the crystalline β -D-benzyl ribofuranoside was used in GC derivatization and analysis. Yield = 47% and m.p. = 94-95°C.

Preparation of analytical derivatives

All derivatizations were carried out in dry "Reacti-vials" (typically 0.3 ml. screw-top, teflon-lined-septum capped borosilicate glass vials) purchased from Pierce Chemical Co. If reaction temperatures other than ambient were required, the vials could snugly fit into holes in an electrically heated aluminum block. Derivatizations were carried out with the following silylating reagents:-

A = 1M SCTASiCl and 2M imidazole in DMF

B = 1 M SCTASiCl and 2M imidazole in PYR

C = Tri-Sil Z (1.2 M TMSi·Im in PYR)

D = 1.2 M TBDMSi·Im in PYR

Persilylation

Two methods of persilylation were used:-

- 1) 20 micromoles of substrate was weighed into a vial; excess silylating reagents were put in all at the same time; and
- 2) 20 micromoles of substrate was first dissolved in a suitable solvent; silylating reagents were added in after 24 hours.

The reagent/substrate ratio was kept at 10 to 1. Vials were shaken manually for 5 minutes after they were mixed to ensure a homogeneous reaction mixture.

Partial silylation

Substrates (20 micromoles) were treated with silylation reagent/substrate ratios of 1:1, 2:1, 3:1, 4:1 etc. according to the number of "blocked" hydroxyl groups desired for the silylated substrate.

Mixed derivatization

Partially derivatized compounds were further derivatized using more powerful reagents. Usually, Tri-Sil Z, TFAIm and AcIm were used as "second" protecting reagents, because their action has been proven to be "fast". Excess reagents were used to ensure "complete" blocking of all polar groups before analysis.

Gas chromatography

Two different instruments were used in the study. The first one was a Hewlett-Packard 5711A isothermal gas chromatograph equipped with a dual flame ionization detector (FID). Glass inserts were employed to line the off-column injector block and also the detector, which were kept at 250°C and 300°C respectively. Glass columns A and B (1m x 2mm ID) were packed with 10% OV-1 and 10% OV-17, respectively, on 80/100 mesh Gas Chrom Q. Column C was glass (3.75m x 2.4mm ID) packed with 10% OV-1 on 80/100 mesh Gas Chrom Q. Nitrogen carrier gas flow rates were maintained at 30 ml/min. The oven was operated isothermally at temperatures which gave convenient retention times. Columns were routinely de-activated by injection of Silyl-8 (Pierce Chemical Co.). Also prior to packing the columns, the glass tubing was treated with 5% dimethyldichlorosilane/toluene, washed with methanol, and dried. There was a splitter arrangement before the detector. 20% of an effluent peak was channelled to the FID while the other 80% was allowed to emerge through a collector port. Detailed construction of the detector/collector/splitter arrangement has been described by Quilliam (44). Effluent from a chromatographic column could be condensed onto the inner walls of a glass capillary tube (1/16" OD x 0.01" ID) inserted into the collector port.

The second instrument was a Varian 1700 gas chromatograph equipped with a FID and interfaced to a Finnigan 1015 RF-quadrupole mass spectrometer. The glass-lined injector port and (FID + separator) were kept at 225°C and 250°C, respectively. Column D (10% OV-1, dimensions and materials identical to column A) was operated with He carrier gas flow

at 40 ml/min. The Varian model could be temperature-programmed, and also allowed GC/FID/MS operation.

The "solvent wash" technique was employed for sample introduction into the GC. A "plug" of solvent was first drawn into the barrel of a 10 μ l Hamilton glass syringe, followed by a small volume of air, and then the sample mixture. The sample was flushed with solvent onto the column through an injector port septum.

The Kovats' isothermal retention index (I) system was employed to record GC retention values. A special Hewlett-Packard 9100A calculator program enabled the conversion of GC retention times into Kovats' indices, against the retention times of a homologous series of *n*-alkanes co-injected with the sample. Separation factors (retention time ratios) of isomeric derivatives were also calculated for closely eluted peaks.

Each GC peak was checked for possible isomeric conversion and decomposition on the column by re-chromatographing the eluted peak and observing any changes in retention times.

Quantitative GC

1) Measurement of signals:

Peak areas of a gas chromatogram were measured by the method of "Height x Width at Half-height". Normal chromatographic peaks often approximate a triangle, and the area can be calculated by the triangle formula.

$A = H \times W_{1/2}$, where A = area of the peak, H = height of the peak and $W_{1/2}$ = width of peak at half-height. The method involves: 1) drawing of the baseline; 2) determining the height; and 3) measuring the height and the width at half height. For overlapping peaks, the outlines of each peak were extrapolated for the measurement of peak areas.

2) Conversion of GC signals to compositions of samples:

The method of "area normalization" was used to calculate the composition of isomeric or anomeric derivative mixtures, because all components had the same response to the FID. The percentage of X (a component in a sample) is calculated by,

$$\% \text{ of } X = \frac{100A_x}{A_x + A_y + A_z} = \frac{100A_x}{\sum_i^n A_i}$$

where A_x = area of peak X,

X, Y and Z are three components in the mixture,

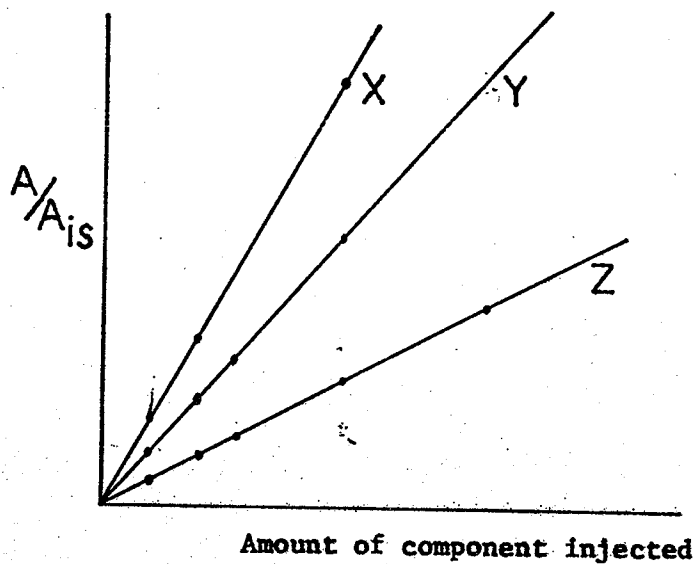
and A_i = area of a component peak i.

It should be noted that all components should be totally free from column adsorption as well as decomposition.

3) Internal standard:

For accurate measurement of a component in a GC sample, the "internal standard" method was used.

Several solutions containing the same amount of a standard and varying amounts of the component of interest were prepared. After chromatographing and obtaining peak areas, a calibration curve was obtained by plotting A/A_{is} versus amount of component injected.



A = peak area of a component,

A_{is} = peak area of internal standard,

X, Y, and Z are samples under study.

The ratios of slopes on the plot give relative molar response between components if A is in units of concentration in moles/litre.

Individual components of a mixture can be quantitated from the calibration graph.

Mass spectrometry

All mass spectral data were obtained from a Finnigan 1015 RF-quadrupole mass spectrometer. GC eluates were collected in glass capillary tubes and introduced into the mass spectrometer with a solid probe inlet. Alternatively, GC/MS was performed on samples through the Varian GC/Finnigan MS system. The ionization chamber was kept at 200°C and ionization energy was 70 eV. The instrument was tuned to "unit resolution" (44) which was very close to the arrangement proposed by Eichelberger (45).

Due to the transmission characteristics of the quadrupole mass analyser (46), correction for mass discrimination was made by multiplying the intensity of each ion by its mass before the spectrum was normalized.

For each mass spectrum, the following procedure was employed:-

The height of each ion with $m/z > 50$ was measured manually, and the values key-punched into IBM-computer cards. A computer program, after Lin (47), automatically performed mass-discrimination compensation and mass peak normalization. The resulting plot (relative abundance versus each m/z value) was also produced by the IBM computer.

GAS CHROMATOGRAPHY

Introduction

The separation and analysis of sugars in biological samples call for many different chromatographic techniques. Established methods include: paper chromatography (48); thin layer chromatography (49); ion-exchange chromatography (50); and recently, high performance liquid chromatography (HPLC) which makes use of different separation principles: adsorption; size exclusion and partition (normal and reverse phase) phenomena (51,52, 53). HPLC has the advantages of high resolution and reproducible results; and is steadily replacing some of the above-mentioned low-resolution techniques. A complementary and yet powerful method for sugar analysis is gas chromatography by which one can quantify a large number of components in a sample during one operation or "run".

The application of gas chromatography to sugar analysis is not without problems. A major one is that many monosaccharides give rise to multiple peaks. These anomeric and isomeric sugar peaks tend to overlap each other and sometimes identification of individual peaks can be laborious. Other investigators have tried to reduce this difficulty by derivatization of the anomeric carbon atom. Conversion of sugars into structures such as alditols (54), methyl oximes (55), lactones (41) and aldono-nitriles (40) was attempted so as to simplify derivatization and gas chromatographic operations.

In recent years, new types of derivative, SCTASi ethers, have been found to be applicable to steroids and nucleosides in both qualitative as well as quantitative GC analyses (36). It was also shown that SCTASi-ethers do have certain advantages over the moisture-sensitive TMSi-ethers. In order to extend the analytical usefulness of SCTASi-ethers to other types of biologically important molecules, the present investigation was undertaken. The main objective of this study, however, was to explore the GC/MS properties of fully and partially SCTASilylated sugars and related compounds so that conditions for quantitative analysis could be developed.

Retention Indices

Retention indices in this study are reported according to the Kovats' system (57). Briefly, I_b^a , which denotes Kovats' retention index at a °C and on liquid stationary phase, b, can be defined as,

$$I_b^a = 100(N) = \frac{\log t'_{r(s)} - \log t'_{r(N)}}{\log t'_{r(N+2)} - \log t'_{r(N)}}$$

where N = number of carbon atoms of an even-number-carbon n-alkane standard,

$t'_{r(s)}$ = adjusted retention time for sample, s;

$t'_{r(N)}$ = adjusted retention time for n-alkane, N;

$t'_{r(N+2)}$ = adjusted retention time for an n-alkane with N+2 carbon atoms;

and $\log t'_{r(N)} < \log t'_{r(s)} < \log t'_{r(N+2)}$.

Since $\log t'_{r^*} \propto I$ or N ; I_b^a can be obtained from a linear plot of $\log t'_{r(N)}$ vs. N by interpolation. Usually, the value of I_b^a for a sample is more accurately determined from such a calibration graph than from the above equation. The Kovats' retention index (isothermal) was found to be relatively reproducible and free from operating-condition differences among laboratories. Also, physical (58) and structural properties (59) of separated sample components could be correlated with respect to their Kovats' indices. The analogous programmed-temperature methylene unit (MU) indices ($I = 100\text{MU}$) have been used previously for various compounds including TMSi-derivatives of sugars (60).

GC system

All GC analyses were carried out on columns packed with 10% OV-1 (a non-polar methyl silicone liquid phase), coated onto Gas Chrom Q support. An OV-17 liquid phase column was used initially in the study; but was found to be unable to give reasonable isomeric separation for TBDMSi-sugar anomers due to low number of theoretical plates (around 750 to 1,000). OV-17 was not pursued further in this study.

OV-1 is able to withstand high temperatures (up to 300° C.). Some SCTASI-sugars, which may contain up to 5 silyl groups per molecule, were eluted around $I = 3000$. Other liquid phase columns such as EGS (ethylene-glycolsuccinate) and phenyl silicones, though useful for TMSi-derivatives, are not stable enough at high temperature for SCTASI-sugar analysis.

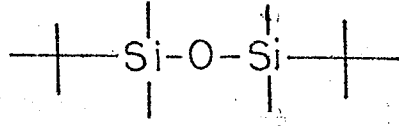
It must be noted that 10% liquid phase columns are only "semi-analytical" to suit this project where both GC analysis as well as peak collection for mass spectrometry were required. The typical numbers of

of theoretical plates for columns used in this study were estimated to be about 1,000 to 2,000, depending on individual samples.

Solvent system

Both N,N-dimethyl formamide (DMF) and pyridine (PYR) are excellent solvents as well as reaction media for silylation of polyhydroxy compounds. While pyridine was not recommended for low-temperature GC (below 200 C), because of its "tailing" characteristic, nonetheless it has great solubilizing power for carbohydrates as well as for the derivatized products. It is also a hydrogen chloride receptor in organochlorosilane reactions. In this study, due to the bulkiness of SCTASi groups and the polyhydroxy nature of sugars, GC was necessarily carried out at much higher temperatures, at which the pyridine "tail" no longer obscured sample peaks (61).

N,N-dimethylformamide suffered one disadvantage: a biphasic reaction mixture was formed when silylation was contaminated even with only a trace of moisture. The upper layer was found to consist of mainly di-tert-butyltetramethyl-disiloxane in which silylated compounds are highly soluble. Analogous products were formed when Ellis (62) performed trimethylsilylation with DMF as solvent. The structure of di-tert-butyltetramethyldisiloxane is shown as follows:-



The identity of di-tert-butyltetramethyldisiloxane was established when a temperature-programmed GC run was performed on the upper reaction-layer (figure 4a), and the GC peak subsequently analysed by mass spectrometry (figure 4b).

It was shown by C.C. Sweeley (28) that when crystalline monosaccharides were trimethylsilylated, the rate of reaction was fast compared with mutarotation; hence essentially one derivatized product was formed for each sugar. On the other hand, when monosaccharides were first dissolved and refluxed and allowed to equilibrate in pyridine, peaks corresponding to the isomeric proportions were obtained in the gas chromatogram.

The derivatizations of monosaccharides were thus carried out in 2 ways:-

- 1) Crystalline sugars were reacted with silylating reagents directly; or
- 2) Crystalline sugars were dissolved and heated to 50° C for 24 hrs. before second derivatization.

Reaction products were analysed at various time intervals until there was no change in the chromatographic peak-profiles. In the first method, it was found that SCTASI-ethers were not formed "instantaneously" and considerable anomeric peaks were always observed. The mutarotation rate was obviously competitive with the silylation rate. Variable proportions of anomeric sugar peaks were observed over a 24-hour-period of the silylation reaction. On the other hand, sugars equilibrated at 50° C in pyridine for 24 hrs. always showed a reproducible pattern of anomeric peaks after 20 min. of silylation reaction.

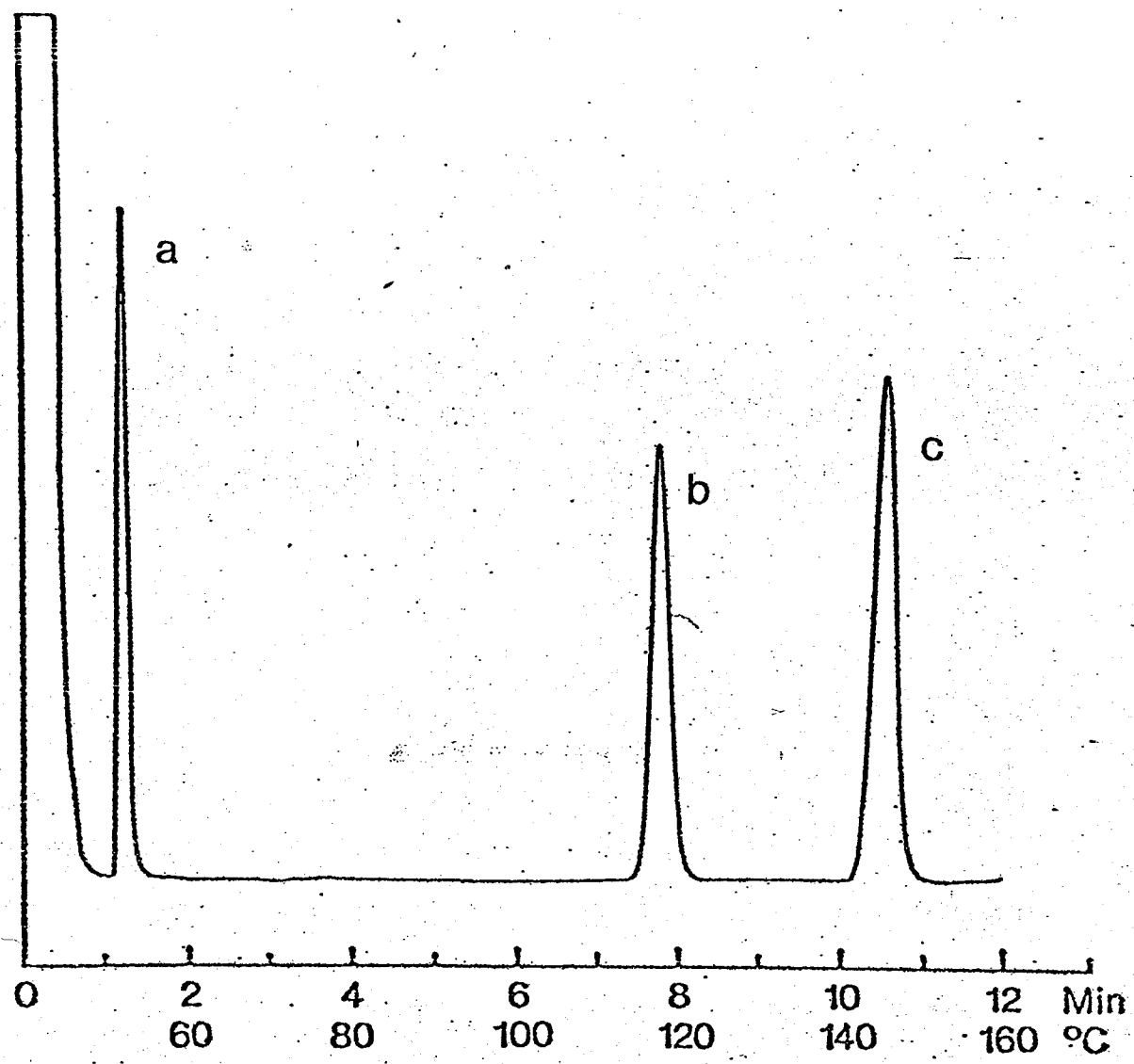


Figure 4a

Gas chromatogram of the upper layer of a silylated sugar reaction mixture when DMF was used as a solvent. Peak identities: a = tert-butyldimethylsilyl chloride; b = di-tert-butyltetramethyl-disiloxane; and c = tert-butyldimethylsilylimidazole.

Temperature programming started from 40° C at 10° C/min. increase in temp.

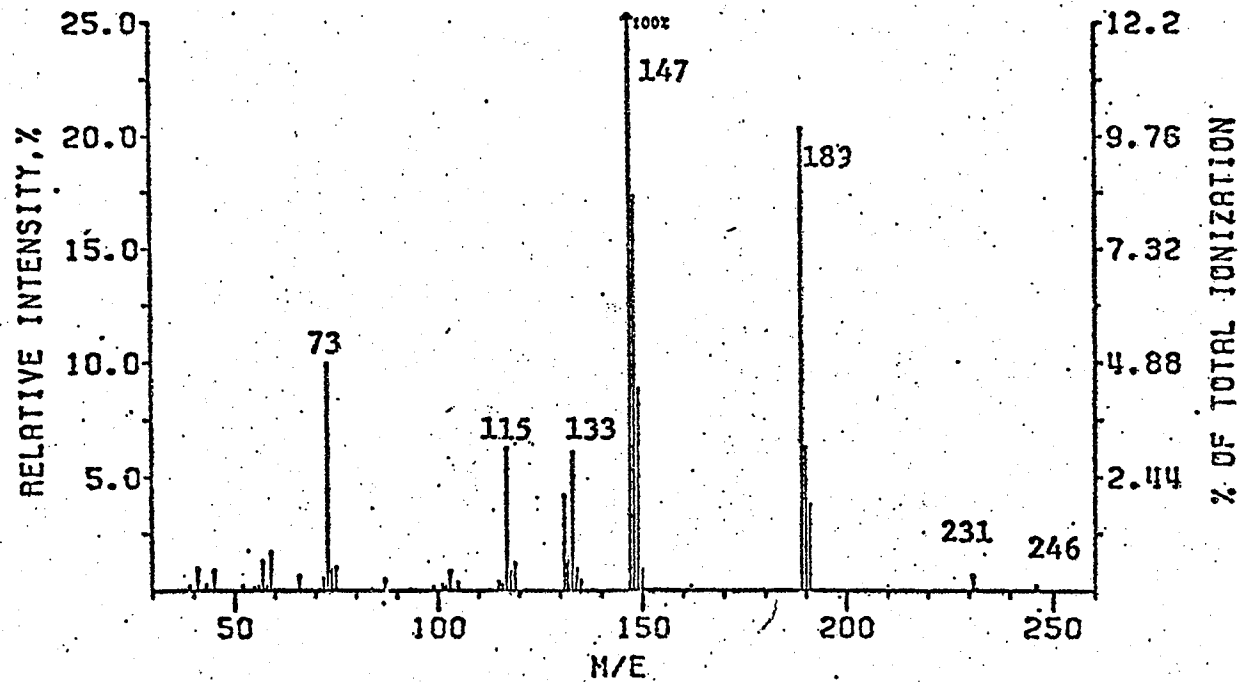


Figure: 4b Mass spectrum of di-*tert*-butyltetramethyldisiloxane. Peak identification:

73 = Me_3Si^+ ; 115 = $t\text{-BuMe}_2\text{Si}^+$; 147 = $\text{Me}_3\text{SiOSiMe}_2^+$; 189 = $t\text{-BuMe}_2\text{SiOSiMe}_2^+$;
231 = M-CH_3^+ ; and 246 = M^+ .

Silylated monosaccharides

In the case of trimethylsilylation of sugars, it was found that reaction was almost instantaneous and completed within 5 minutes upon manual shaking. Both methods of derivatization, namely, 1 and 2, gave identical TMSi-sugar chromatogram profiles because TMSi-reagents are extremely fast in action.

No separations of TMSi-sugar anomers were observed, except in the case of fructose, which formed two peaks. I values of TMSi-sugars have not been reported in the literature. Table 6 shows the I values measured in this work. Partial TMSi-sugars were not observed when insufficient TMSi-reagents were used to silylate sugars. It is believed that heat-induced reaction occurred on the column with the formation of a small peak due to the per-silylated sugar, and the rest of the sugar molecules decomposed or absorbed onto the column. Immediate injection of Silyl-8, however, did not elute any "ghost" peaks.

While partial TMSi-sugars were not chromatographed at all, partial TBDMSi-sugars were found to be volatile enough to afford some separation on GC. Examples are shown in figures 5-8, with results summarized in Table 7. The number of silyl groups on each silylated species was confirmed by mass spectrometry as well as by comparing GC retention times. Usually they have lower I values than corresponding fully silylated compounds. Multiple peaks were observed for partially silylated sugars and their presence might be useful in "finger-printing" or confirming a particular sugar in a sample mixture. Though the number of silyl groups on a molecule could be obtained from mass spectral data, the exact positions of substituents were difficult to assign. The number of possible cyclic struc-

tures for a "simple" partially silylated molecule, such as bis-O-TBDMSi-D-2-deoxyribose, can amount to 6, as in fig. 8. Thus, no attempts have been made to assign positions of substituent groups on the partially substituted sugars.

It is interesting to note that the replacement of TMSi-group by TBDMSi moieties on sugar hydroxyl groups greatly increased the I values of derivatized sugars; better separation of anomers was also observed. (Table 8) Similar results have been reported for SCTASi-steroids and SCTASi-nucleosides (44). The increase in bulkiness on the protecting group modifies the derivatives to such an extent that improved separation over TMSi-analogues on a low resolution column results. Table 9 gives a comparison of GC data for silylated sugars from various references.

Table 6. GC retention data of per-O-TMSi-sugars

Compound Number ^a	Compound Name ^a	GC Data ^(b) I_{OV-1}^{180}	I_{OV-1}^{210} (α) Separation factor
I aaa	tris-O-TMSi-D-2-deoxyribose	1496	
II aaaa	tetrakis-O-TMSi-D-ribose	1681	
IIIaaaa	tetrakis-O-TMSi-D-xylose	1735	
IV aaaaa	pentakis-O-TMSi-D-glucose		1854
V aaaaa	pentakis-O-TMSi-D-galactose		1862
VI aaaaa	pentakis-O-TMSi-D-mannose		1953
VII aaaaa	pentakis-O-TMSi-D-fructose		1.17 1865 1931

^a Refer to nomenclature Scheme for structures and numbering;

^b Kovats' retention indices, and α = separation factor (always ≥ 1).

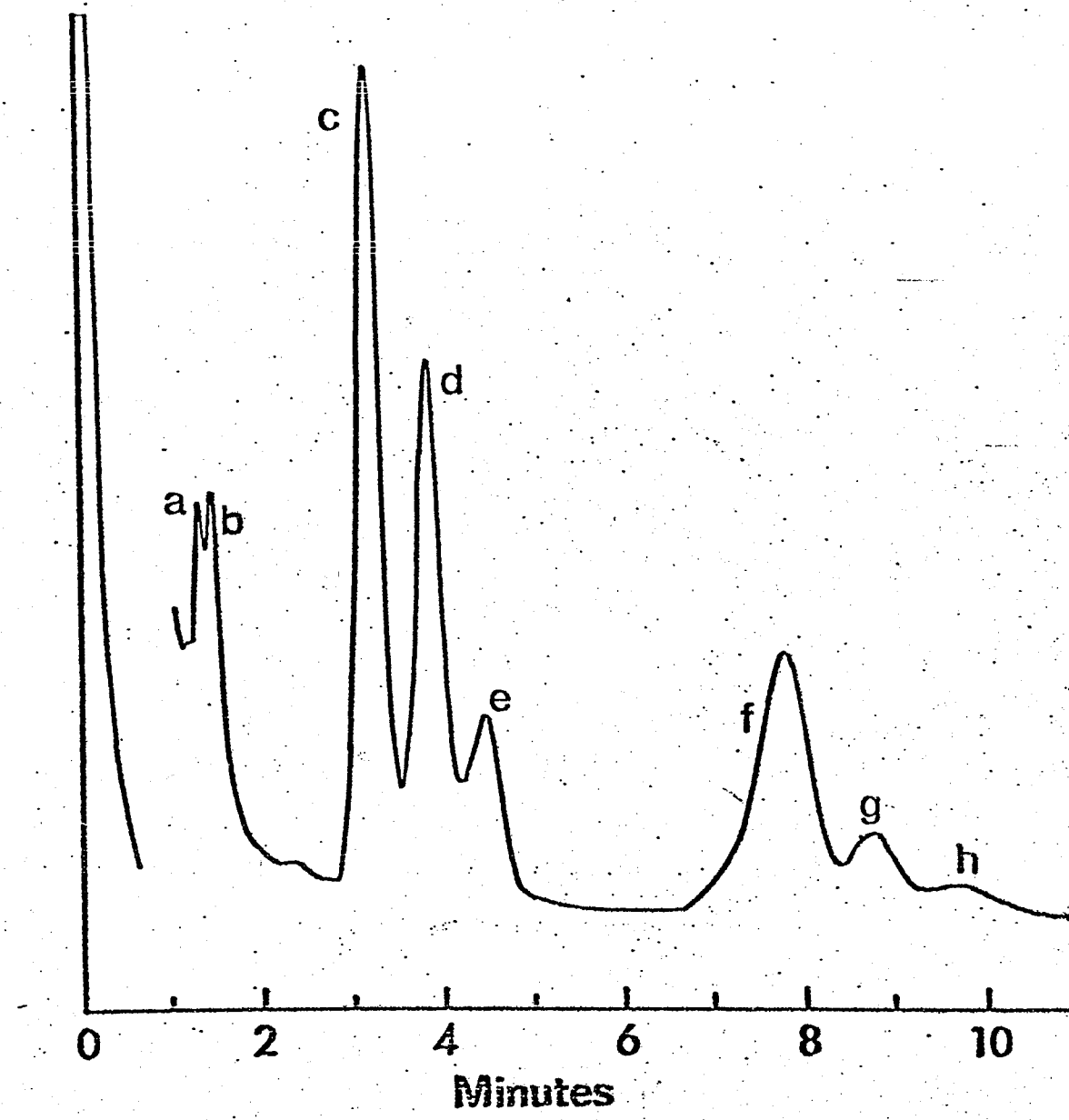


Figure: 5 Gas chromatogram of silylated D-ribose : a and b = mono-O-TBDMSi-D-ribose; c and d = bis-O-TBDMSi-D-ribose; e, f, g, and h = tris-O-TBDMSi-D-ribose. All assignments were confirmed by mass spectrometry.
Conditions: Column A (OV-1, 10%; 1m x 2mm ID), 210°C,
 N_2 flow = 30 ml/min.

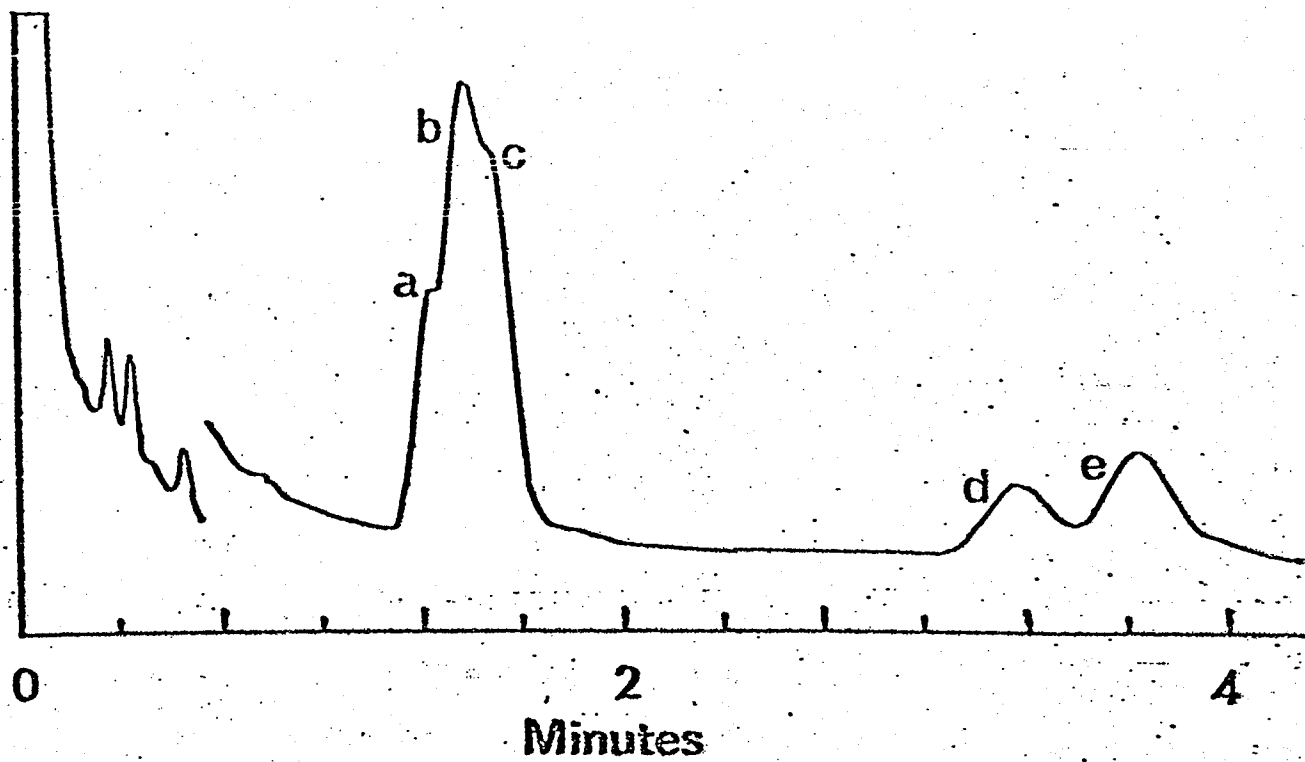


Figure: 6 Gas chromatogram of TBDMSi-D-2-deoxyribose.

a, b and c = bis-O-TBDMSi-D-2-deoxyriboses; d and e = tris-O-TBDMSi-D-2-deoxyribose.

Conditions: Column A (OV-1, 10%; 1mx 2mm. ID) 210° C.

N₂ flow = 30 ml./min.

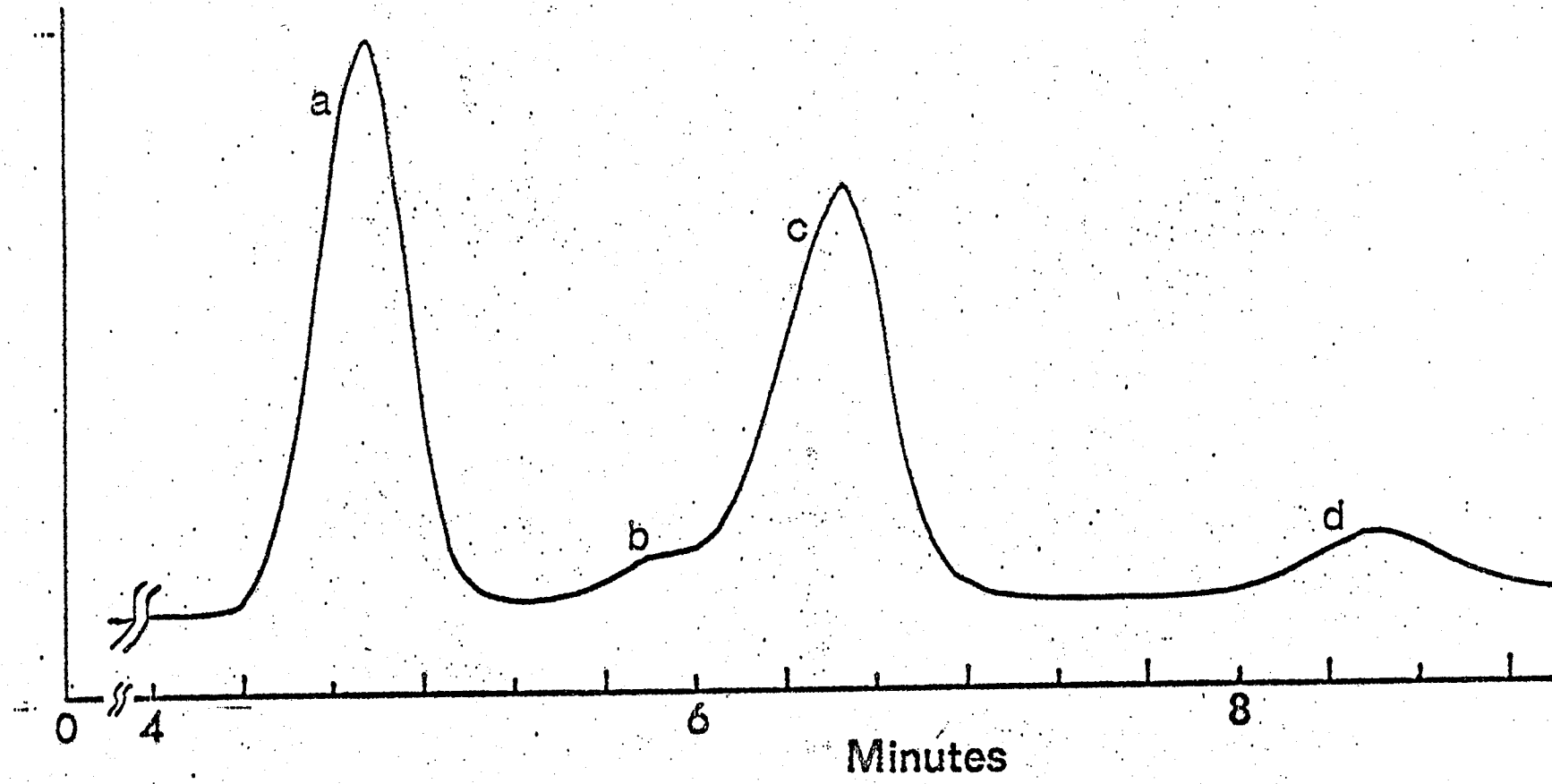


Figure: 7 Gas chromatogram of silylated D-ribose: a, b,c and d are all tetrakis-O-TBDMSi-D-ribose derivatives.

Conditions: Column A (OV-1, 10%; 1m x 2mm ID), 280°C, N₂ flow = 30 ml/min.

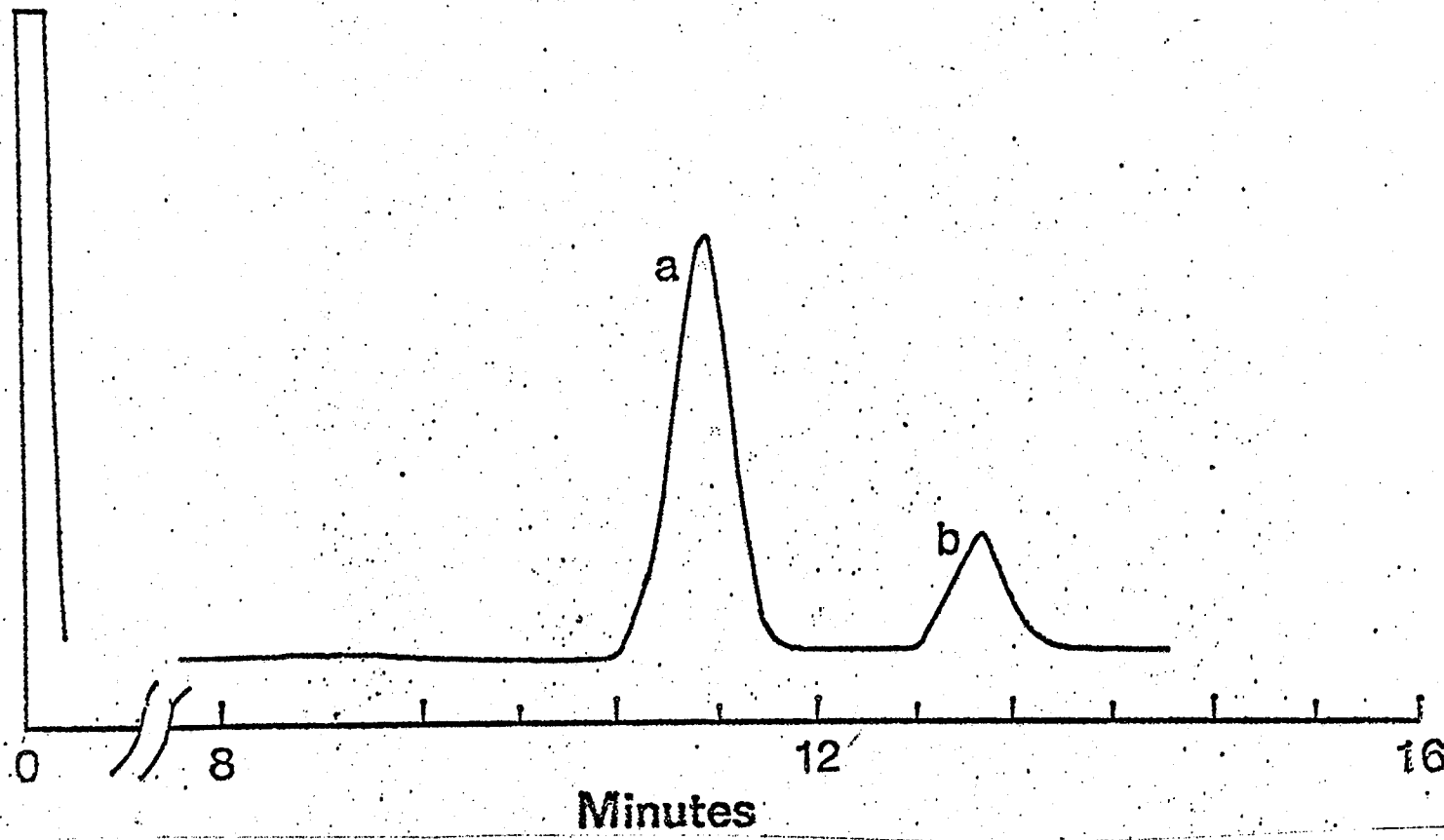


Figure: 8 Gas chromatogram of TBDMSi-D-galactose.

a and b = pentakis-O-D-galactose. Conditions: (Column A, 10% OV-1; 1m x 2mm ID)
240°C, N₂ flow rate = 30 ml/min.

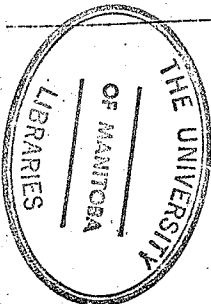
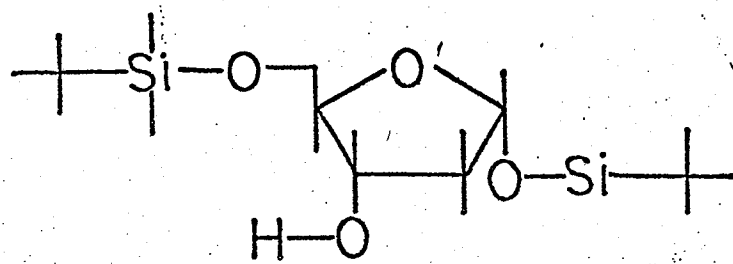


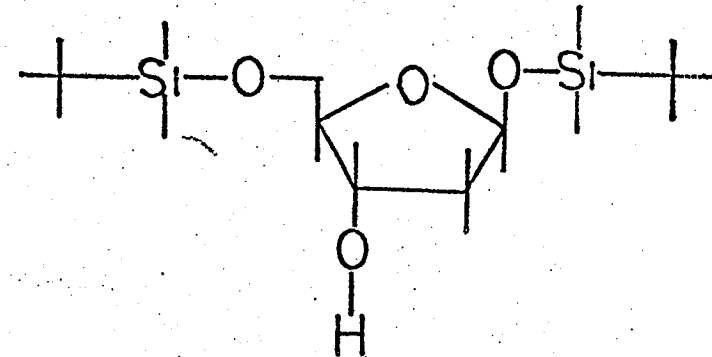
Table 7 GC retention data for partial-O-TBDMSi-sugars

^a Compound Number	^a Compound Name	GC Data ^b I_{OV-1}^{210} I_{OV-1}^{240}	Separation factor
I (bb)	bis-O-TBDMSi-D-2-deoxyribose	1802 1850	1.09
II (bbb)	tris-O-TBDMSi-D-ribose	2240 2271	1.08
III (bbb)	tris-O-TBDMSi-D-xylose	2246 2270	1.07
IV (bbb)	tris-O-TBDMSi-O-glucose	2602	
IV (bbbb)	tetrakis-O-TBDMSi-D-glucose	2647 2674	1.07
V (bbbb)	tetrakis-O-TBDMSi-D-galactose	2712	
VI (bbb)	tris-O-TBDMSi-D-mannose	2611	
VI (bbbb)	tetrakis-O-TBDMSi-D-mannose	2688 2742	1.15
VIII (bbbb)	tetrakis-O-TBDMSi-D-fructose	2711	

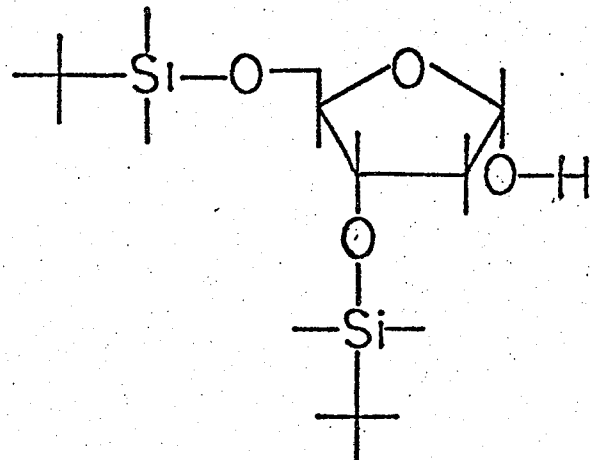
^a refer to Nomenclature Scheme,^b I = Kovats' retention indices α = separation factor



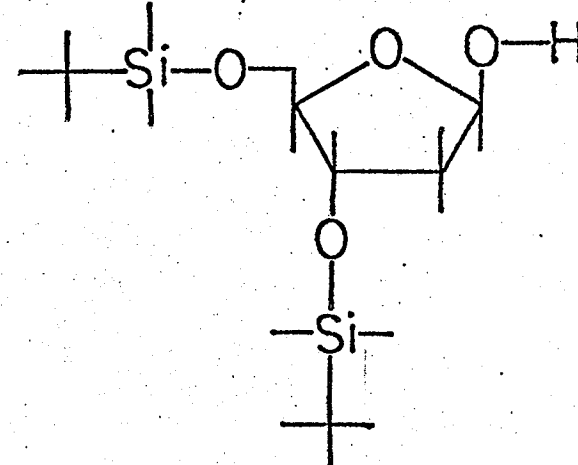
Bis-O-1,5-TBDMSi- α -D-2-deoxyribose



Bis-O-1,5-TBDMSi- β -D-2-deoxyribose

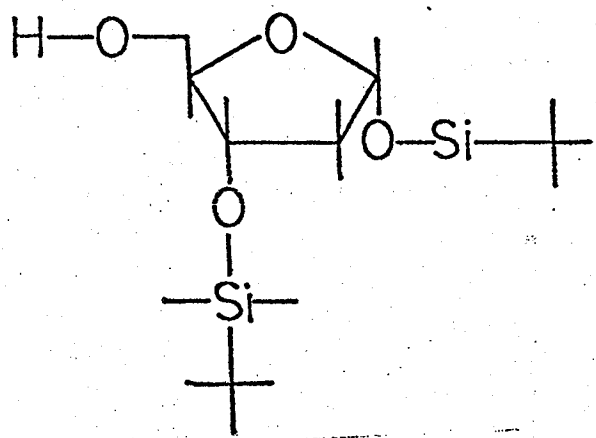


Bis-O-3,5-TBDMSi- α -D-2-deoxyribose

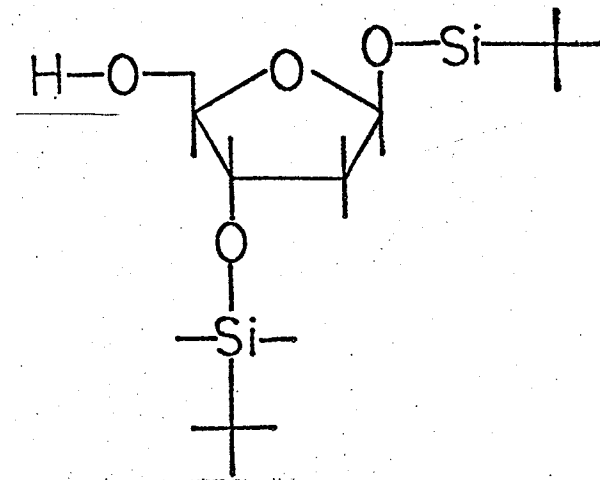


Bis-O-3,5-TBDMSi- β -D-2-deoxyribose

Figure: 9 Possible structures of bis-O-TBDMSi-2-deoxyribose (cont'd)



Bis-O-1,3-TBDMSi- α -D-2-deoxyribose



Bis-O-1,3-TBDMSi- β -D-2-deoxyribose

Figure 9 (cont'd) Possible structures of bis-O-TBDMSi-2-deoxyribose

Table 8 GC retention data for per-O-TBDMSi-sugars

Compound Number ^a	Compound Name ^a	b I ²¹⁰ OV-1	b I ²⁴⁰ OV-1	Separation factor
I _{bbb}	tris-O-TBDMSi-D-2-deoxyribose	2092 2152		1.09
II _{bbbb}	tetrakis-O-TBDMSi-D-ribose	2454 2512 2544 2624		1.22 1.11 1.28
III _{bbbbb}	tetrakis-O-TBDMSi-D-xylose	2460 2500		1.15
IV _{bbbbb}	pentakis-O-TBDMSi-D-glucose		2807 2925	1.44
V _{bbbbb}	pentakis-O-TBDMSi-D-galactose		2868 2895	1.13
VI _{bbbbb}	pentakis-O-TBDMSi-D-mannose		2900 2936	1.10
VII _{bbbbb}	pentakis-O-TBDMSi-D-fructose		2888 2940	1.34

^arefer to nomenclature scheme for numbering and structures; ^bKovats' retention indices.

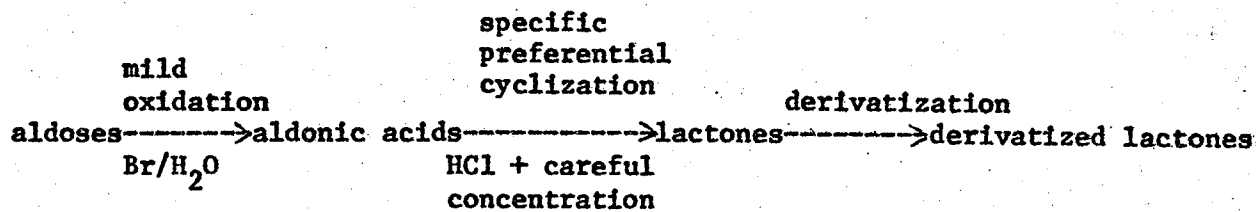
Table 9 Comparisons between studies of silylated sugars

Sugars	Number of resolved GC peaks			
	TMSi derivatives (63)	TMSi derivatives (38)	TMSi derivatives this study	TBDMSi derivatives this study
D-2-deoxyribose	-	1	1	2
D-ribose	4	3	1	4
D-xylose	2	3	1	2
D-glucose	2	2	1	2
D-galactose	3	3	1	2
D-mannose	2	2	1	2
D-fructose	4	1	2	2
Column liq. phase	SE-30 OV-101	SE-52	OV-1	OV-1
Number of theoretical plates per column	capillary col. 70,000	packed col. no. of plates not stated	packed col. 1,000-2,000	packed col. 1,000 to 2,000

Abbreviation: liq. = liquid; - = not done

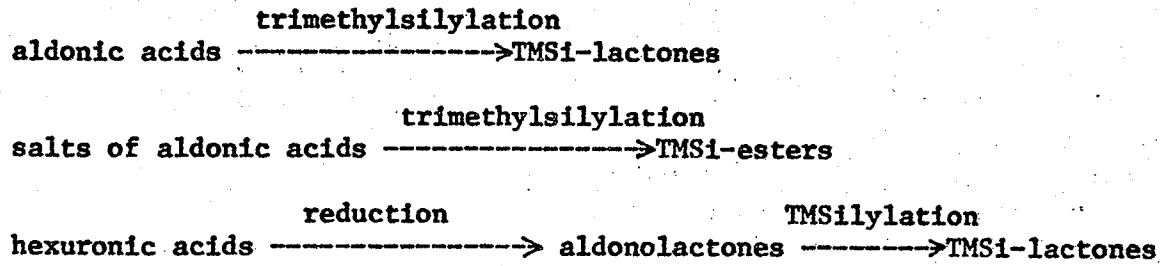
1,4-Ribonolactone

Another way of avoiding the problem of anomeric and configurational isomerism in GC analysis of monosaccharides is to convert aldoses into aldonic acids which cyclize preferentially into 1,4- and/or 1,3-lactones. Further derivatization of resulting lactones gives a single peak in the gas chromatogram for each sugar. The general scheme runs as follows:



Scheme: 4 ref(60)

Together with neutral saccharides, aldonic acids and salts of aldonic acids can also be simultaneously examined:-



Scheme 5 ref(41)

1,4-ribonolactone was selected as a prototype of sugar lactones in this study for the following reasons: 1) it is relatively simple in structure (3 hydroxyl groups); 2) it is readily available in a highly purified form; and 3) it assumes a cyclic structure in most solvent systems. GC retention data for 1,4-ribonolactone derivatives are given in Table 10.

Excess SCTASi reagents on 1,4-ribonolactone gave one per-silylated product (as detected by GC and mass spectrometry). Reaction times for reagents A and B were almost identical. For TBDMSCl/imidazole/solvent, a quantitative yield of persilylated product was formed in less than 30 minutes at 50°C. No spurious peak due to the straight chain ribonic acid derivative could be detected. As in the case of sugars, partial SCTASi-1,4-ribonolactones were also chromatographed (figs 10-12).

Mixed derivatization using TFAIm and Ac₂O was not successful because 1,4-ribonolactone was labile in the acidic by products.

Table 10(GC retention data of silylated 1,4-ribonolactone)

Compound Number ^a	Compound Name ^a	I_{OV-1}^{180}	I_{OV-1}^{210}	I_{OV-1}^{240}	I_{OV-1}^{280}	Separation factor
IX _(b)	mono-O-TBDMSi-1,4-ribonolactone	1696 1722 1805				1.11 1.35
IX _(bb)	bis-O-TBDMSi-1,4-ribonolactone	2003 2053 2078				1.21 1.07
IX _{bbb}	tris-O-TBDMSi-1,4-ribonolactone		2321			
IX _(d)	mono-O-TMTBSi-1,4-ribonolactone	2026 2103				1.26
IX _(dd)	bis-O-TMTBSi-1,4-ribonolactone			2518 2564 2608		1.65 1.15
IX _{ddd}	tris-O-TMTBSi-1,4-ribonolactone			3170		
IX _(aaa)	tris-O-TMSi-1,4-ribonolactone	1700				
IX _{ccc}	tris-O-TMIPSi-1,4-ribonolactone			3045		
IX _{eee}	tris-O-TMHSi-1,4-ribonolactone			3560		
IX _(aab)	bis-O-TMSi-mono-O-TBDMSi-1,4-ribonolactone	1902				
IX _(abb)	mono-O-TMSi-bis-O-TBDMSi-1,4-ribonolactone	2120				

^a: refer to nomenclature scheme for numbering and structures; ^b: I = Kovats' retention indices.

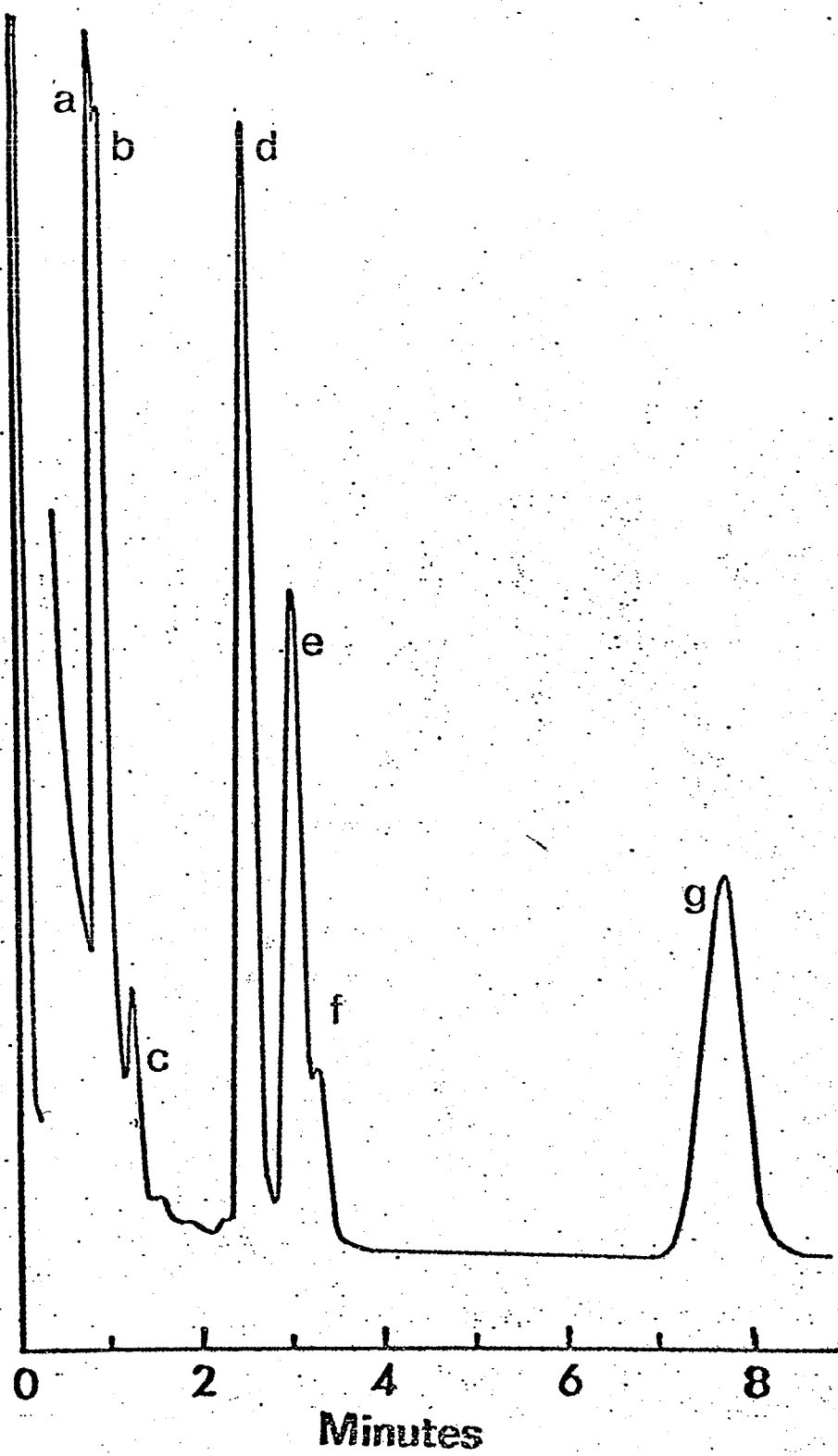


Figure 10 Gas chromatogram of silylated 1,4 ribonolactones.

a, b and c = mono-O-TBDMSi-1,4 ribonolactones. d, e, and f = bis-O-TBDMSi-1,4-ribonolactones. g = tris-O-TBDMSi-1,4ribonolactone.

Conditions: Column A (OV-1, 10%; 1m x 2mm ID) 210°C, N₂ flow = 30 ml/min.

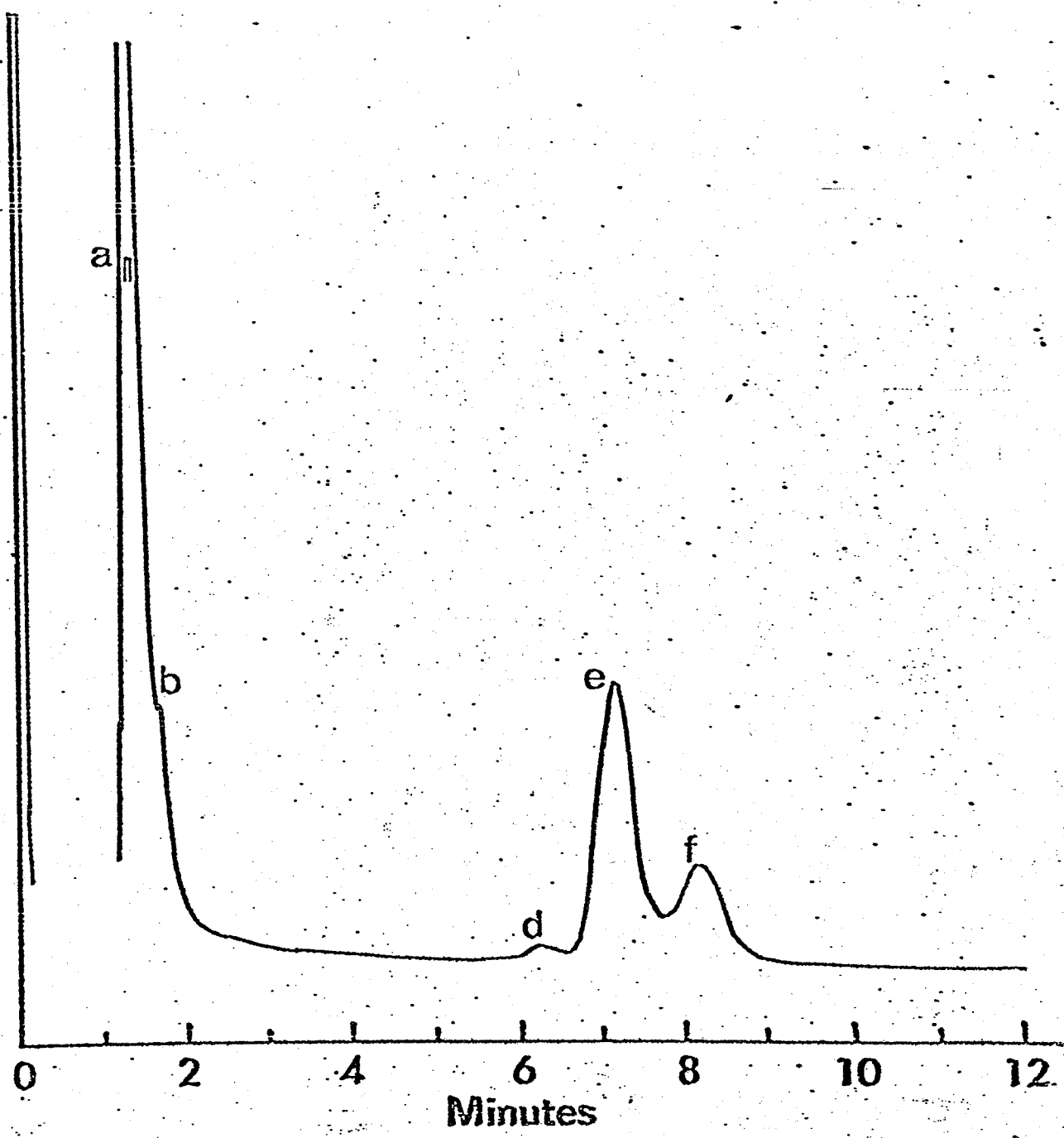


Figure: 11 Gas chromatogram of partially silylated 1,4-ribonolactones.

a, b = mono-0-TMTBSi-1,4 ribonolactones; d,e and f = bis-0-TMTBSi-1,4 ribonolactones.

Conditions: column A (OV-1, 10%; 1m x 2mm, ID) 210°C, N₂ flow = 30 ml/min.

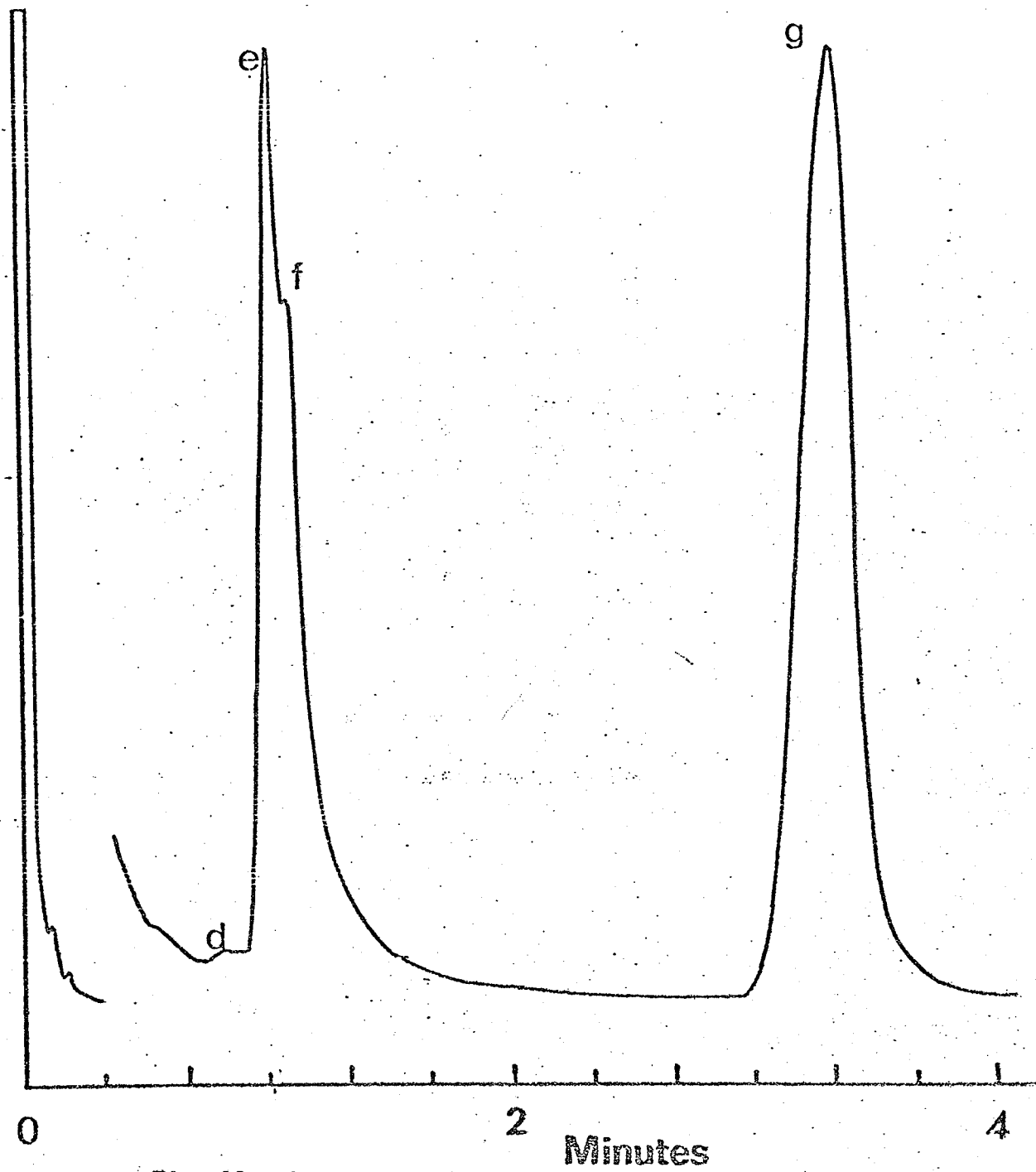


Fig. 12

Gas chromatogram of O-TMTBSi-1,4-ribonolactones. Peak identities: d, e and f = bis-O-TMTBSi-1,4-ribonolactones; g = tris-O-TMTBSi-1,4-ribonolactone.
Conditions: Column A (OV-1, 1m x 2mm ID) 280°C, N₂ flow = 30 ml/min.

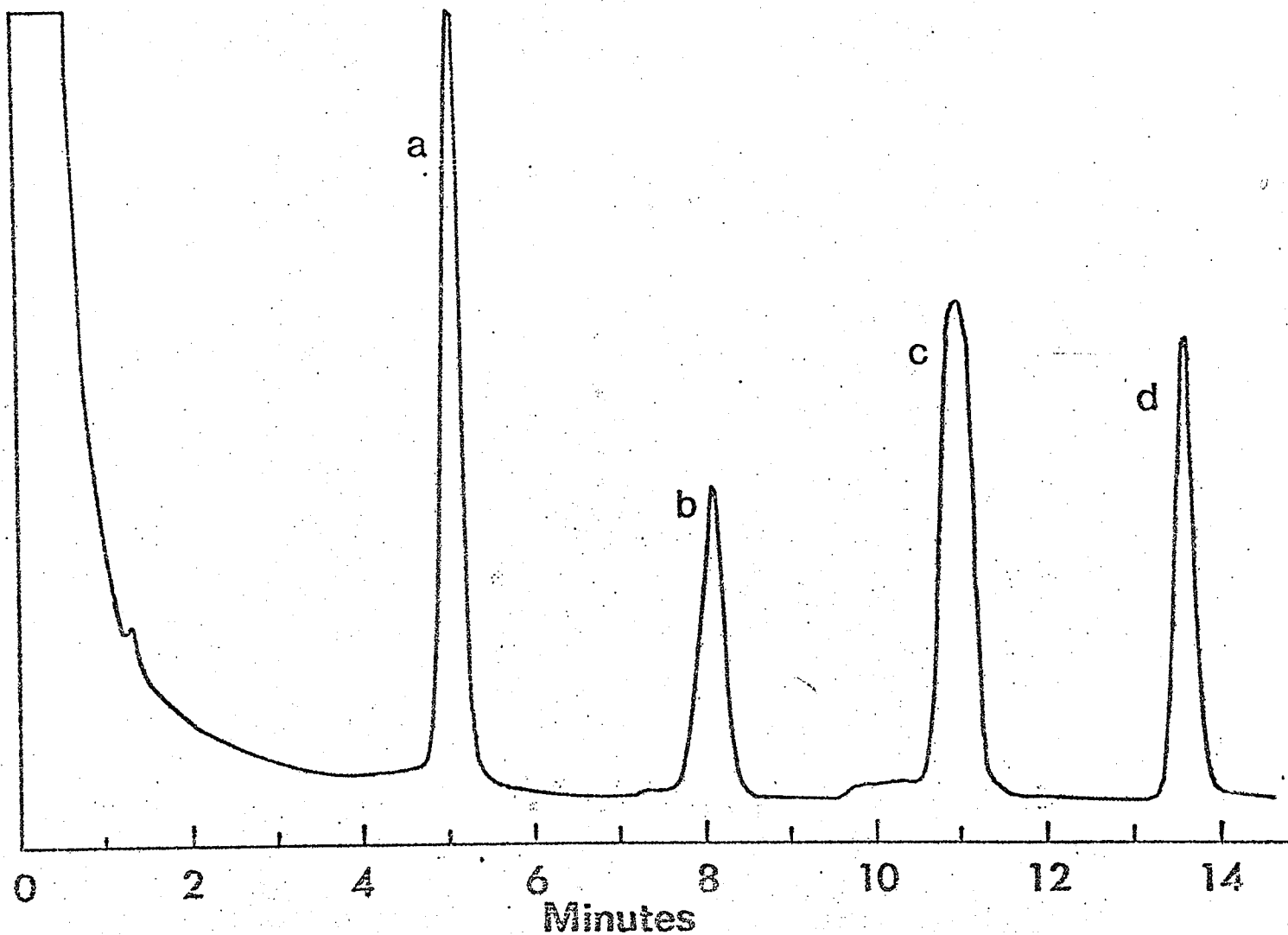


Figure: 13 Gas chromatogram of mixed TMSi/TBDMSi derivatives of 1,4-ribonolactone. Peak identification: a = tris-O-TMSi-1,4-ribonolactone; b = bis-O-TMSi-mono-O-TBDMSi-1,4-ribonolactone(s); c = mono-O-TMSi-bis-O-TBDMSi-1,4-ribonolactone(s); and d = tris-O-TBDMSi-1,4-ribonolactone. Conditions: Column A (OV-1, 10%; 1mx2mm ID), N₂ flow = 30 ml/min. Temp. program: 150 to 300°C, 10 degrees/min.

SCTASi- β -D-benzylribofuranosides

Further studies on the SCTASi-reagents were carried out on a synthesized sample of β -D-benzylribofuranoside. In carbohydrate analysis, complex molecules are often methanolysed and the resulting methyl glycosides separated to give structural information. This approach has been very popular in glycolipid and glycoprotein studies, because fatty acids are simultaneously obtained as their methyl esters and aminodeoxyhexoside bonds are more readily methanolysed than hydrolysed. Also, neuraminic acid is more stable as its methyl ester.

β -D-benzylribofuranoside possesses a UV absorbing benzene ring and a simple definite structure (three hydroxyls and a β -furanoid conformation). The UV absorbing properties are also compatible with TLC visualization and HPLC detection and quantitation. With the characteristic O-benzyl group on the anomeric carbon atom, mass spectral interpretation should be greatly facilitated.

GC data for derivatized β -D-benzylribofuranosides are given in Table 11, the chromatograms being shown in figs. 14-20.

Table 11 . GC retention data for derivatives of β -D-benzyl ribofuranoside

Compound Number ^a	Compound Name ^a	t_{R}^{210} OV-1	t_{R}^{240} OV-1	t_{R}^{280} OV-1	Separation faxtor
VIII (b)	mono-O-TBDMSi- β -D-benzyl-ribofuranoside	2241 2273 2337			1.09 1.20
VIII (bb)	bis-O-TBDMSi- β -D-benzyl-ribofuranoside		2521 2569 2604		1.15 1.10
VIII (d)	mono-O-TMTBSi- β -benzyl-ribofuranoside		2510 2546 2629		1.12 1.29
VIII (dd)	bis-O-TMTBSi- β -D-benzyl-ribofuranoside			3058 3159	1.26
VIII _{bbb}	tris-O-TBDMSi- β -D-benzyl-ribofuranoside			2824	
VIII _{ccc}	tris-O-TMIPSi- β -D-benzyl-ribofuranoside			3454	
VIII _{ddd}	tris-O-TMTBSi- β -D-benzyl-ribofuranoside			3578	
VIII _{aaa}	tris-O-TMSi- β -D-benzyl-ribofuranoside	2140			
VIII _{qqq}	tris-O-Ac- β -D-benzyl-ribofuranoside	2272			

Table 11 (cont'd) GC retention data for derivatives of β -D-benzyl ribofuranoside

Compound Number ^a	Compound Name ^a	I ₁₈₀ ^b OV-1	I ₂₁₀ ^b OV-1	I ₂₄₀ ^b OV-1	Separation factor
VIII _(aab)	bis-O-TMSi-mono-O-TBDMSi- β -D-benzyl-ribofuranoside	2371			
VIII _(abb)	mono-O-TMSi-bis-O-TBDMSi- β -D benzyl-ribofuranoside	2600			
VIII _(qqb)	bis-O-Ac-mono-O-TBDMSi- β -D-benzyl-ribofuranoside	2395 2432 2482			1.1 1.16
VIII _(qbb)	mono-O-Ac-bis-O-TBDMSi- β -D-benzyl-ribofuranoside	2591 2650 2697			1.16 1.14
VIII _(ppb)	bis-O-TFA-mono-O-TBDMSi- β -D-benzyl-ribofuranoside	1971 2043 2090			1.29 1.19
VIII _(pbb)	mono-O-TFA-bis-O-TBDMSi- β -D-benzyl-ribofuranoside	2392 2411 2464			1.07 1.21
VIII _{ppp}	tris-O-TFA- β -D-benzyl-ribofuranoside	1668			

a: refer to nomenclature scheme for numbering and structures; b: I = Kovats' retention indices.

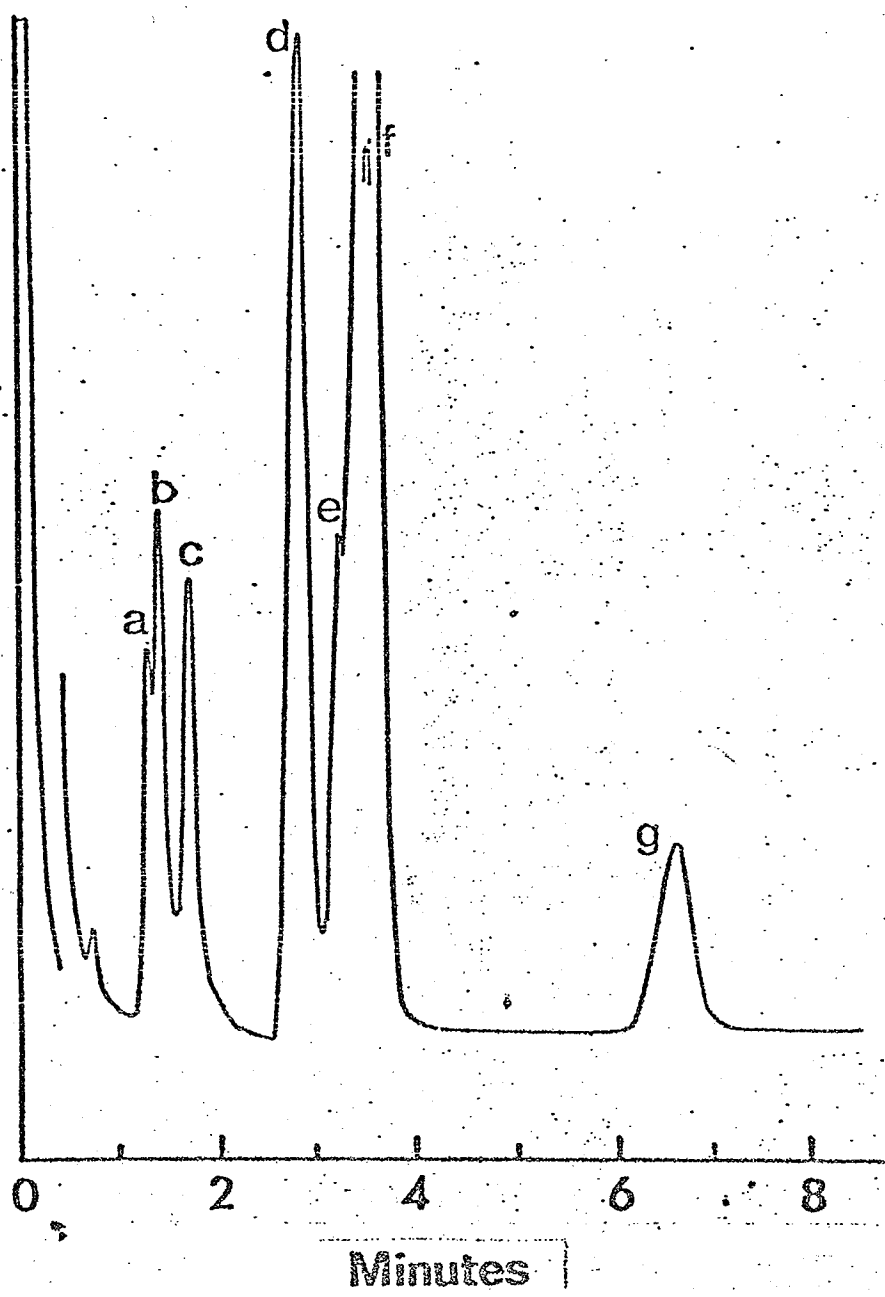


Figure: 14 Gas chromatogram of O-silylated β -D-benzylribofuranosides.

a, b and c = mono-O-TBDMSi- β -D-benzylribofuranosides

d, e, and f = bis-O-TBDMSi- β -D-benzylribofuranosides

g = tris-O-TBDMSi- β -D-benzylribofuranoside

Conditions: Column A (OV-1, 10%, 1m x 2mm ID), 240°C, N₂ flow = 30 ml/min.

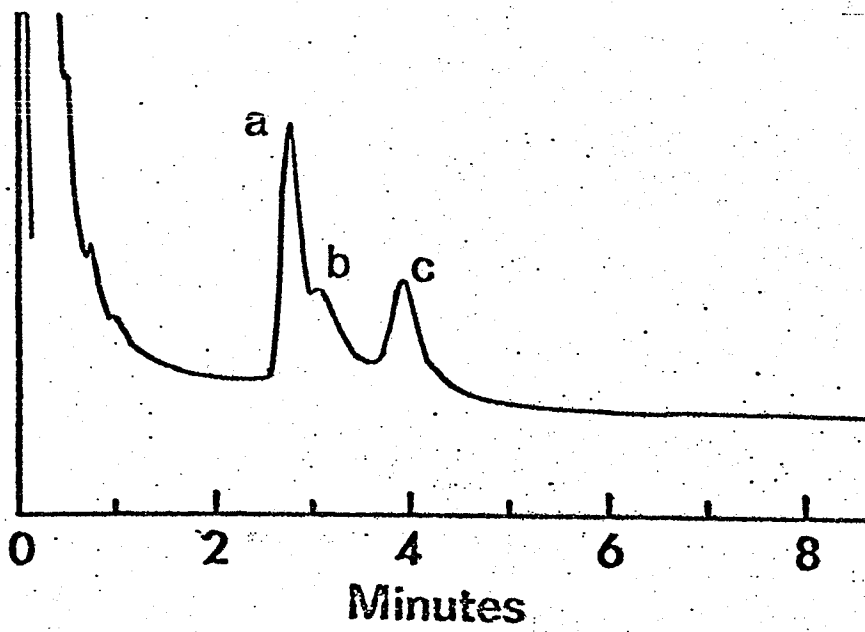


Figure 15 Gas chromatogram of mono-O-TMTBSi- β -D-benzyliribofuranosides.

a, b and c are all mono-silylated species.

Conditions: Column A (OV-1, 1m x 2mm ID) 240°C, N₂ flow = 30 ml/min.

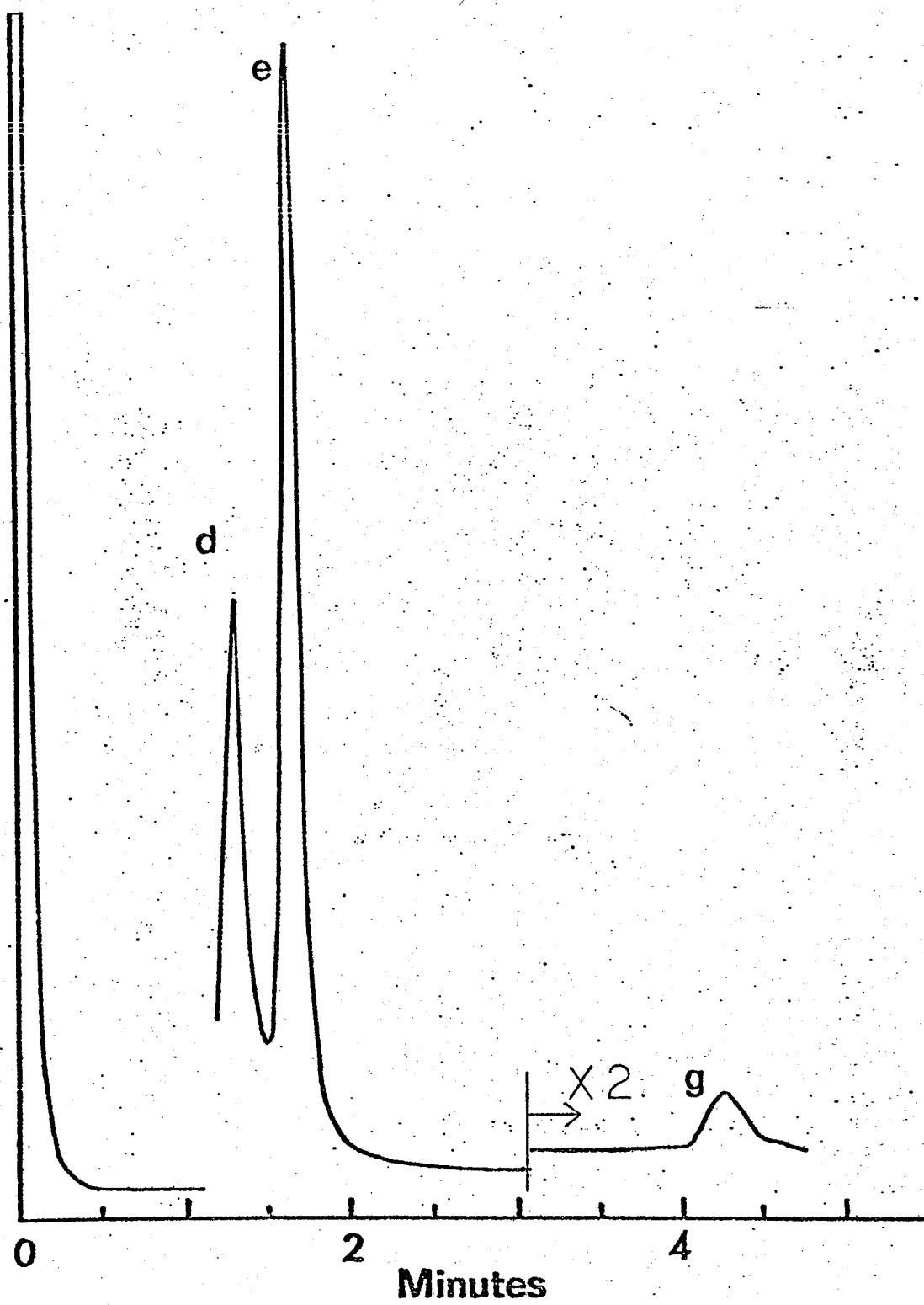


Figure 16 Gas chromatogram of O-TMTBSi- β -D-ribofuranosides. Peak identities:
d and e = bis-O-TMTBSi- β -D-benzylribofuranosides ; g = tris-O-TMTBSi- β -D-
benzylribofuranoside. Only 2 peaks were observed for di-substituted species.
Conditions: Column A (OV-1, 1m x 2mm ID) 280°C, N₂ flow = 30 ml/min.

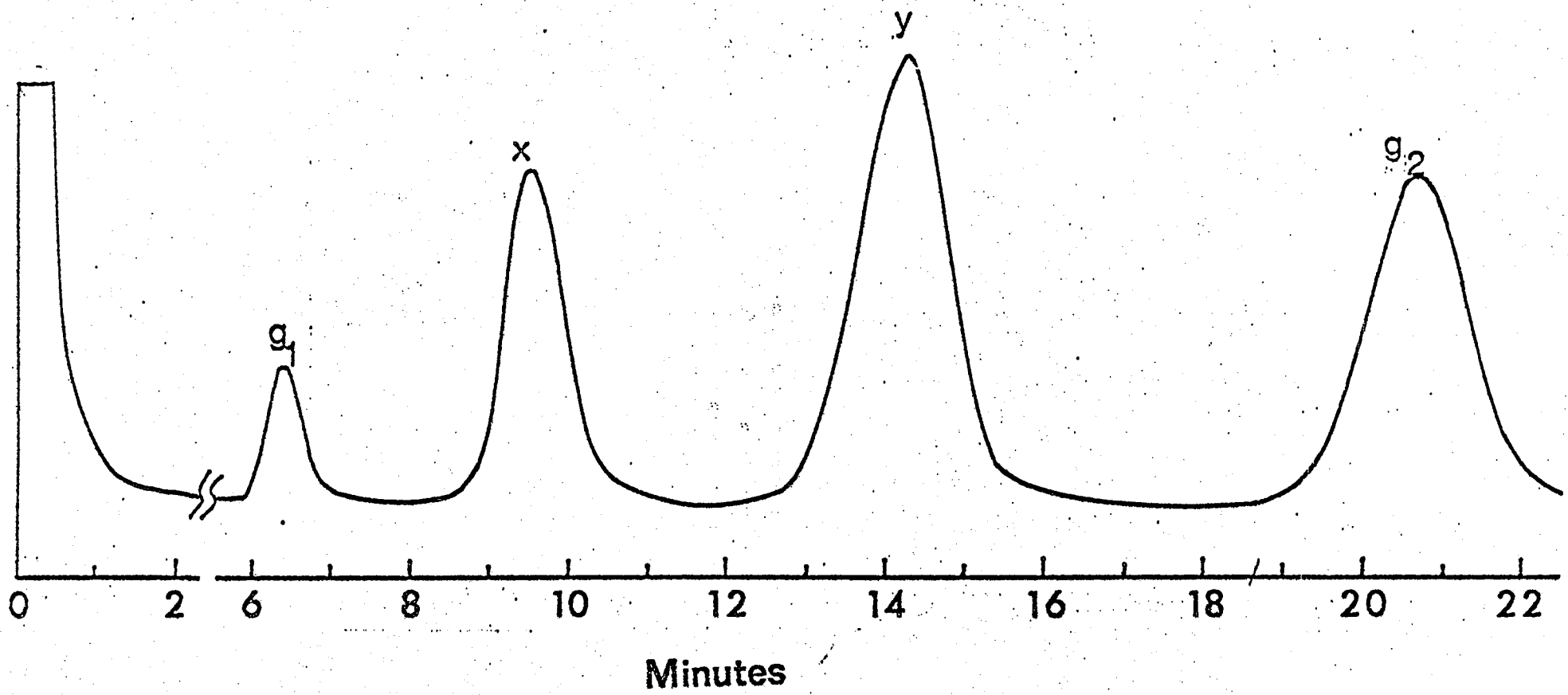


Figure 17. Gas Chromatogram of TMIPSi₃- β -D-benzylribofuranoside. Due to impurities in TMIPSiCl preparation, one of which was TMHSiCl (cyclo-tetramethylene-hexyl-chlorosilane), the 4 last eluted peaks in the order of elution were: *g*₁ = tris-O-TMIPSi- β -D-benzyl-ribofuranoside; *x* = bis-O-TMIPSi-mono-TMHSi- β -D-benzyl-ribofuranoside; *y* = mono-O-TMIPSi-bis-O-TMHSi- β -D-ribofuranoside and *g*₂ = tris-O-TMHSi- β -D-benzylribofuranoside.

Conditions: Column A (OV-1 10%, 1m x 2mm ID), 270 °C, N₂ flow = 30 ml/min.

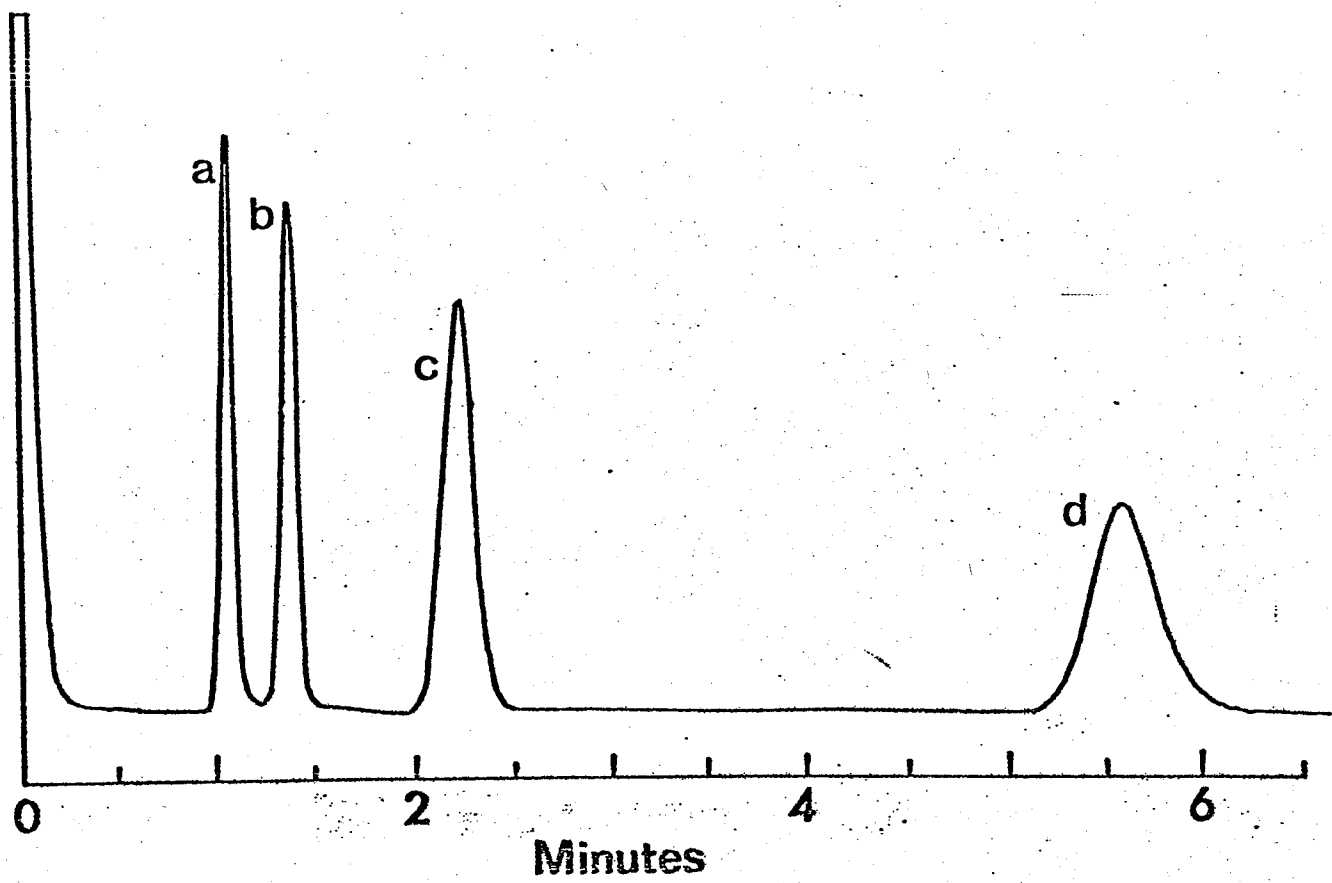


Figure: 18 Gas chromatogram of mixed TMSi/TBDMSi derivatives of β -D-benzyl-ribofuranoside. a = tris-O-TMSi- β -D-benzylribofuranoside; b = bis-O-TMSi-mono-O-TBDMSi- β -D-benzylribofuranoside; c = mono-O-TMSi-bis-O-TBDMSi- β -D-benzyl-ribofuranoside; and d = tris-O-TBDMSi- β -D-benzylribofuranoside.

Conditions: (Column A, OV-1 10%) 210°C,

N_2 flow = 30 ml./min.

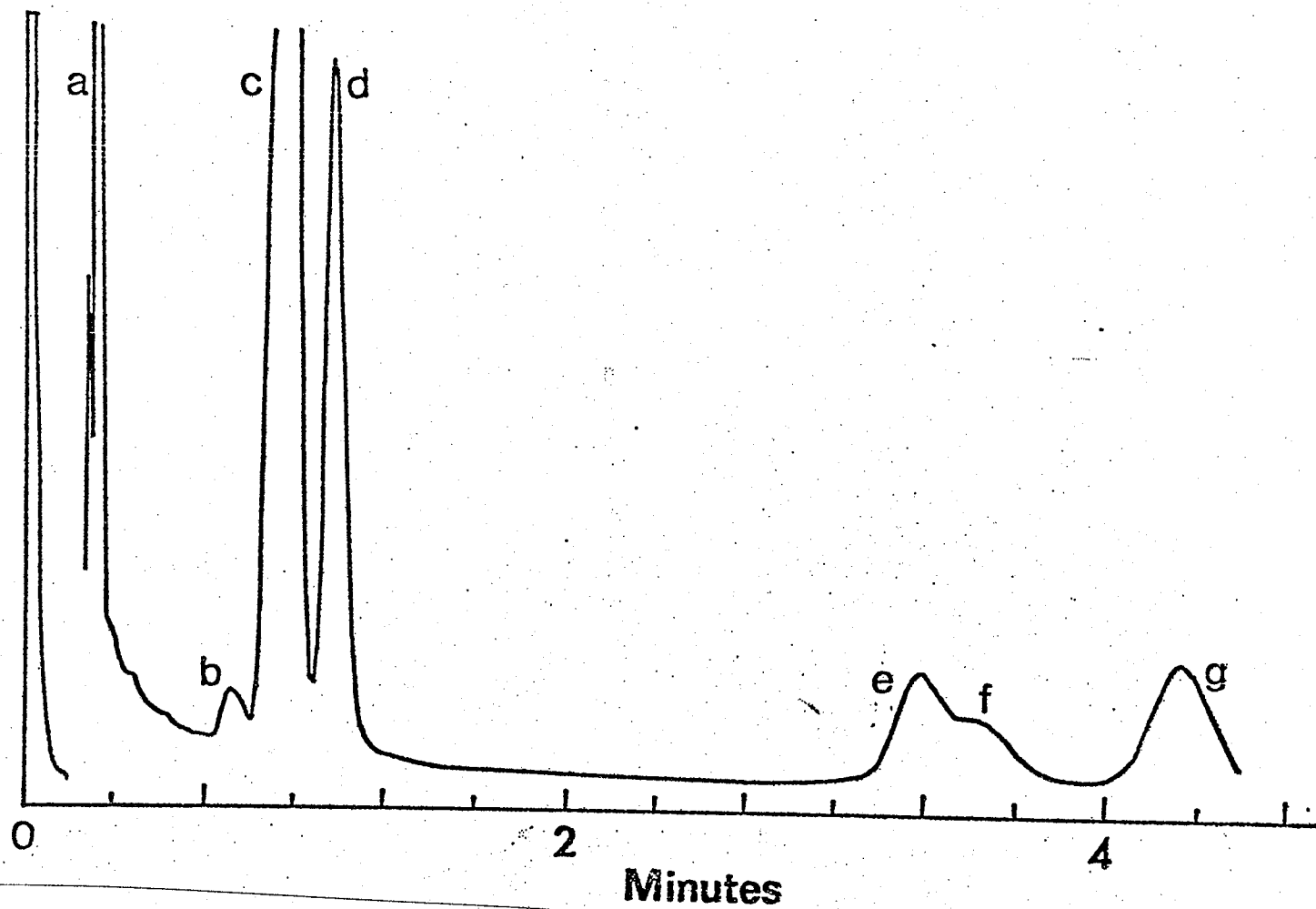


Figure: 19 Gas chromatogram of TFA/TBDMSi mixed derivatives of β -D-benzylribofuranosides.

Peak identities: a = tris-O-TFA- β -D-benzylribofuranoside; b, c and d = bis-O-TFA-mono-O-TBDMSi- β -D-benzylribofuranosides; e, f and g = mono-O-TFA-bis-O-TBDMSi- β -D-benzylribofuranosides.

Conditions: Column A (10% OV-1, 1m x 2mm ID) 210 °C, N₂ = flow = 30 ml/min.

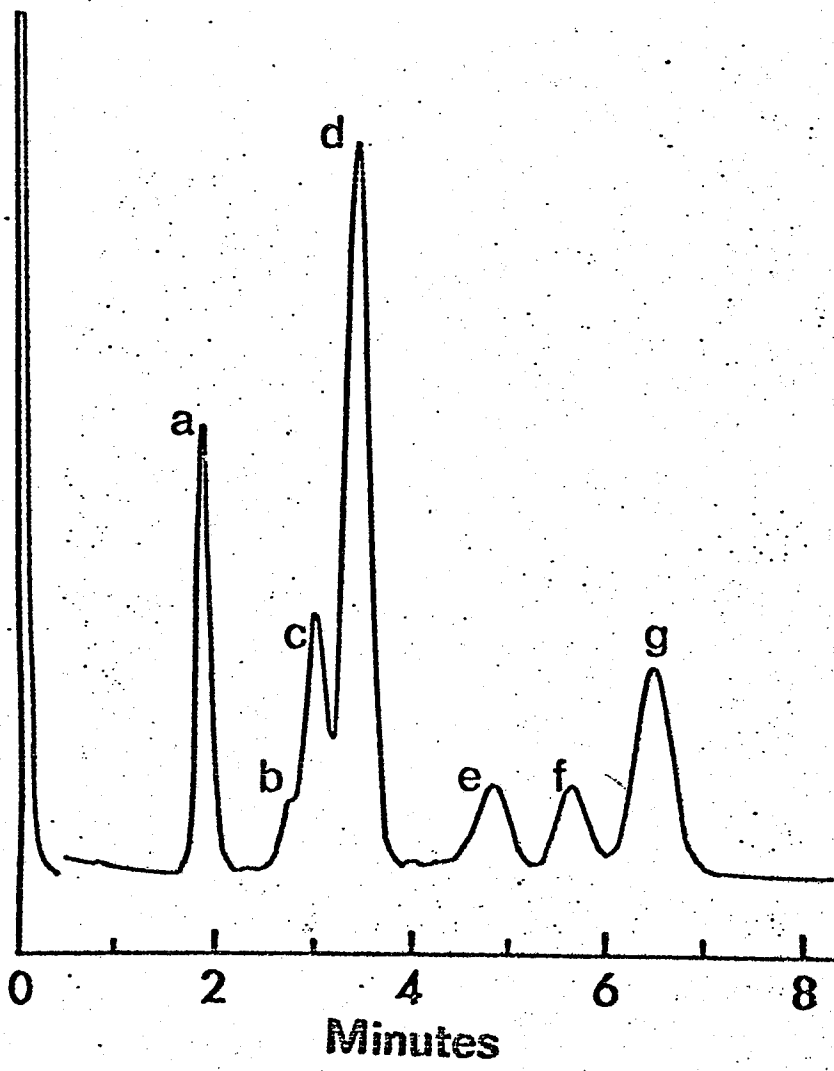


Figure: 20 Gas chromatogram of mixed derivatives of β -D-benzylribofuranoside.

a = tris-0-acetyl- β -D-benzylribofuranoside; b, c and d = bis-0-acetyl-mono-0-TBDMSi- β -D-benzylribofuranosides; e, f and g = mono-0-acetyl-bis-0-TBDMSi- β -D-benzylribofuranosides.

Conditions: Column A (OV-1, 10%, 1m x 2mm ID) 240°C, N₂ flow = 30 ml/min.

Quantitative GC

The application of SCTASi-sugars in quantitative GC was also investigated. Although quantitation by GC has been well documented (64) one should make sure that errors due to handling, decomposition and chemical transformation of derivatized samples are minimized.

Some derivatized samples are known to decompose on columns. This may happen when "active sites" are present in injection ports, columns and detectors. Catalytic decomposition at hot metal surfaces has also led to serious errors in sample analysis. In other cases derivatization by-products could hydrolyse derivatized samples e.g. acid catalysed elimination of TFA from pertrifluoroacetates (65).

Chemical transformation of samples include both intra-molecular and intermolecular reactions. As a result of 2 \leftrightarrow 3 silyl group migration, extra GC peaks were observed when either 2'-0 or 3'-0 unprotected partial SCTASi-nucleosides were chromatographed (44).

The third kind of quantitation error is due to poor sample handling and poor injection techniques. It would be erroneous if we assume that the signal from the GC detector represents fully the amount of sample introduced into the instrument. Dead volumes are common problems in injection needles as well as injection port connections.

One way of preventing sample handling errors is to "spike" samples with "internal standards". The chemical nature of internal standards to be used is still open to controversy. Some workers prefer standards that

are structurally very similar to samples being analysed. Others advocate the use of chemically inert universal GC internal standards e.g. pyrene, triphenylene, etc. In this study the latter type of standard was employed. Generally, internal standards should possess: good GC behavior (symmetrical peaks; total elution, etc.); inertness; freedom from overlapping sample peaks and linearity of detector response. Aromatic polycyclic compounds are commonly used in routine analyses as internal standards.

Typically, a plot of ratio of sample peak response to response of internal standard vs. amount injected can provide much information about sample decomposition and possible chemical transformation, as well as linearity of response. Fig. 21 shows the response of tris-O-TBDMSi- β -D-benzyliribofuranoside with respect to the amount injected onto the column. The straight line plot is an indication of good linear response of the SCTASI derivatives. Also, the graph extrapolates through the origin of the plot, implying no decomposition of derivatized sample on the column.

Figure 22 shows the responses of other SCTASI-derivatives.

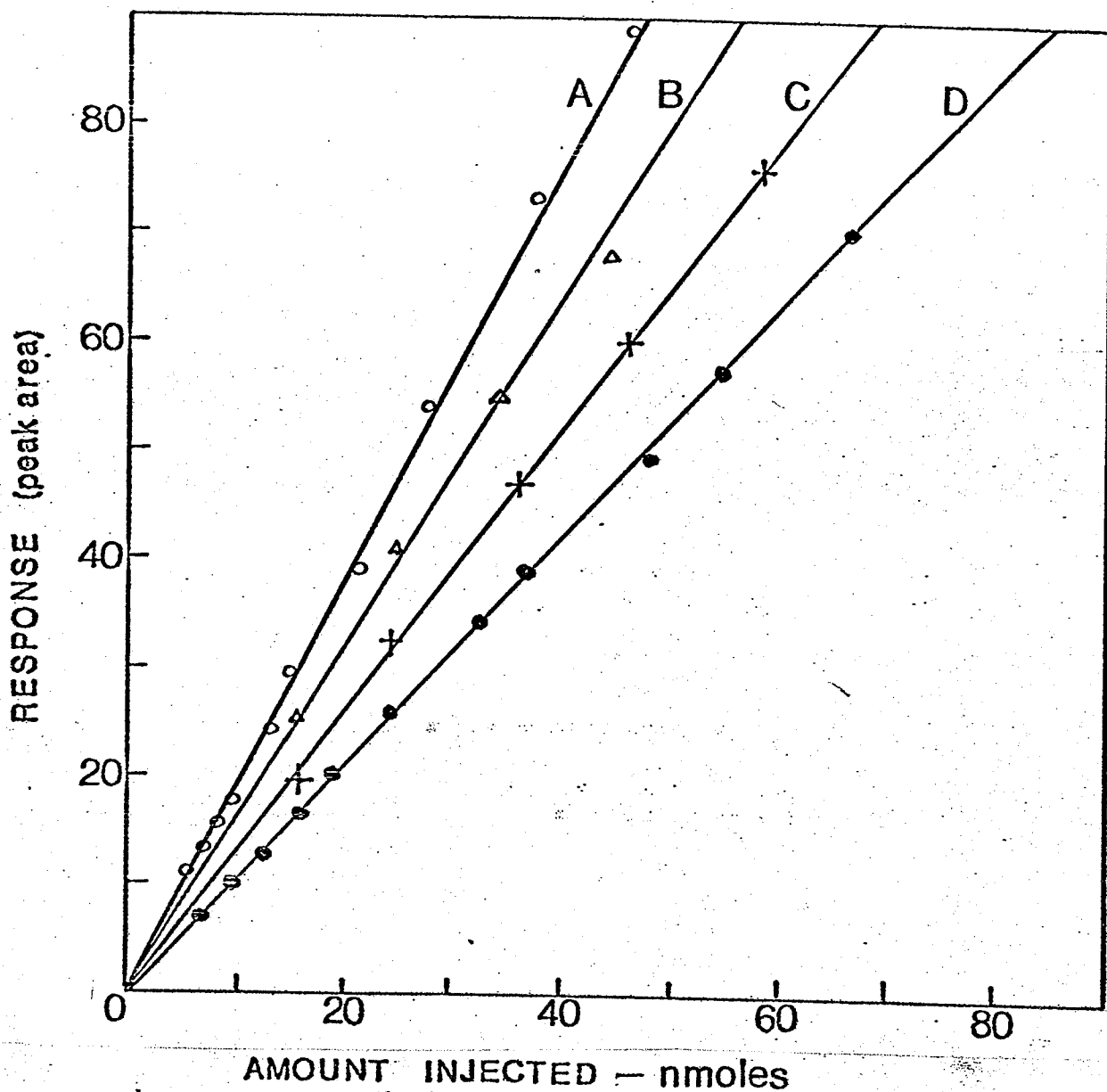
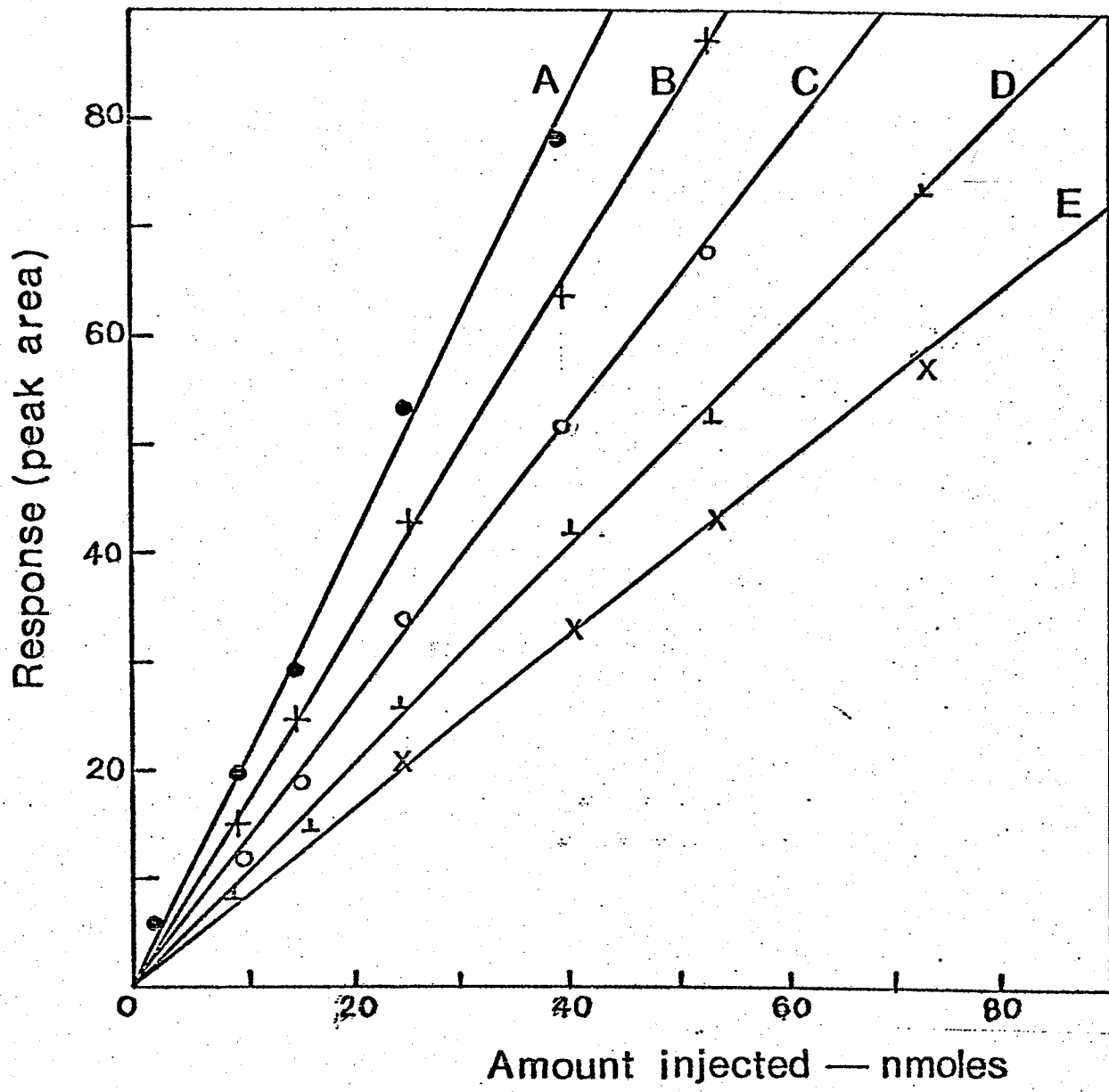


Figure 21 FID response curves for silylated β -D-benzylribofuranosides and 1,4-ribonolactones: (A) tris-0-TBDMSi- β -D-benzylribofuranoside; (B) tris-0-TBDMSi-1,4-ribonolactone; (C) tris-0-TMSi- β -D-benzylribofuranoside; (D) tris-0-TMSi-1,4-ribonolactone. All areas were calculated against internal standards. Both TMSi- and TBDMSi- derivatives show good linear responses. The ratio between slopes of 2 curves gives the relative molar response (RMR) between 2 derivatives.



Figure; 22 FID response curves of silylated hexose, pentose and D-2-deoxyribose: (A) pentakis-0-TBDMSi-D-galactose; (B) tetrakis-0-TBDMSi-D-ribose; (C) tris-0-TBDMSi-D-2-deoxyribose; (D) tetrakis-0-TMSi-O-D-ribose; (E) tris-0-TMSi-O-D-2-deoxyribose.

Mutarotation of sugars

It is suggested, from indirect evidence, that mutarotation of a crystalline sugar involves two consecutive events. First, an isomerization takes place and then equilibrium is eventually established. The isomerization process involves not only conversion into constitutional isomers, i.e. furanoses, pyranoses and septanoses (known as lactol ring isomerization); but also anomeration ($\alpha \leftrightarrow \beta$ form interconversion). (66, 67). The equilibrium process which depends on relative free energies of components in a particular solvent system, determines the relative proportions of the isomerization products (fig. 23).

It was shown by C.C. Sweeley that anomeric forms of an equilibrated sugar could be quantitatively determined by trimethylsilylation of a mutarotated sugar, followed by subsequent GC analysis (38). The relative areas of the component represented the relative proportions of individual anomers. Unfortunately, in the present study, the identity of an individual anomer could not be assigned. However, ratios of peaks for each sugar examined are presented in Table 12 and compared with other data from various sources.

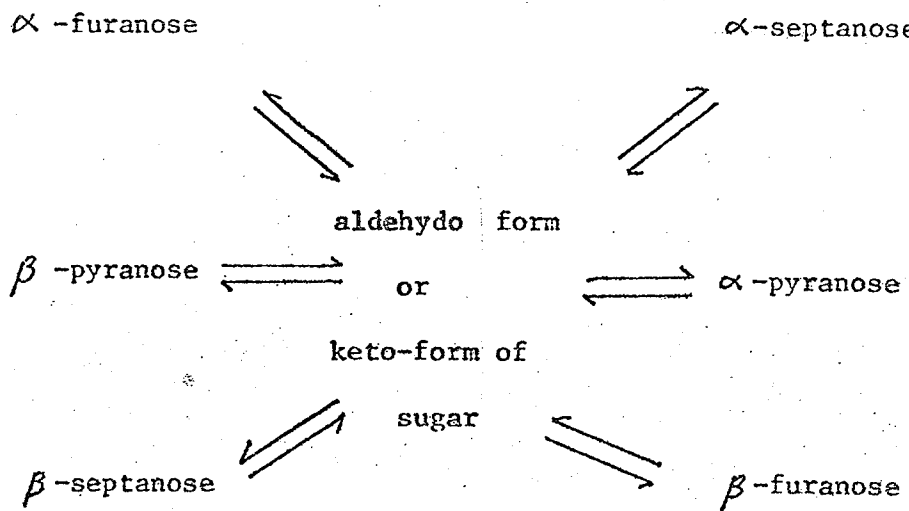


Figure: 23. Equilibrium processes in mutarotation of sugars

Table 12. Comparison of mutarotation studies (in pyridine).

Sugars	This study		Other studies		reference
	no. of peaks resolved	Ratio of peak areas	γ : α -f. : β -f. : \times -p. : β -p.	ratios	
D-2-deoxy-ribose	2	13.4:86.6			
D-ribose	4	45.7:5.8:40.6:7.9		21 : - : - : 17 : 62	(68a)
D-xylose	2	81.5 : 18.5		30 : - : - : 22 : 48	(68b)
D-galactose	2	88.2 : 11.8		11.3: - : - : 45.9 : 42.8 : 13.7 : 23.4 : 31.7 : 31.2 : 5.1 : 62.1 : 33.8 : 49.0	(38) (69a) (69b)
D-glucose	2	13.4 : 86.6		24.3: - : - : 29.9 : 45.8 - : - : - : 43 : 57	(38) (70)
D-mannose	2	61.3 : 38.7		3.2 : - : - : 47.3 : 49.5	(38)
D-fructose	2	70.9 : 28.7			

(cont'd)

Table 12 (cont'd)

Abbreviations: α -f. = α -furanose; β -f. = β -furanose; α -p. = α -pyranose; β -p. = β -pyranose; γ = γ -sugar.

Conditions: (68_a)--room temp.; (68_b)--70°C; values obtained by NMR.

(38) ---not specified; values obtained by GC.

(69_a)--room temp.; (69_b)--25°C; values obtained by GC.

(70)---room temp.; values obtained by GC.

In this study, temp. = 50°C.

Ir It is evident from the data in Table 12 that conditions are important in the determination of the equilibrium composition, e.g. in galactose determination. Thus, temperature seemed to change the distribution of components to a very drastic extent. Other studies have shown that mutarotation was also sensitive to the purity of the solvent system and/or impurities, especially traces of moisture or cations (71).

MASS SPECTROMETRY

Introduction

Mass spectrometric analysis of a substance involves conversion of atomic or molecular species into ions; and subsequent separation of these ions on the basis of their mass-to-charge ratio (m/z) by magnetic or electrostatic means. Mass spectrometry was first applied to carbohydrates in 1958 by P.A. Finan and co-workers (72). In that investigation, appearance potentials of $C_6H_{11}O^+$ ions were measured from undervatized monosaccharides. Later works, however, were directed towards protected carbohydrates which, due to their enhanced volatilities, were more amenable to the mass spectral instrumentation. Derivatization methods are essentially similar to those for GC. Excellent techniques for protection of hydroxyl and/or carbonyl groups on carbohydrates include: alkylation (73); acetylation (74); isopropylidation (75); boronation (76); and trimethylsilylation (77).

Much information can be obtained from the mass spectra of these derivatives. Very often molecular weights can be deduced easily from characteristic peaks, e.g. M^+ and masses of fragments derived from it. In high resolution mass spectrometry the elemental composition of each ionic peak can be determined. Because substitution of protecting groups profoundly influences fragmentation patterns, diagnostic and characteristic features associated with certain types of derivatives could be examined as distinct classes. Prediction of fragmentation pathways can also be

made on new samples. Modes of fragmentation are also closely related to the stereochemistry as well as to the linkages between monosaccharide sub-units of carbohydrate molecules. Mass spectrometry has become an indispensable tool in carbohydrate research.

Newer methods of ionization, such as field ionization (FI), field desorption (FD) and chemical ionization (CI), though giving prominent M^+ and/or related peaks, provide little fragmentation for M^+ ions and thus less structural information. In this study, electron impact (EI) ionization was employed throughout.

Electron impact mass spectrometry

Electron impact ionization makes use of an electron beam of "uniform" kinetic energy to bombard a sample to generate ionic species for mass separation and recording. Typically, an energy of 70 eV is employed. This method usually results in large amounts of energy transferred to the molecule, causing extensive ionization, fragmentation and rearrangement depending on the thermodynamics and stabilities as well as chemical nature of daughter ions towards further decomposition. Operation with low electron energy minimizes fragmentation but drastically reduces ion yield. A scheme of possible fates of an ionized molecule is shown in figure: 24.

Intensities of mass-analysed ion beams can be plotted out in a bar-graph line diagram, with m/z as the abscissa and relative abundance of ions as the ordinate. The highest peak (base peak) is arbitrarily set to be 100%. Other peaks in the mass spectrum are expressed as relative intensities of the base peak. The resulting spectrum is characteristic of the original specimen.

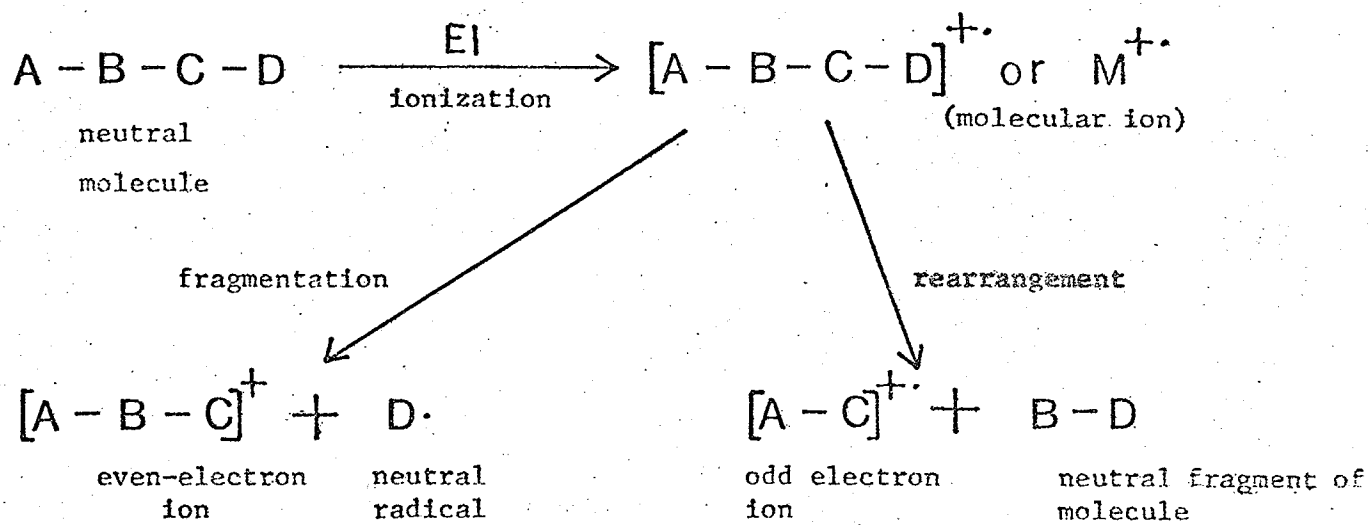


Figure: 24. Formation of different ions from the molecular ion.

The mass spectrum of a compound also depends on the type of instrument used. Decafluorotriphenylphosphine has been recommended as a standard for tuning a mass spectrometer, especially the quadrupole types (45). In order to obtain similar mass spectra for the same compound on quadrupole as well as magnetic mass spectrometers, "special" tuning procedures were used (44, 36). Fig. 25 shows a mass spectrum of the standard, decafluorotriphenylphosphine, recorded on our Finnigan quadrupole mass spectrometer after correction for mass discrimination.

Electron impact behavior of trialkylsilyl ethers of carbohydrates

An understanding of trialkylsilylated ethers of carbohydrates best starts with the chemistry of silicon. Silicon belongs to Group IV of the Periodic Table. Usually silicon attains a co-ordination number of 4, with orbital hybridization of sp^3 . ($p \rightarrow d$)₇ bonding may sometimes be operational in Si-N and Si-O bonding systems. Silicon has an electronegativity of 1.8 and a covalent radius of 1.17 Å (78, 79). Thus, silicon can accommodate more substituent groups around it than can carbon; and silicon has more affinity for positive charge. Also, Si-O and Si-O bond dissociation energies are 127 ± 10 and 85 ± 10 kcal/mol, respectively (80). The exceptional strength of the Si-O bond is a major determining factor in the fragmentation of trialkylsilyl ethers of organic compounds. In general, fission of Si-C bonds is much favoured over that of Si-O bonds.

It is generally believed that for silyl ethers electron impact causes the formation of a molecular ion with positive charge on the oxygen atom as shown in scheme 6, although a positively charged centre remote from the silyl ether site is possible.

MS-24/8/76 DFTPP W-TUNING
FINNIGAN-1015 RF-QUADRUPOLE MASS SPECTRUM
CORRECTED FOR MASS DISCRIMINATION

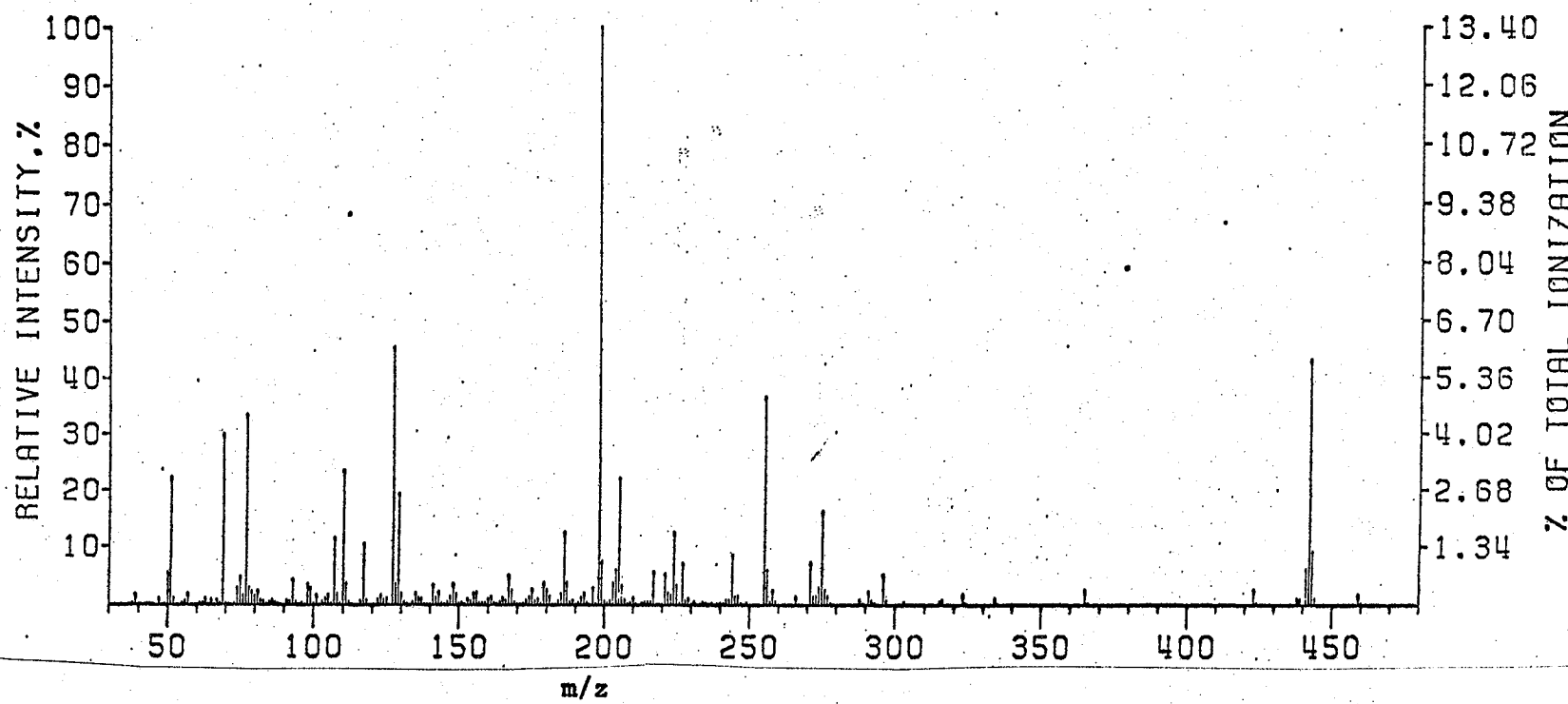
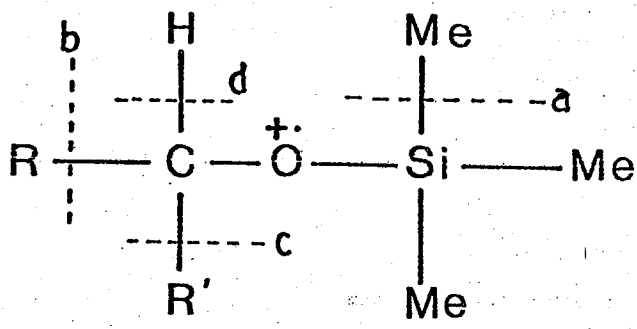


Figure: 25. Mass spectrum of decafluorophenylphosphine under "standard" conditions,
with correction for mass discrimination.



Scheme 6. Possible fissions of a trimethylsilyl ether.

R and R' denote alkyl groups remote from the silyl group.

Fragmentation can be brought about by α -cleavages at a, b, c and d.

Due to the relative stabilities of C-C, C-H and Si-O bonds, fission at a is the preferred route. $(M-CH_3)^+$ in trimethylsilyl ethers is the most often observed product from the M^+ ion. $(M-CH_3)^+$ is relatively stable, because expulsion of CH_3 eases the steric crowding at the Si atom. In TBDMSi ethers, expulsion of the bulky tert-butyl group is the norm.

In cyclic systems, e.g. TMSi-glucopyranose, loss of silanols is always observed because of the ease of abstraction of a hydrogen from an adjacent carbon (fig. 26). There is also an absence of metastable peaks at the high end of the mass spectra of TMSi-sugars. Cleavage of C-C bonds within the furanose or pyranose rings occurs to a smaller extent and this gives rearrangement-ions at the middle and lower range of the mass spectrum (77). $M^+/(M-CH_3)^+$ abundance ratios are also dependent on operating temperatures of the ionization source and inlet probe while SCTASi-ethers are found to be more predictable. $(M-R)^+$ is an abundant ion in the mass spectrum ($R = t\text{-}Bu$ or $i\text{-}Pr$). Generally, fragmentation patterns of SCTASi-ethers are simpler, and with less rearrangements. SCTASi groups have also unique properties of 'directing' fragmentations for some derivatives (36).

Different SCTASi groups produce characteristic shifts in mass spectra. Replacement of a TBDMSi by a TMTBSi moiety would cause a shift of +26 u, whereas replacing a TBDMSi by a TMPSi only produces a change of +12 u. By using different kinds of SCTASi reagents, corresponding mass peaks can be labelled for differently silylated molecules.

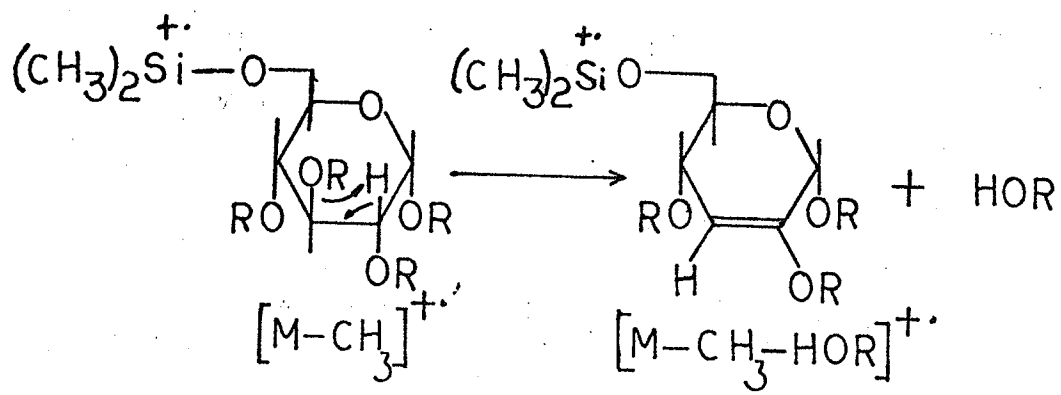


Figure: 26.

Loss of trimethylsilanol from $M-15^+$: $R = \text{TMSi}$ and $R' = \text{TMSi}-\text{CH}_3$

Molecule shown here is pentakis-O-TMSi- α -D-glucose.

Much work has been done on the TMSi-sugars (77,81,82). High resolution mass spectrometry and deuterium labelling of TMSi-monosaccharides have helped to elucidate fragmentations and geneses of many ionic species. The mass spectral behavior of SCTASi-sugars, however, have not been described in the literature. The following is an attempt to interpret some high-lights of the mass spectra of some SCTASi-monosaccharides. The discussion is divided into 4 parts:

- a) pyranose systems which include TBDMSi-D-glucoses, -mannoses, and -fructoses;
- b) the D-2-deoxyribose system which consists of SCTASi-D-2-deoxyribooses;
- c) ribofuranose systems which include SCTASi- β -D-benzylribofuranosides, -D-riboses and -D-xyloses; and,
- d) SCTASi-ribonolactone furanoid systems.

(a) Mass spectra of TBDMSi-hexopyranose systems

1) Pentakis-O-TBDMSi-D-glucoses:

Analogous to TMSi-hexoses, GC of TBDMSi-D-glucoses gave more than one peak. Mass spectral analysis of the 2 eluted peaks (figs. 27,28) reveals similar or analogous fragmentation patterns to those for TMSi-glucoses reported by DeJongh *et al* (77).

Scheme 7 shows the loss of tert-butyl radical from the molecular ion, M^+ , to form the $(M-57)^+$ ion at m/z 693. Non-specific or (specific ?) losses of tert-butyldimethylsilanol molecules give $(M-57-132)^+$, m/z 561, and $(M-57-132-132)^+$, m/z 429.

The $(M^+)-\text{t-Bu}$ ion (m/z 693) can be postulated to give an ion m/z 561 through loss of t-butyldimethylsilanol. Further loss of Me_2SiO is believed to produce m/z 487. On the other hand, elimination of CH_2CO from m/z 693 could produce m/z 519 which can in turn gives m/z 445 with the loss of Me_2SiO . This is outlined in scheme 8.

Other ionic species of medium abundances, e.g. m/z 231, m/z 245 and m/z 375 can arise from the M^+ ion through some even mass intermediates as shown in scheme 9.

TBDMS5 GLUCOSE PK I
SPECTRUM RECORDED ON 1015 QUADRUPOLE MASS SPECTROMETER
AND NORMALIZED TO CONSTANT SENSITIVITY

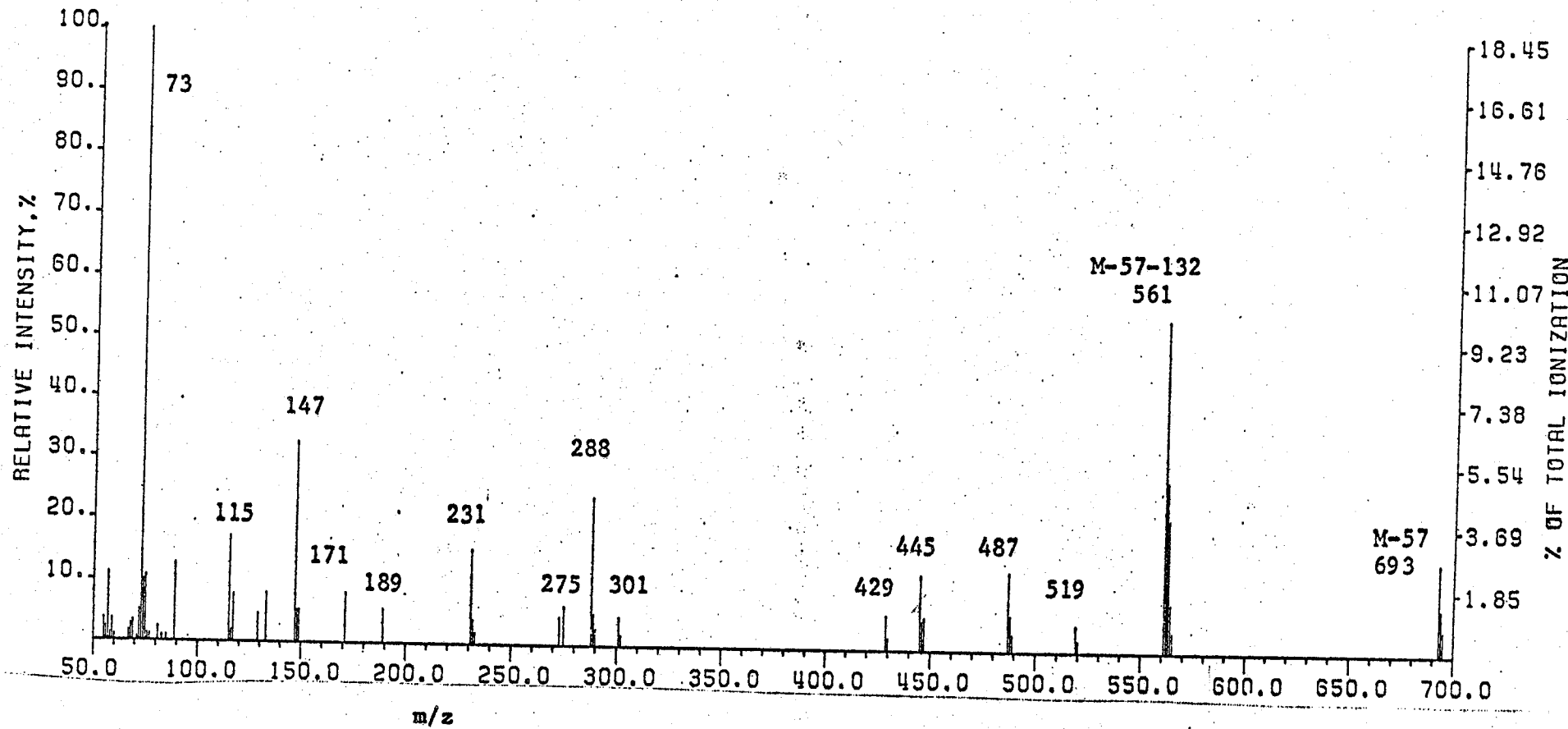


Figure: 27. Mass spectrum of pentakis-O-TBDMSi-D-glucose (MW 750), $I_{\text{OV-1}}^{240} = 2807$, recorded on Finnigan 1015 mass spectrometer at 70 eV.

TBDMS5 GLUCOSE PK2
SPECTRUM RECORDED ON 1015 QUADRUPOLE MASS SPECTROMETER
AND NORMALIZED TO CONSTANT SENSITIVITY

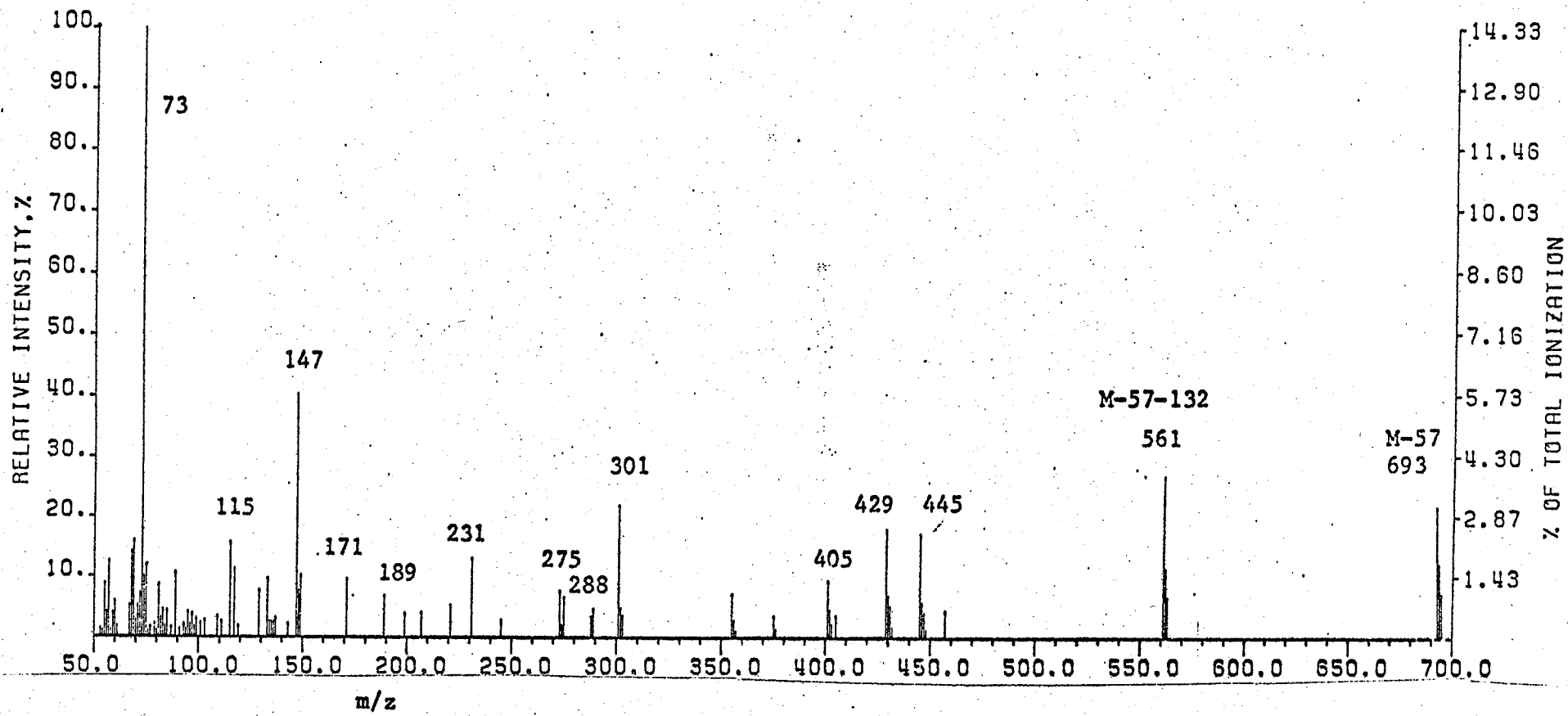
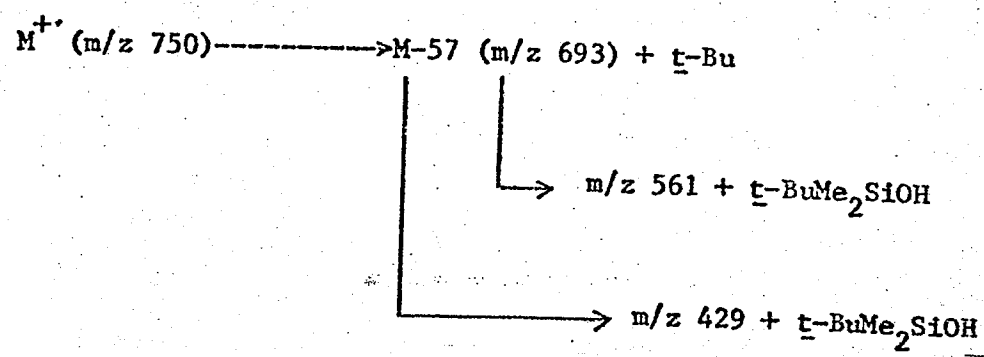
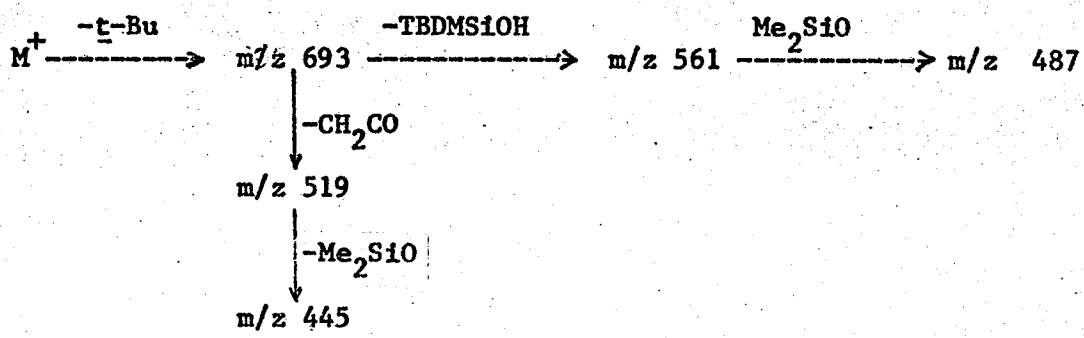


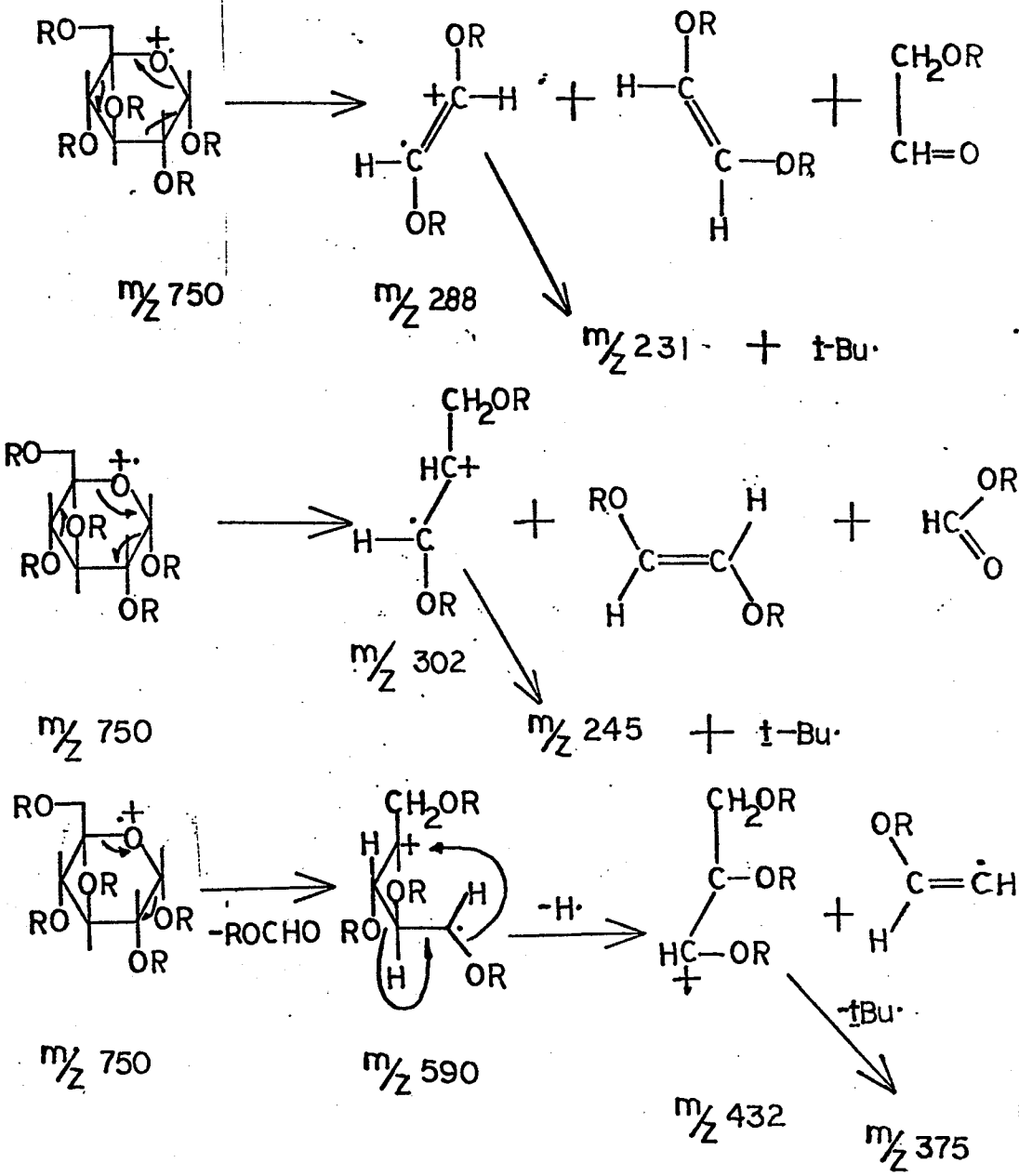
Figure: 28. Mass spectrum of pentakis-O-TBDMSi-D-glucose (MW 750, I_{Ov-1}^{240} 2925) recorded on Finnigan 1015 mass spectrometer at 70 eV.



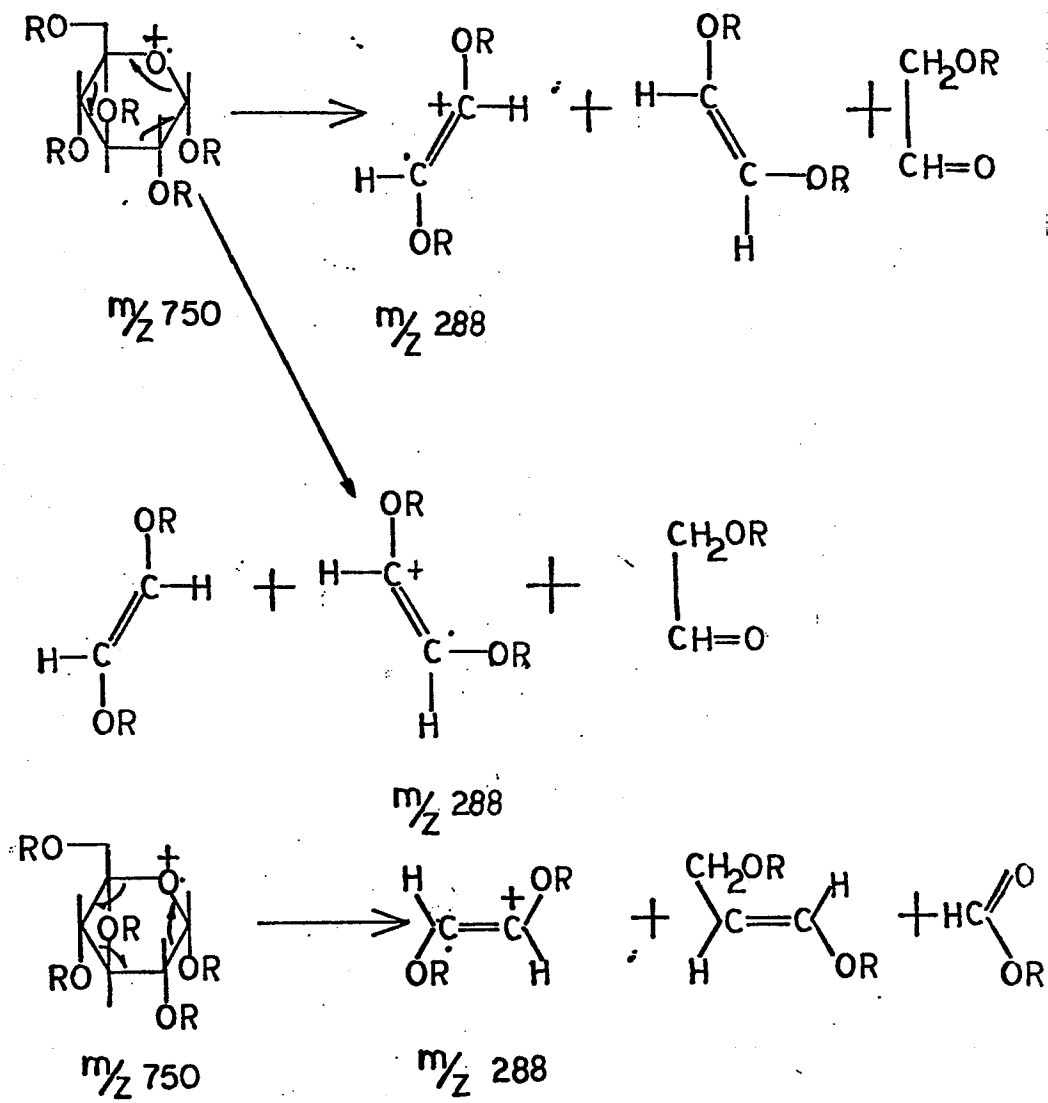
Scheme 7 Formation of m/z 693, m/z 561 and m/z 429



Scheme: 8. Geneses of $m/z\ 487$, $m/z\ 519$ and $m/z\ 445$ from $m/z\ 693$.



Scheme 9. Formation of $m/z\ 231$, $m/z\ 245$ and $m/z\ 375$ from M^+ ion, through some even- mass intermediates. ($R=\text{TBDMSI}$)

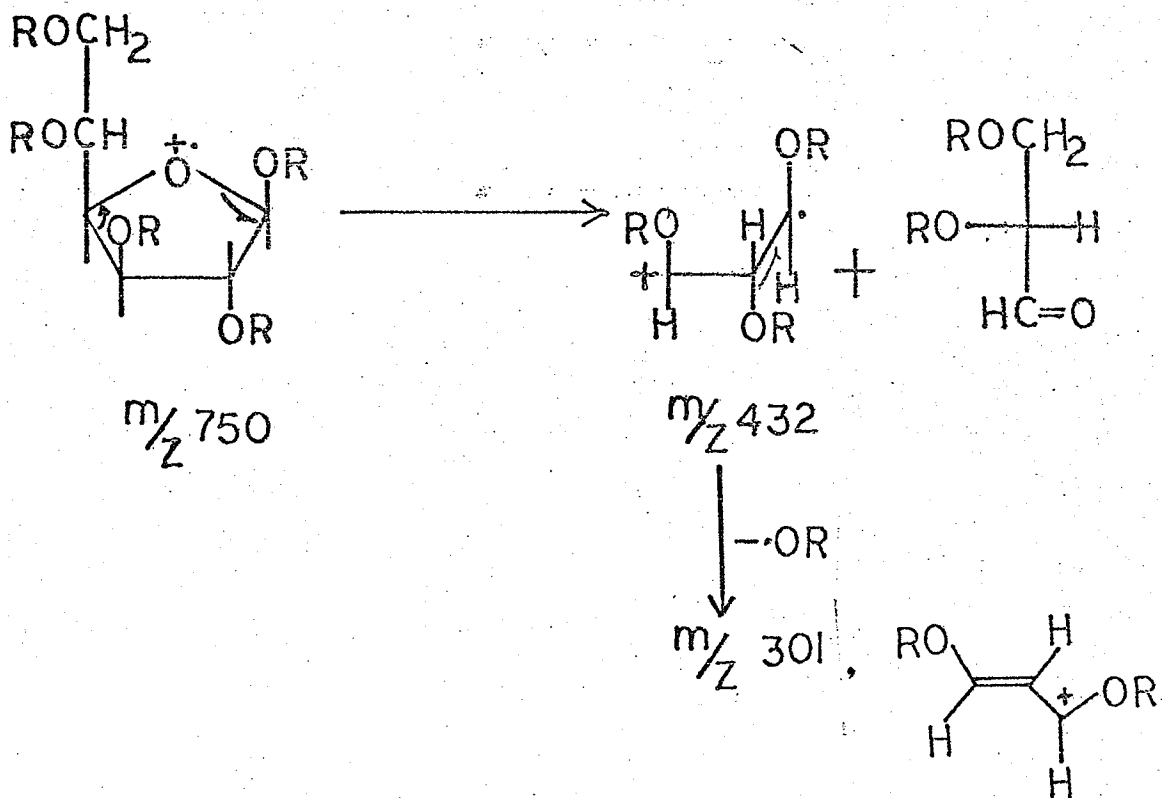


Scheme: 10. Formation of m/z 288, from M^+ ion. ($R=TBDMSI$).

One ionic species which is characteristic of TBDMSi-pyranose is the m/z 288 peak (m/z 204 in TMSi-pyranoses). Its facile formation involves cyclic migration of electrons around the pyranose rings. Three possible routes of formation are shown in scheme 10. Furanoid systems could not undergo similar electron shifts and for them m/z 288 tends to be very small.

However, furanoid systems can undergo another type of fragmentation to give m/z 301 (m/z 217 in TMSi-furanoses) which is much more intense than that from the pyranoses (scheme 11).

Judging from the rather high m/z 301 peak in the mass spectrum of pentakis-O-TBDMSi-glucose (GC peak 2), there could have been contamination by furanose(s) in the GC peak (figs. 27,28)



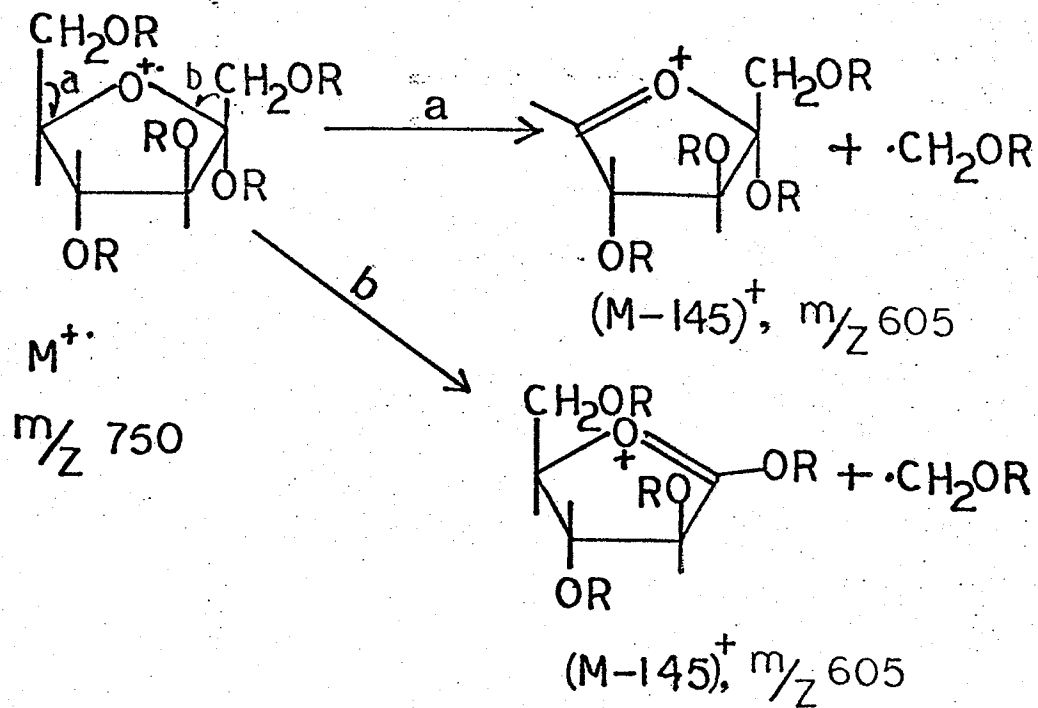
Scheme: 11 Formation of m/z 301 from pentakis-O-TBDMSi-D-glucose.
(R = TBDMSi; m/z 750 corresponds to M^+ ion)

ii) Pentakis-O-TBDMSi-D-mannose:

The mass spectra of TBDMSi-D-mannoses are very similar to those of TBDMSi-D-glucoses. The differences between them amount to variations of intensities of major ionic peaks (mass spectra figs. 29,30).

iii) Pentakis-O-TBDMSi-D-fructoses:

Mass spectra (figs. 31,32) were obtained from the 2 resolved GC peaks pf VII_{bbbbbb}. Prominent m/z 301 peaks in both mass spectra indicate that both are furanoid systems. The α or β anomers, however, could not be distinguished since the spectra are almost identical. The characteristic peak is (M-145) or (M-TBDMSiOCH₂)⁺. (scheme 12)



Scheme: 12 Formation of (M-145)⁺ ion from M⁺ of pentakis-O-TBDMSi-D-fructose. (m-145)⁺ is an ion characteristic of TBDMSi-2-ketofuranoses. (R = TBDMSi).

TBDMS5 MANNOSE PK1
FINNIGAN-1015 RF-QUADRUPOLE MASS SPECTRUM
CORRECTED FOR MASS DISCRIMINATION

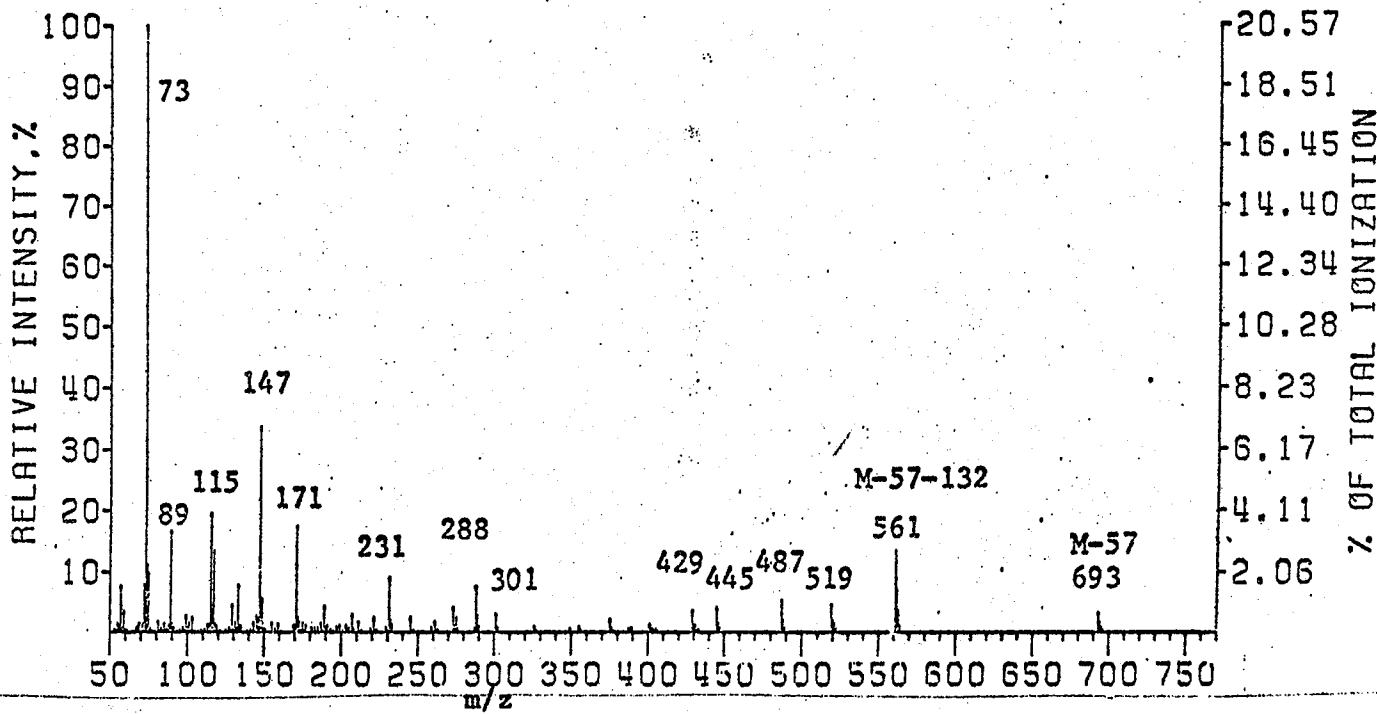


Figure: 29. Mass spectrum of pentakis-O-TBDMS-D-mannose (VI_{bbbbbb}, MW 750, $I_{OV-1}^{240} = 2900$) recorded on Finnigan 1015 mass spectrometer at 70 eV.

TBDMS5 MANNOSE PK2
 FINNIGAN-1015 RF-QUADRUPOLE MASS SPECTRUM
 CORRECTED FOR MASS DISCRIMINATION

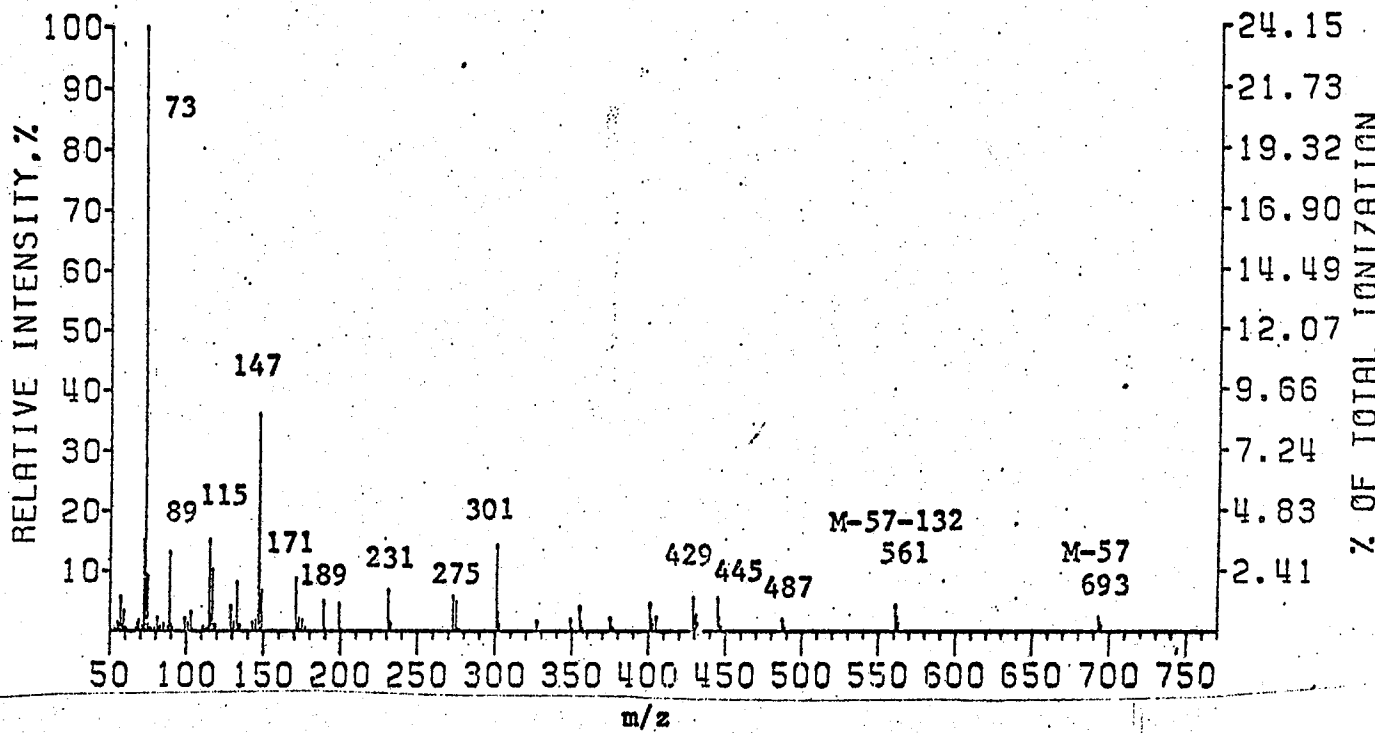


Figure: 30. Mass spectrum of pentakis-O-TBDMSi-D-mannose (VI_{bbbbbb}, MW 750, $I_{OV-1}^{240} = 2936$), recorded on Finnigan 1015 mass spectrometer at 70 eV.

TBDMS5 FRUCTOSE PK1
 FINNIGAN-1015 RF-QUADRUPOLE MASS SPECTRUM
 CORRECTED FOR MASS DISCRIMINATION

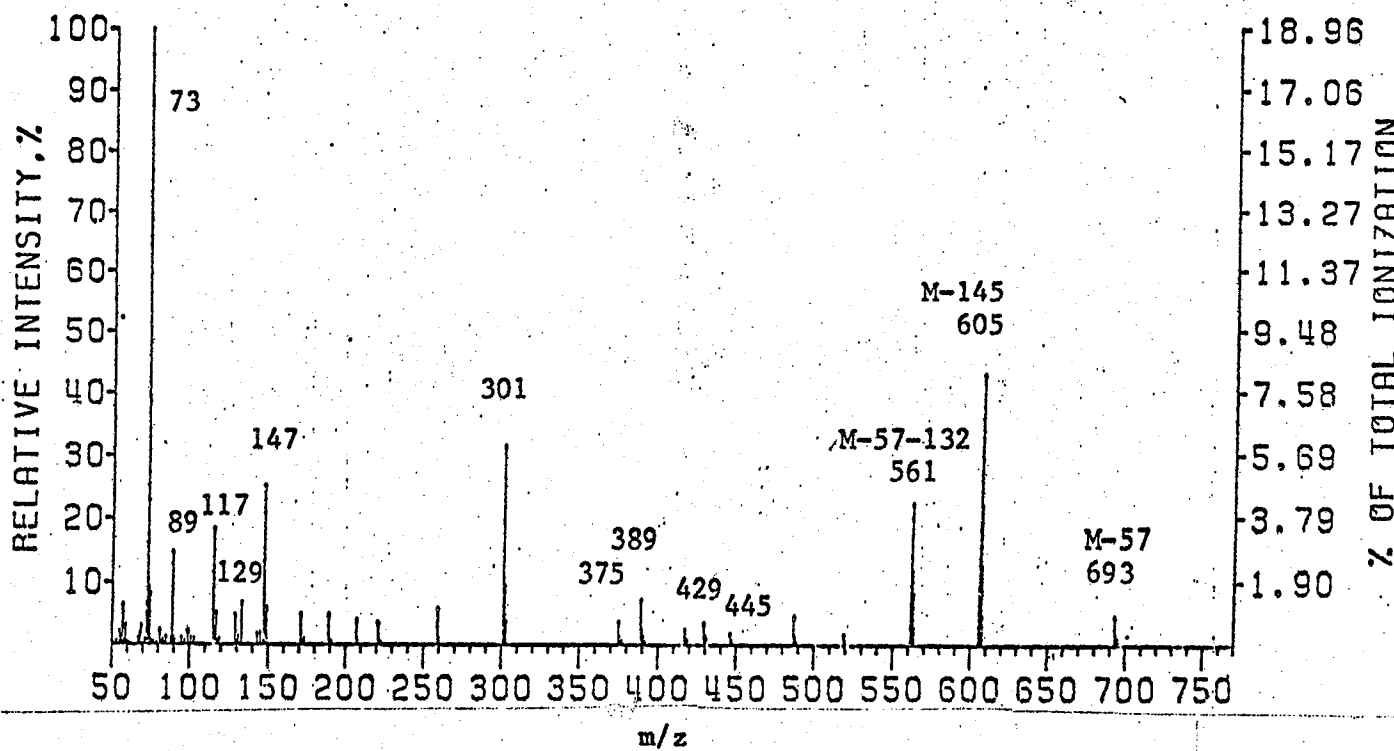


Figure: 31. Mass spectrum of pentakis-O-TBDMSi-D-fructose (VII_{bbbbbb}, MW 750, $I_{OV-1}^{240} = 2888$), recorded on Finnigan 1015 mass spectrometer at 70 eV.

TBDMS5 FRUCTOSE PK 2
 FINNIGAN-1015 RF-QUADRUPOLE MASS SPECTRUM
 CORRECTED FOR MASS DISCRIMINATION

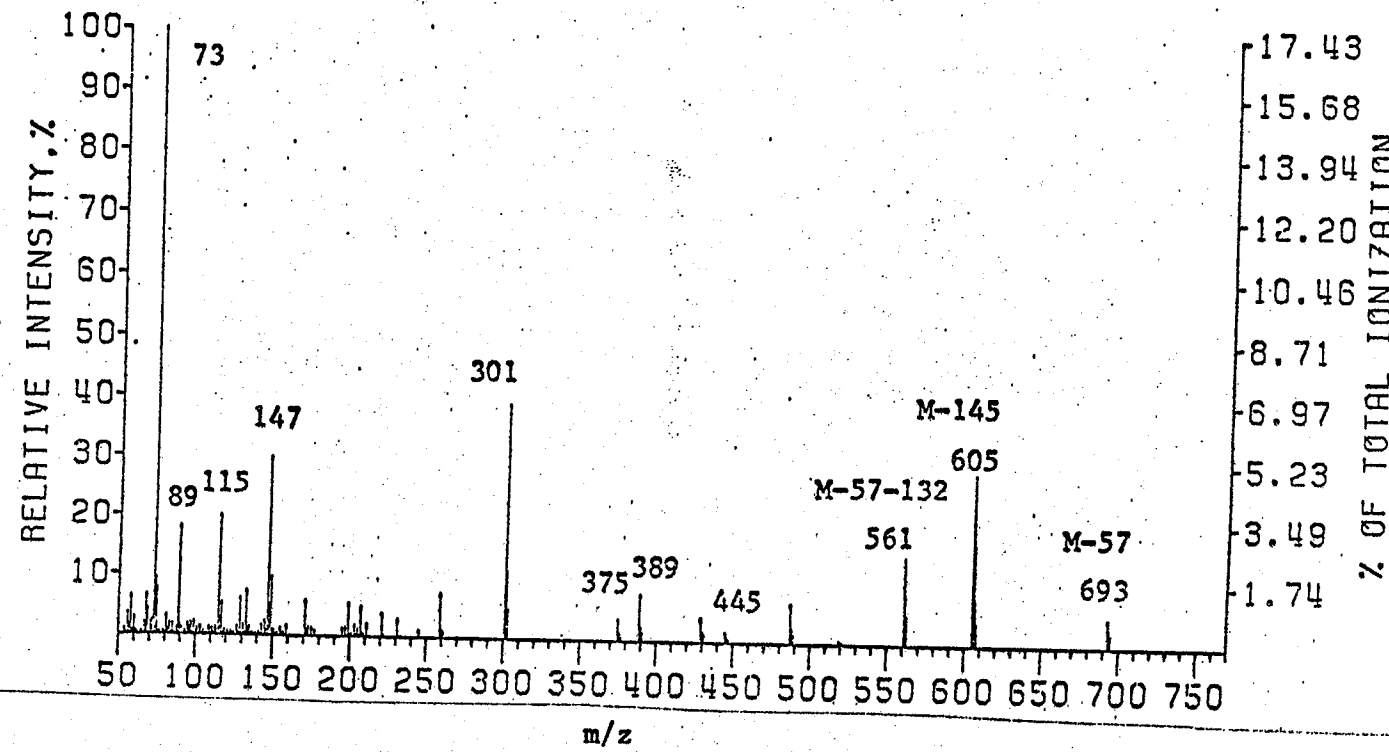


Figure: 32. Mass spectrum of pentakis-O-TBDMSi-D-fructose (VII_{bbbbbb}, MW 750, $I_{OV-1}^{240} = 2940$), recorded on Finnigan 1015 mass spectrometer at 70 eV,

(b) Mass spectra of SCTASI-D-2-deoxyriboses

i) Per SCTASI-D-2-deoxyriboses:

The following three sections deal with the furanose systems in general. The mass spectra of the TMSi-furanoses (77); and TMSi-deoxyribofuranosides as well as TMSi-ribonucleosides (83) have been investigated before. Subsequent work by Quilliam (44) of this laboratory on O-SCTASI-2'-deoxyribonucleosides and O-SCTASI-ribonucleosides helped to elucidate many of the fragmentation patterns of the above-mentioned molecules. He employed techniques such as high resolution mass spectrometry, measurement of decomposition of metastable ions, deuterium labelling and mixed derivatization, to interpret geneses of various fragments.

SCTASI-D-2-deoxyriboses bear many similarities towards SCTASI-2'-deoxyribonucleosides. Figures 33 depicts common structural features between the 2 classes of compounds.

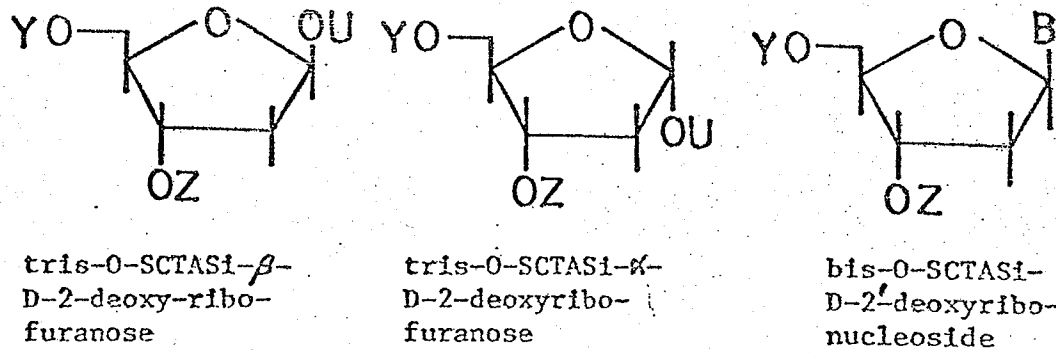


Figure: 33. Comparison between SCTASI-deoxyribonucleosides and SCTASI-D-2-deoxyriboses. Y, Z and U are SCTASI groups at the oxygens of C₅, C₃ and C₁ respectively. B denotes the base unit in the nucleoside.

If the group OU is regarded as analogous in behavior to the base B in mass spectral fragmentation schemes, SCTASi-2-deoxyriboses can be interpreted as if they were the SCTASi-deoxyribonucleosides, except perhaps with minor modifications.

It is convenient to label certain fragments of the SCTASi-2-deoxyribose molecule since this would simplify much in the explanation of the fragmentations. Referring to figure 34, numbers 1 to 5 denote the carbon atoms in the molecule, (B = base moiety; S = sugar and J = fragment containing C₁, C₂ and B or OU)

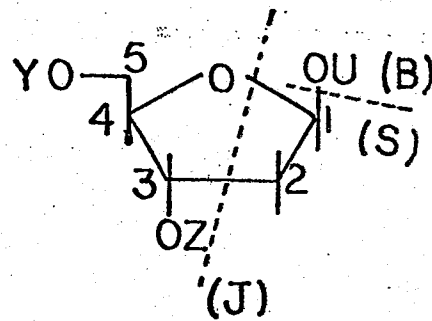


Figure: 34.

Major fragments of SCTASi-2-deoxyribose.

The mass spectra of tris-O-TBDMSi and -TMTBSi ethers of 2-deoxyribose are shown in figs. 35 to 38. One of the major precursors of SCTASi-ethers has been found to be the $(M-R)^+$ ion, where the SCTASi group is represented by RX_2Si with R = t-Bu or i-Pr. It is not surprising that most of the fragments of SCTASi-2-deoxyribose come from $(M-R)^+$ as shown in scheme 13.

MSGC TBDMS3 2-DEOXYRIBOSE PK1
FINNIGAN-1015 RF-QUADRUPOLE MASS SPECTRUM
CORRECTED FOR MASS DISCRIMINATION

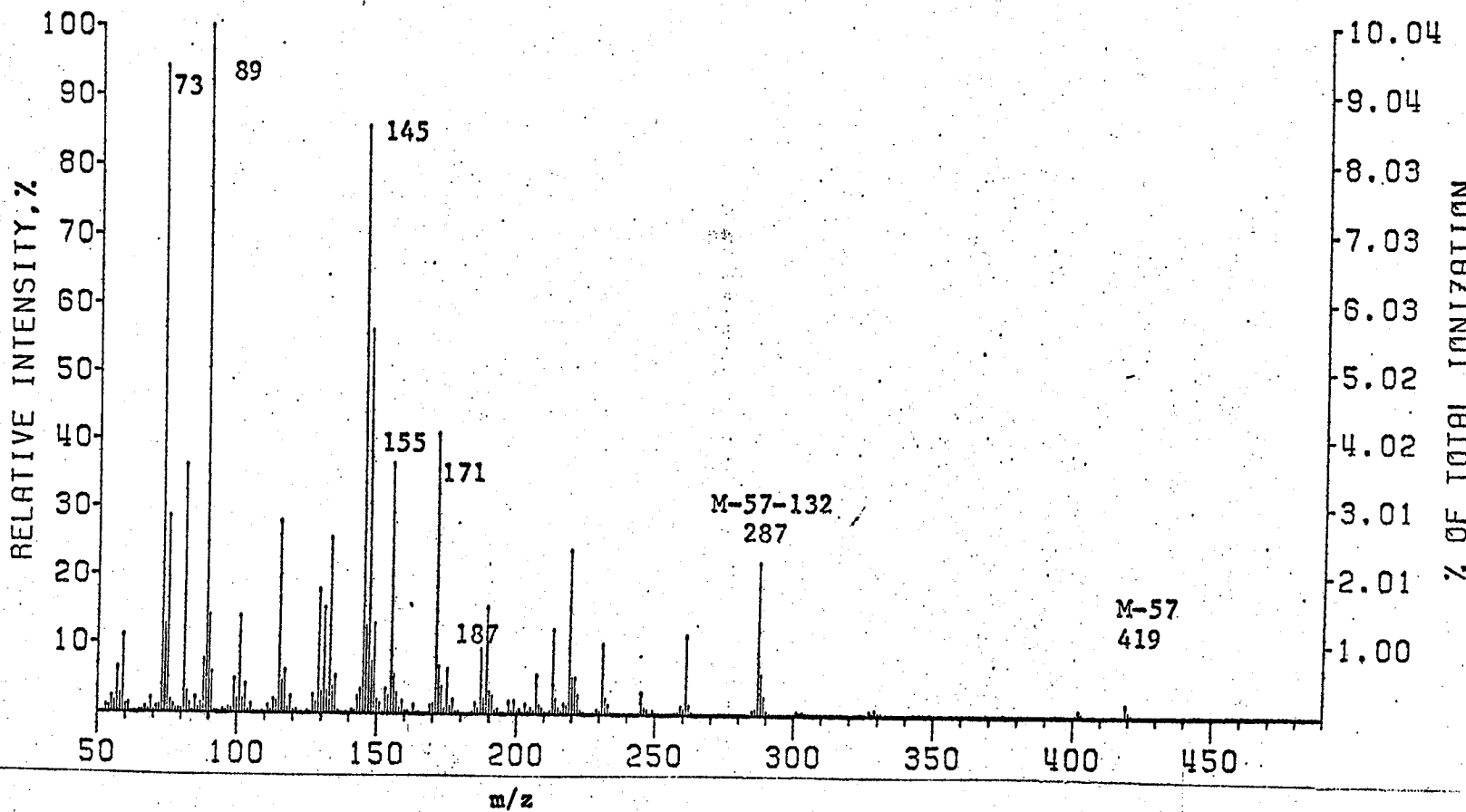


Figure: 35. Mass spectrum of tris-O-TBDMSi-D-2-deoxyribose (I_{bbb}^{210} , MW 476, $I_{OY-1}^{210} = 2092$), recorded on Finnigan mass spectrometer at 70 eV.

99

96
MSGC TBDMS3 2-DEOXYRIBOSE PK2
FINNIGAN-1015 RF-QUADRUPOLE MASS SPECTRUM
CORRECTED FOR MASS DISCRIMINATION

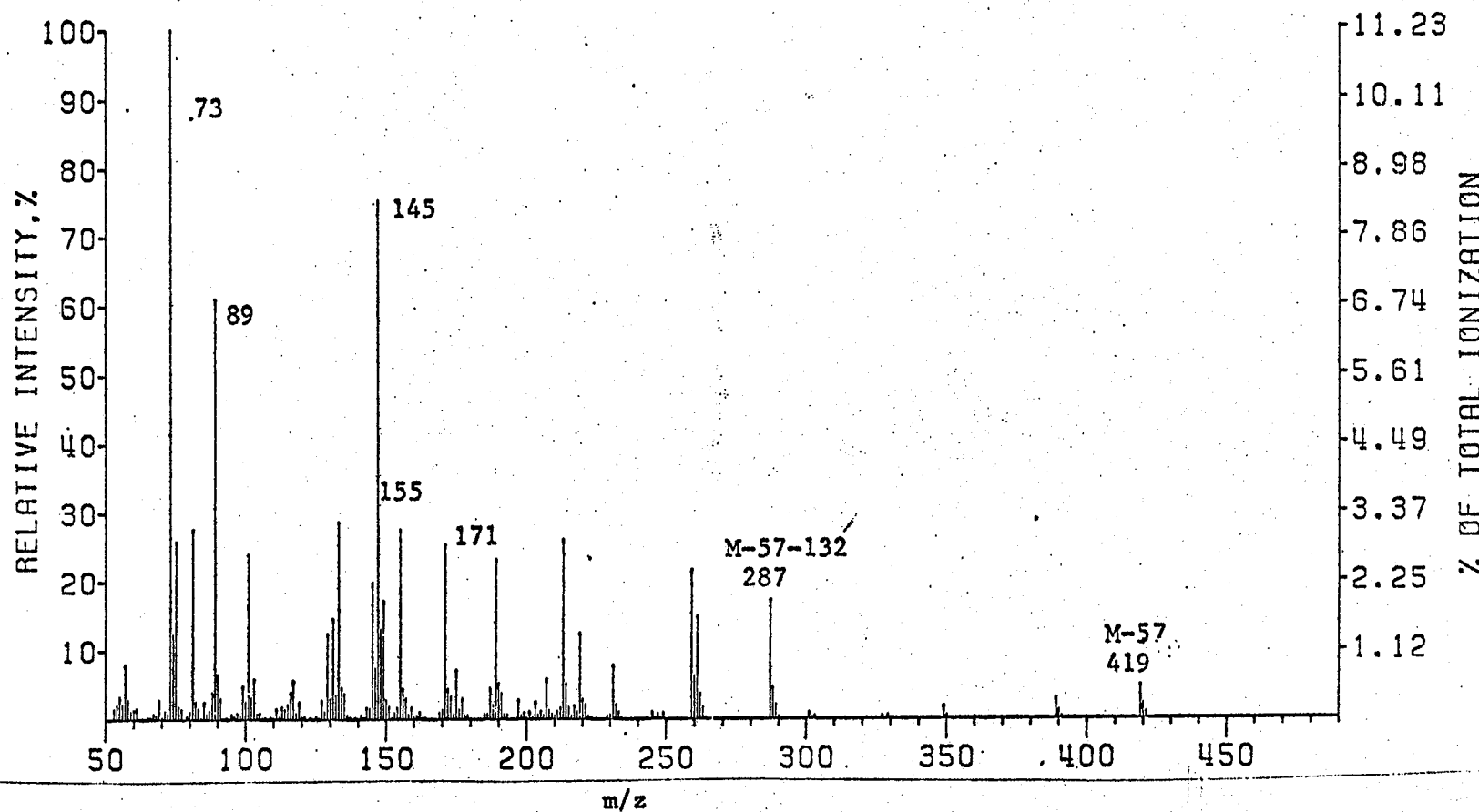


Figure: 36. Mass spectrum of tris-O-TBDMSi-D-2-deoxyribose (I_{bbb} , MW 476, $I_{OY-1}^{240} = 2152$), recorded on Finnigan 1015 mass spectrometer at 70 eV.

MSGC-3-12/8/76 TMTBS3 2'-DEOXY-RIB. PK9
SPECTRUM RECORDED ON 1015 QUADRUPOLE MASS SPECTROMETER
AND NORMALIZED TO CONSTANT SENSITIVITY

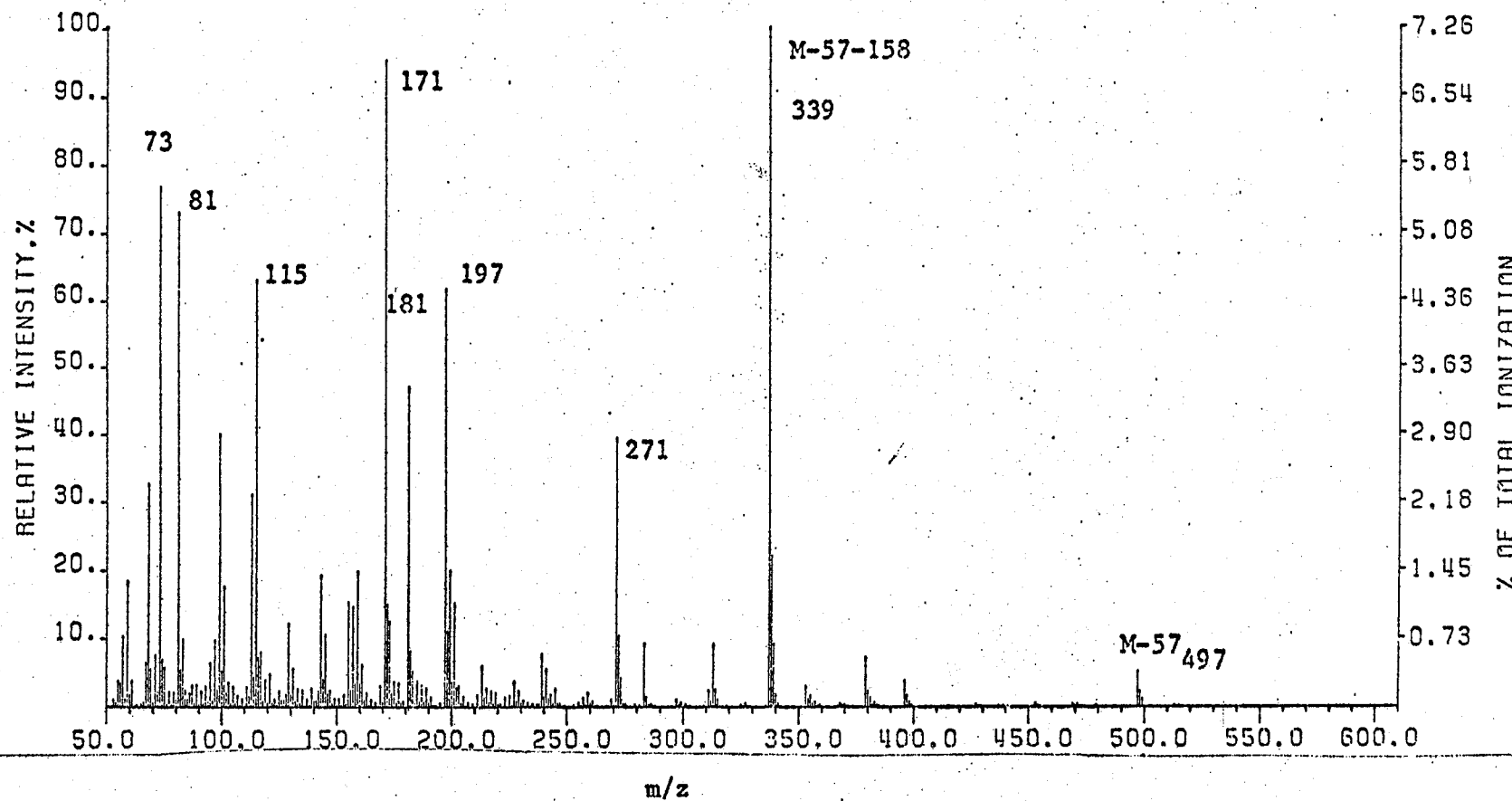


Figure: 37. Mass spectrum of tris-O-TMTBSi-D-2-deoxyribose (I_{ddd} , MW 554, $I_{\text{OV-1}}^{280} = 2878$),
recorded on Finnigan mass spectrometer (model 1015) at 70 eV.

MSGC-3-12/8/76 TMTBS3 2-DE-OXY. RIB.
FINNIGAN-1015 RF-QUADRUPOLE MASS SPECTRUM
CORRECTED FOR MASS DISCRIMINATION.

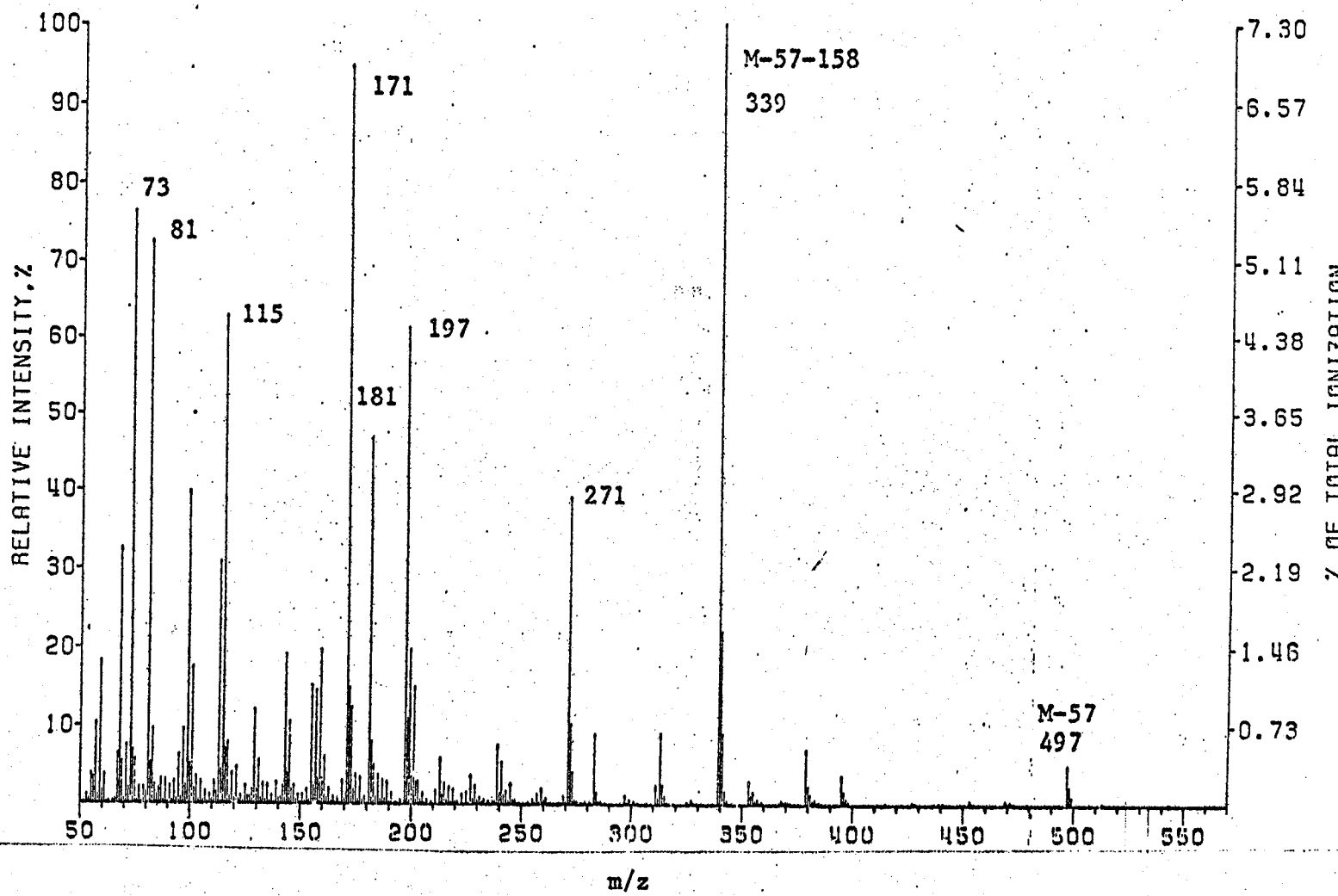
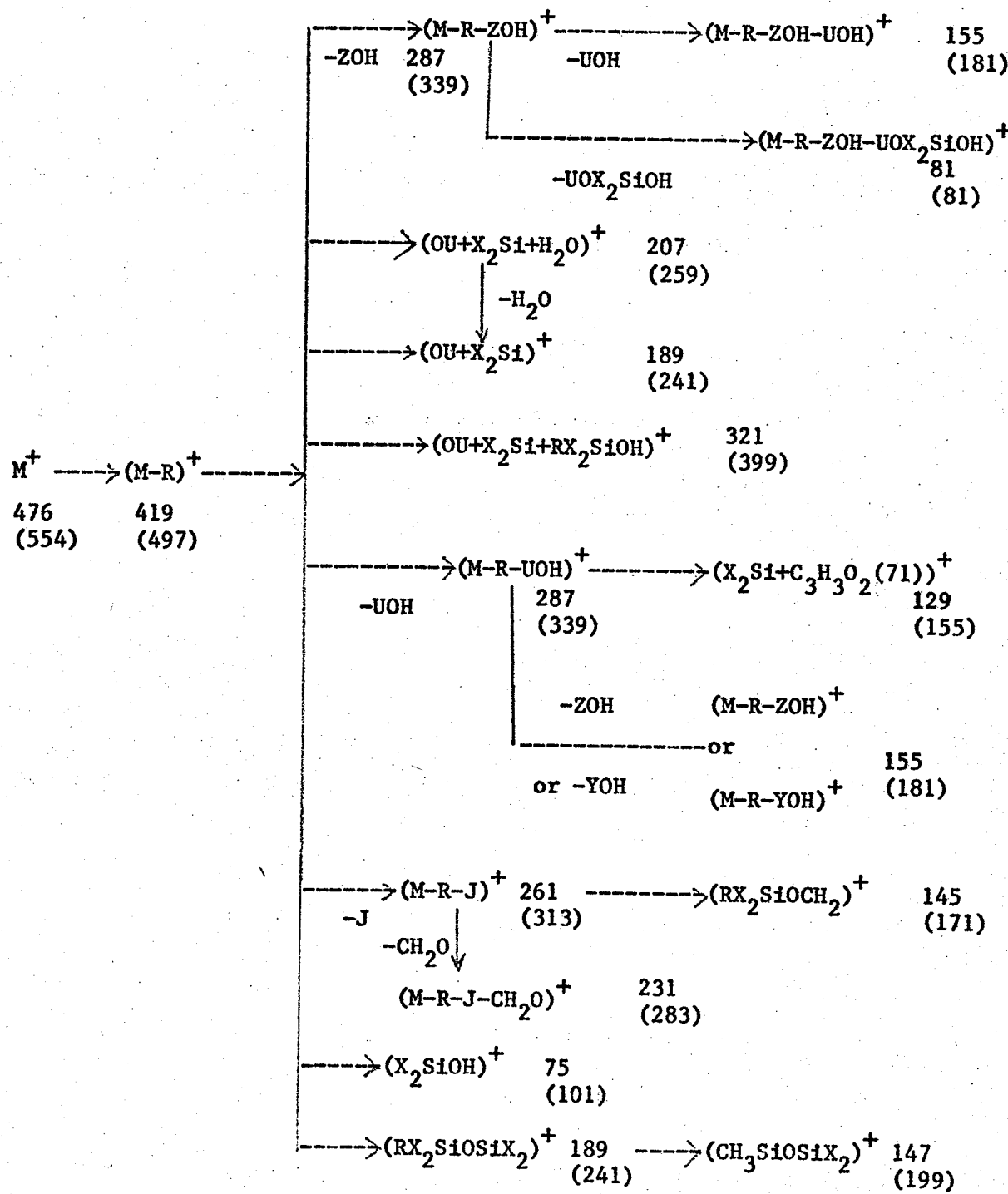


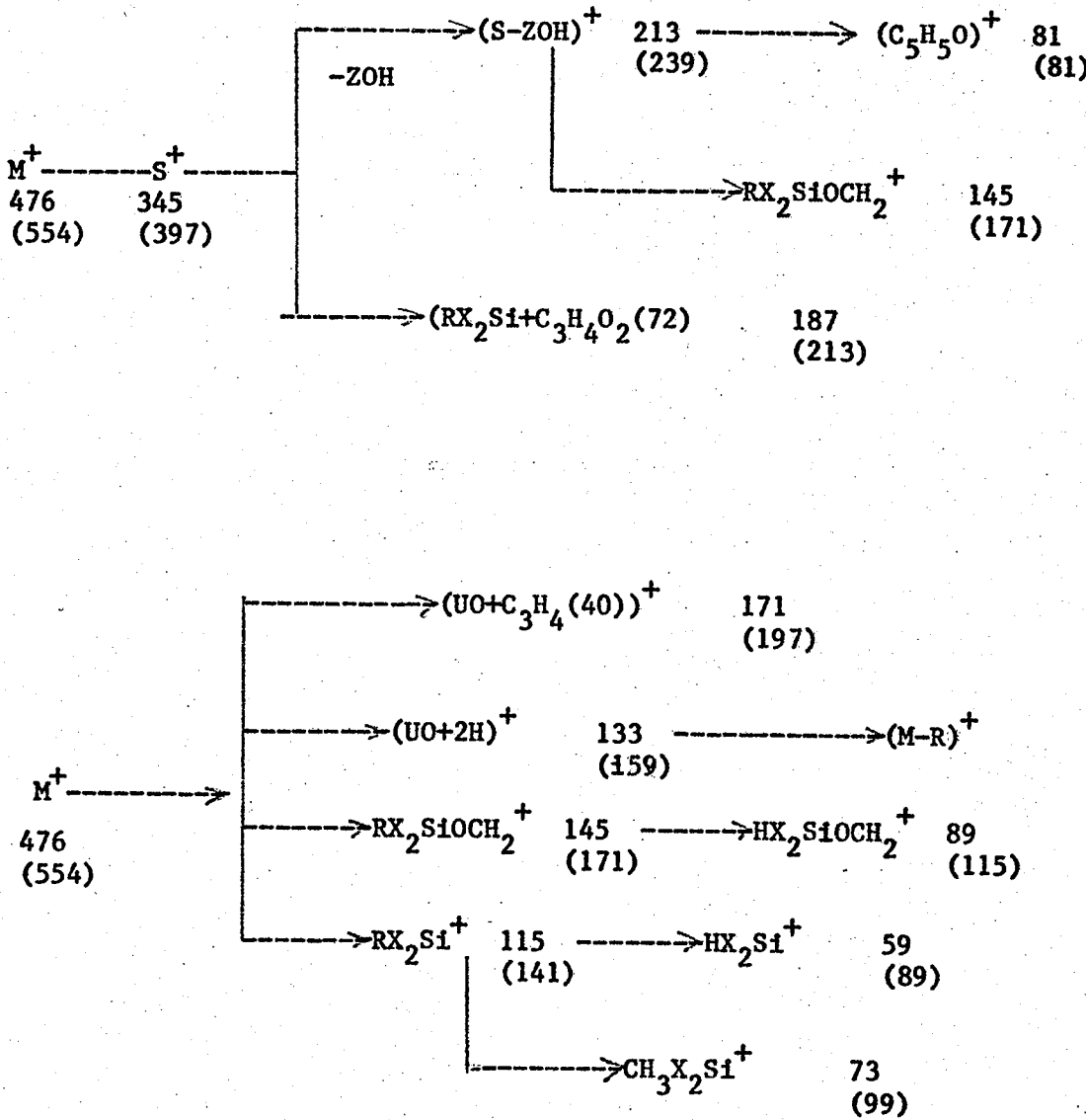
Figure:38. Mass spectrum of tris-O-TMTBSi-D-2-deoxyribose (I_{ddd} , $I_{Ov-1}^{280} = 2932$, MW 554),
recorded on Finnigan 1015 mass spectrometer at 70 eV,

Scheme 13. Mass spectral fragmentation of SCTASi-D-2-deoxyriboses, by analogy with 2'-deoxyribonucleosides (77). All assignments are tentative. Numbers adjacent to ions denote masses of ions for TBDMSi derivatives (no brackets) and for TMTBSi derivatives (with brackets).



Scheme: 13. (Cont'd)

Mass spectral fragmentation of SCTASi-2-deoxyriboses.



(ii) Mass spectral fragmentation of partial SCTASi-D-2-deoxyriboses

Gas chromatography of the reaction mixture gave two peaks corresponding to bis-O-D-2-deoxyriboses. The mass spectra of I_(bb), (figs. 39, 40) show similar breakdown patterns to I_{bbb}. One characteristic ion which is not found in the mass spectra of I_{bbb} is (M-R-H₂O)⁺ at m/z 287, as there is a free hydroxyl group on the molecule. It is extremely difficult to assign correct positions to the silyl groups in the molecule. The maximum number of isomers is six, whereas only two GC peaks were obtained. It is strongly suspected that the GC column did not resolve all the isomers present though it is probable that some were formed in minor amounts.

(iii) Mass spectra of mixed TMSi/TBDMSi derivatives of D-2-deoxyriboses

For I_(abb), which gave a single GC peak rather than the maximum of 6, the mass spectrum (fig. 41) shows only (M-t-Bu)⁺ and a small peak for (M-CH₃)⁺ ion, due to the facile elimination of the bulky t-butyl radical from the TBDMSi-moiety. That there was one TMSi group and two TBDMSi groups in the derivative is shown by the presence of m/z 155 which corresponds to the (M-t-Bu-TBDMSiOH-TMSiOH)⁺ ion.

Conversely, in the mass spectrum of I_(aab) (fig. 42) m/z 155 is represented by (M-t-Bu-2TMSiOH)⁺ which selfexplains the formula of the derivative. (A single GC peak was observed instead of the maximum of 6). Also the TBDMSi group exerts stronger fragmentation 'directing' properties than does the TMSi group. The ion at m/z 103 in the mass spectrum of I_(aab) probably represents TMSiOCH₂⁺.

MSGC-29/7/76 TBDMS2 2-DE-OXY-RIB. PK1
FINNIGAN-1015 RF-QUADRUPOLE MASS SPECTRUM
CORRECTED FOR MASS DISCRIMINATION

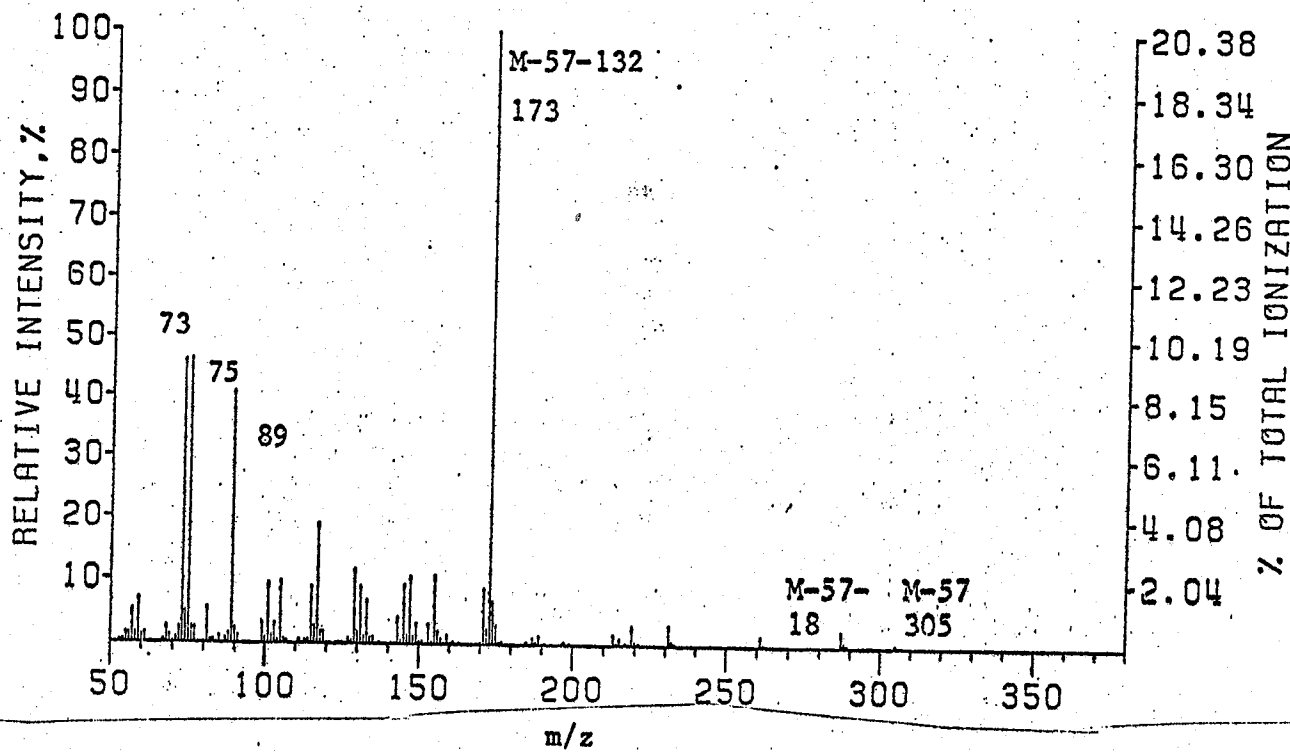


Figure: 39. Mass spectrum of bis-O-TBDMSi-D-2-deoxyribose ($I_{(bb)}$, MW 362, $I_{OV-1}^{210} = 1802$), recorded on Finnigan 1015 mass spectrometer at 70 eV.

MSGC-29/7/76 TBDMS2 2-DE-OXY-RIB. PK2
FINNIGAN-1015 RF-QUADRUPOLE MASS SPECTRUM
CORRECTED FOR MASS DISCRIMINATION

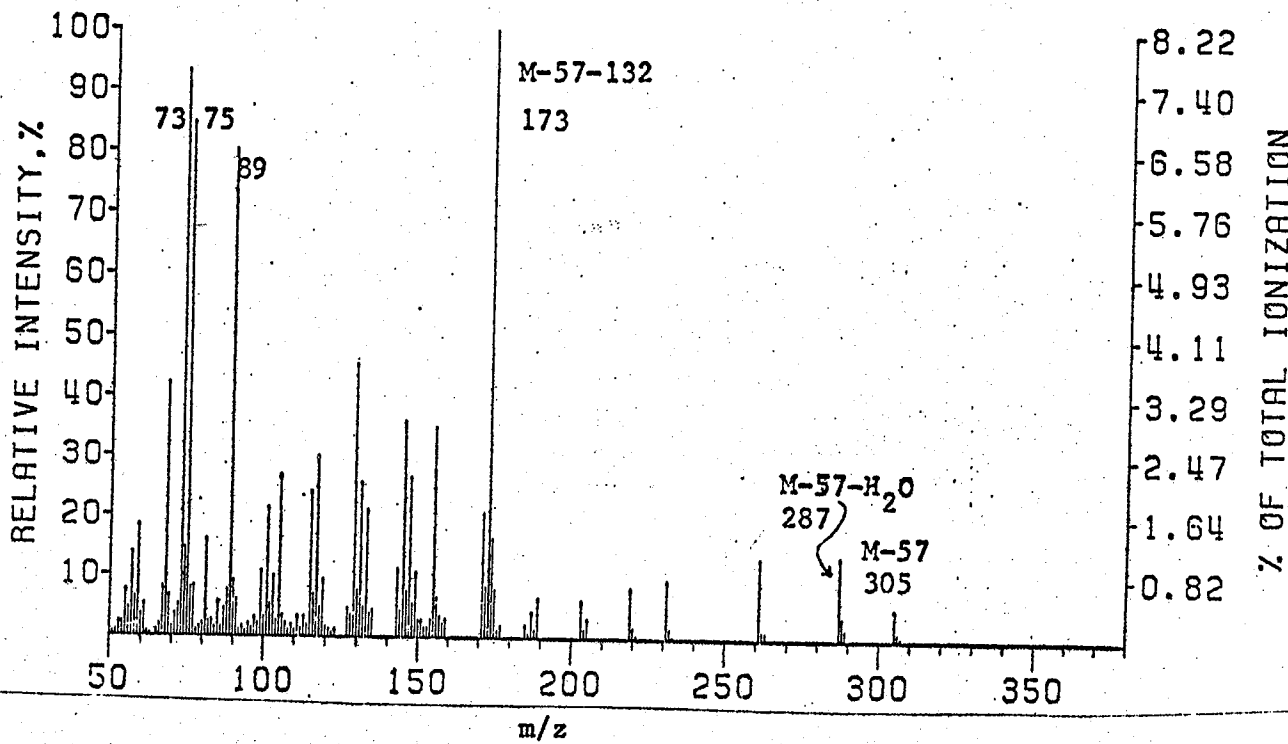


Figure: 40. Mass spectrum of bis-O-TBDMSi-D-deoxyribose(I_(bb)), MW 362, $I_{OV-1}^{210} = 1850$, recorded on Finnigan 1015 mass spectrometer at 70 eV.

MS TMS1 TBDMS2 2-DE-OXY-RIB.
FINNIGAN-1015 RF-QUADRUPOLE MASS SPECTRUM
CORRECTED FOR MASS DISCRIMINATION

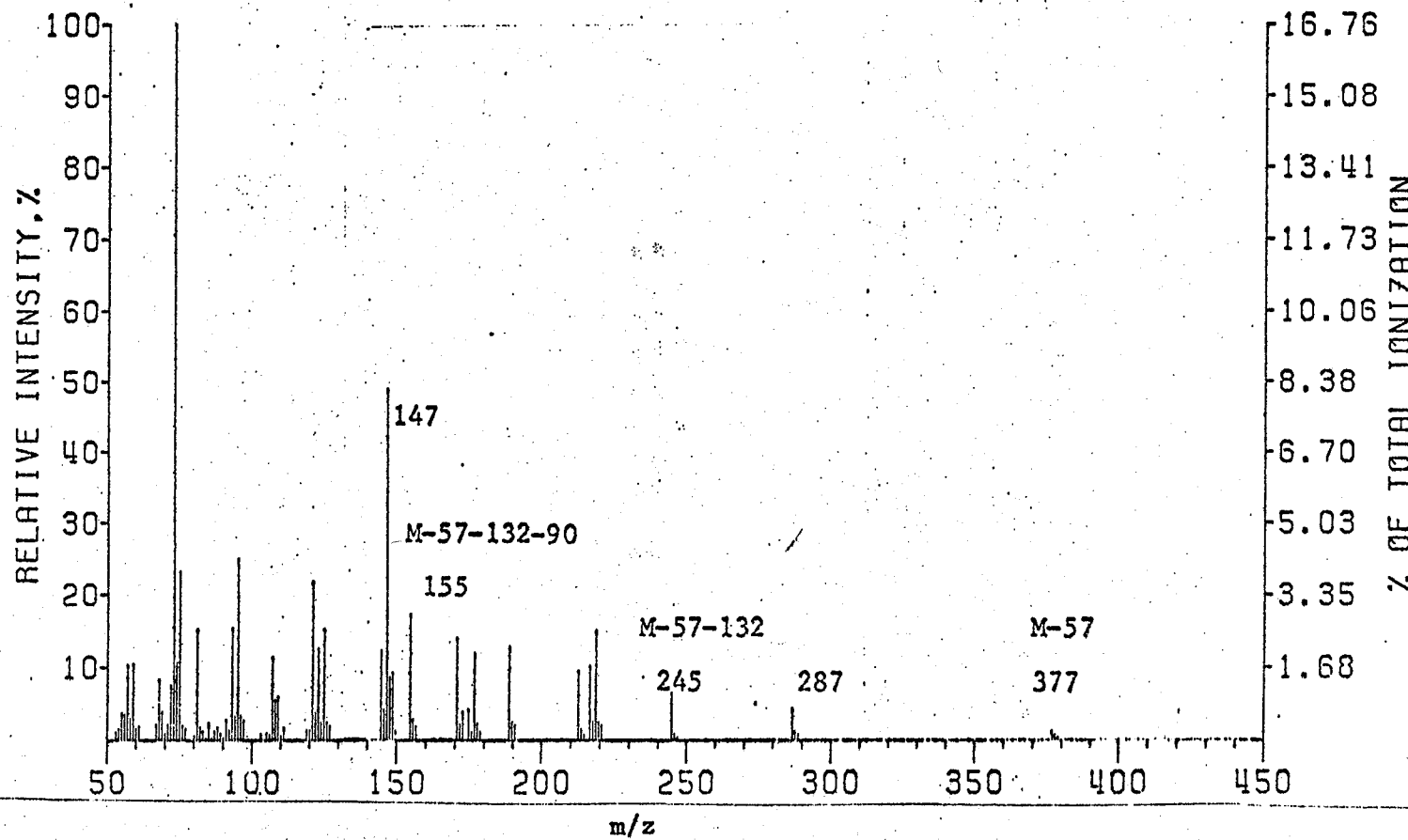


Figure: 41. Mass spectrum of mono-O-TMSi-bis-O-TBDMSi-D-2-deoxyribose ($I_{(abb)}$), MW 434,
recorded on Finnigan 1015 mass spectrometer at 70 eV.

MS TMS2 TBDMS1 2-DE-OXY-RIBOSE
FINNIGAN-1015 RF-QUADRUPOLE MASS SPECTRUM
CORRECTED FOR MASS DISCRIMINATION

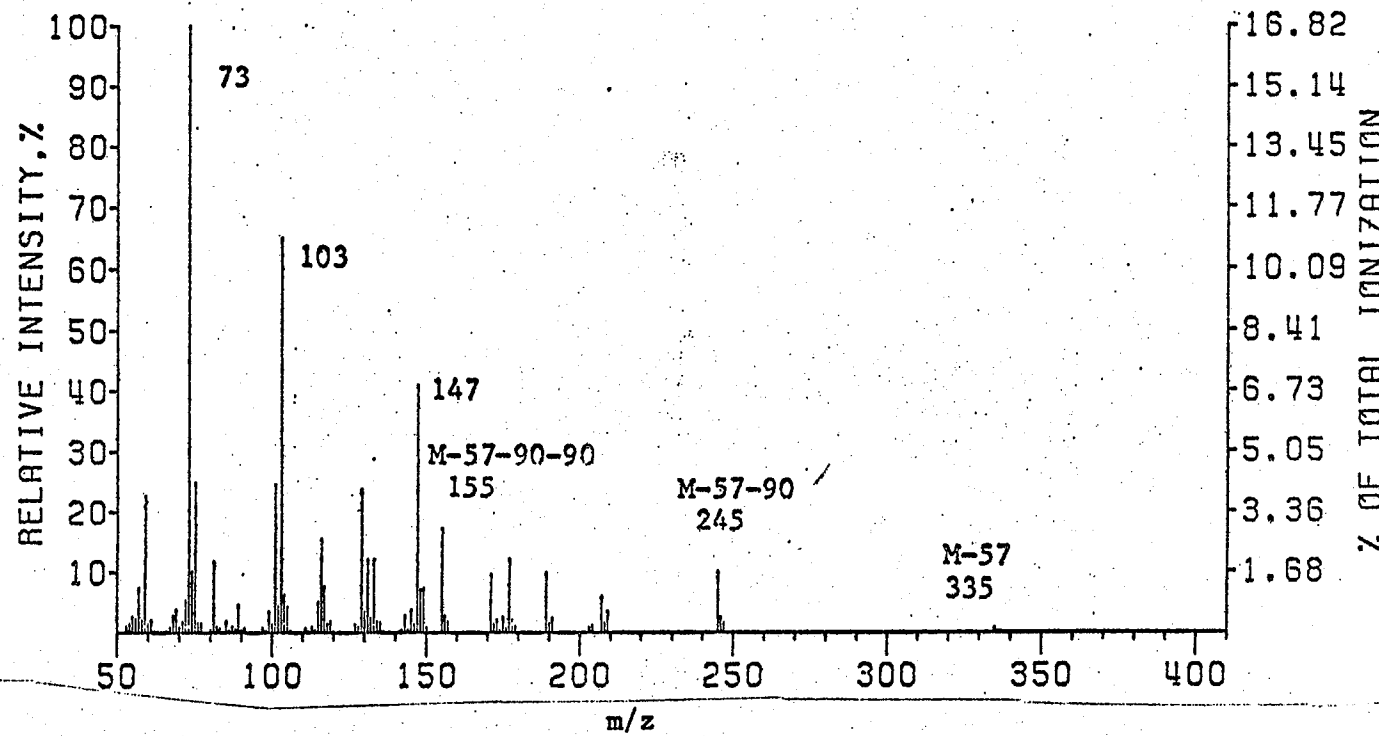


Figure: 42. Mass spectrum of bis-0-TMSi-mono-OTBDMSi-D-2-deoxyribose ($I_{(aab)}$, MW 392), recorded on Finnigan 1015 mass spectrometer at 70 eV.

(c) Mass spectra of SCTASI- β -D-ribofuranosides

i) Whereas mass spectral fragmentation patterns of SCTASI-D-2-deoxyriboses can be explained by analogy with the SCTASI-deoxyribonucleosides, silylated β -D-benzylribofuranosides and silylated D-ribofuranoses are also analogues of silylated ribonucleosides in MS. As figure 43 shows OU and Bz (benzyl) can also be regarded the same as the nucleobase B for mass spectral interpretation purposes. The mass spectra of silyl derivatives of β -D-benzylribofuranosides are shown in figures 44-47, with fragmentation pathways (deduced by analogy with ribonucleosides) given in scheme 14.

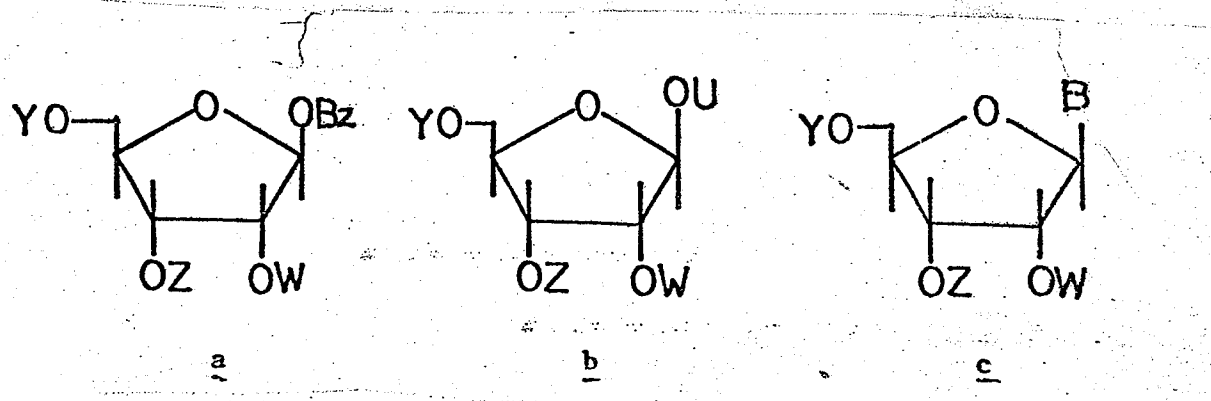


Figure: 43a Comparison of c (SCTASI-ribonucleoside) with a (SCTASI- β -D-ribofuranoside and b (SCTASI-D-ribofuranose). Y, Z, W and U represent SCTASI groups on the oxygen atoms of C₅, C₃, C₂ and C₁ respectively. (B = base and Bz = benzyl)

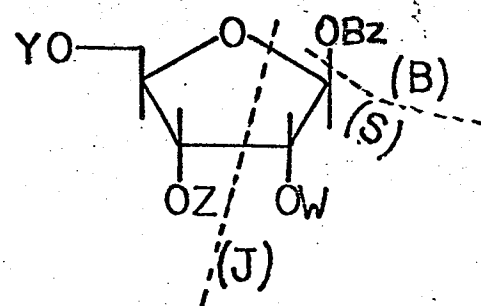


Figure: 43b. Diagram showing major fragments of SCTASI- β -D-ribofuranosides.

MSGC TMS3 BEN. RIB.
FINNIGAN-1015 RF-QUADRUPOLE MASS SPECTRUM
CORRECTED FOR MASS DISCRIMINATION

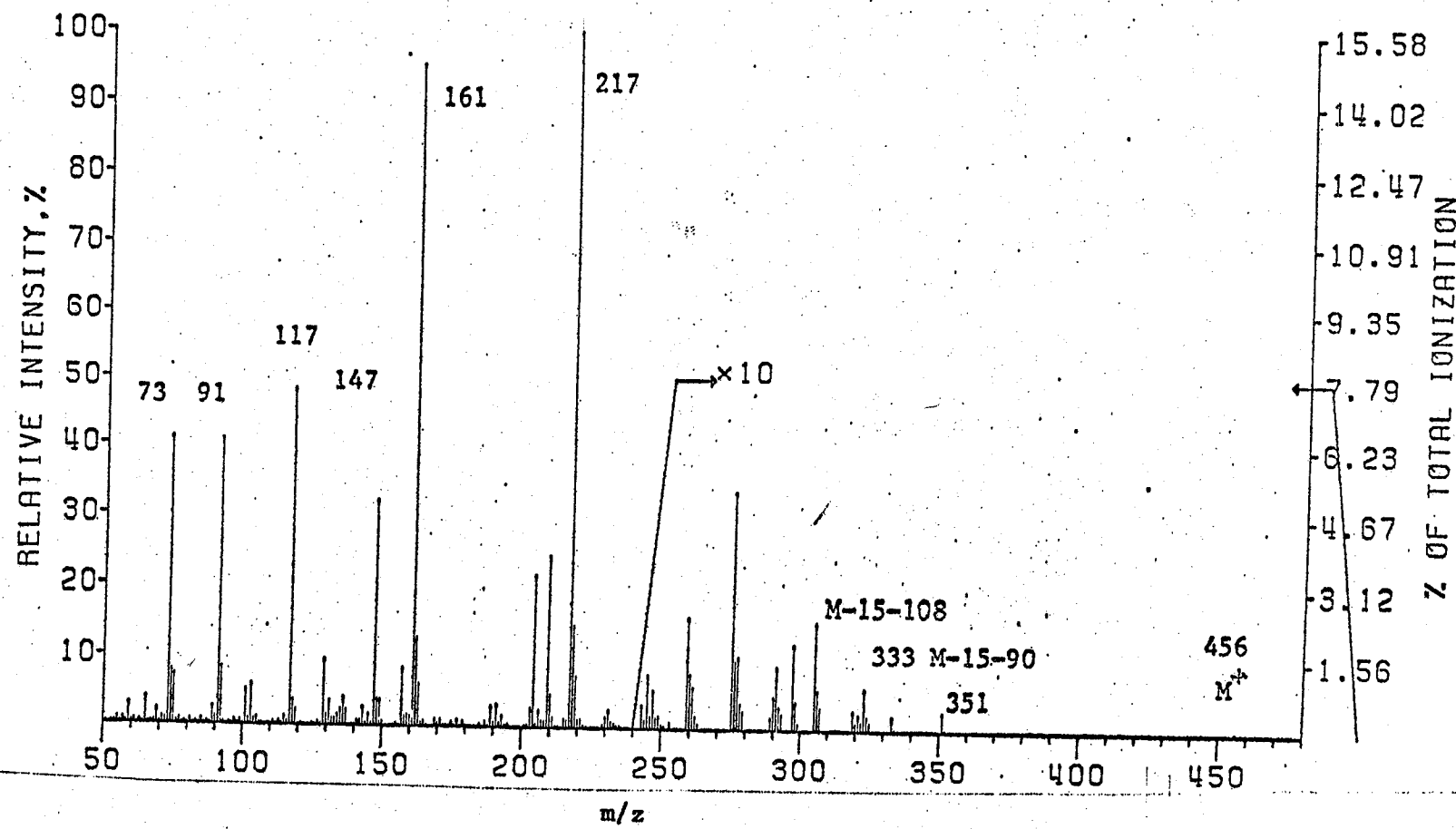


Figure: 44. Mass spectrum of tris-O-TMSi- β -D-benzyl-ribofuranoside (VIII_{aaa}, $I_{OV-1}^{210} = 2140$, MW 456), recorded on Finnigan 1015 mass spectrometer at 70 eV.

MSGC TBDMS3 BEN. RIB.
FINNIGAN-1015 RF-QUADRUPOLE MASS SPECTRUM
CORRECTED FOR MASS DISCRIMINATION

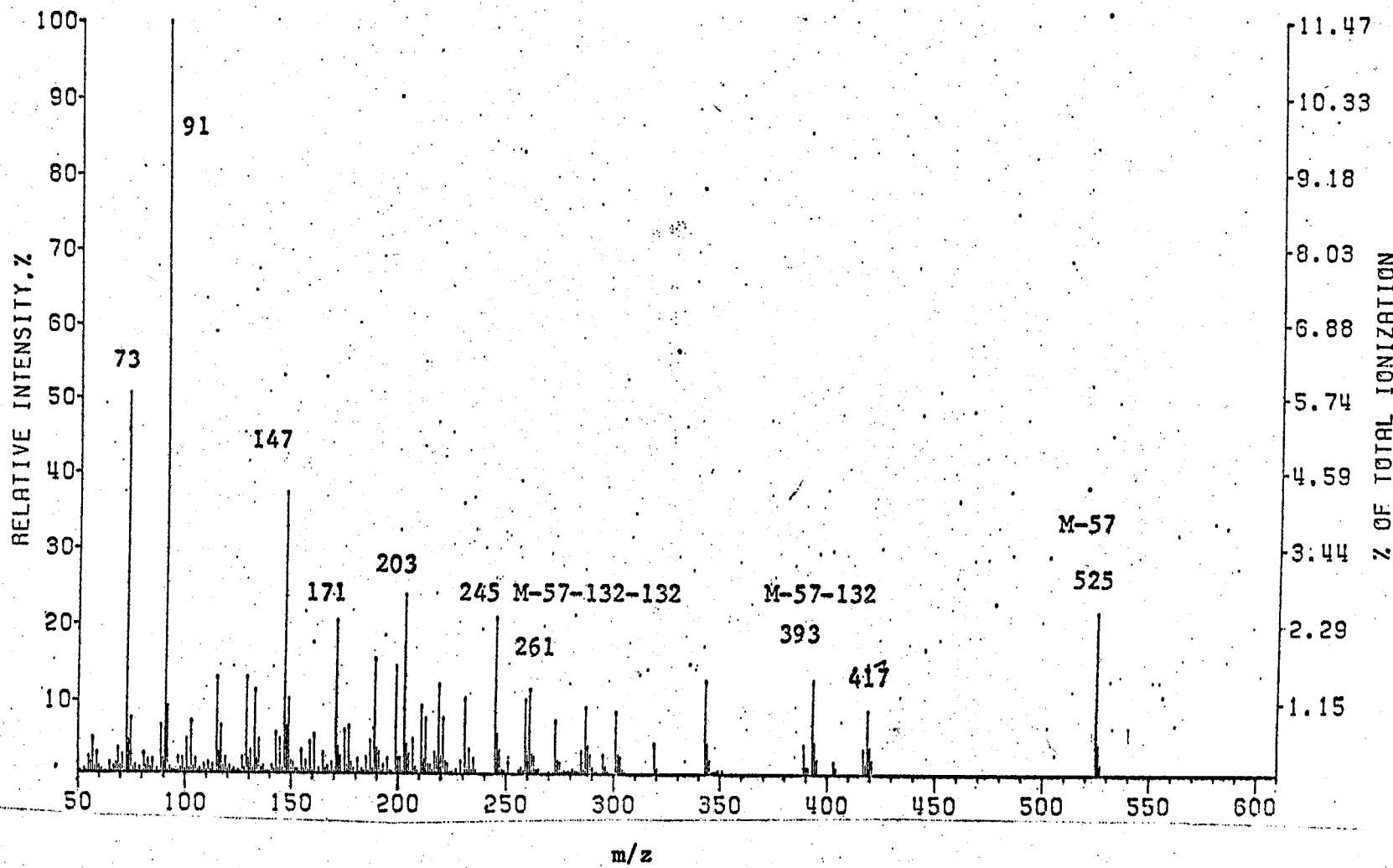


Figure: 45. Mass spectrum of tris-O-TBDMSi- β -D-benzyl-ribofuranoside (VIII_{bbb}, MW 582, $I_{Ov-1}^{280} = 2824$), recorded on Finnigan 1015 mass spectrometer at 70 ev.

MSGC-22-14/8/76 TMIPS3 BEN. RIB. PKS
FINNIGAN-1015 RF-QUADRUPOLE MASS SPECTRUM
CORRECTED FOR MASS DISCRIMINATION

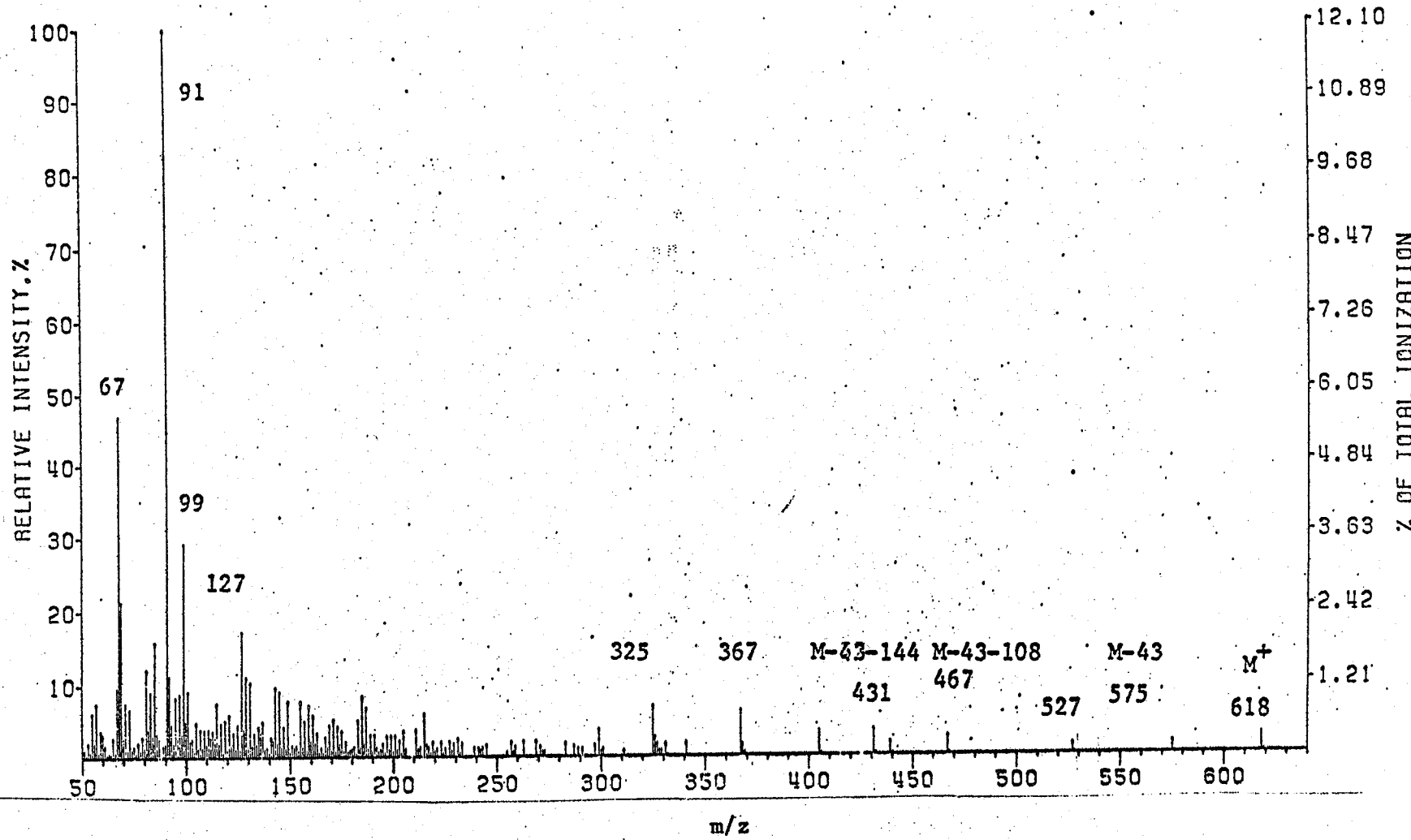


Figure: 46. Mass spectrum of tris-O-TMIPS- β -D-benzyl-ribofuranoside (VIII_{ccc}, MW 618, I_{OV-1}^{280} = 3454), recorded on Finnigan 1015 mass spectrometer at 70 eV.

MSGC-4-14/8/76 TMTBS3 BEN. RIB.
FINNIGAN-1015 RF-QUADRUPOLE MASS SPECTRUM
CORRECTED FOR MASS DISCRIMINATION

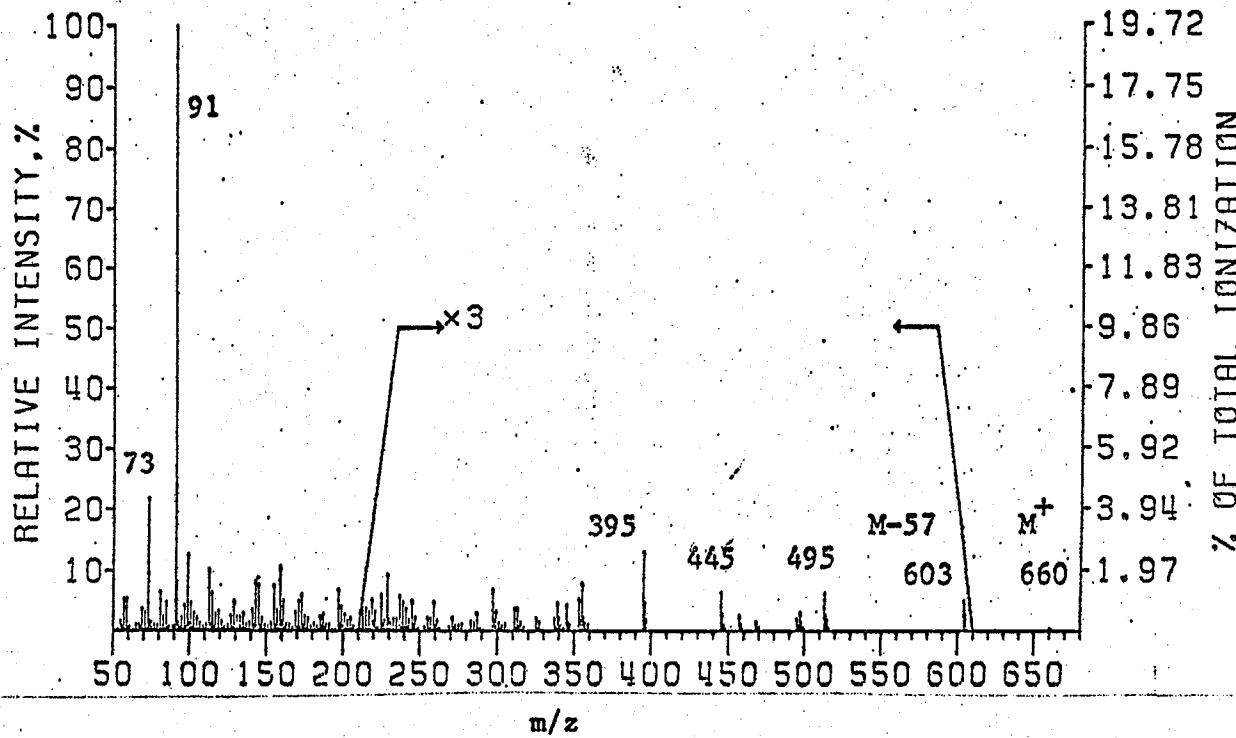
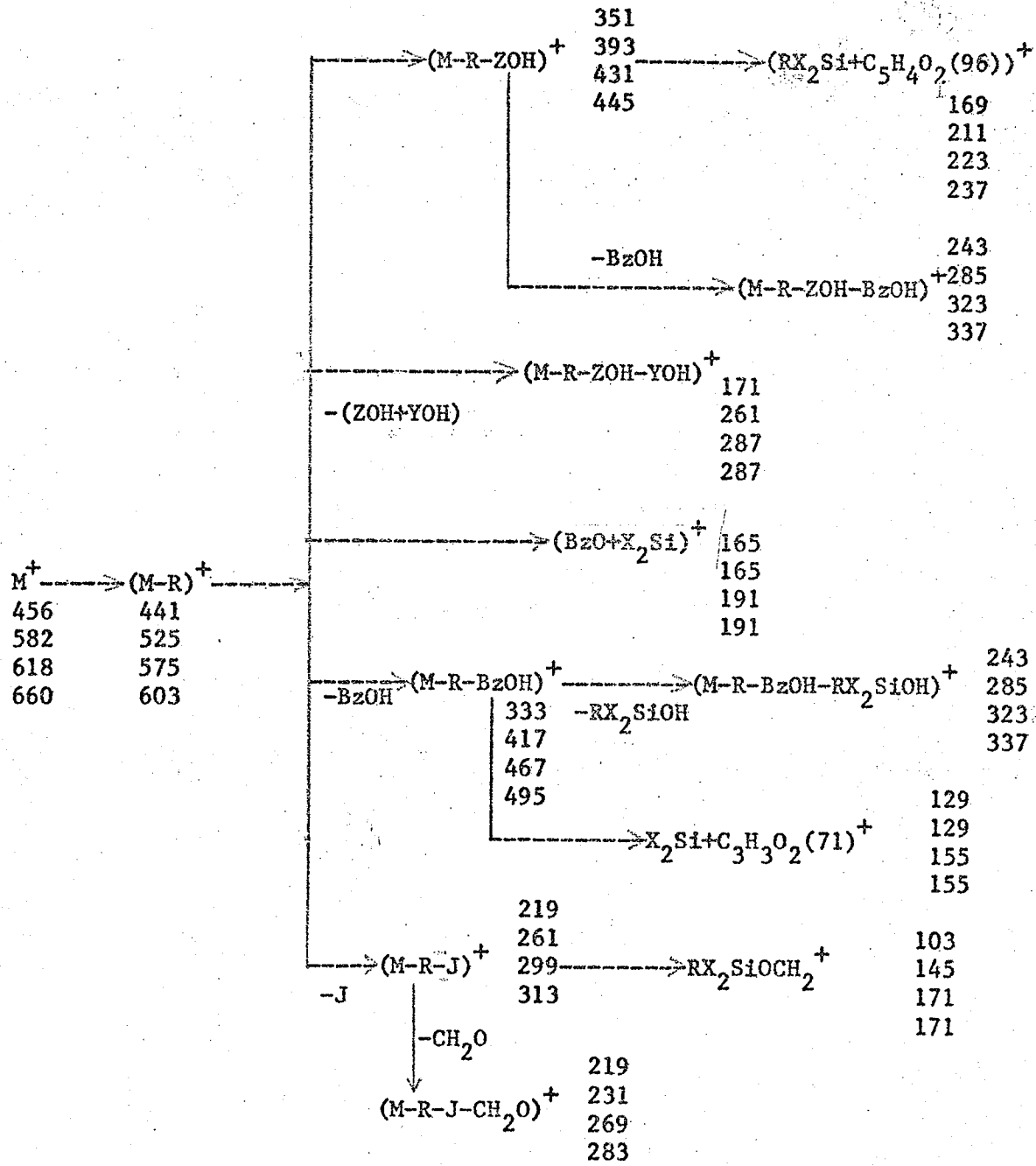
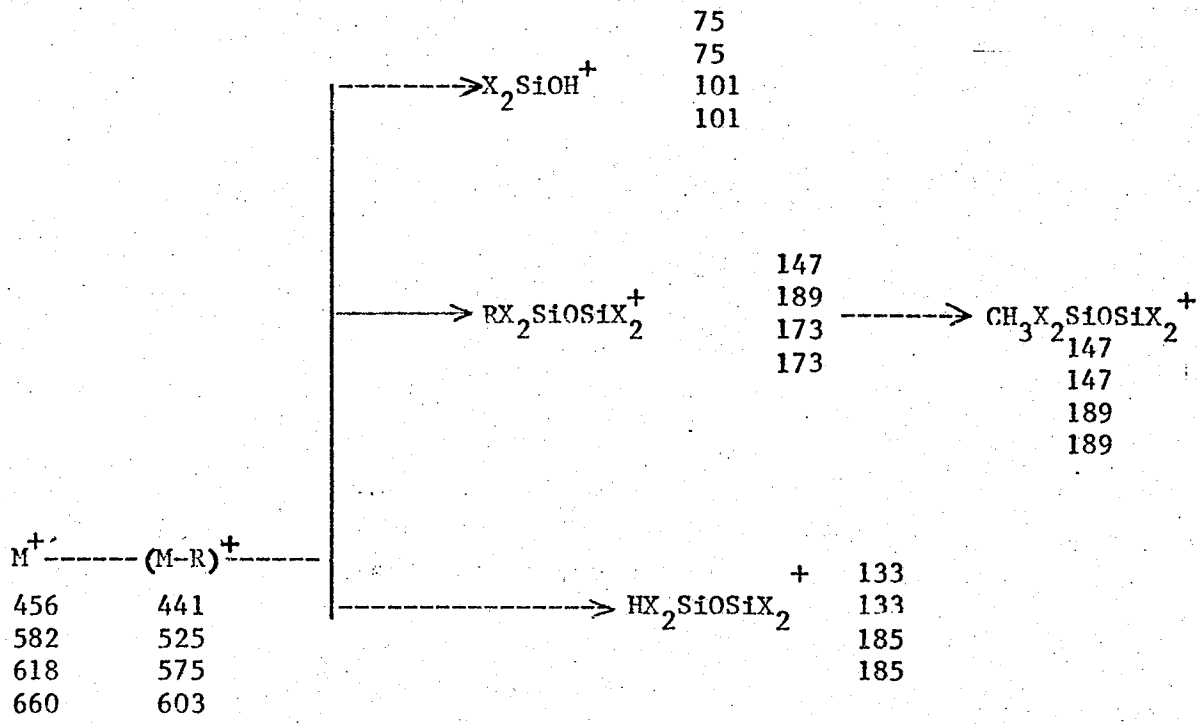


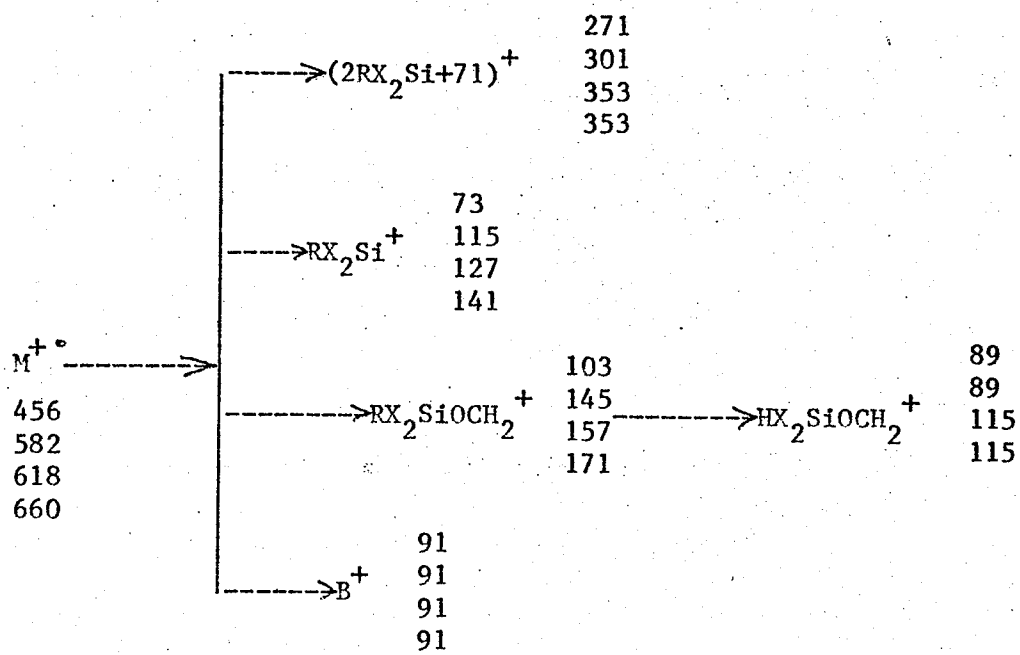
Figure: 47. Mass spectrum of tris-O-TMTBSi- β -D-benzyl-ribofuranoside (VIII_{ddd}, MW 660, I²⁸⁰_{OV-1} = 3578), recorded on Finnigan 1015 mass spectrometer at 70 eV,

Scheme: 14. Mass spectral fragmentation pattern of SCTASi- β -D-benzyl-ribofuranosides. The four numbers adjacent to ions are masses of ions for TMSi, TBDMSi, TMPSi and TMTBSi derivatives respectively.





Scheme: 14 (cont'd) Lower mass ions such as 101, 173, 189 and 185 which contain cyclo-tetramethylene group as X_2 decompose further to give smaller fragments.



Scheme: 14 (cont'd)

Some lower mass ions such as 127, 141, 129, 157, 171 and 115 which contain cyclo-tetramethylene group as X_2 decompose further into smaller fragments.

$J = B + C_2H_2 + OW$; J for $VIII_{aaa} = 222$; for $VIII_{bbb} = 264$; for $VIII_{ccc} = 276$ and for $VIII_{ddd} = 290$.

ii) Partial SCTASI- β -D-benzylribofuranosides

The mass spectra of mono-TBDMSi and mono-TMTBSi derivatives (all three isomers were separated by GC in each case-figs. 14,15) are shown in figs. 48-53. The mass spectra of bis-TBDMSi derivatives (three GC peaks fig.14) and bis-TMTBSi derivatives (two GC peaks, fig. 16) are shown in figs. 54-58. All mass spectra show characteristic $(M-t\text{-Bu}-H_2O)^+$ ions as well as $(M-t\text{-Bu}-BzOH)^+$ ions. $C_7H_7^+$ is the base peak in all spectra, showing the well-known stability of this ion (usually assigned the tropylion structure).

Some variations in peak heights in the mass spectra of isomeric derivatives are also observed.

SPECTRUM RECORDED ON 1015 QUADRUPOLE MASS SPECTROMETER
AND NORMALIZED TO CONSTANT SENSITIVITY.

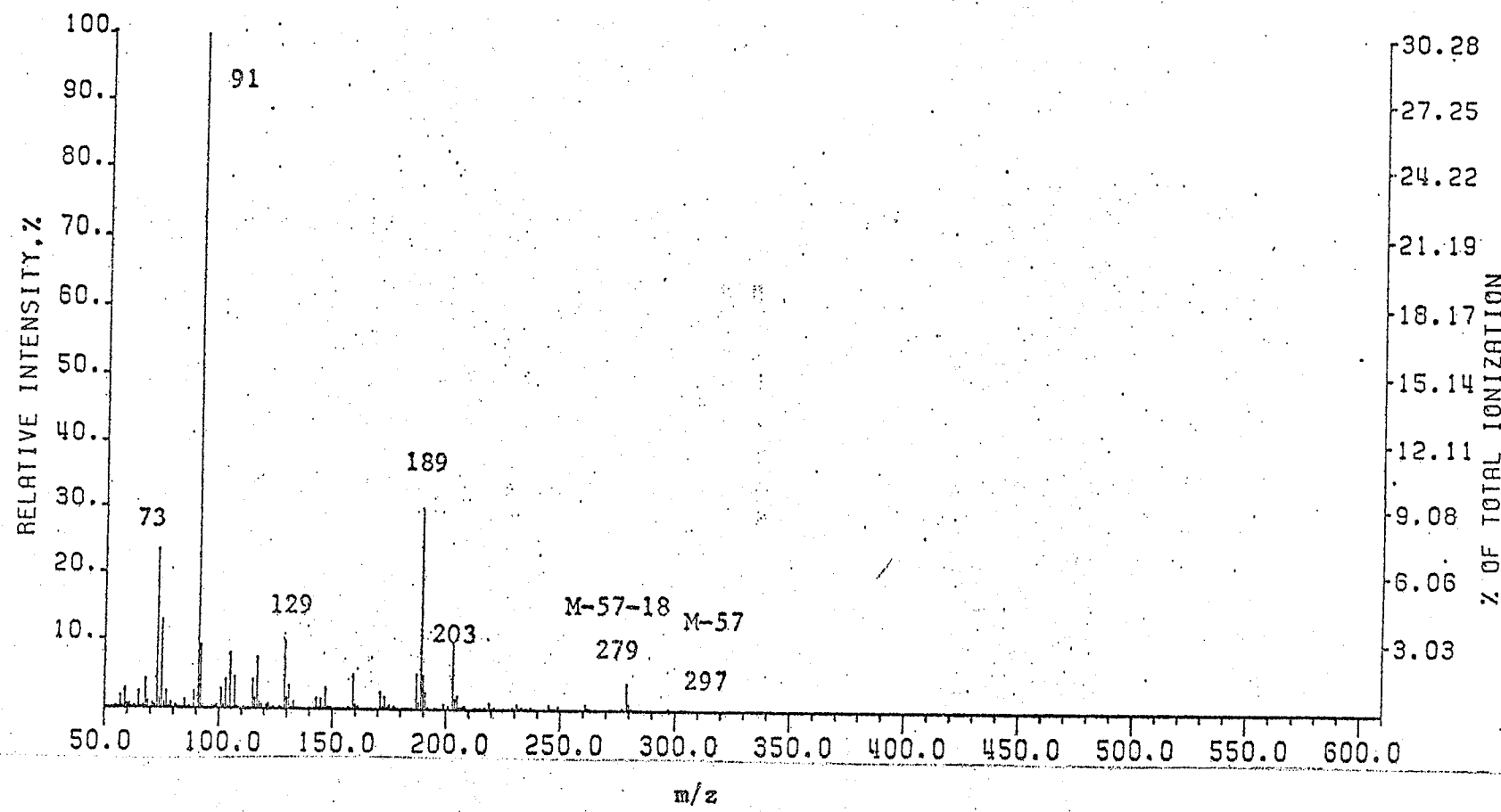


Figure: 48. Mass spectrum of mono-O-TBDMSi- β -D-benzylribofuranoside (VIII_(b)), MW 354, $I_{\text{OV-1}}^{240} = 2241$, recorded on Finnigan 1015 mass spectrometer at 70 eV.

TBDMS1 BEN. RIBOSIDE PK2
FINNIGAN-1015 RF-QUADRUPOLE MASS SPECTRUM
CORRECTED FOR MASS DISCRIMINATION

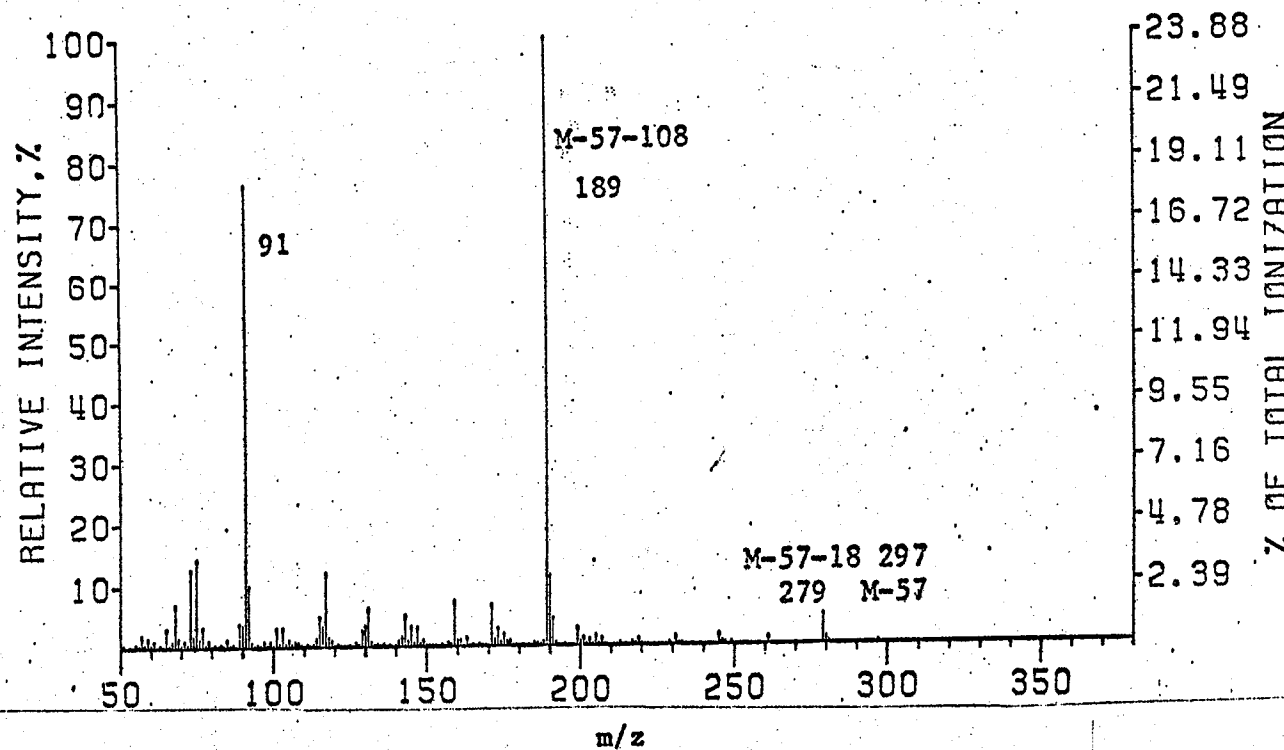


Figure: 49. Mass spectrum of mono-O-TBDMS1- β -D-benzyl-ribofuranoside (VIII(b)), MW 354, $I_{OV-1}^{240} = 2273$, recorded on Finnigan 1015 mass spectrometer at 70 eV.

MSGC-4-24/7/76 TBDMSI BEN. RIB. PK3
FINNIGAN-1015 RF-QUADRUPOLE MASS SPECTRUM
CORRECTED FOR MASS DISCRIMINATION

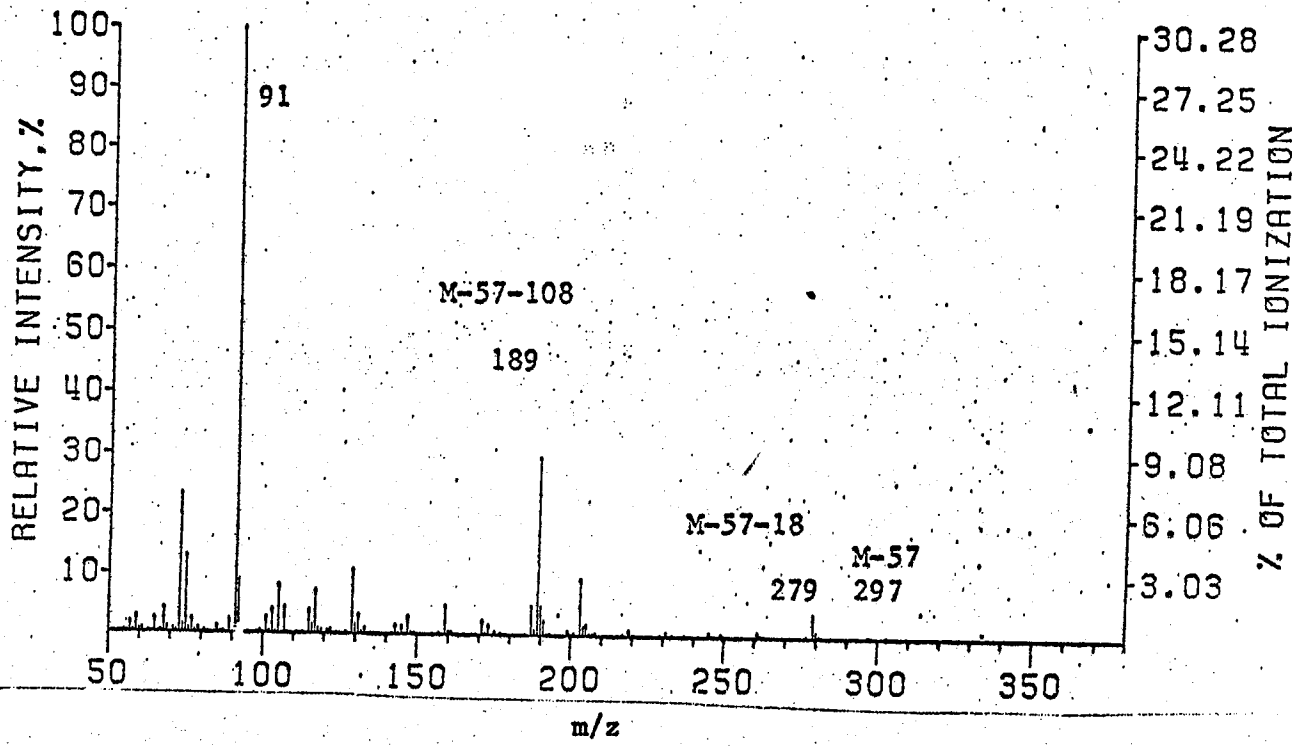


Figure: 50. Mass spectrum of mono-O-TBDMSI- β -D-benzyl-ribofuranoside (VIII_(b), MW 354, $I_{OV-1}^{240} = 2337$), recorded on Finnigan 1015 mass spectrometer at 70 eV.

MSGC-12-16/8/76 TMTBS1 BEN. RIB. PK21
FINNIGAN-1015 RF-QUADRUPOLE MASS SPECTRUM
CORRECTED FOR MASS DISCRIMINATION

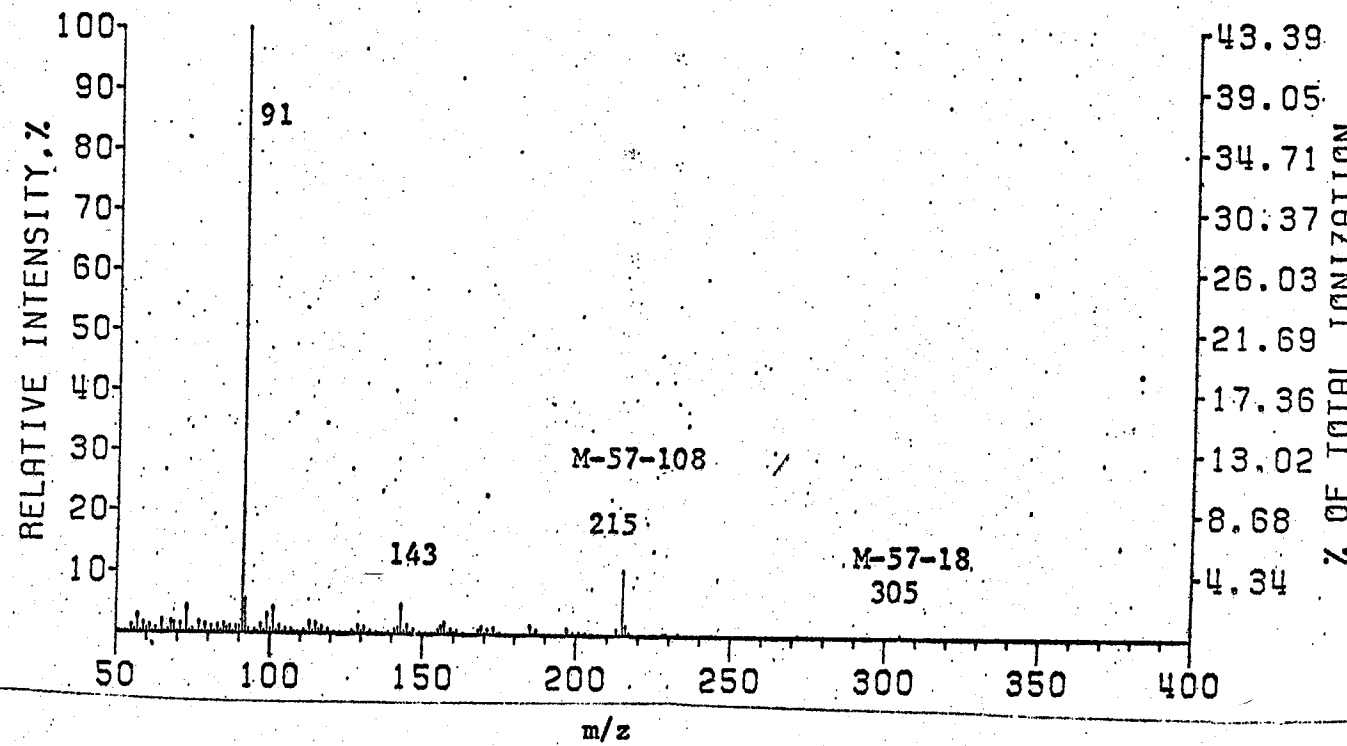


Figure: 51. Mass spectrum of mono-O-TMTBS1- β -D-benzyl-ribofuranoside (VIII_(d), MW 380, $I_{Ov-1}^{240} = 2510$), recorded on Finnigan 1015 mass spectrometer at 70 eV.

TMTBSI BEN. RIB. MSGC-12-16/8/76 PK22
FINNIGAN-1015 RF-QUADRUPOLE MASS SPECTRUM
CORRECTED FOR MASS DISCRIMINATION

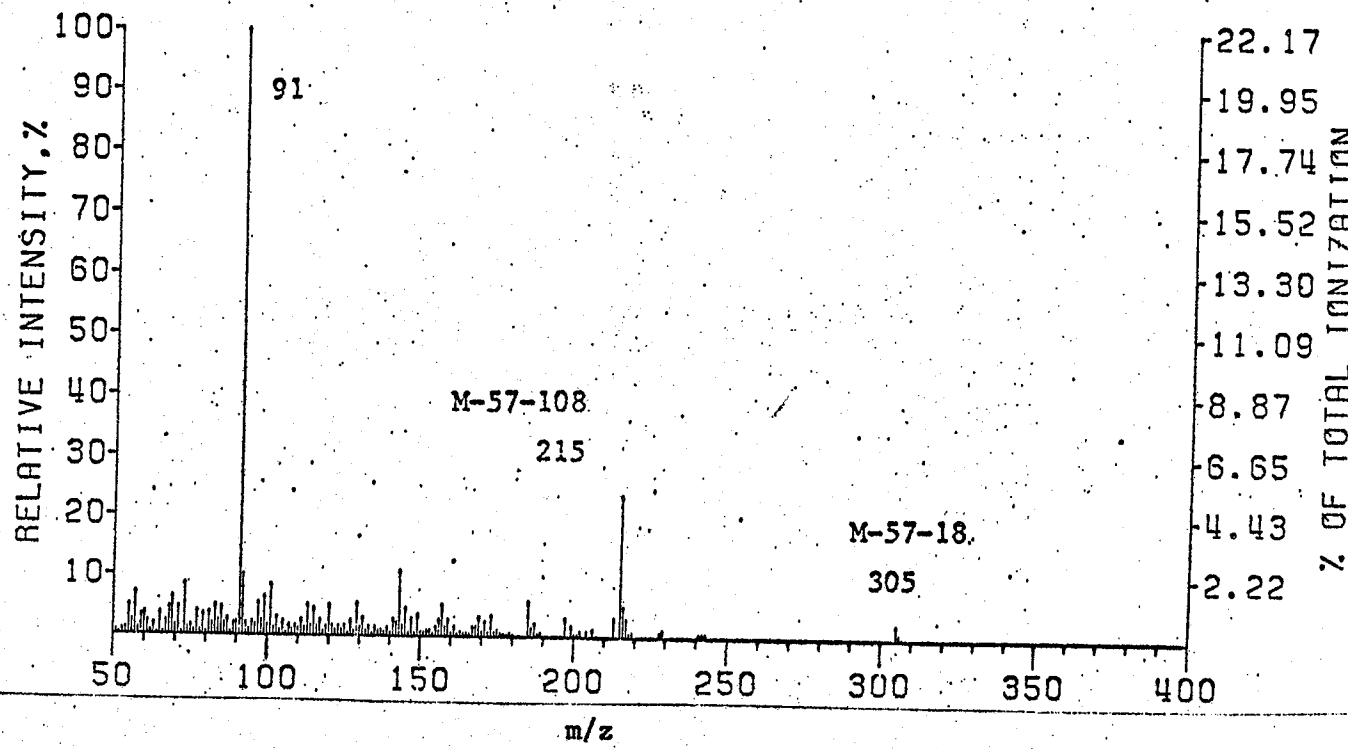


Figure: 52. Mass spectrum of mono-O-TMTBSi- β -D-benzyl-ribofuranoside (VIII_(d), MW 380, $I_{\text{OV-1}}^{240} = 2546$), recorded on Finnigan 1015 mass spectrometer at 70 eV.

MSGC-12-16/8/76 TMTBS BEN. RIB. PK23
FINNIGAN-1015 RF-QUADRUPOLE MASS SPECTRUM
CORRECTED FOR MASS DISCRIMINATION

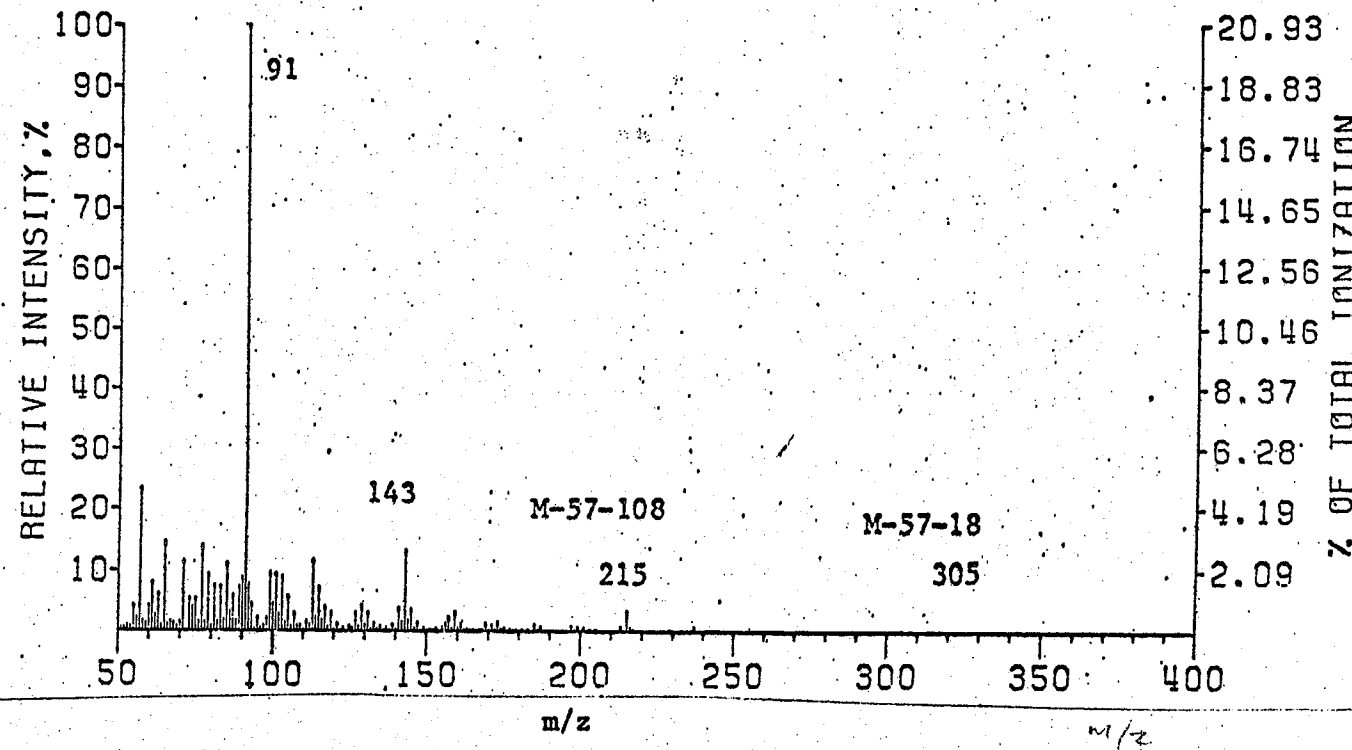


Figure: 53. Mass spectrum of mono-O-TMTBSi- β -D-benzyl-ribofuranoside (VIII_(d), MW 380, $I_{OV-1}^{240} = 2629$), recorded on Finnigan 1015 mass spectrometer at 70 eV.

MSGC-4-24/7/76 TBDMS2-BEN. RIB. PK4
 FINNIGAN-1015 RF-QUADRUPOLE MASS SPECTRUM
 CORRECTED FOR MASS DISCRIMINATION

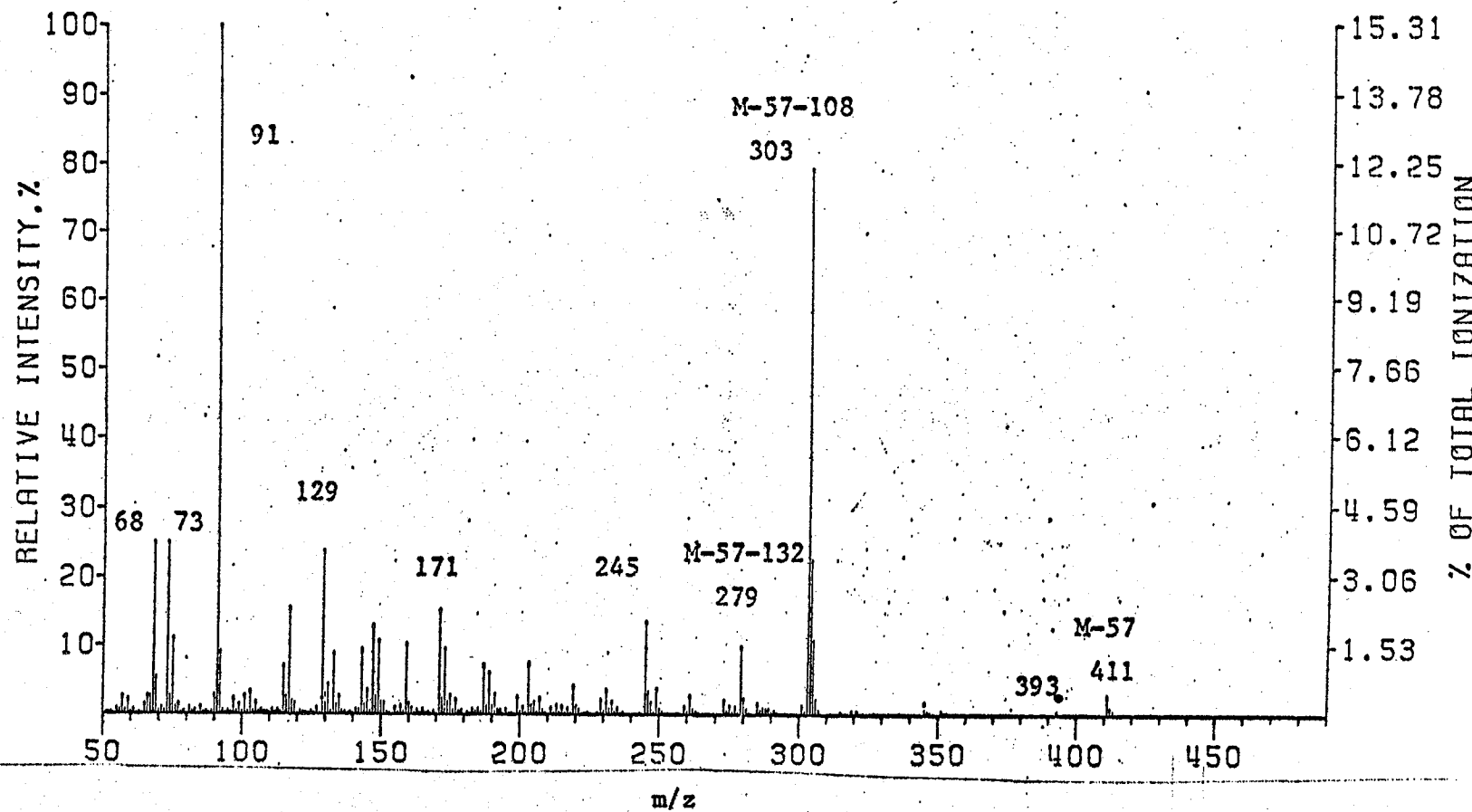


Figure: 54. Mass spectrum of bis-O-TBDMS- β -D-benzyl-ribofuranoside (VIII_(bb), MW 468, $I_{OV-1}^{240} = 2521$), recorded on Finnigan 1015 mass spectrometer at 70 eV.

MSGC-4-24/7/76 TBDMS2-BEN.RIB. PK5
 FINNIGAN-1015 RF-QUADRUPOLE MASS SPECTRUM
 CORRECTED FOR MASS DISCRIMINATION

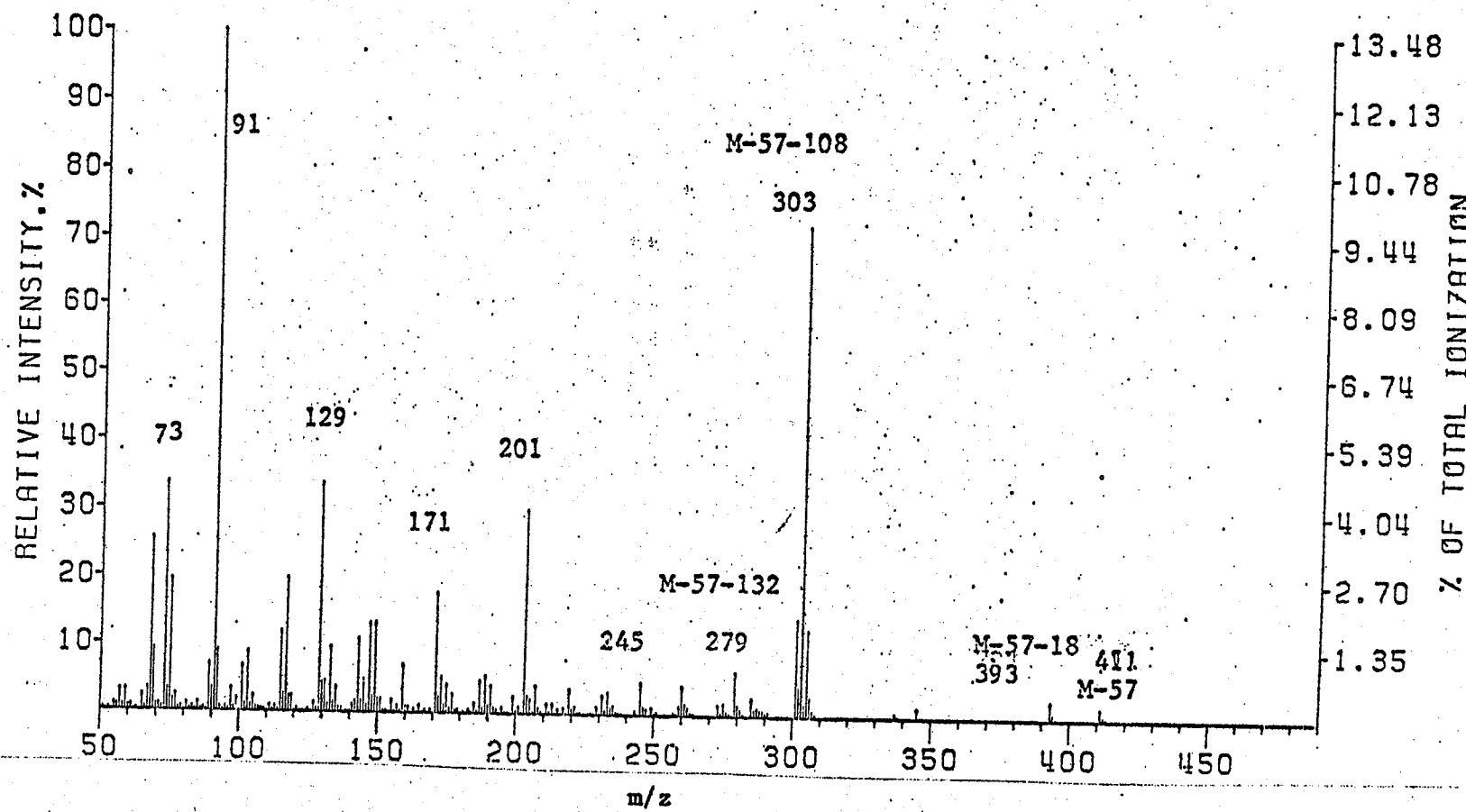


Figure: 55. Mass spectrum of bis-O-TBDMS- β -D-benzyl-ribofuranoside (VIII_(bb)), MW 468, $I_{Ov-1}^{240} = 2569$, recorded on Finnigan 1015 mass spectrometer at 70 eV.

MSGC-4-24/7/76 TBDMS2-BEN. RIB. PK6
FINNIGAN-1015 RF-QUADRUPOLE MASS SPECTRUM
CORRECTED FOR MASS DISCRIMINATION

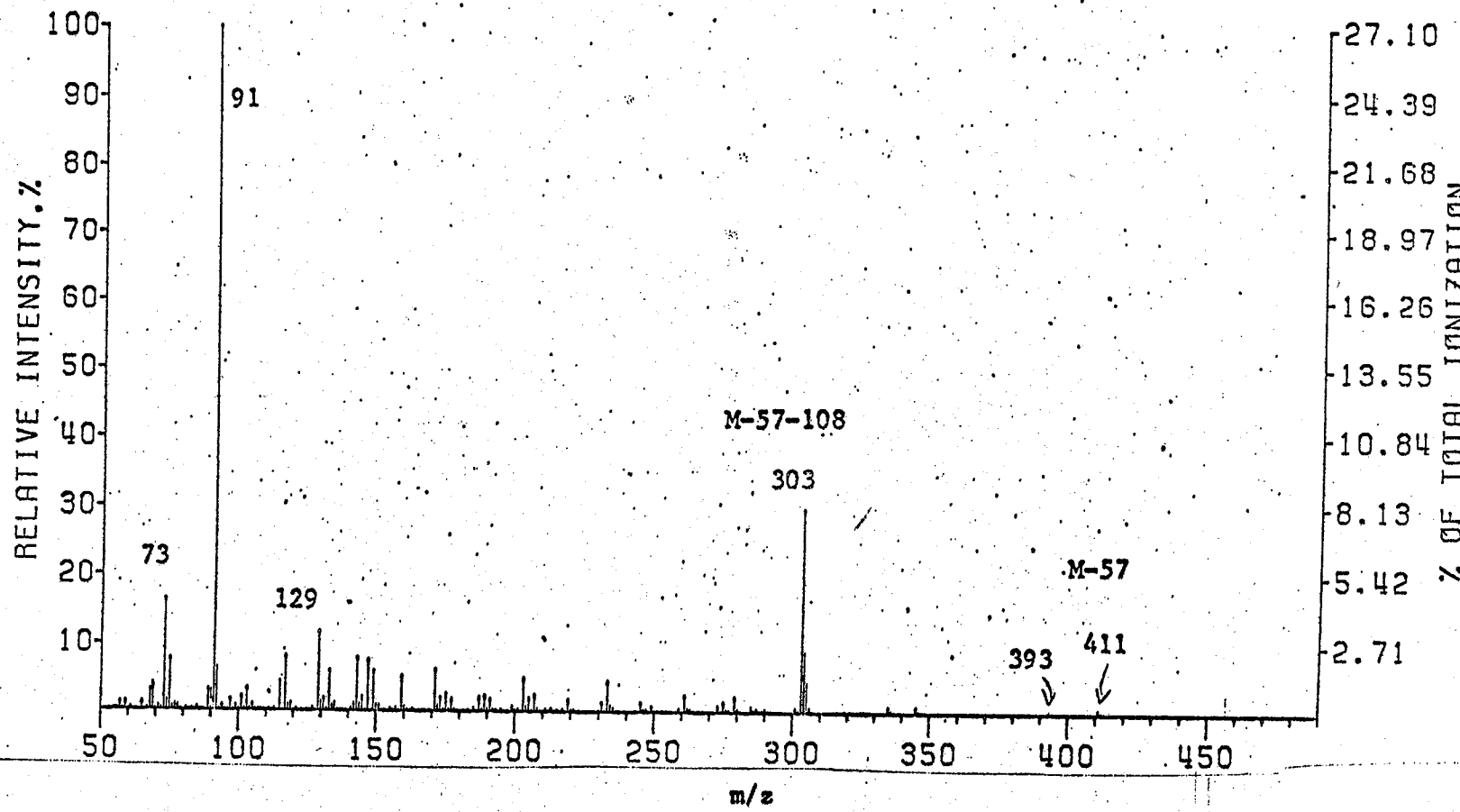


Figure: 56. Mass spectrum of bis-O-TBDMS- β -D-benzyl-ribofuranoside (VIII_(bb)), MW 468, $I_{OV-1}^{240} = 2604$, recorded on Finnigan 1015 mass spectrometer at 70 eV.

MSGC-1-12/8/76 TMTBS2 BEN. RIB. PK1
FINNIGAN-1015 RF-QUADRUPOLE MASS SPECTRUM
CORRECTED FOR MASS DISCRIMINATION

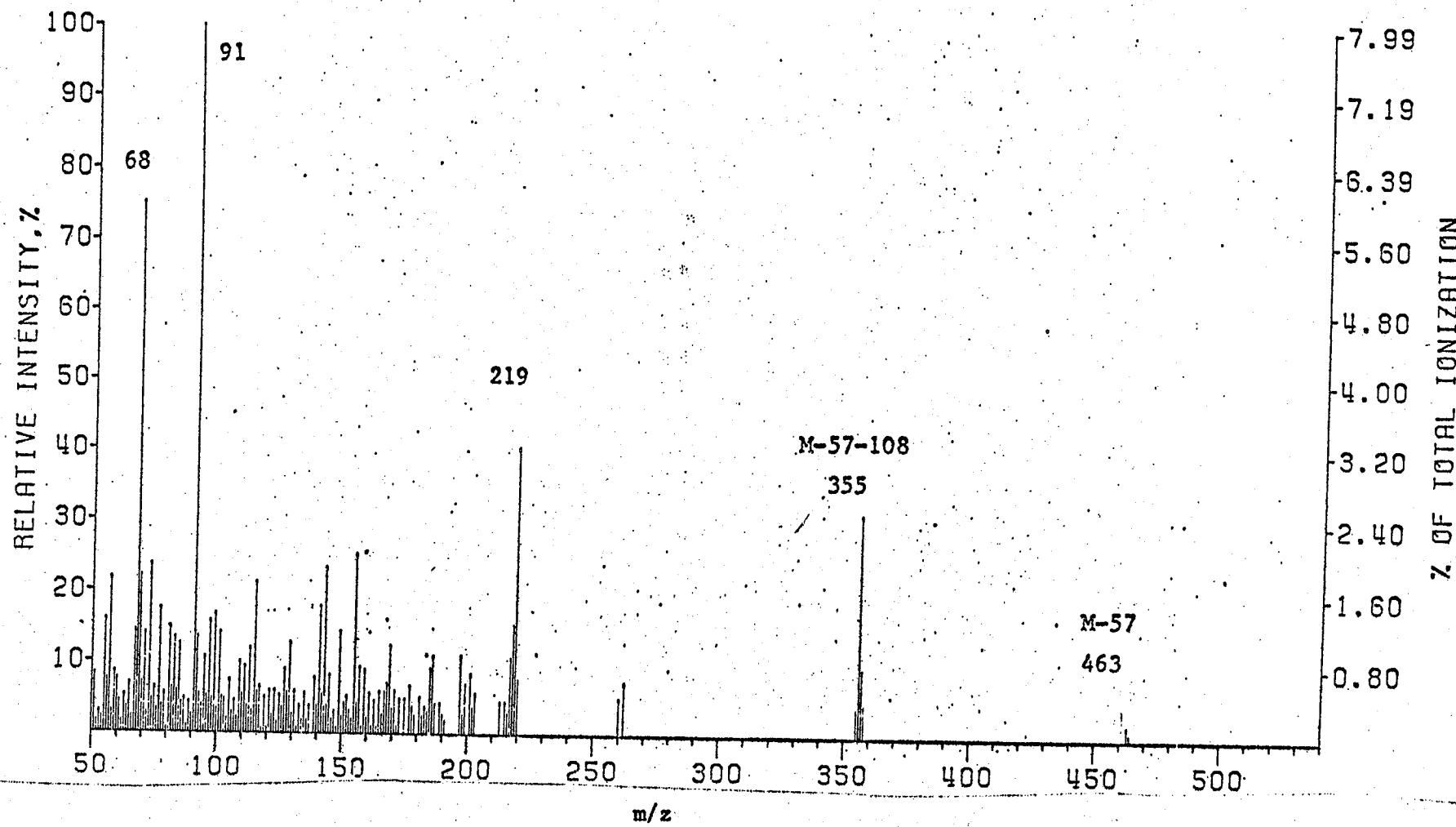


Figure:57. Mass spectrum of bis-O-TMTBSi- β -D-benzyl-ribofuranoside (VIII) (dd), MW 540, $I_{Ov-H}^{280} = 3058$, recorded on Finnigan 1015 mass spectrometer at 70 ev.

MSGC-2-12/8/76 TMTBS2 BEN. RIB. PK2
FINNIGAN-1015 RF-QUADRUPOLE MASS SPECTRUM
CORRECTED FOR MASS DISCRIMINATION

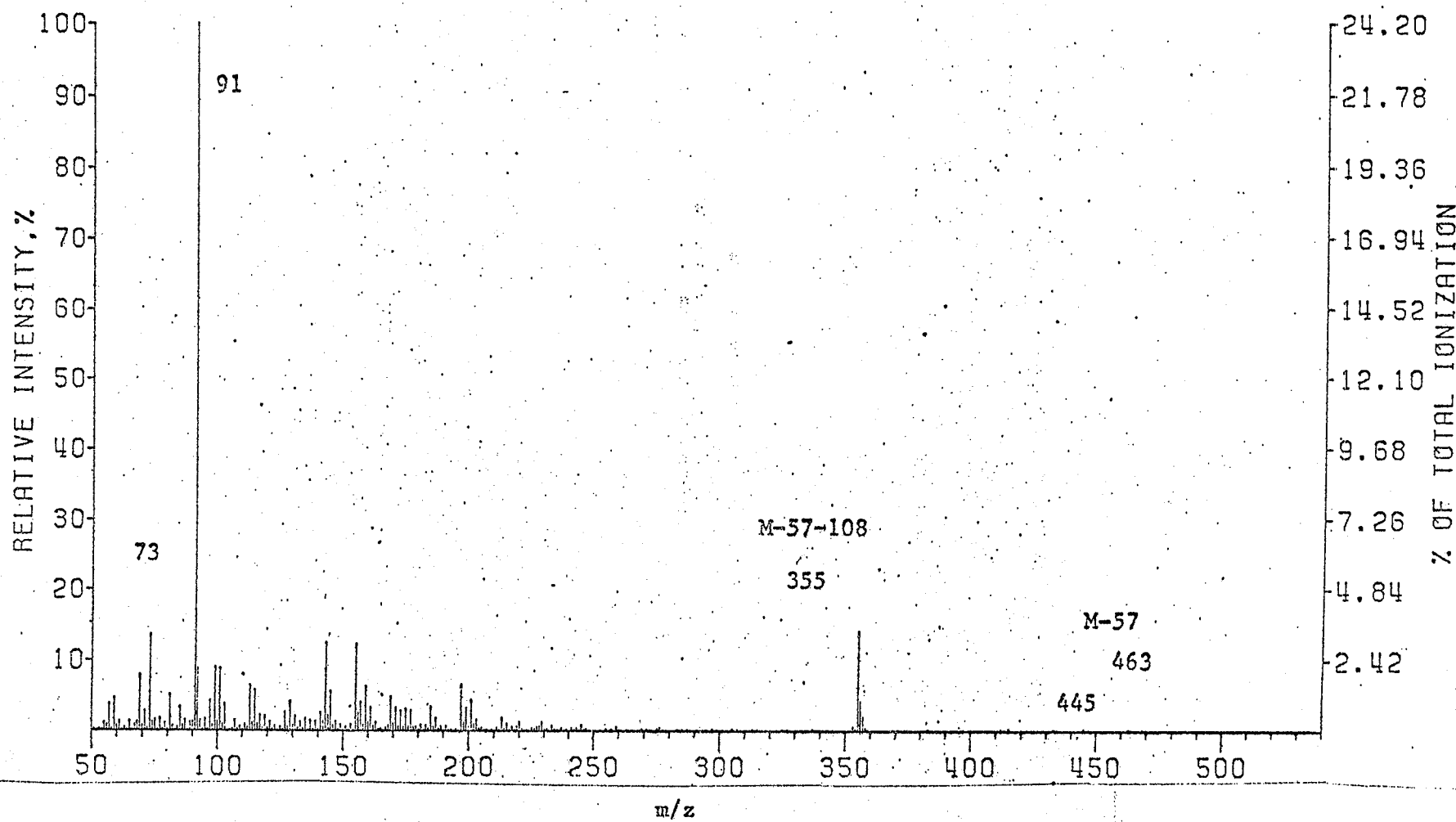


Figure: 58. Mass spectrum of bis-O-TMTBSi- β -D-benzylribofuranoside (VIII) (dd), MW 540, $I_{OV-1}^{280} = 3159$, recorded on Finnigan 1015 mass spectrometer at 70 eV.

iii) Mixed Ac/TBDMSi derivatives of β -D-benzylribofuranosides

The mass spectra of mono-TBDMSi-bis-acetyl- β -D-benzylribofuranoside are shown in figs. 59-61; of bis-TBDMSi-mono-acetyl derivatives in figs. 62-64. In each case, all three isomers were separated by GC (fig. 20). Figure 65 shows the mass spectrum of the tris-acetyl derivative.

The mass spectra analyses show characteristic $(M-57)^+$ for all derivatives. Further studies should provide detailed mechanisms of fragmentation of mixed derivatives.

GCMS AC2TBDM51 BEN. RIB.
 FINNIGAN-1015 RF-QUADRUPOLE MASS SPECTRUM
 CORRECTED FOR MASS DISCRIMINATION

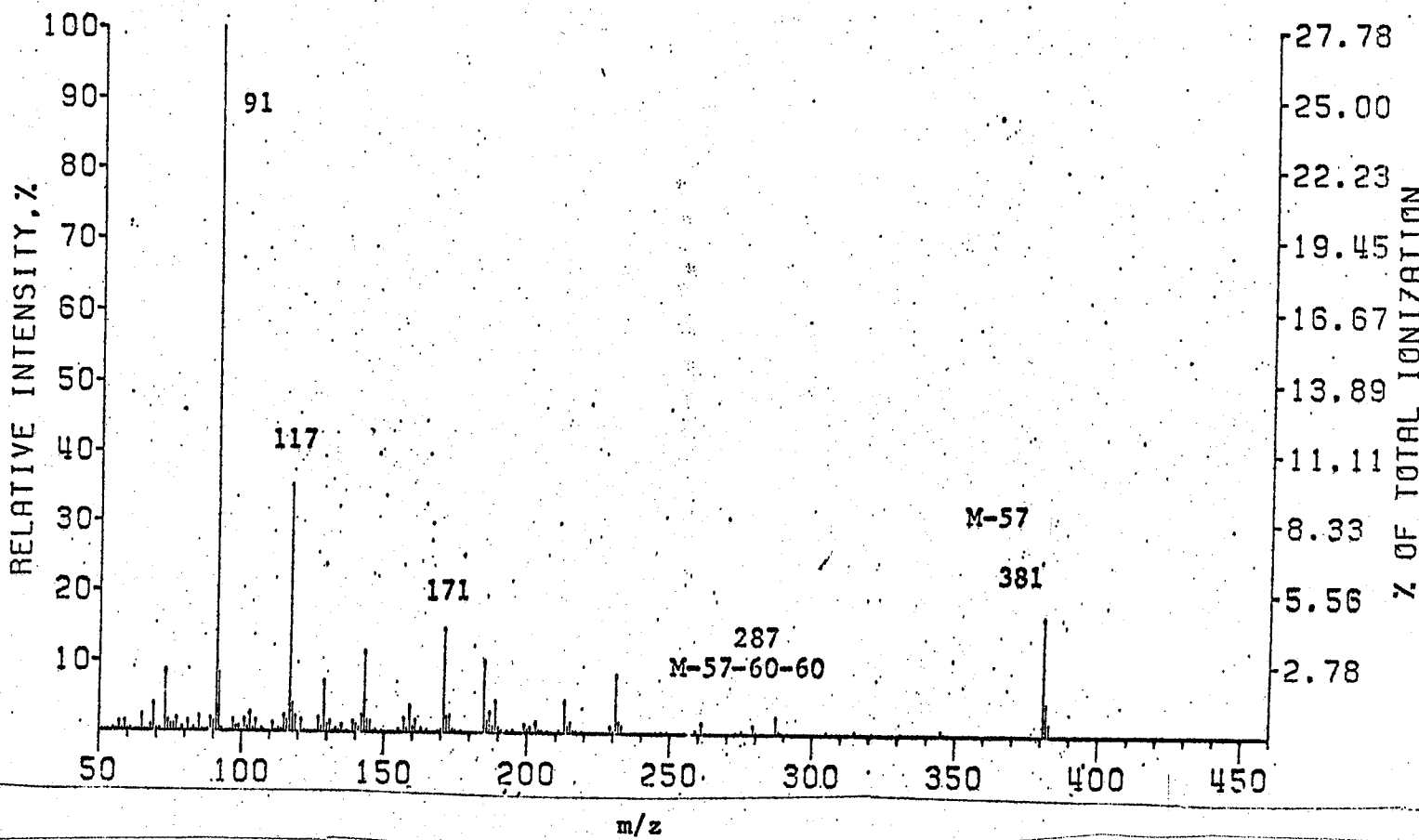


Figure:59. Mass spectrum of mono-O-TBDMSi-bis-O-Ac- β -D-benzylribofuranoside (VIII_{bqq}), MW 438,
 $I_{OV-1}^{210} = 2395$), recorded on Finnigan 1015 mass spectrometer at 70 eV.

MSGC-3-25/7/76 TBDMSI AC2 BEN. RIB: PK2
FINNIGAN-1015. RF-QUADRUPOLE MASS SPECTRUM
CORRECTED FOR MASS DISCRIMINATION

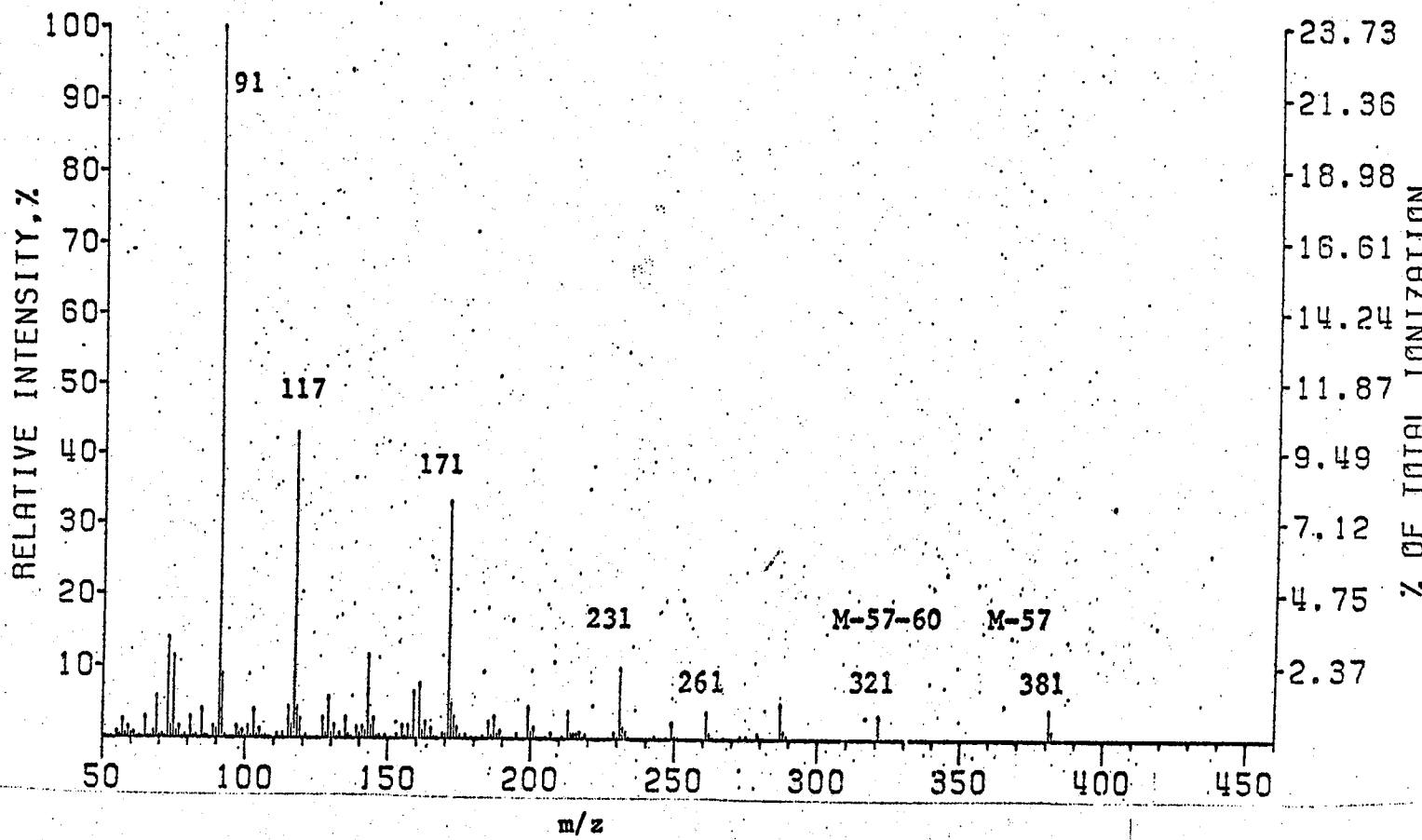


Figure: 60. Mass spectrum of mono-O-TBDMSi-bis-O-Ac- β -D-benzyl-ribofuranoside (VIII_(qqb), MW 438,
I_{OV-1}²¹⁰ = 2432), recorded on Finnigan 1015 mass spectrometer at 70 eV.

MSGC-3-25-7-76 TBDMS1 AC2 BEN. RIB. PK3
FINNIGAN-1015 RF-QUADRUPOLE MASS SPECTRUM
CORRECTED FOR MASS DISCRIMINATION

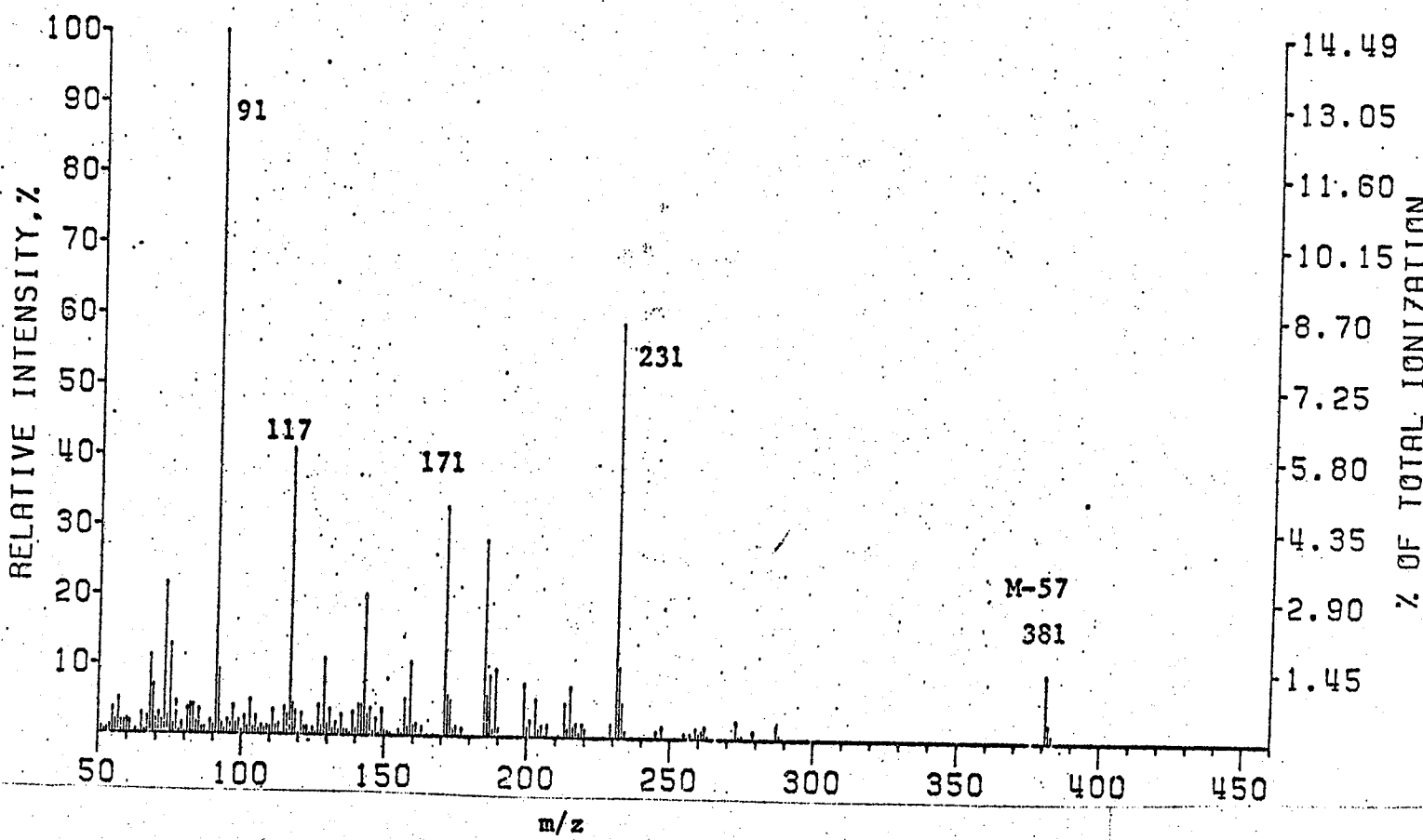


Figure: 61. Mass spectrum of mono-O-TBDMSi-bis-O-Ac- β -D-benzyl-ribofuranoside (VIII, bqq), MW 438,
 $I_{OV-1}^{210} = 2482$, recorded on Finnigan 1015 mass spectrometer at 70 eV,

MSGC-3-25/7/76. TBDMS2 AC1 BEN. RIB. PK4
FINNIGAN-1015 RF-QUADRUPOLE MASS SPECTRUM
CORRECTED FOR MASS DISCRIMINATION

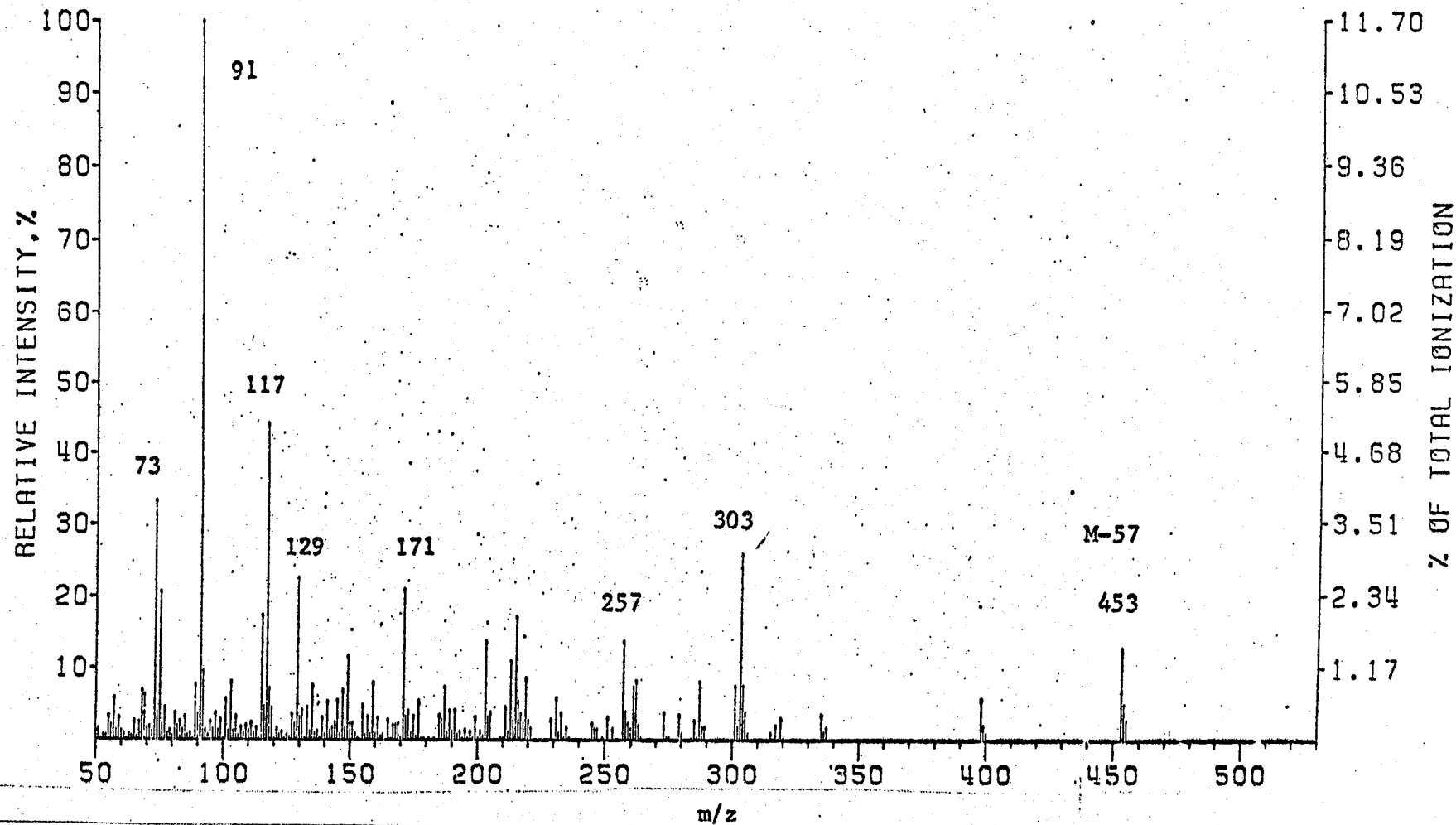


Figure: 62. Mass spectrum of mono-O-Ac-bis-O-TBDMS- β -D-benzyl-ribofuranoside (VIII), MW 510,
 $I_{OV-1}^{210} = 2591$, recorded on Finnigan 1015 mass spectrometer at 70 eV.

MSGC-3-25/7/76 TBDMSS2 AC1 BEN. RIB. PK5
FINNIGAN-1015 RF-QUADRUPOLE MASS SPECTRUM
CORRECTED FOR MASS DISCRIMINATION

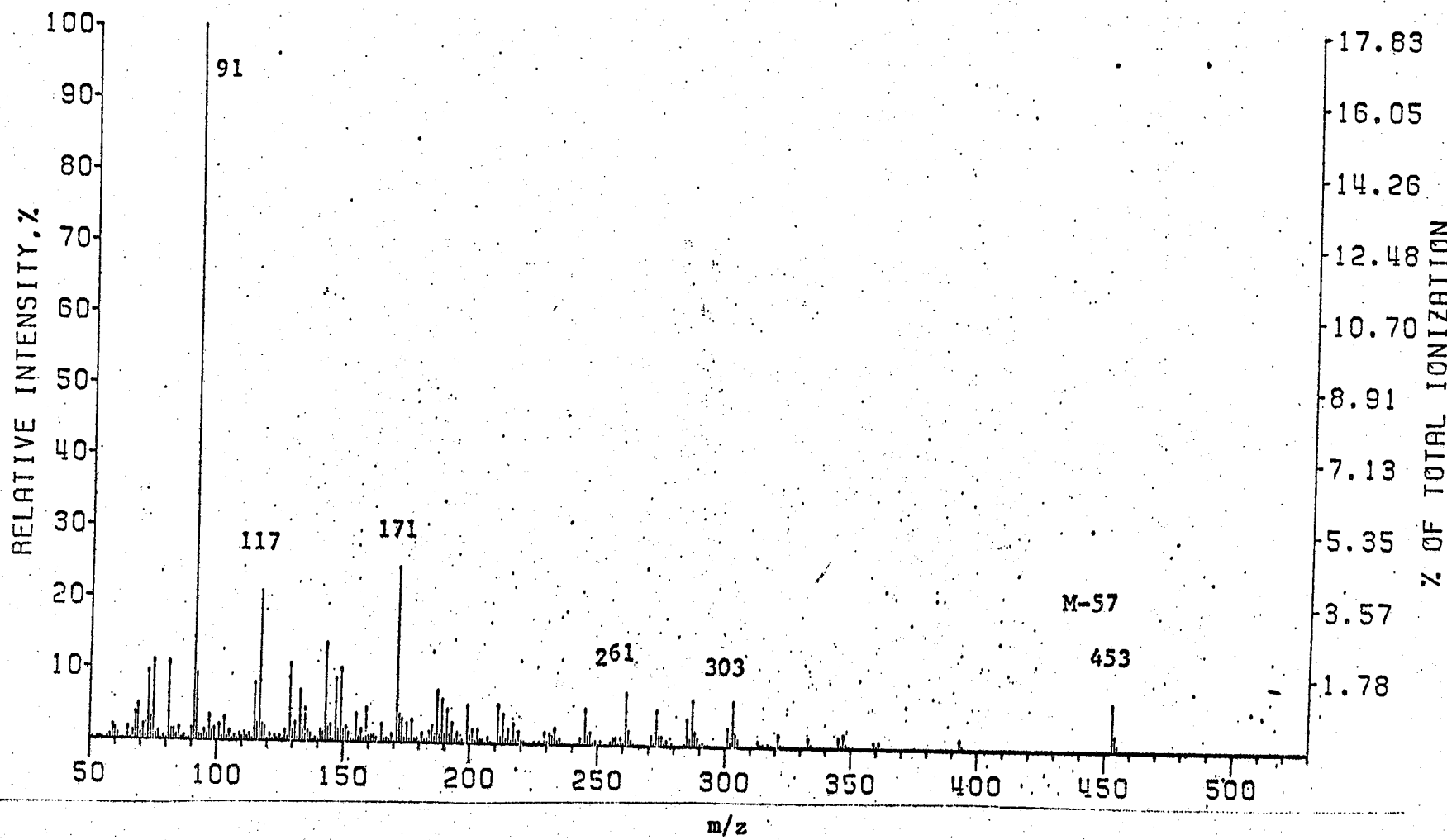


Figure: 63. Mass spectrum of mono-O-Ac-bis-O-TBDMS- β -D-benzyl-ribofuranoside (VIII_{qbb}), MW 510,
 $I_{Ov-1}^{210} = 2650$, recorded on Finnigan 1015 mass spectrometer at 70 eV.

MSGC-3-25/7/76 TBDMS2 AC1 BEN. RIB. PK6
FINNIGAN-1015 RF-QUADRUPOLE MASS SPECTRUM
CORRECTED FOR MASS DISCRIMINATION

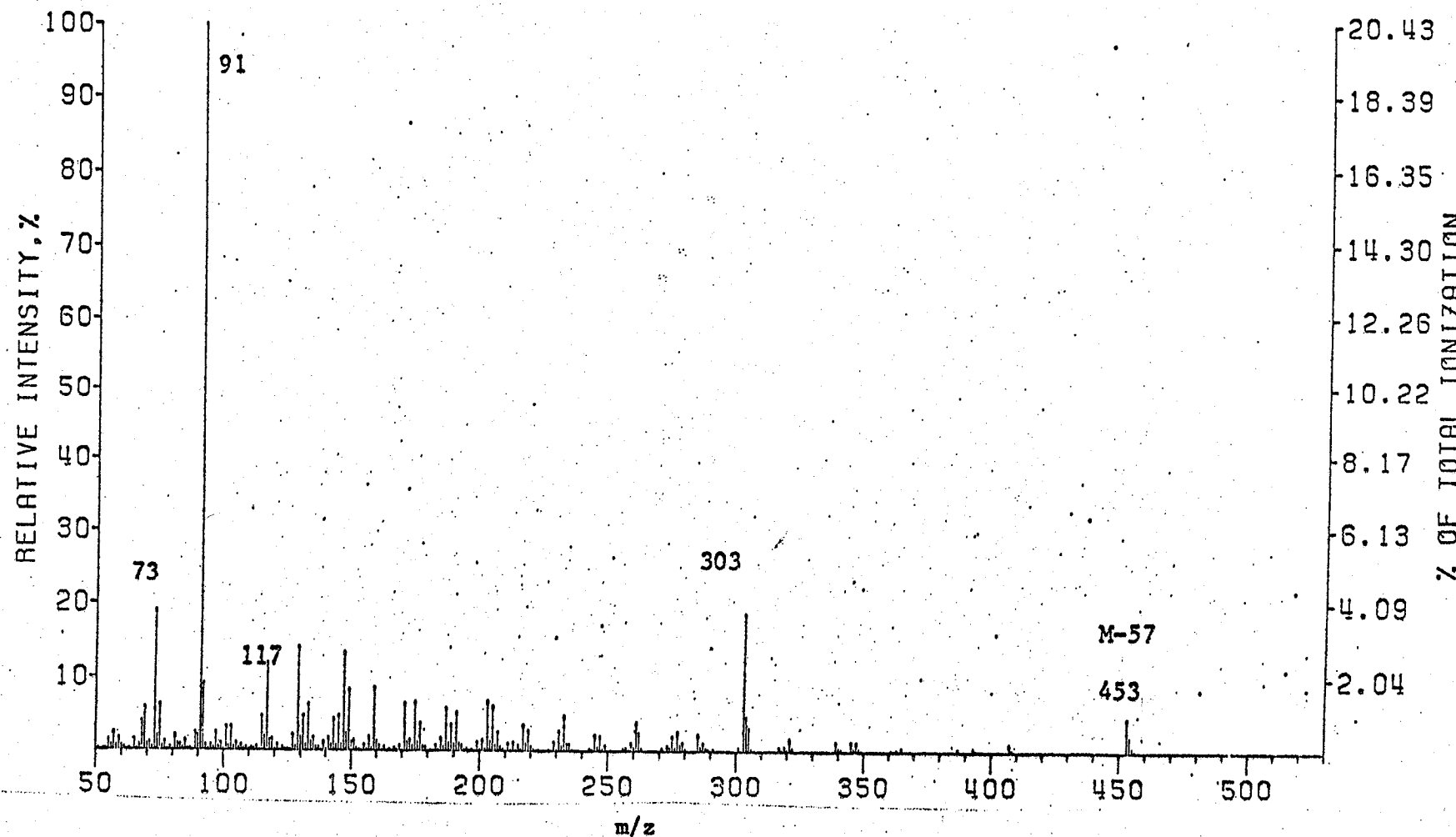


Figure: 64. Mass spectrum of mono-O-Ac-bis-O-TBDMS- β -D-benzyl-ribofuranoside (VIII_(qbb)), MW 510,
 $I_{OV-1}^{210} = 2697$), recorded on Finnigan 1015 mass spectrometer at 70 eV.

MSGC-AC3 BEN. RIB. PK1
FINNIGAN-1015 RF-QUADRUPOLE MASS SPECTRUM
CORRECTED FOR MASS DISCRIMINATION

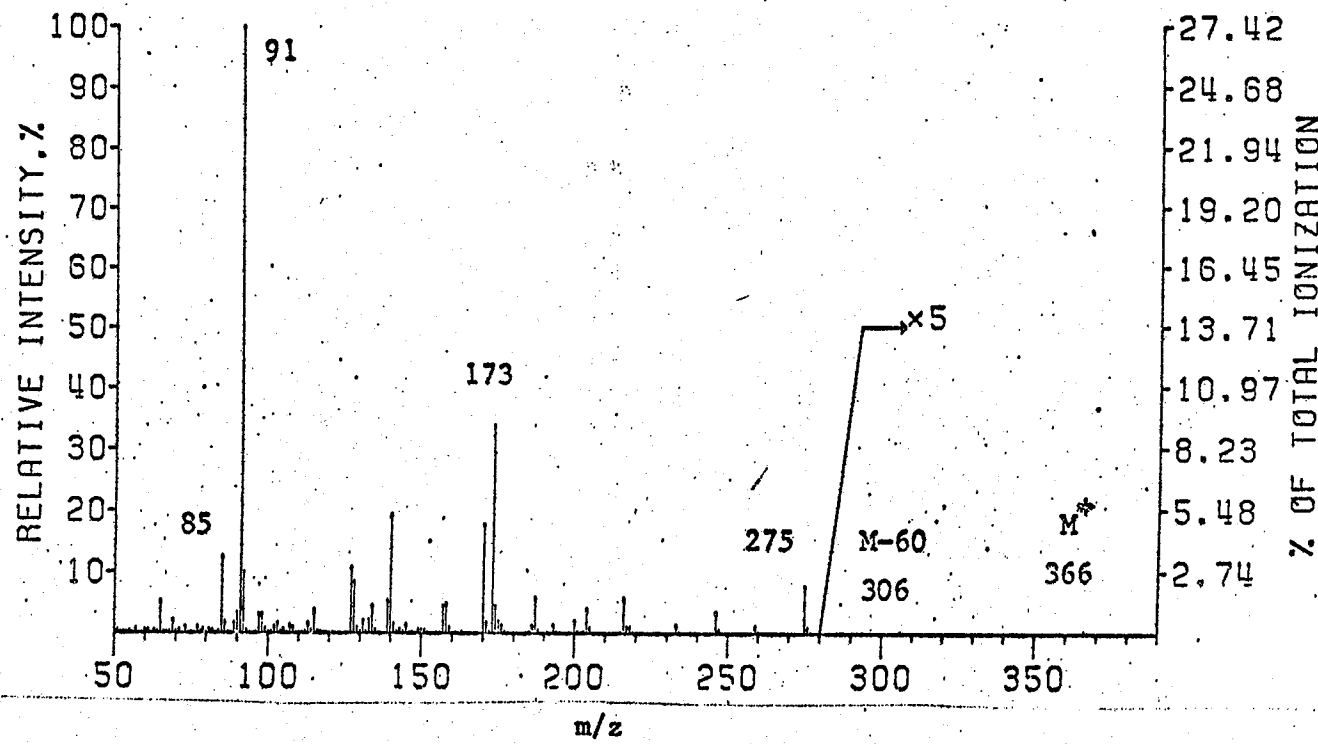


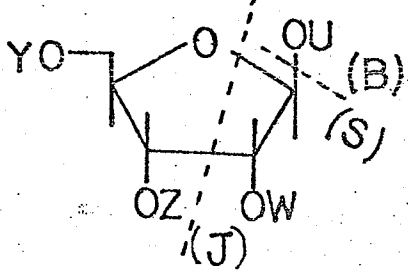
Figure: 65. Mass spectrum of tris-O-Ac- β -D-benzyl-ribofuranoside (VIII_(qqq), MW 366, $I_{OV-1}^{210} = 2272$), recorded on Finnigan 1015 mass spectrometer at 70 eV.

iv) Mass spectral fragmentation of SCTASi-D-ribose

Four GC peaks were obtained for II_{bbbb} indicating the presence of four isomers (fig. 7). It is believed that two of the structures should correspond to the furanose system and the other two to the pyranose system. The mass spectra are shown in figs 66-69. A distinctive feature of TBDMSi-furanose is the peak at m/z 301. A furanoid system should be distinguished from the pyranose form by the m/z 301 to m/z 288 ratio.

The mass spectrum of tetrakis-O-TMTBSi-D-ribose (single GC peak) is shown in fig. 70.

Here, interpretation is analogous to that for SCTASi-ribonucleosides (scheme 15).



v) Mass spectra of SCTASi-D-xyloses

Gas chromatography gave two peaks corresponding to tetrakis-O-TBDMSi-D-xylose, the α and β anomers. The mass spectra are shown in figs. 71 and 72. Generally, the spectra parallel those of the riboses, with variations in heights of peaks.

GCMS TBDMS4-RIB. MU=24.54
FINNIGAN-1015 RF-QUADRUPOLE MASS SPECTRUM
CORRECTED FOR MASS DISCRIMINATION

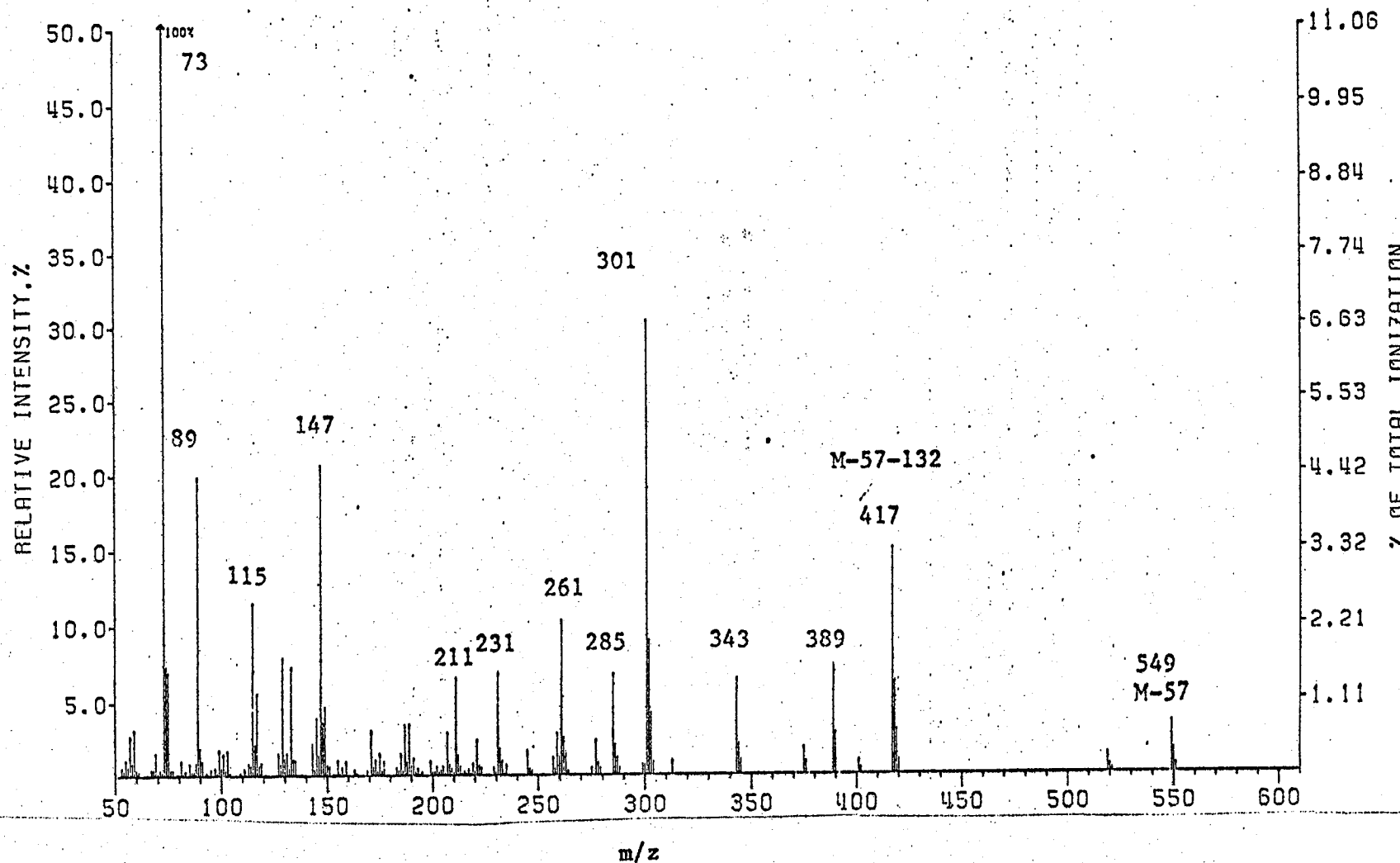


Figure: 66. Mass spectrum of tetrakis-O-TBDMS-D-ribose (II_{bbbb}, MW 606, $I_{OV-1}^{210} = 2454$) recorded on Finnigan 1015 mass spectrometer at 70 eV.

MSGC TBDMS4 RIB. MU=25.12
FINNIGAN-1015 RF-QUADRUPOLE MASS SPECTRUM
CORRECTED FOR MASS DISCRIMINATION

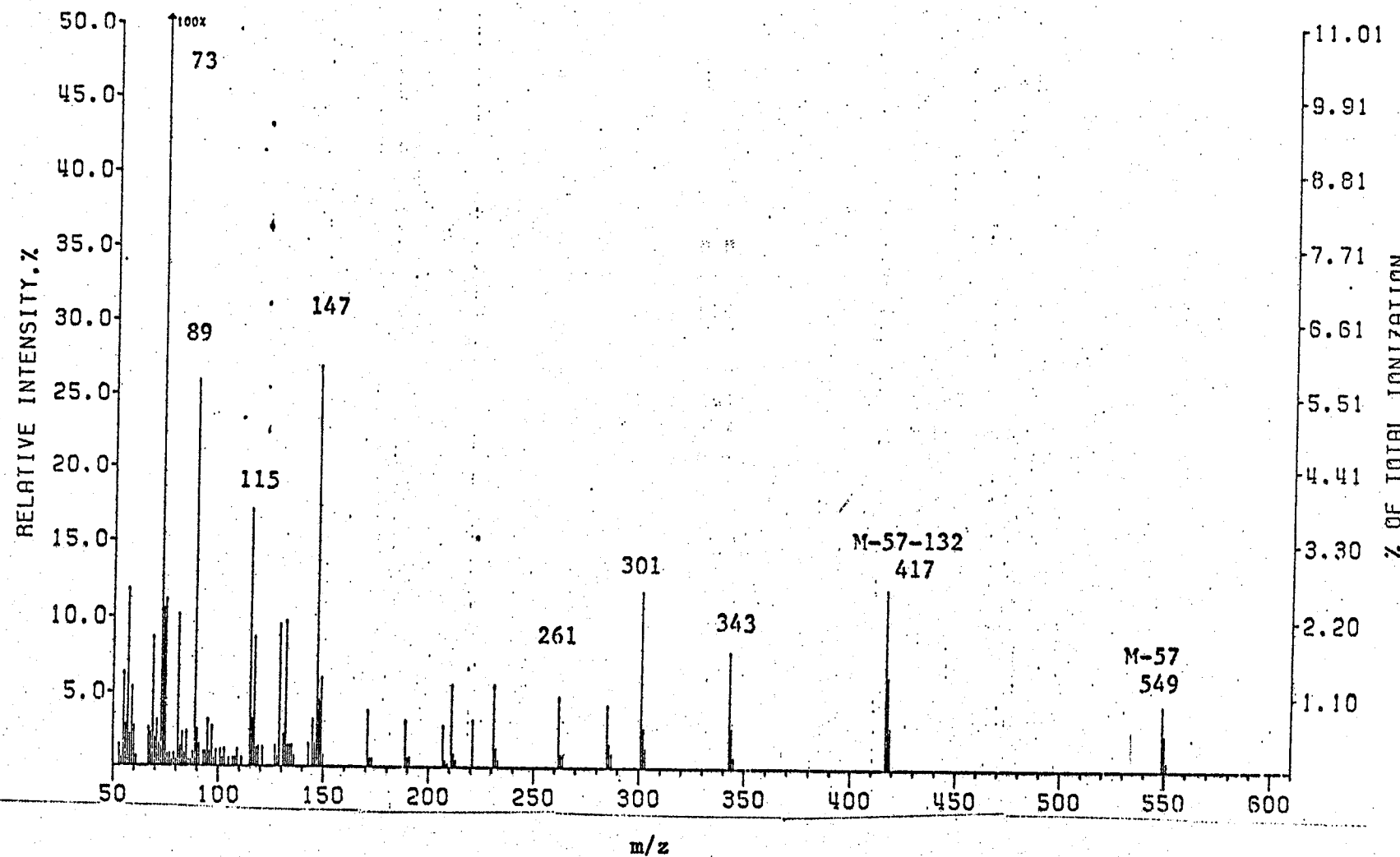


Figure: 67. Mass spectrum of tetrakis-O-TBDMS-D-ribose (II_{bbbb}, MW 606, I_{OV-1}²¹⁰ = 2512), recorded on Finnigan 1015 mass spectrometer at 70 eV.

MSGC TBDMS4 RIB. MU=25.44
FINNIGAN-1015 RF-QUADRUPOLE MASS SPECTRUM
CORRECTED FOR MASS DISCRIMINATION

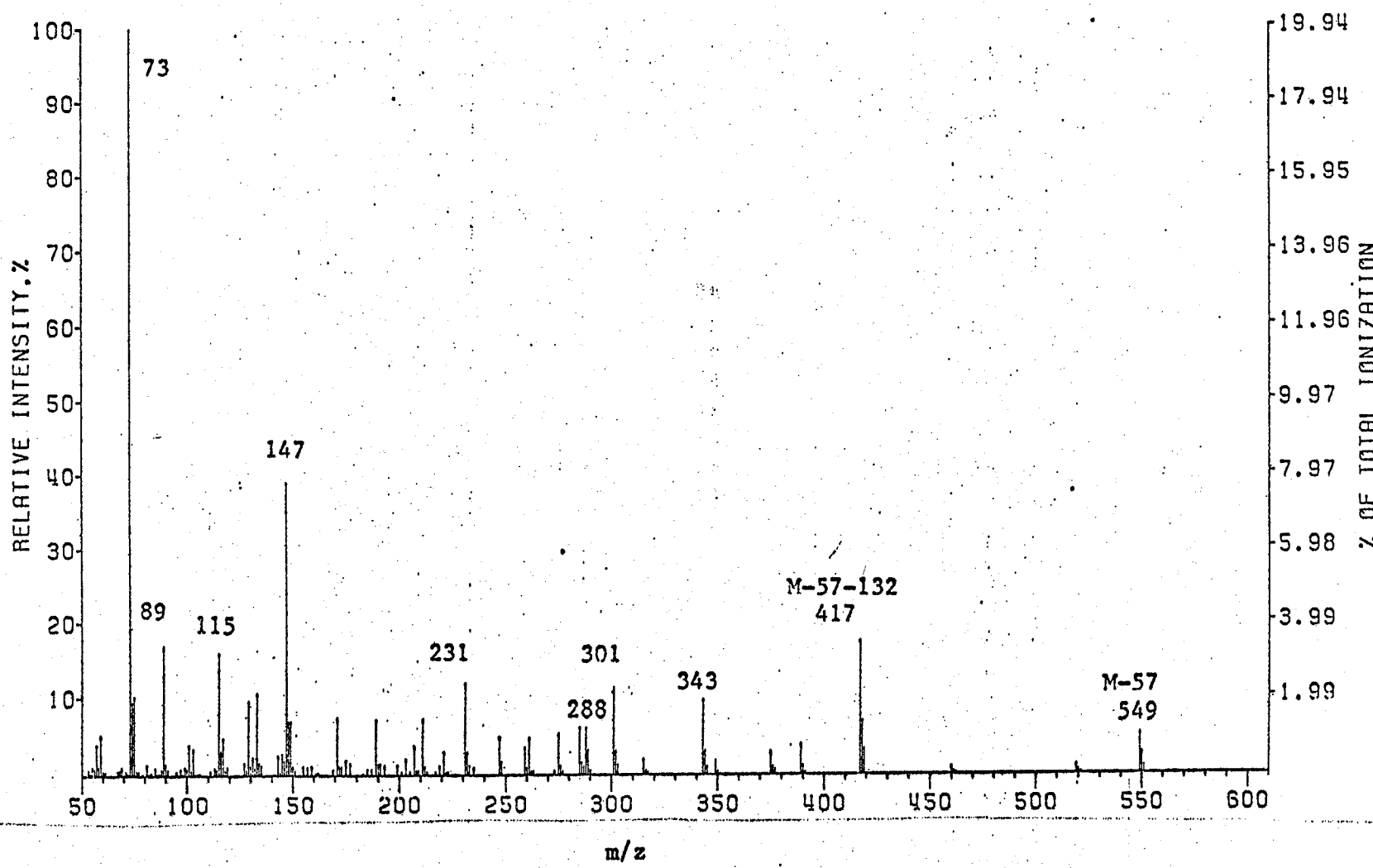


Figure: 68. Mass spectrum of tetrakis-O-TBDMSi-D-ribose (II_{bbbb}, MW 606, I_{OV-1}²¹⁰ = 2544), recorded on Finnigan 1015 mass spectrometer at 70 eV.

MSGC TBDMS4 RIB. MU=26.24
SPECTRUM RECORDED ON 1015 QUADRUPOLE MASS SPECTROMETER
AND NORMALIZED TO CONSTANT SENSITIVITY

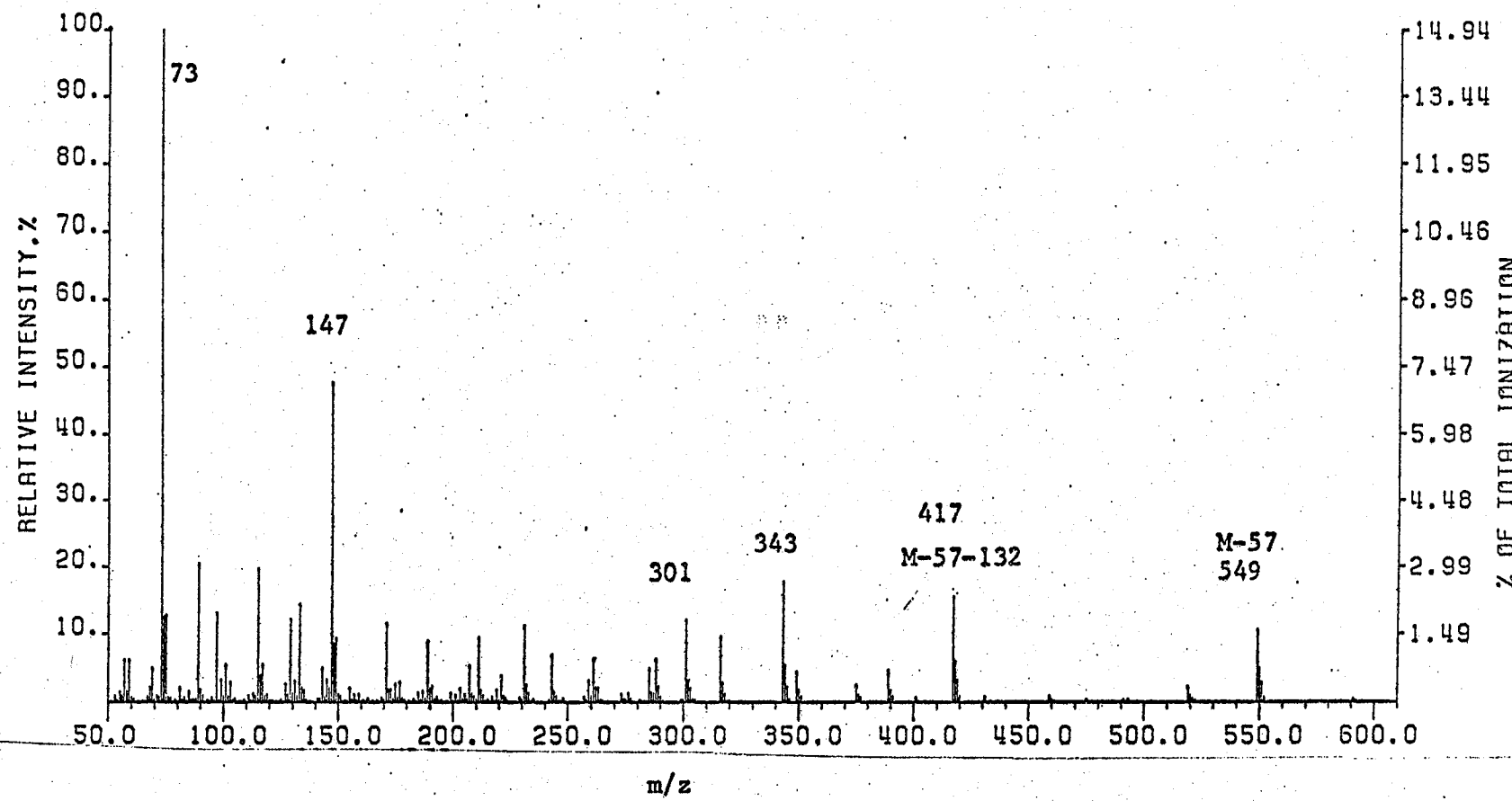
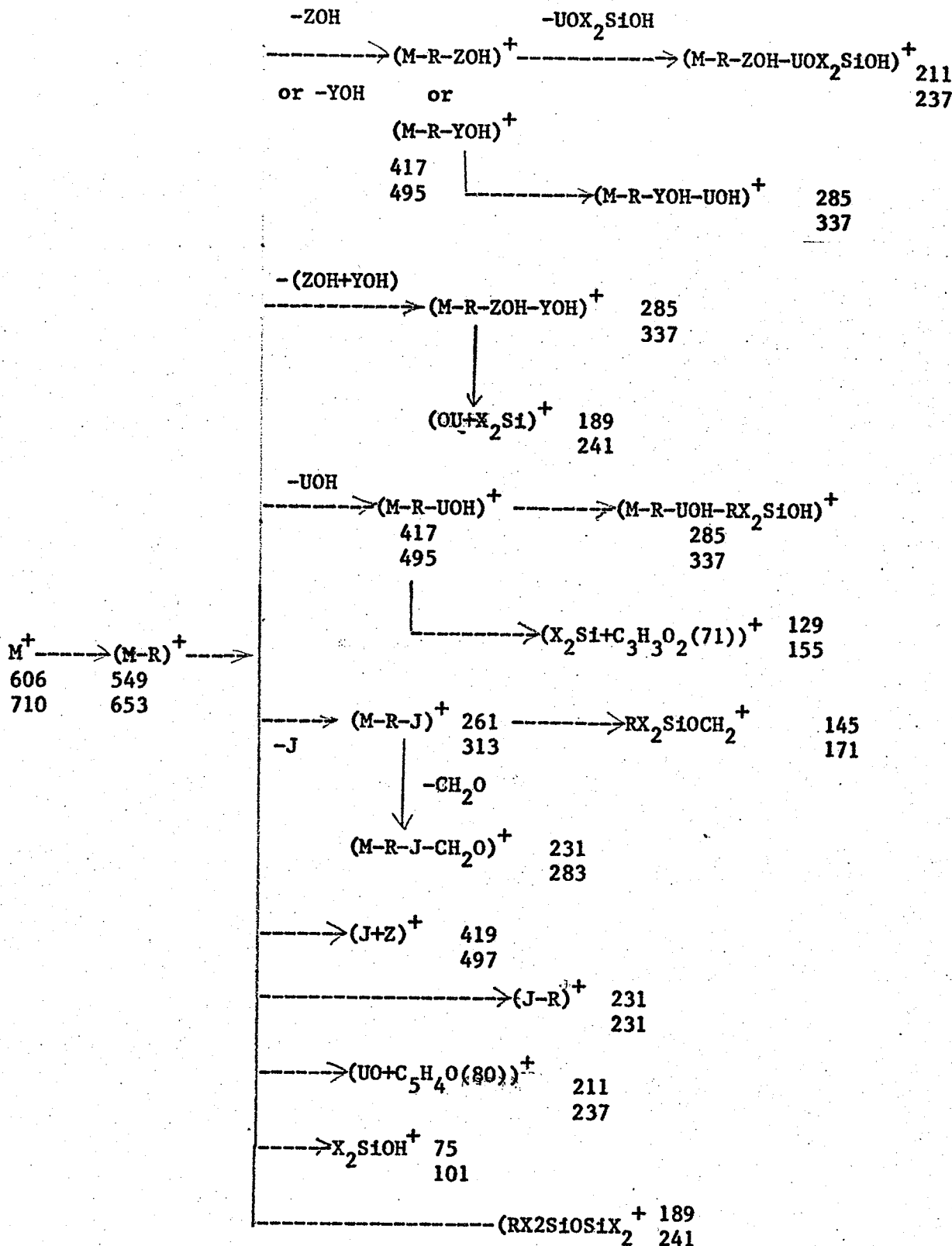
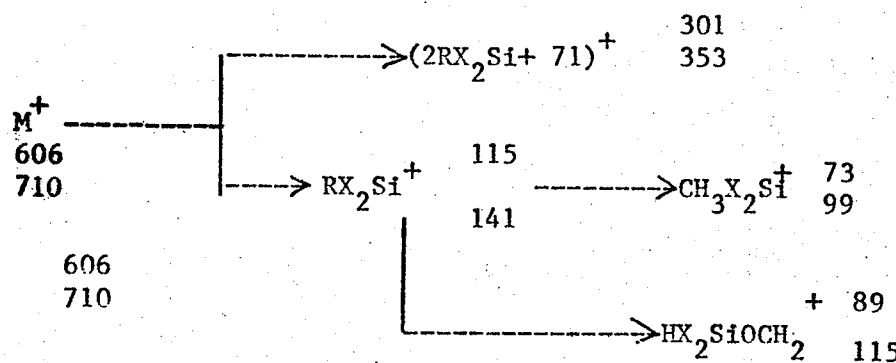


Figure: 69. Mass spectrum of tetrakis-O-TBDMS-D-ribose (II_{bbbb}, MW 606, $I_{\text{OV-1}}^{210} = 2624$), recorded on Finnigan 1015 mass spectrometer at 70 eV.



Scheme 15 Mass spectral fragmentation patterns of SCTASi-D-ribofuranoses.

Numbers following ionic species are masses for TBDMSi and TMTBSi derivatives respectively.



Scheme: 15 (cont'd)

MSGC-11-15/8/76 TMTBS4 RIB. I=34.4
FINNIGAN-1015 RF-QUADRUPOLE MASS SPECTRUM
CORRECTED FOR MASS DISCRIMINATION

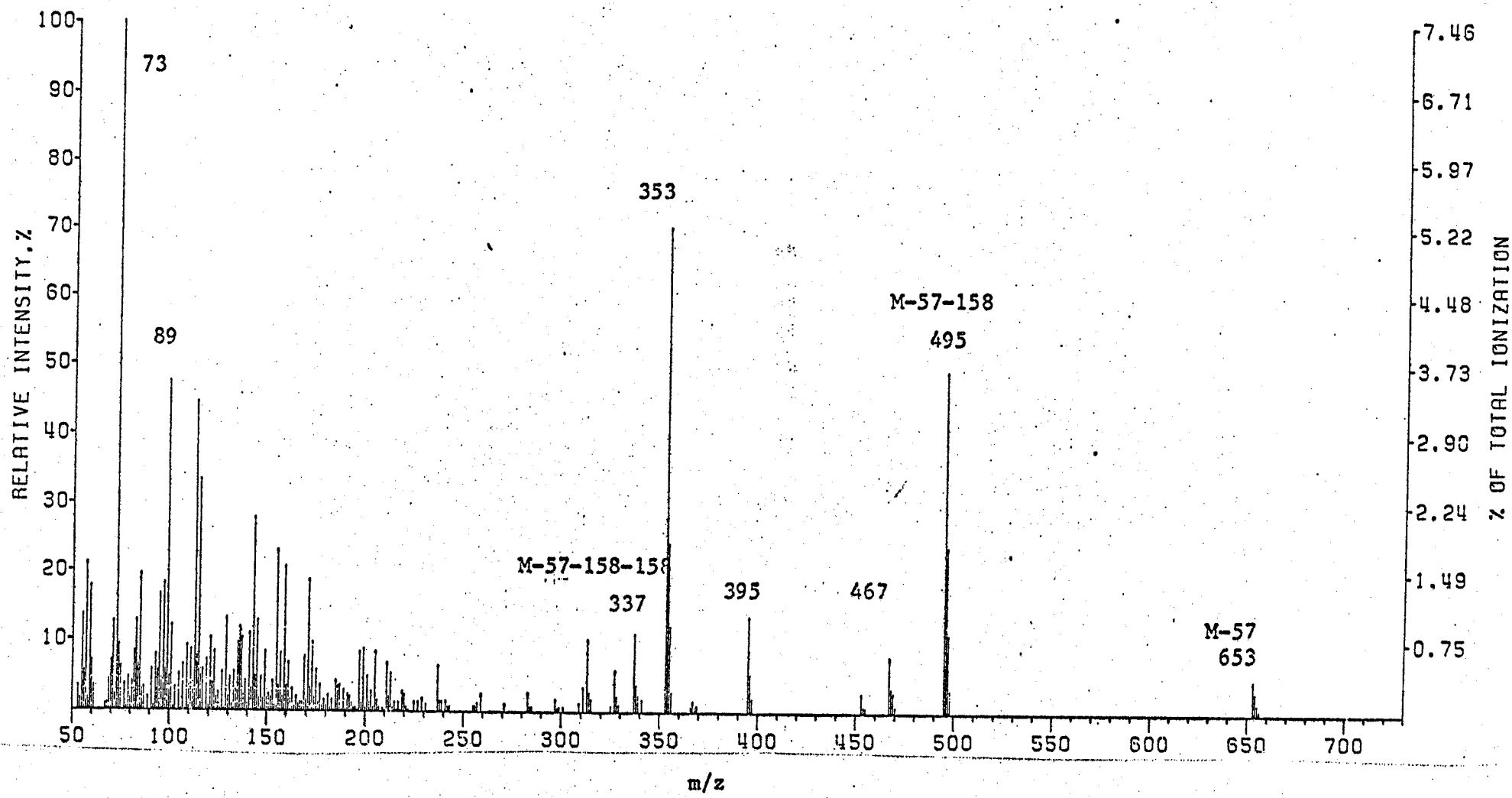


Figure 70. Mass spectrum of tetrakis-O-TMTBS4-D-ribose (II_{ddd}, MW 710, $I_{Ov-1}^{280} = 3442$), recorded on Finnigan 1015 mass spectrometer at 70 eV.

TBDMS₄ XYLOSE PK1
FINNIGAN-1015 RF-QUADRUPOLE MASS SPECTRUM
CORRECTED FOR MASS DISCRIMINATION

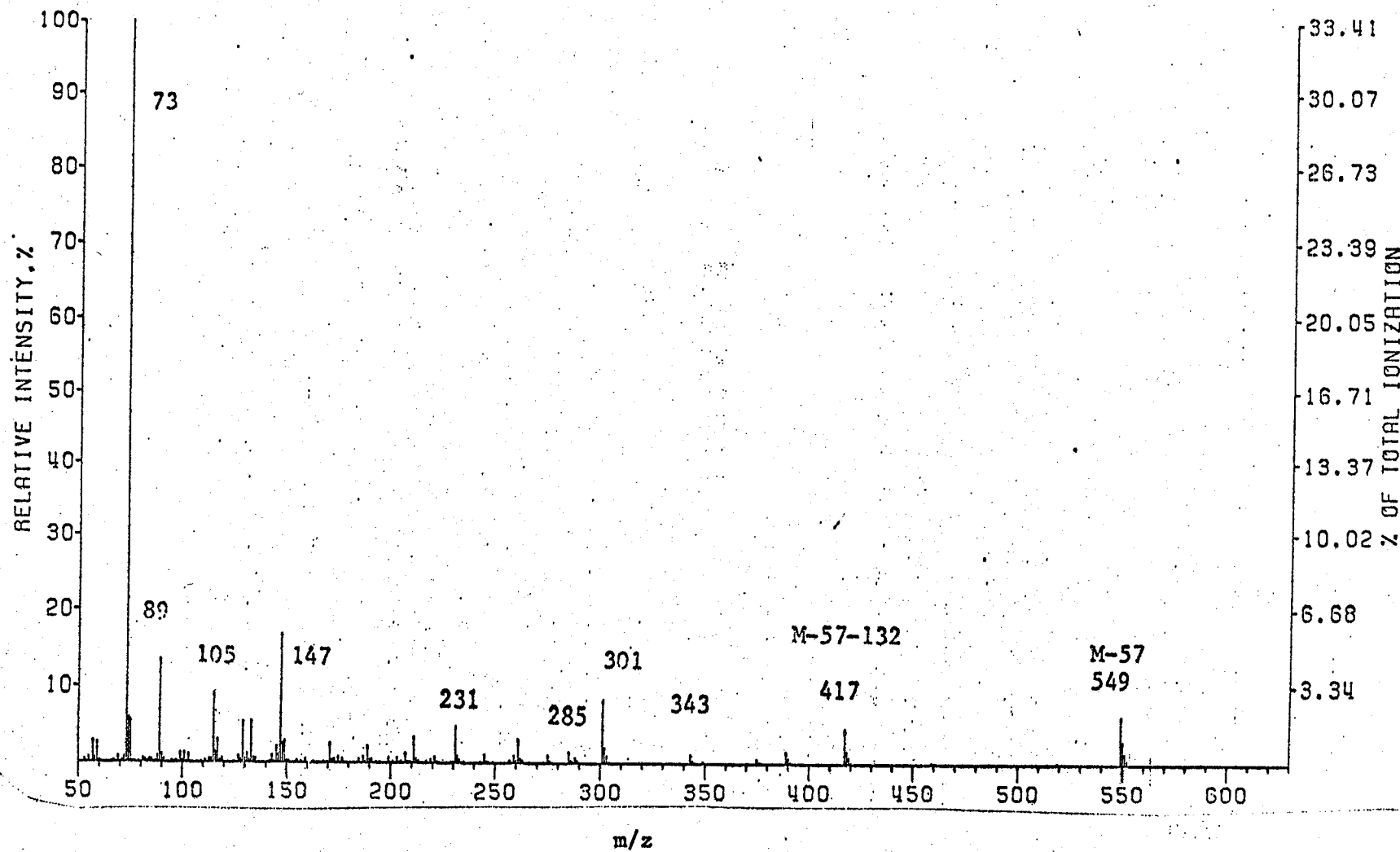


Figure: 71. Mass spectrum of tetrakis-O-TBDMS-D-xylose (III_{bbbb}, MW 606, $I_{OV-1}^{210} = 2460$), recorded on Finnigan 1015 mass spectrometer at 70 eV.

TBDMS4 XYLOSE PK 2
FINNIGAN-1015 RF-QUADRUPOLE MASS SPECTRUM
CORRECTED FOR MASS DISCRIMINATION

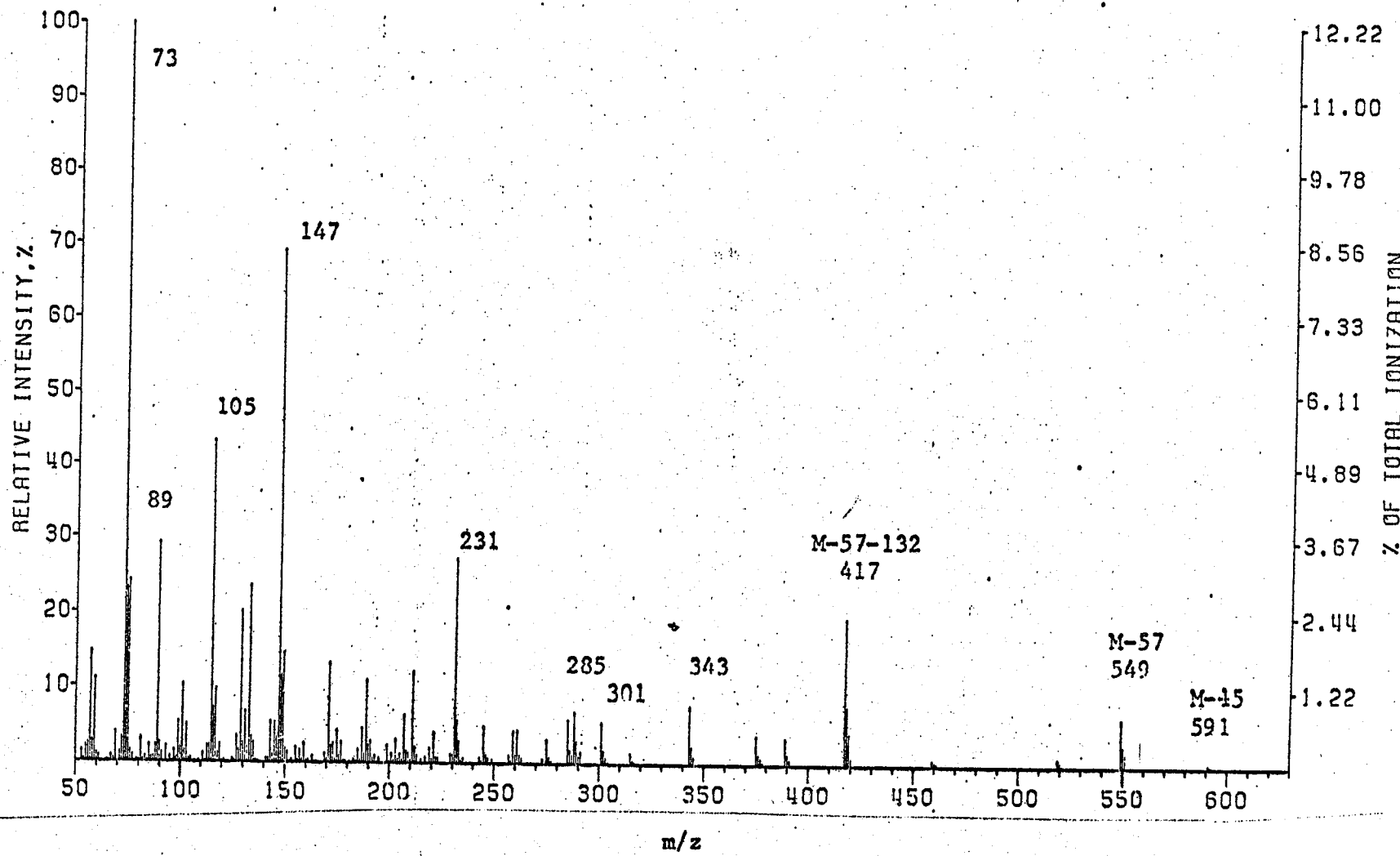


Figure: 72. Mass spectrum of tetrakis-O-TBDMS-D-xylose (III_{bbbb}, MW 606, $I_{OV-1}^{210} = 2500$), recorded on Finnigan 1015 mass spectrometer at 70 eV.

(d) Mass-spectra of SCTASi-1,4 ribonolactones

i) Fully silylated 1,4-ribonolactones.

The mass spectral interpretation of TMSi-aldonolactones was performed by Petersson and co-workers (84). They showed that diastereomers could be differentiated from each other by examining the differences in intensities for various fragmentation products. In this study, SCTASi-1,4 ribonolactones were selected for investigation because of their simple structures (three substituent groups). The mass spectra of tris-TMSi, TBDMSi, TMIPSi, TMTBSi 1,4-ribonolactones are shown in figs. 73-76. Molecular weights can easily be obtained from $(M-R)^+$ ions. Characteristic ions include loss of CO from $(M-R)^+$, i.e. the $(M-R-28)^+$ ion; and also the $(M-R-SCTASiOH)^+$ ions. Other ionic species are common fragments most frequently encountered in the mass spectra of SCTASi-ethers.

MSGC 1/6/76 TMS3 RIB.LAC.
FINNIGAN-1015 RF-QUADRUPOLE MASS SPECTRUM
CORRECTED FOR MASS DISCRIMINATION

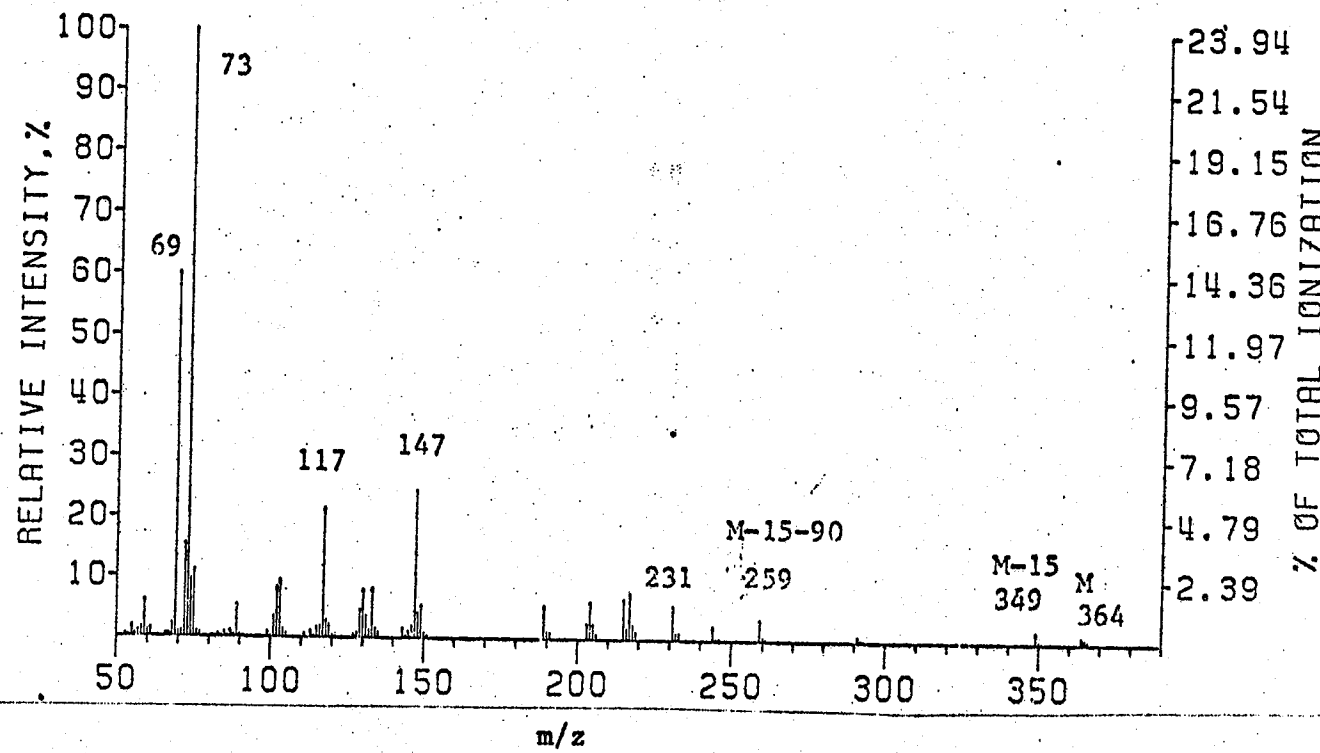


Figure: 73. Mass spectrum of tris-O-TMSi-1,4-ribonolactone(IX_{aaa}, MW 364, I¹⁸⁰_{OV-1} 1700), recorded on Finnigan 1015 mass spectrometer at 70 eV.

MSGC-1/6/76 TBDMS3-RIBONOLACTONE
FINNIGAN-1015 RF-QUADRUPOLE MASS SPECTRUM
CORRECTED FOR MASS DISCRIMINATION

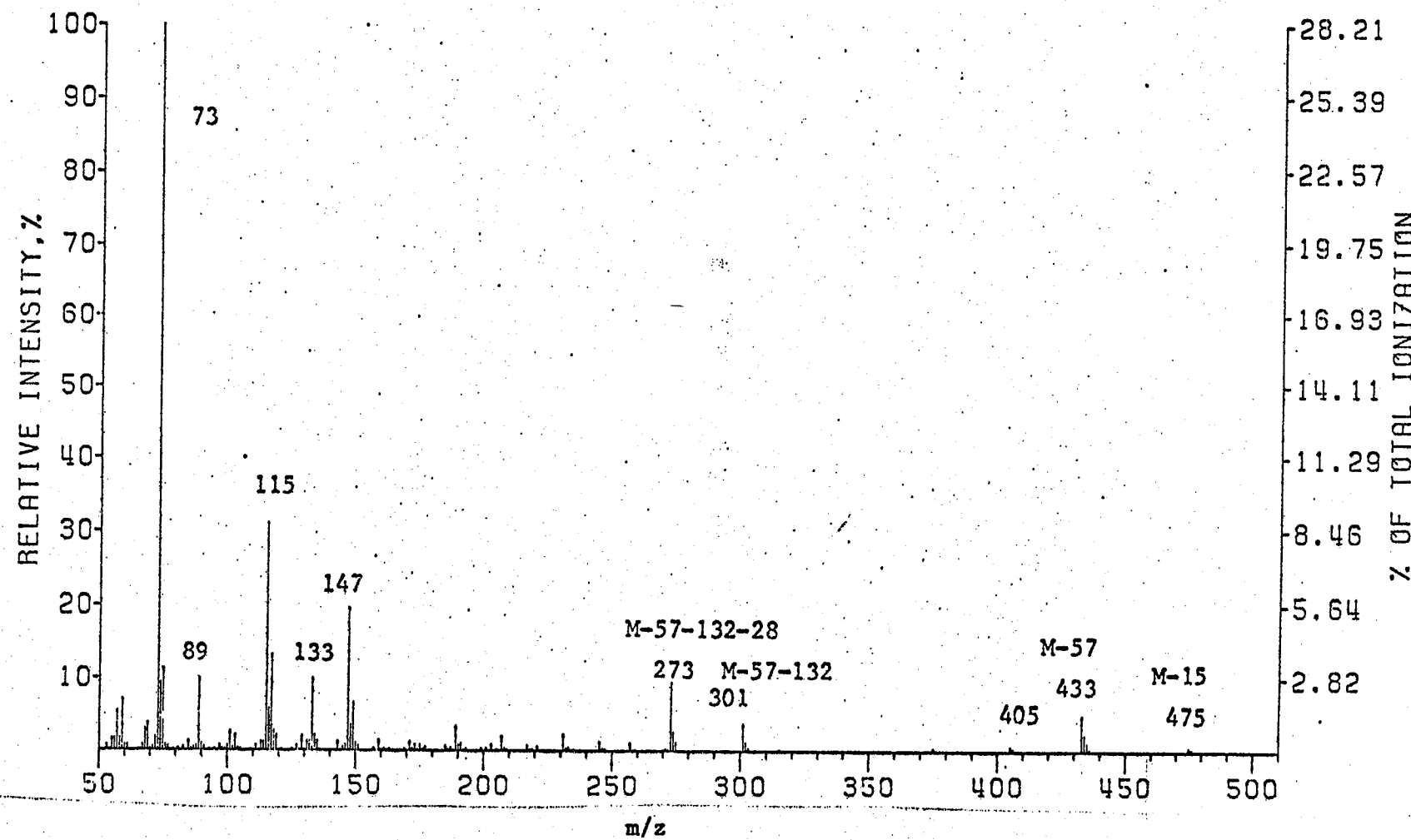


Figure: 74. Mass spectrum of tris-O-TBDMSi-1,4-ribonolactone (IX, MW 490, $I_{\text{OV-1}}^{210} = 2321$), recorded on Finnigan 1015 mass spectrometer at 70 eV.

MSGC-10-12/8/76 TMIPS3 RIB. LAC. PK1
FINNIGAN-1015 RF-QUADRUPOLE MASS SPECTRUM
CORRECTED FOR MASS DISCRIMINATION

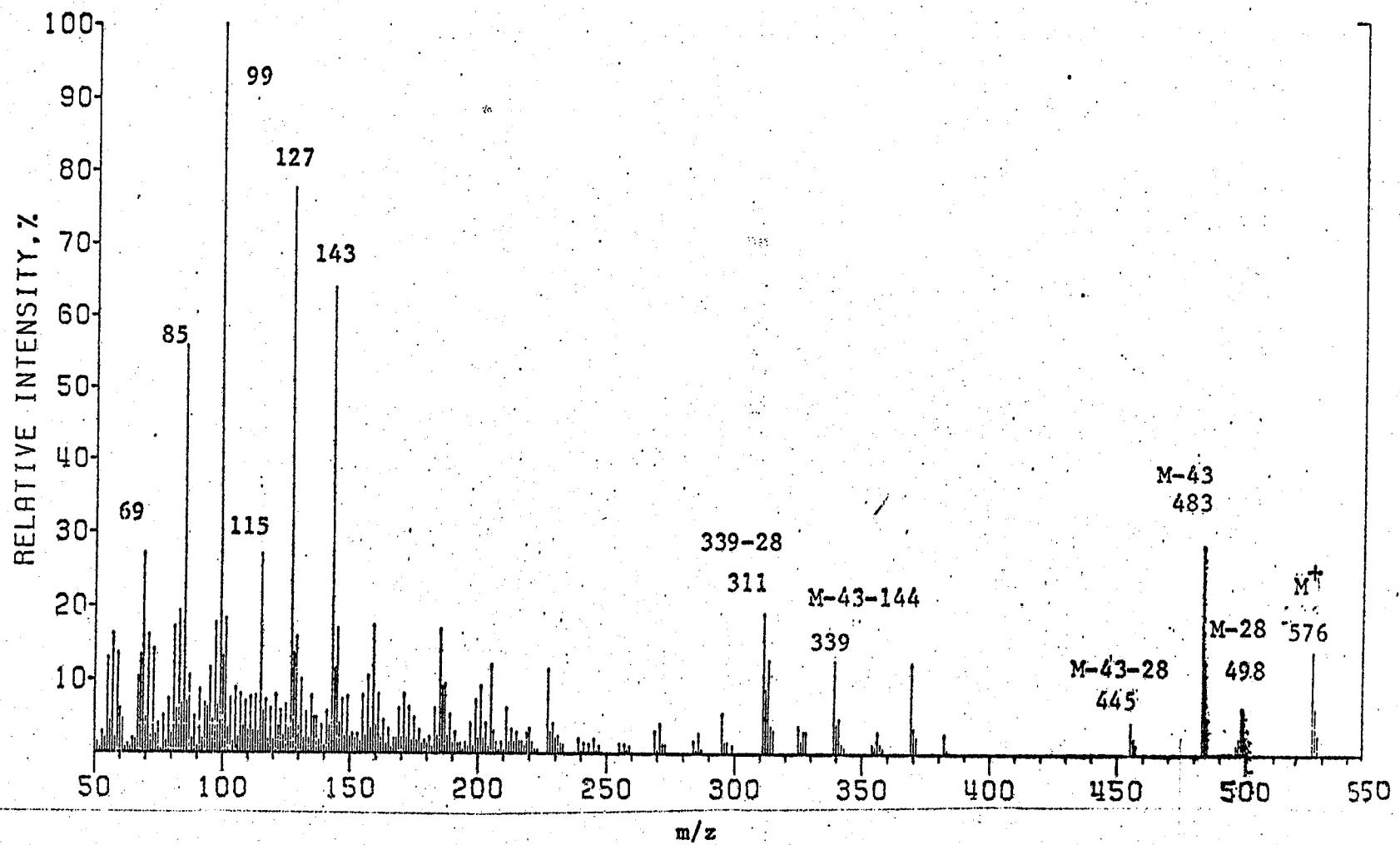


Figure: 75. Mass spectrum of tris-O-TMIPS1-1,4-ribonolactone (IX_{ccc}, MW 576, $I_{OV-1}^{280} = 3045$), recorded on Finnigan 1015 mass spectrometer at 70 eV.

MSGC-4-12/8/76 TMTBS3 RIB. LAC. PK5
SPECTRUM RECORDED ON 1015 QUADRUPOLE MASS SPECTROMETER
AND NORMALIZED TO CONSTANT SENSITIVITY

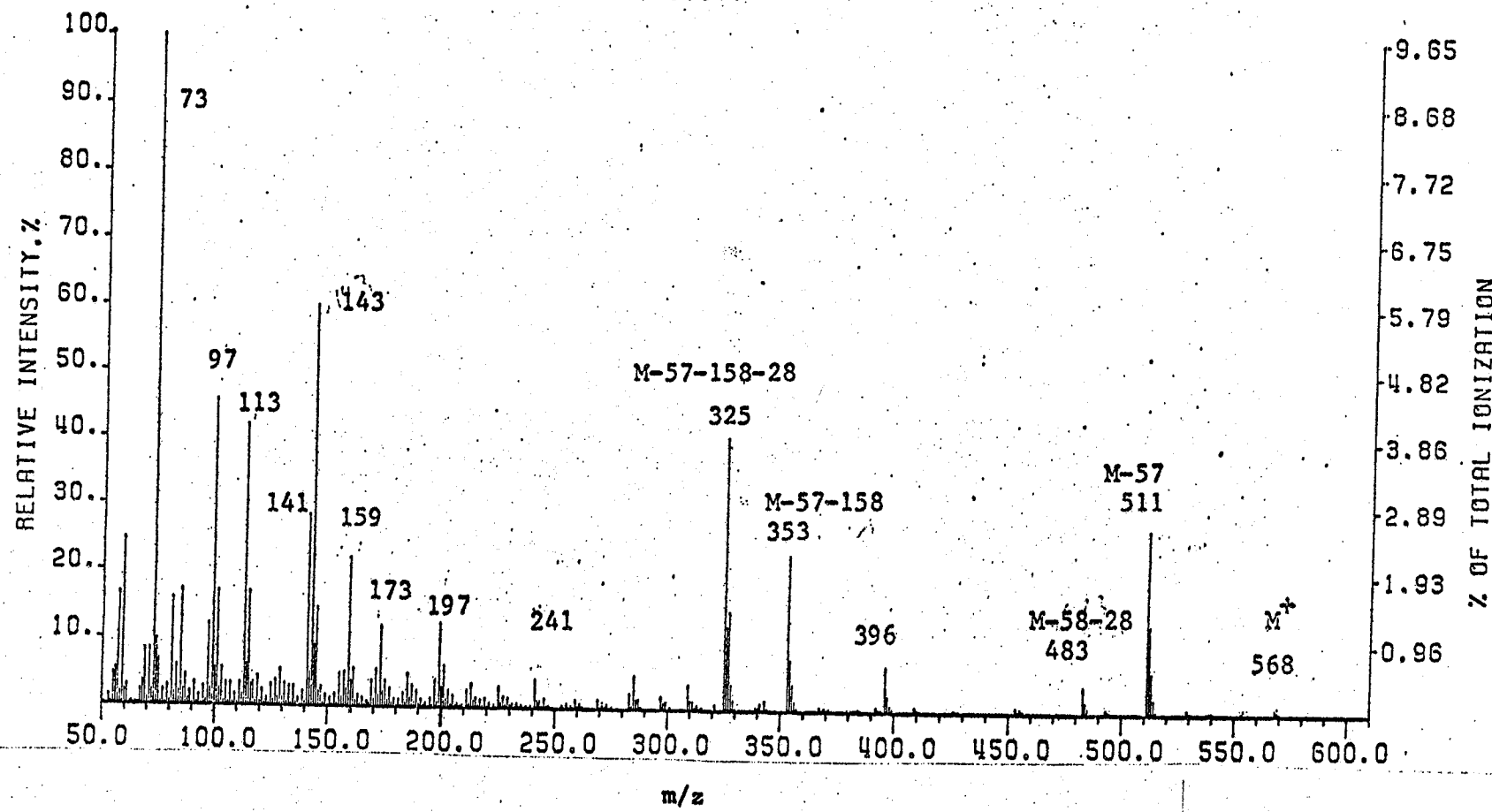


Figure: 76. Mass spectrum of tris-O-TMTBSi-1,4-ribonolactone (IX_{ddd}, MW 568, I²⁸⁰_{OV-1} = 3170),
recorded on Finnigan 1015 mass spectrometer at 70 eV.

ii) Partial O-SCTASi-1,4-ribonolactones:

The mass spectra of the mono-TBDMSi, mono-TMTBSi, bis-TBDMSi, and bis-TMTBSi ethers of 1,4-ribonolactones are shown in figs. 77-87. Three isomers could occur in each case, and with the exception of the mono-TMTBSi derivatives (which gave two GC peaks, fig. 11), three GC peaks were obtained (figs. 10-12). As in the mass spectra of other partially silylated polyhydroxy compounds, loss of water from some of the fragments is common. The ion at m/z 159 represents loss of water from $(M-57-28)^+$ while m/z 117 and m/z 143 are both unique to partial SCTASi-1,4-ribonolactones.

MSGC-2-1/8/76 TBDMSI-RIB. LAC. PK1
FINNIGAN-1015 RF-QUADRUPOLE MASS SPECTRUM
CORRECTED FOR MASS DISCRIMINATION

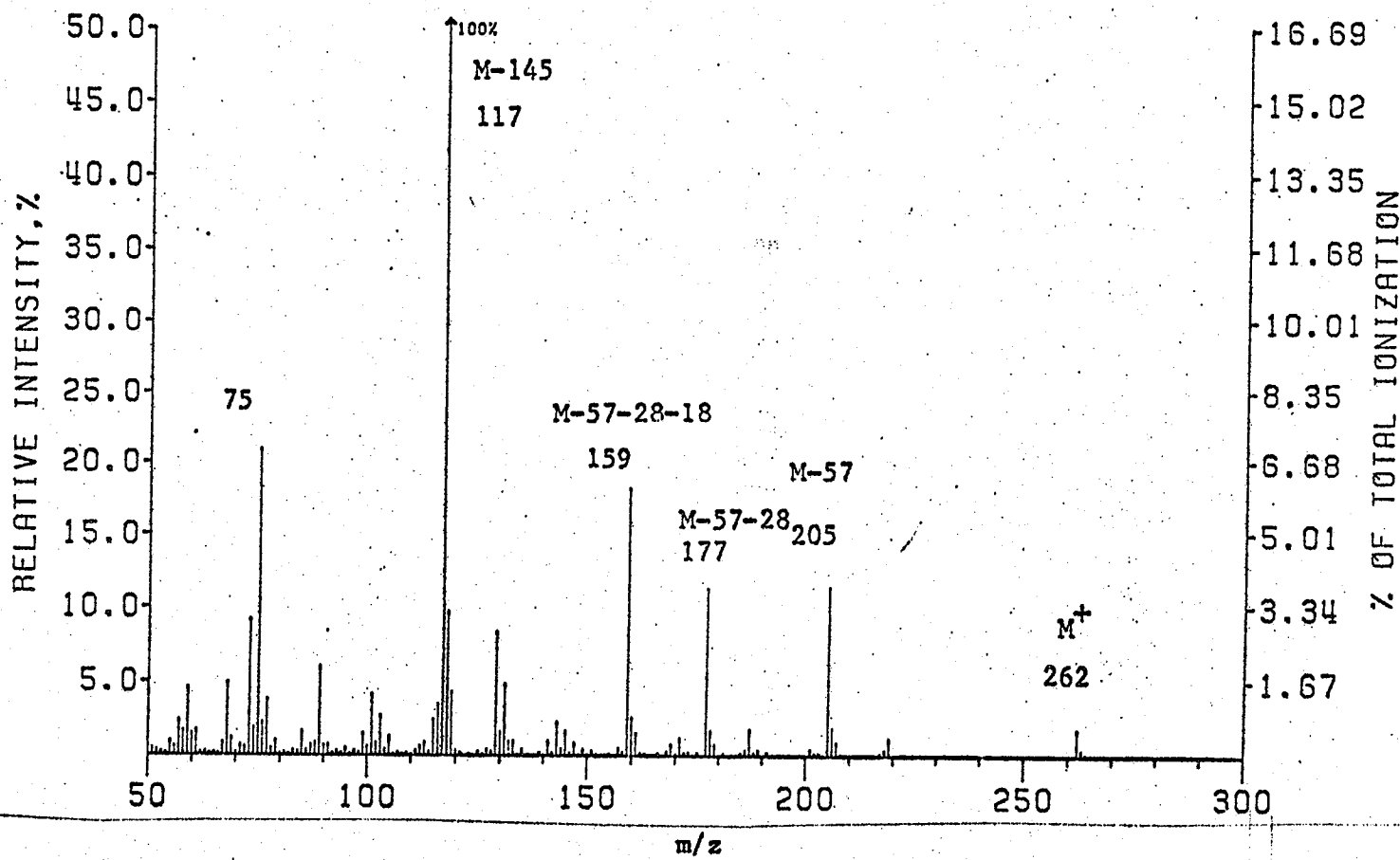


Figure: 77. Mass spectrum of mono-O-TBDMSI-1,4-ribonolactone (IX_(b), MW 262, $I_{\text{OV-1}}^{180} = 1696$), recorded on Finnigan 1015 mass spectrometer at 70 eV.

MSGC-2-1/8/76 TBDMS1-RIB. LAC. PK2
 FINNIGAN-1015 RF-QUADRUPOLE MASS SPECTRUM
 CORRECTED FOR MASS DISCRIMINATION

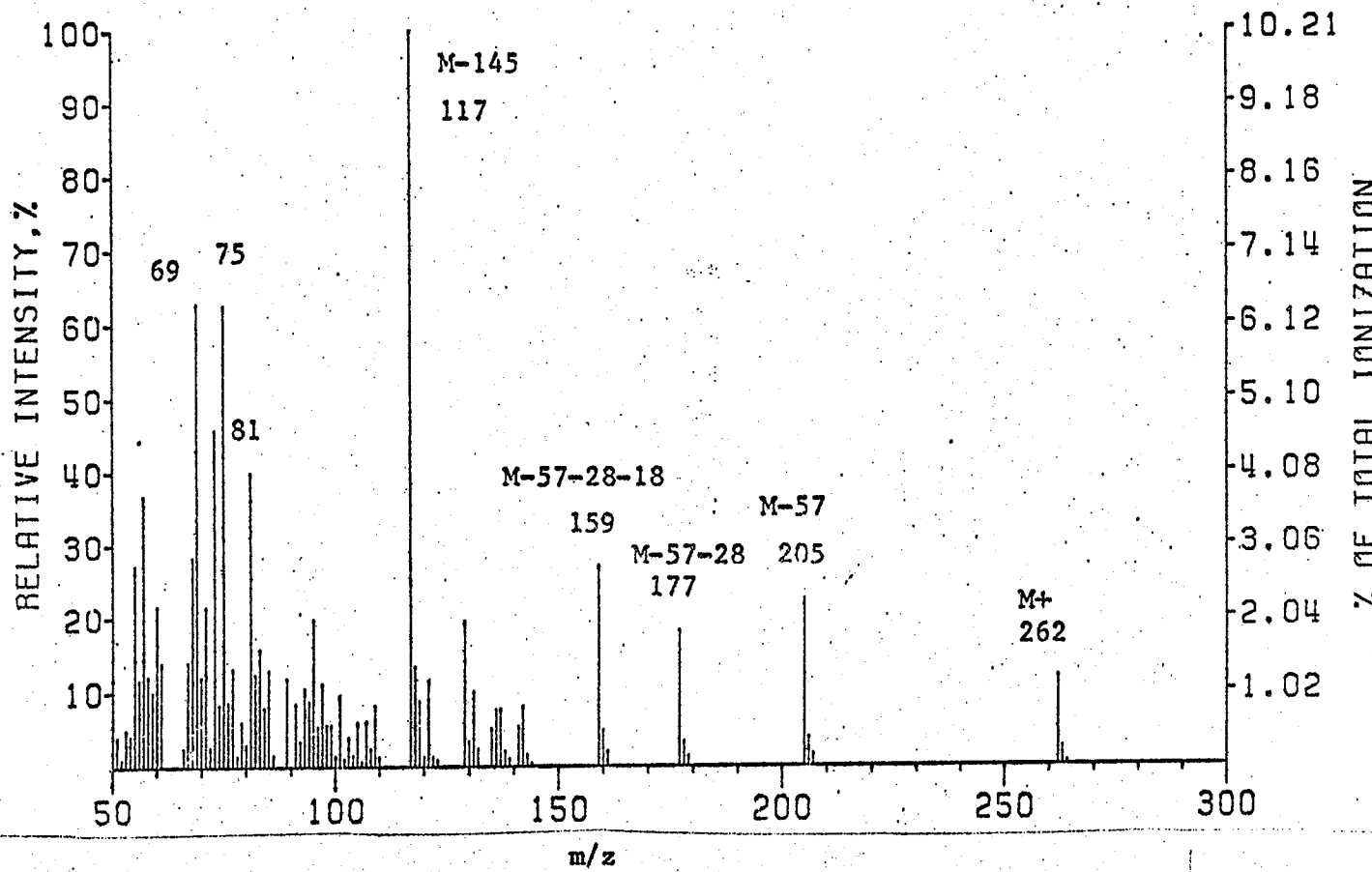


Figure: 78. Mass spectrum of mono-O-TBDMSi-1,4-ribonolactone (IX_(b)), MW 262, $I_{OV-1}^{180} = 1722$, recorded on Finnigan 1015 mass spectrometer at 70 eV.

MSGC-2-1/8/76 TBDMS1-RIB. LAC. PK3
FINNIGAN-1015 RF-QUADRUPOLE MASS SPECTRUM
CORRECTED FOR MASS DISCRIMINATION

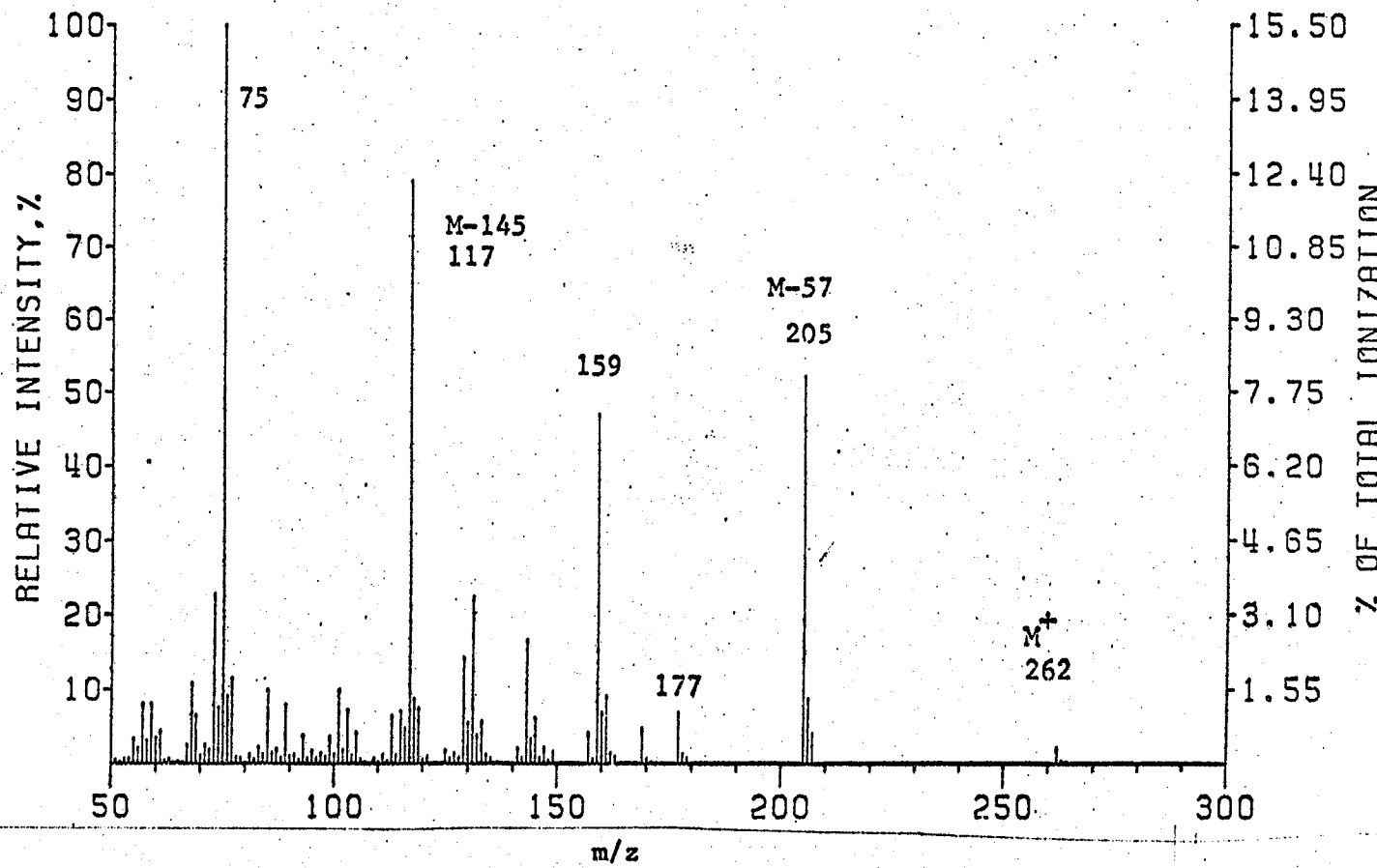


Figure: 79. Mass spectrum of mono-O-TBDMSi-1,4-ribonolactone (IX_(b), MW 262, $I_{OV-1}^{180} = 1805$), recorded on Finnigan 1015 mass spectrometer at 70 eV,

MSGC-6-15/8/76 TMTBS1 RIB. LAC. PK11
FINNIGAN-1015 RF-QUADRUPOLE MASS SPECTRUM
CORRECTED FOR MASS DISCRIMINATION

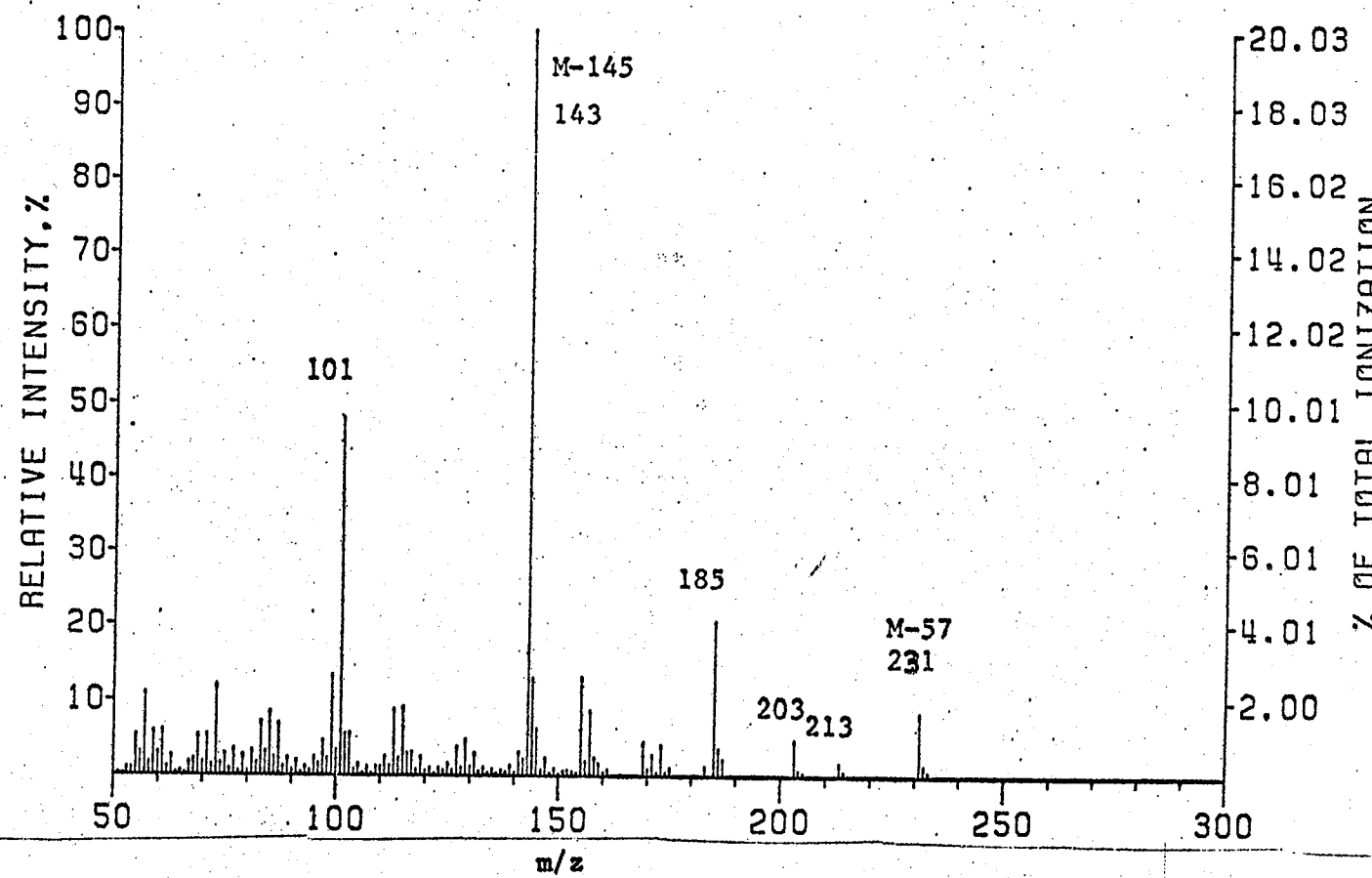


Figure: 80. Mass spectrum of mono-O-TMTBSi-1,4-ribonolactone ($\text{IX}_{(d)}$), MW 288, $I_{\text{OY}-1}^{180} = 2026$, recorded on Finnigan 1015 mass spectrometer at 70 eV.

MSGC-6-15/8/76 TMTBS1 RIB. LAC. PK12
FINNIGAN-1015 RF-QUADRUPOLE MASS SPECTRUM
CORRECTED FOR MASS DISCRIMINATION

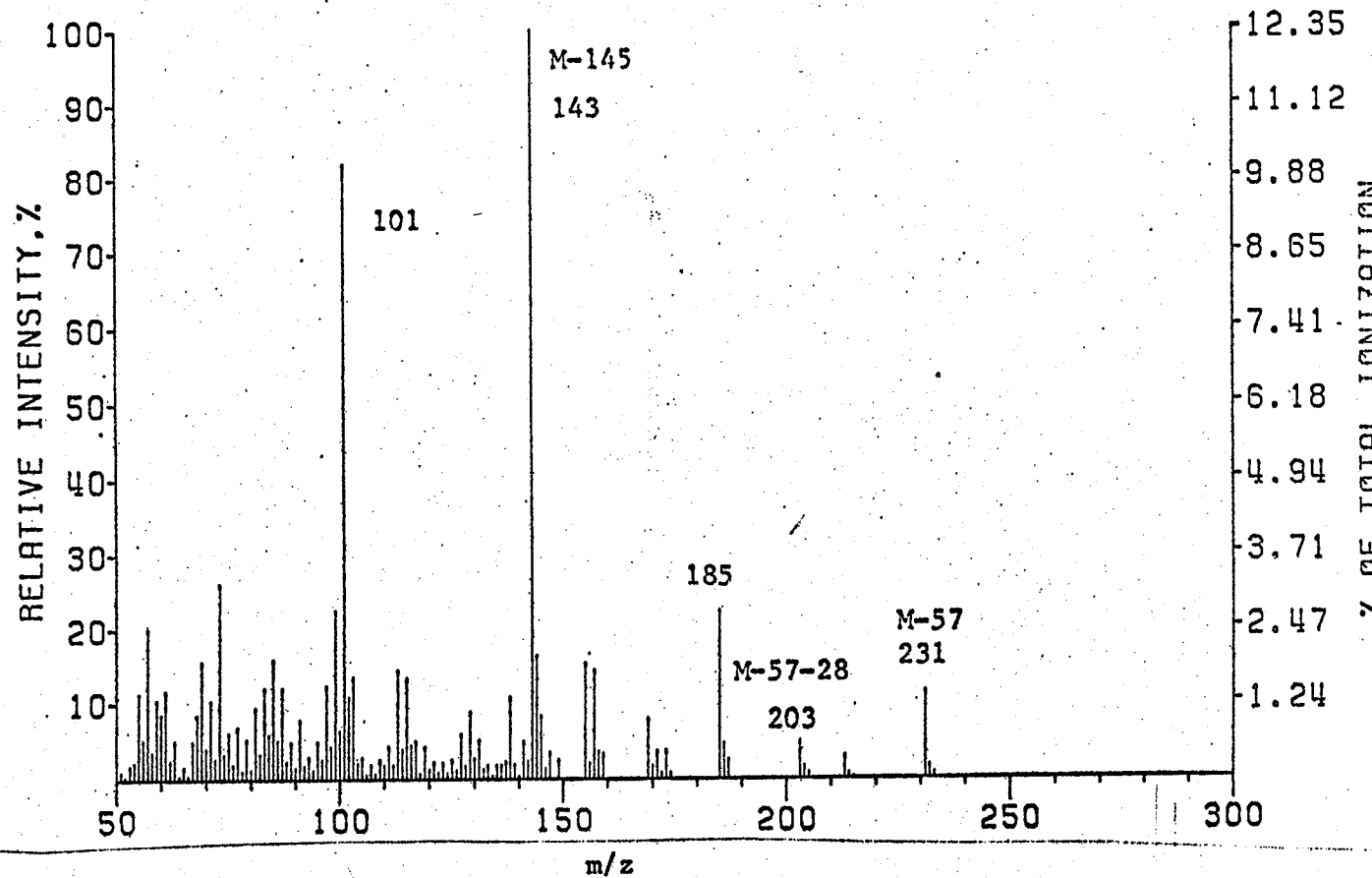


Figure: 81. Mass spectrum of mono-O-TMTBS1-1,4-ribonolactone (IX_(d)), MW 288, $I_{\text{OV}-1}^{180} = 2103$, recorded on Finnigan 1015 mass spectrometer at 70 eV.

MSGC TBDMS2 RIB. LAC. PK1 1/6/76
FINNIGAN-1015 RF-QUADRUPOLE MASS SPECTRUM
CORRECTED FOR MASS DISCRIMINATION

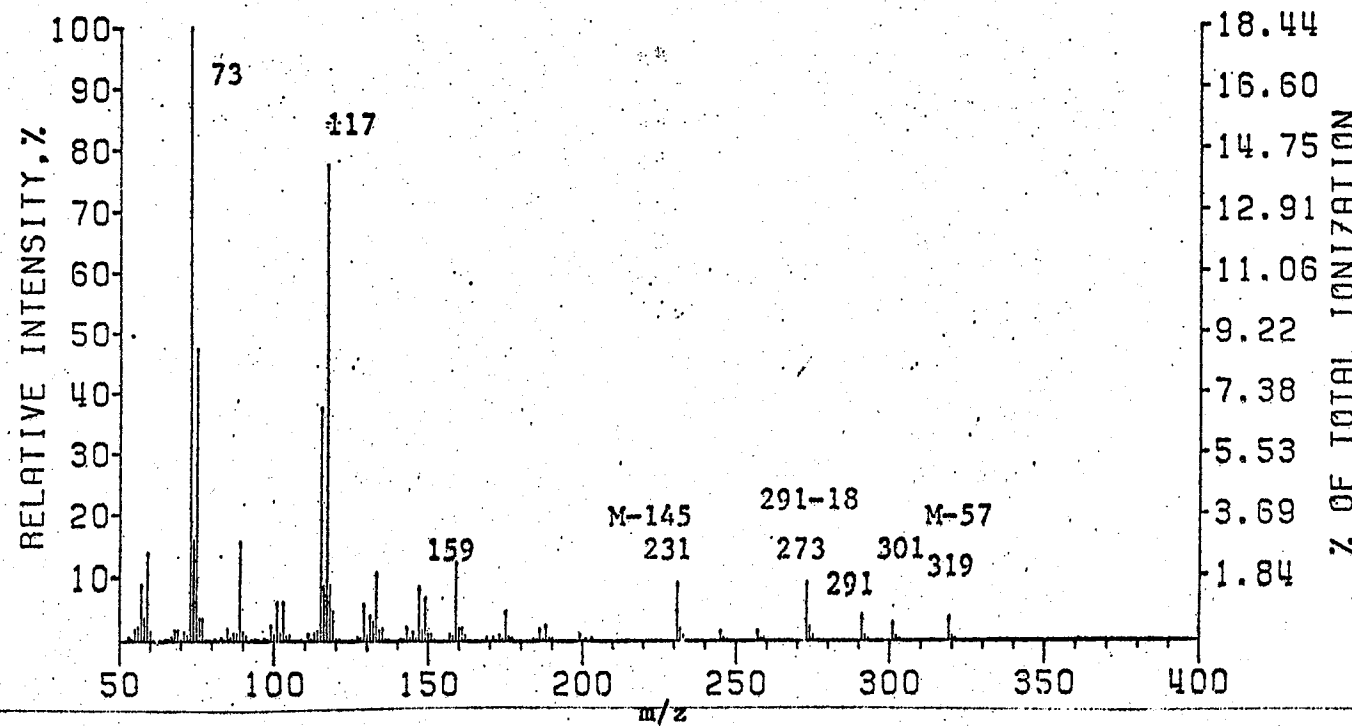


Figure: 82. Mass spectrum of bis-O-TBDMSi-1,4-ribonolactone (IX_(bb)), MW 376, $I_{OV-1}^{180} = 2003$, recorded on Finnigan 1015 mass spectrometer at 70 eV.

GCMS: 1/6/76 TBDMS2 RIB.LAC. PK2
FINNIGAN-1015 RF-QUADRUPOLE MASS SPECTRUM
CORRECTED FOR MASS DISCRIMINATION.

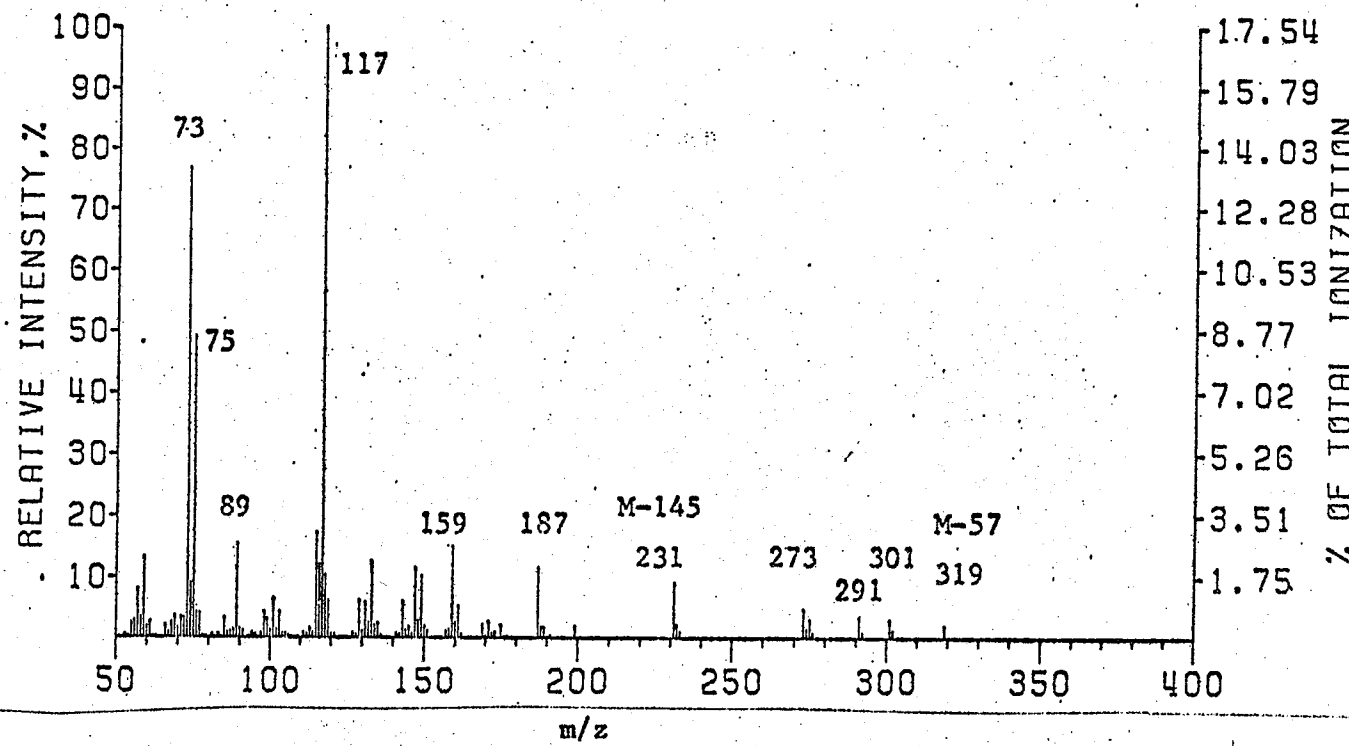


Figure: 83. Mass spectrum of bis-O-TBDMSi-1,4-ribonolactone (IX_(bb), MW 376, I¹⁸⁰_{OV-1} 2053), recorded on Finnigan 1015 mass spectrometer at 70 eV.

SPECTRUM RECORDED ON 1015 QUADRUPOLE MASS SPECTROMETER
AND NORMALIZED TO CONSTANT SENSITIVITY

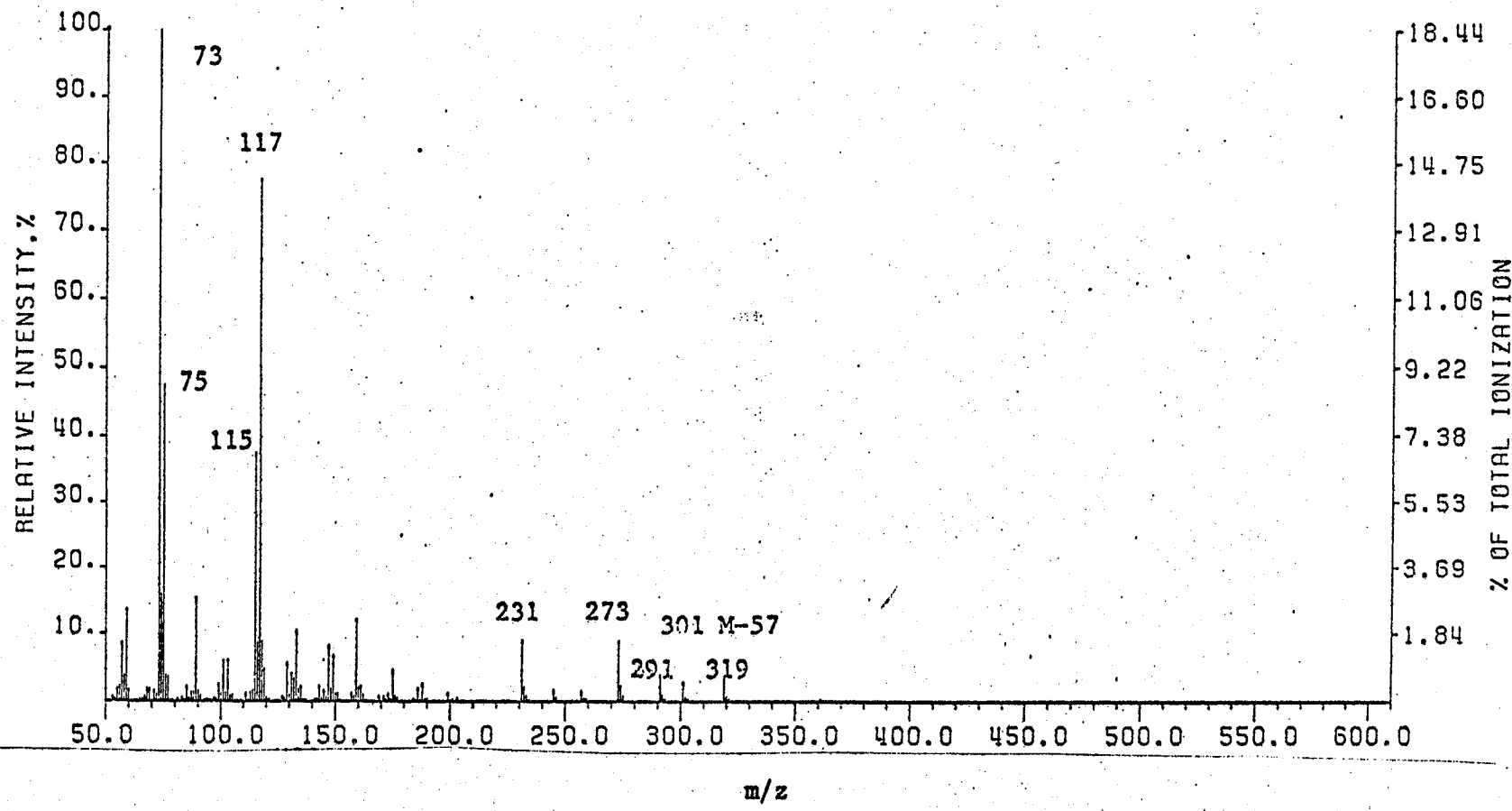


Figure: 84. Mass spectrum of bis-O-TBDMSi-1,4-ribonolactone (IX_{bb}), MW 376, $I_{Ov-1}^{180} = 2078$, recorded on Finnigan 1015 mass spectrometer at 70 eV.

MSGC-4-12/8/76 TMTBS2 RIB. LAC. PK4
FINNIGAN-1015 RF-QUADRUPOLE MASS SPECTRUM
CORRECTED FOR MASS DISCRIMINATION

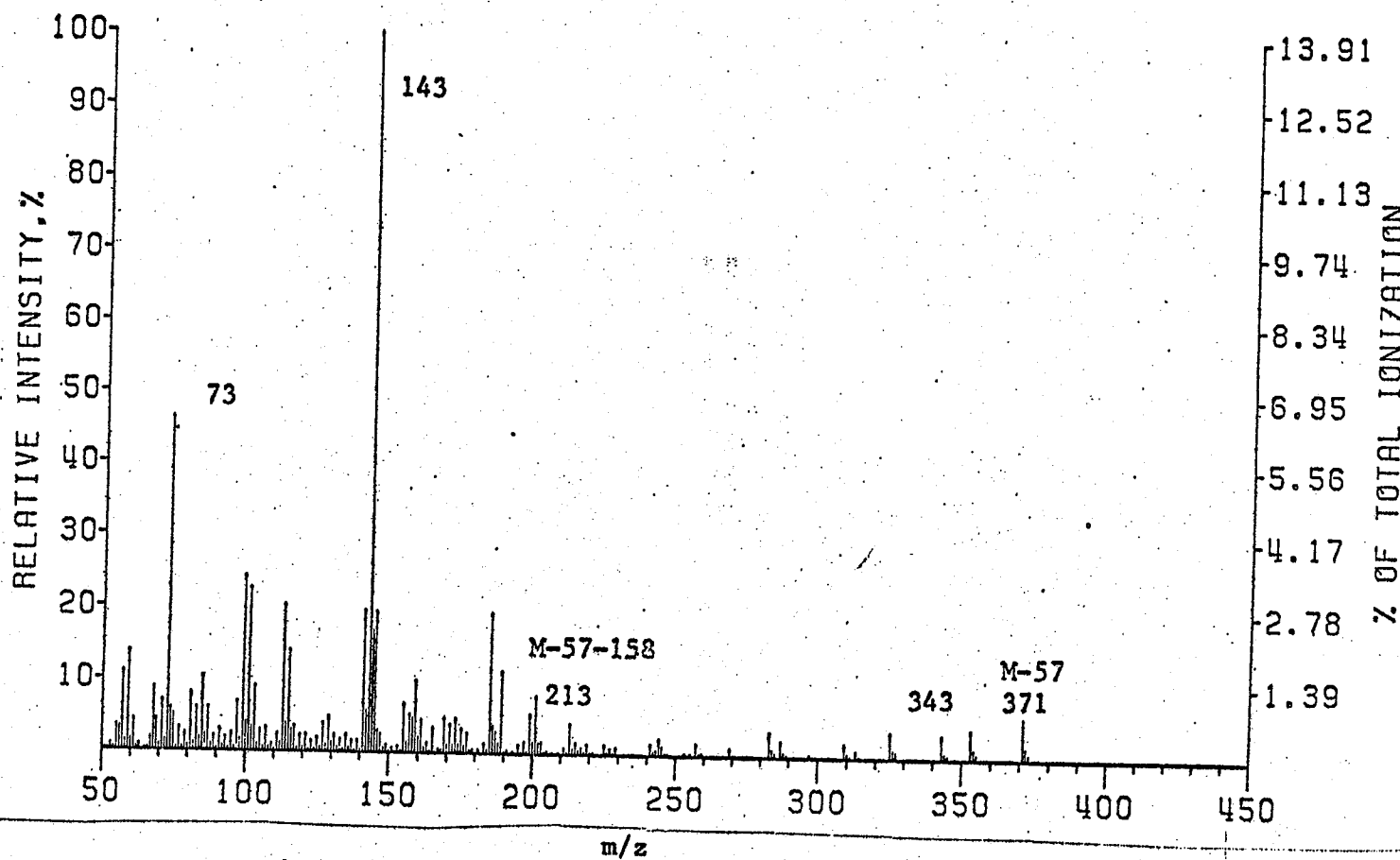


Figure: 85. Mass spectrum of bis-O-TMTBS1-1,4-ribonolactone (IX_(dd), MW 428, $I_{\text{QV-1}}^{240} = 2518$), recorded on Finnigan 1015 mass spectrometer at 70 eV.

MSGC-6/15/8/76 TMTBS2 RIB.LAC. PK15
FINNIGAN-1015 RF-QUADRUPOLE MASS SPECTRUM
CORRECTED FOR MASS DISCRIMINATION

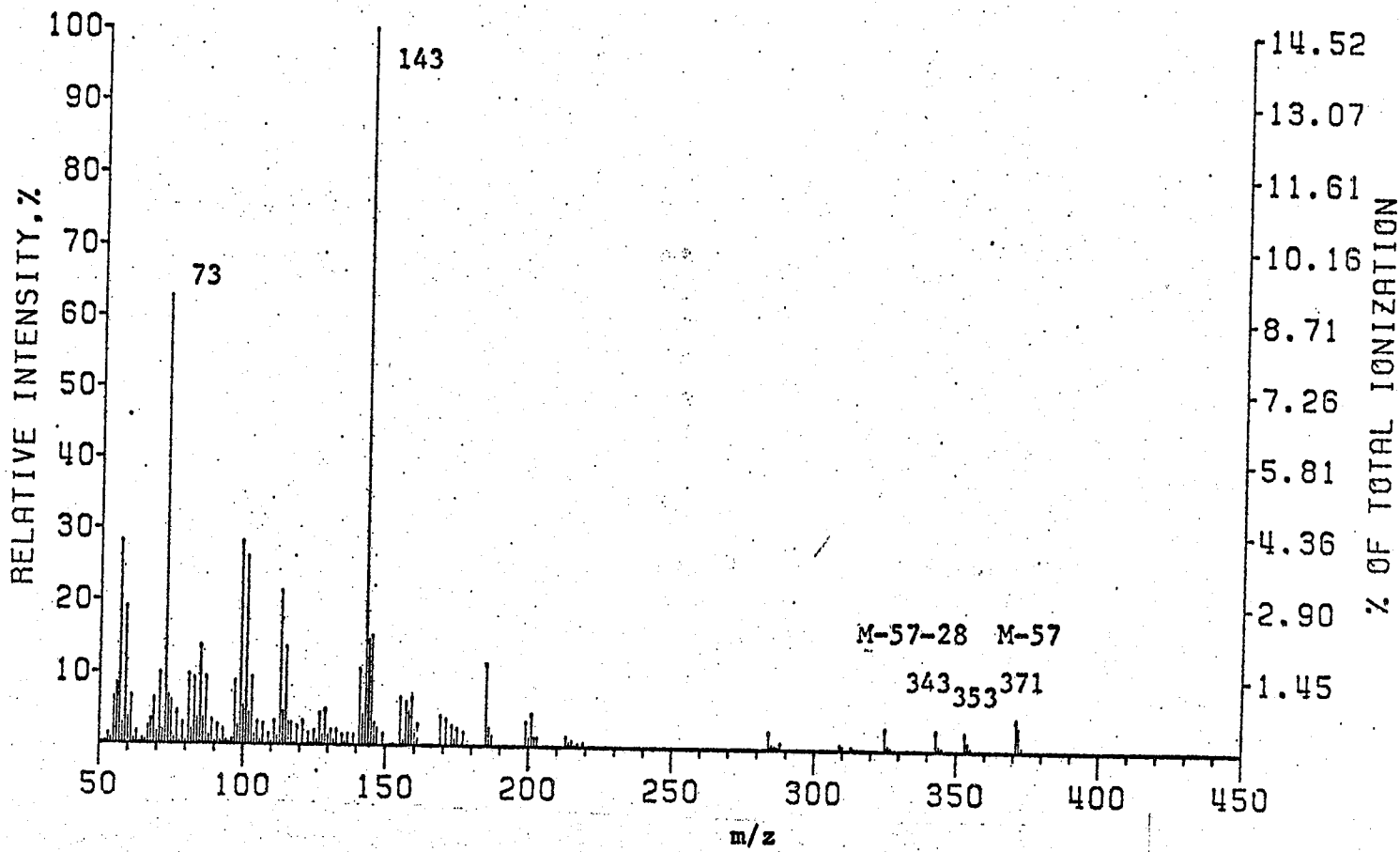


Figure: 86. Mass spectrum of bis-O-TMTBSi-1,4-ribonolactone (IX_{dd}), MW 428; $I_{Ov-1}^{240} = 2564$, recorded on Finnigan 1015 mass spectrometer at 70 eV.

SPECTRUM RECORDED ON 1015 QUADRUPOLE MASS SPECTROMETER
AND NORMALIZED TO CONSTANT SENSITIVITY

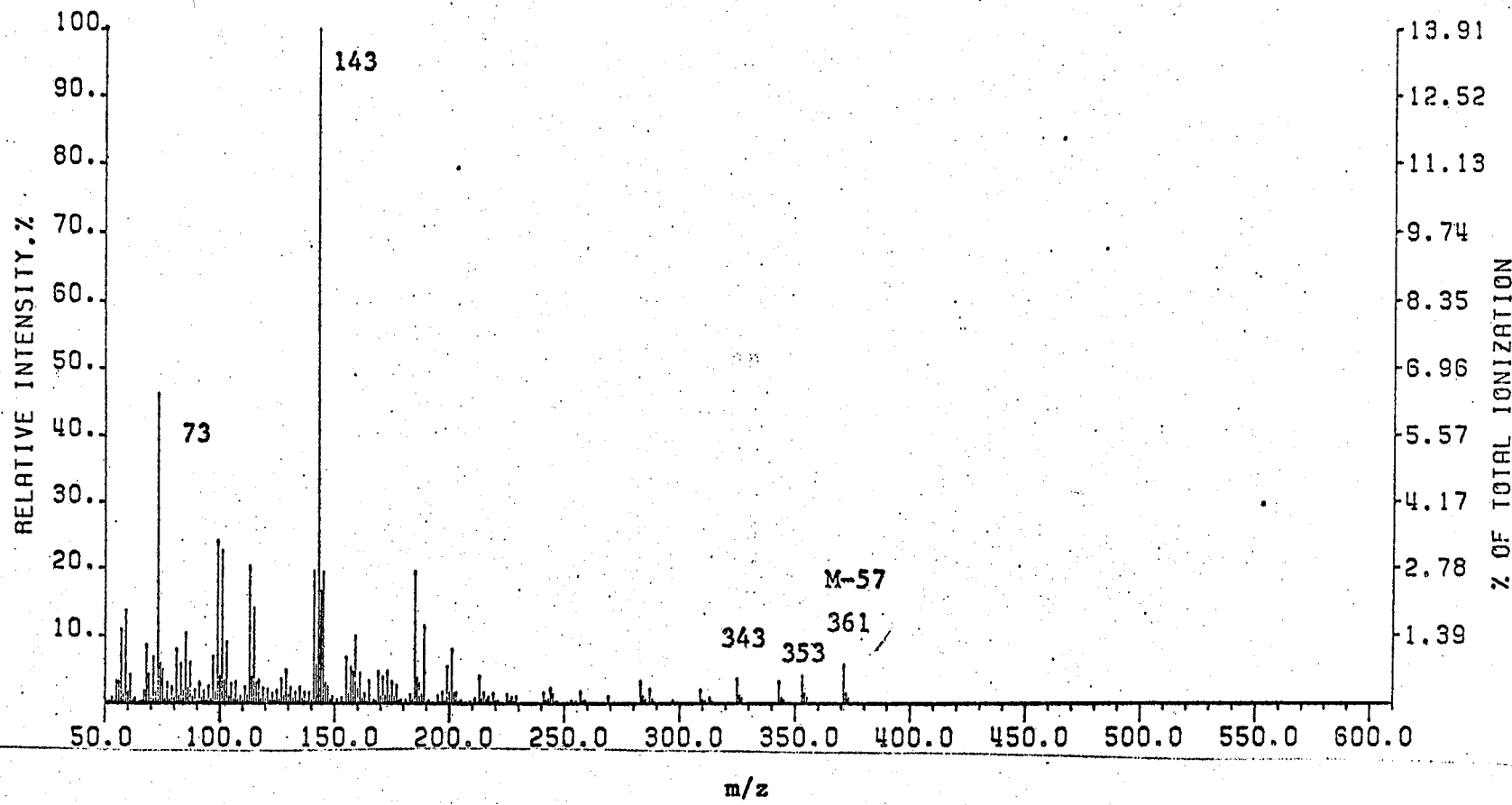


Figure: 87. Mass spectrum of bis-O-TMTBSi-1,4-ribonolactone (IX_(dd), MW 428, $I_{0V-1}^{240} = 2608$), recorded on Finnigan 1015 mass spectrometer at 70 eV.

Conclusion:

Derivatization of monosaccharide molecules with SCTASi reagents drastically increases the GC retention times of the compounds compared with TMSi analogues. The separations of anomers as well as stereoisomers are much enhanced. Evidently, the sterically crowded silyl groups introduced into the molecules modify greatly the interactions between the derivatives and the liquid phase of the column used (in this case OV-1). SCTASi-ethers of monosaccharides are not only stable to high GC column temperatures; they are also very resistant to hydrolysis, thus enabling ease in handling. For polyhydroxyl molecules, the TBDMSi-moiety (the least bulky among the three silyl groups studied) seems to be quite compatible with GC analysis. When the number of free hydroxyl groups on the molecule exceeds 6, the molecular weight of the derivative may become exceedingly high for mass spectral purposes. However, partially silylated monosaccharides could also be chromatographed without loss of peak symmetry and eluted at much lower retention times. Mixed derivatives, possessing characteristic properties of protecting groups, can also be prepared and are very much amenable to gas phase analyses.

Other SCTASi-ethers (namely, TMIPSi and TMTBSi derivatives) suffer from long GC retention times as well as less prominent peaks at high-mass regions in their mass spectra. Sometimes, derivatives tend to have high molecular weights which exceed the normal range of a medium priced mass spectrometer. On the other hand, they provide effective labelling of silicon groups and are complementary to TBDMSi-derivatives in mass spectral interpretations.

SCTASi-moieties by yielding a stable siliconium ion, have both fragmentation 'directing' as well as characteristic silyl rearrangement properties. They afford moderately intense peaks at the high end of the mass spectrum which aid in obtaining molecular weights and other information pertaining to silylated compounds.

Preliminary results on SCTASi-monosaccharide gas phase analysis properties also indicate that much knowledge is still lacking in the absolute mass spectral identification of anomers and epimers; as well as stereoisomers of many silylated monosaccharides. Further studies could be directed to deuterium labelling of the derivatized molecules. High resolution mass spectrometry and the study of metastable peaks should provide much information concerning indisputable interpretation of fragmentation pathways of SCTASi-sugars.

It is hoped that once detailed fragmentation patterns have been worked out mass fragmentography could supply qualitative information at pico-gram levels, and may provide sufficient specificity for a particular structure to enable a positive identification.

Future studies that might be of value to perform would be the investigation of SCTASi-methyl glycosides and SCTASi-glycosamines. The former compounds are important in complex carbohydrate analysis when methanolysis is used. The latter compounds are of significance because of the wide presence of glycosamines in biological systems.

BIBLIOGRAPHY

- 1) Abraham White, P. Handler, E. Smith.
Principles of Biochemistry, 5th edition, McGraw Hill Inc. (1973)
- 2) Thomas D. Brock
Biology of Micro-organisms. 1970 by Prentice Hall, Inc.
Englewood Cliffs, New Jersey.
- 3) E.C. Horning, C.J.W. Brooks, W.J.A. VandenHeuvel
Advances in Lipid Research, 6 273 (1968). Academic Press, N.Y.
- 4) J. Drozd
J. Chromatography, 113 303 (1976).
- 5) A.E. Pierce
"Silylation of Organic Compounds", Pierce Chem. Co. Rockford, Ill.
(1968)
- 6) A.E. Pierce
Pierce Handbook and General Catalogue 1978-1979
Pierce Chem. Co. Rockford, Ill. U.S.A. 61105
- 7) W.J.A. VandenHeuvel
J. of Chromatography 27 (1967) 85
- 8) W.R. Supina, R.F. Kruppa, R.S. Heuly
J. Am. Oil Chem. Soc., 44 (1967) 74
- 9) H. Miyazaki, M. Ishibashi, M. Itoh, T. Nambara
Chem. Pharm. Bull., 23 3033 (1975)
- 10) M.A. Quilliam, K.K. Ogilvie, J.B. Westmore
Biomed. Mass Spectrom. 1 78 (1974)
- 11) G. Phillipou, D.A. Bighan, R.F. Seemark
Steroids 26 516 (1975)

- 12) S.J. Gaskell, C.J.W. Brooks
Biochem. Soc. Trans., 4 111 (1976)
- 13) R.W. Kelly, P.L. Taylor
Anal. Chem., 48 456 (1976)
- 14) E.E. Knaus, R.T. Coutts, C.W. Kazakoff
J. Chromatogr. Sci., 14 525 (1976)
- 15) D.J. Harvey
Biomed. Mass Spectrom., 4 265 (1977)
- 16) G. Phillipou
J. Chromatogr., 129 384 (1976)
- 17) B.S. Thomas, C.Eaborn, D.R.M. Walton
Chem. Commun., (1966) 408
- 18) C. Eaborn, C.A. Holder, D.R.M. Walton, B.S. Thomas
J. Chem. Soc., C, (1969) 2501
- 19) C.J.W. Brooks, B.S. Middleditch
Anal. Lett., 5 611 (1972)
- 20) J.R. Chapman, E. Bailey
Anal. Chem., 45 1636 (1973)
- 21) C. Eaborn, D.R.M. Walton, B.S. Thomas
Chem. Ind. (1967) 827
- 22) E. Bailey
J. Chromatography, 89 215 (1974)
- 23) A. Dutton
Steroids 14 575 (1969)
- 24) C.F. Poole
J. of Chromatography, 89 (1974) 225

- 25) W.D.M. Paton
J. Chromatogr. 109 73 (1975)
- 26) M.A. Quilliam, J.B. Westmore
24th Annual Conference on Mass Spectrometry and Allied Topics,
American Soc. for Mass Spectrometry, San Diego, May 9-14, 1976.
Paper E-3
- 27) M.A. Quilliam, J.B. Westmore
Steroids 29 579 (1977)
- 28) M.A. Quilliam, J.F. Templeton, J.B. Westmore
Steroids 29 613 (1977)
- 29) E.J. Corey, A. Venkateswarlu
J. Am. Chem. Soc., 94 6190 (1972)
- 30) K.K. Ogilvie, E.A. Thompson, M.A. Quilliam, J.B. Westmore
Tetrahedron Lett., 2865 (1974)
- 31) K.K. Ogilvie
Canadian Journal Chem., 3799 (1973)
- 32) K.K. Ogilvie, K.L. Sanada, E.A. Thompson, M.A. Quilliam,
J.B. Westmore
Tetrahedron Lett. 2861 (1974)
- 33) K.K. Ogilvie, S.L. Beauchage, D.W. Entwistle, E.A. Thompson
M.A. Quilliam, J.B. Westmore
J. Carbohydr. Nucleosides Nucleotides 3 197 (1976)
- 34) F.G. Khorana
Science, Vol. 203, 16 Feb. 1979

- 35) K.K. Ogilvie, J. Iwacha
Tetrahedron Lett., 317 (1973)
- 36) M.A. Quilliam, J.B. Westmore
Anal. Chem., 50 59 (1978)
- 37) A.G. McInnes, D.H. Ball, F.G. Cooper, C.T. Bishop
J. Chromatogr. 1 556 (1958)
- 38) C.C. Sweeley, W.W. Wells, M. Makita, R. Bentley
J. Am. Chem. Soc., 85 2497 (1963)
- 39) J. Szafranek, C.D. Pfaffenberger, E.C. Horning
Analyst 6 (6) 479 (1973)
- 40) B.A. Dmitriev, L.V. Backmousky, O.S. Chizov, B.M. Zolotarev
and N.K. Kochetkov
Carbohydr. Research, 19 432 (1971)
- 41) M.B. Perry, R.K. Hulyalkar
Canadian J. Biochem., 43 573 (1965)
- 42) L.H. Sommer, L.T. Taylor
J. Am. Chem. Soc., 76 1030 (1954)
- 43) R. Barker
J. Org. Chem., 26 4605
- 44) M.A. Quilliam
P.D. Thesis, U. of Manitoba. (1977)
- 45) J.W. Eichelberger, L.E. Harris, W.L. Budde
Anal. Chem., 49 995 (1975)

- 46) F.W. Karasek
Research and Development, 55 (Nov. 1970)
- 47) D.C.K. Lin
Ph.D. Thesis, U. of Manitoba. (1972)
- 48) J.W. Walker, J. Tillman
J. of Chromatogr., 132 (1) 172 (1977)
- 49) P. Barlett, L.S. Corsano
Chem. Abstract (1976) 85 74414q
- 50) J.C. Linden, C.L. Lawhead
J. Chromatogr. 105 125 (1975)
- 51) A.D. Jones, S.G. Sellings, J.A. Cox
J. of Chromatogr., 144 169 (1972)
- 52) M. Sinner
J. of Chromatogr., 121 (1976) 122
- 53) Varian Product Line Notes, Separation Science, No. LC 782010,
Varian Instrument Division, 611 Hansen Way, Palo Alto, Ca 94303
- 54) J.S. Sawardeker, J.H. Sloneker, A. Jeanes
Anal. Chem., 37 1602 (1965)
- 55) R.A. Laine, C.C. Sweeley
Anal. Chem. 43 533 (1971)
- 56) C.C. Sweeley
Anal. Chem. 36 1461 (1964)
- 57) E. Kovats
Advances in Chromatogr. 1 329 (1965)

- 58) G. Castello, G. D'Amato
J. chromatogr., 79 23 (1973)
- 59) M. Gassiot, G. Firpo, E. Fernandez, R. Carlo, M. Carlo, M. Martin
J. Chromatogr., 108 337 (1975)
- 60) J. Szafranek, C.D. Phaffenberger, E.C. Horning
J. Chromatogr., 88 149 (1974)
- 61) O.P. Pahl
J. Biological Chem., 245 299 (1970)
- 62) W.C. Ellis
J. Chromatogr., 41 325 (1969)
- 63) K. Tesarik
J. Chromatogr., 65 295 (1972)
- 64) J. Novak
Advances in Chromatography, 11 1 (1974)
- 65) B. Nilsson, S. Svensson
Carbohydrate Research, 65 169 (1978)
- 66) E.L. Eliel, N.L. Allinger, S.J. Angyal, G.A. Morrison
'Conformational Analysis' Wiley-Interscience, N.Y. (1965)
- 67) B. Capron
Chem. Reviews, 69 407 (1969)
- 68) H.S. Isbell, W. Pigman
Advances in Carbohydrate Chem. Biochem., 24 13 (1969)
- 69) T.E. Acree, R.S. Schallengberger, L.P. Mattick
Carbohydrate Research, 6 495 (1968)
- 70) A.S. Hill, R.S. Schallengberger
Carbohydrate Research, 11 541 (1969)

- 71) A. Reine, J.A. Hveding, O. Kjolberg, O. Westbye
Acta Chem. Scand. B28 (1974)
- 72) P.A. Finan, R.I. Reed, W. Snedden
Chem. Ind. (London) 1172 (1959)
- 73) N.K. Kochetkov
Tetrahedron, 21 2029 (1965)
- 74) K. Bieman, D.C. DeJongh, H.K. Schnoes
J. Am. Chem. Soc., 85 1736 (1963)
- 75) D.C. DeJongh, K. Bieman
J. Am. Chem. Soc., 86 67 (1964)
- 76) P.J. Wood, I.R. Siddiqui, J. Weisz
Carbohydrate Research, 42 1 (1975)
- 77) D.C. DeJongh, T. Radford, J.D. Hribar, S. Hanessian, M. Bieber,
G. Dawson, C.C. Sweeley
J. Am. Chem. Soc. 91 1728 (1969)
- 78) L. Pauling
'The Nature of the Chemical Bond' 2nd edition. Cornell University, Ithaca, N.Y. (1948)
- 79) L.O. Brockway, N.R. Davidson
J. Am. Chem. Soc., 63 3287 (1941)
- 80) G.G. Hess, F.W. Lampe, L.H. Sommer
J. Am. Chem. Soc., 87 5327 (1965)
- 81) O.S. Chizov, N.V. Molodtsov, N.K. Kichetkov
Carbohydrate Research, 4 273 (1967)
- 82) H.C. Curtius, J.A. Vollmin, M. Miller
J. Chromatogr., 37 216 (1968)

- 83) J.A. McCloskey
"Basic Principles in Nucleic Acid Chemistry",
Vol. 1 P.O.P. T'so Ed. Academic Press, N.Y. 1974
- 84) G. Petersson, O. Sammuelson, K. Anjou, E. von Sydow
Acta. Chem. Scand, 21 (1967) 1251